



รายงานวิจัยฉบับสมบูรณ์

โครงการ การควบคุมเชิงทำนายแบบจำลองเชิงออฟไลน์สำหรับระบบซึ่งไม่เป็นเชิงเส้นขนาดใหญ่

โดย รองศาสตราจารย์ ดร.สุรเทพ เขียวหอม

มิถุนายน 2558

รายงานวิจัยฉบับสมบูรณ์

โครงการ การควบคุมเชิงทำนายแบบจำลองเชิงออฟไลน์สำหรับระบบซึ่งไม่เป็นเชิงเส้นขนาดใหญ่

รองศาสตราจารย์ ดร.สุรเทพ เขียวหอม ภาควิชาวิศวกรรมเคมี คณะวิศวกรรมศาสตร์ จุฬาลงกรณ์มหาวิทยาลัย

สนับสนุนโดยสำนักงานกองทุนสนับสนุนการวิจัยและจุฬาลงกรณ์มหาวิทยาลัย (ความเห็นในรายงานนี้เป็นของผู้วิจัย สกว. และจุฬาลงกรณ์มหาวิทยาลัย ไม่จำเป็นต้องเห็นด้วยเสมอไป)

บทคัดย่อ

รหัสโครงการ: RSA5680044

ชื่อโครงการ: การควบคุมเชิงทำนายแบบจำลองเชิงออฟไลน์สำหรับระบบซึ่งไม่เป็นเชิงเส้นขนาดใหญ่

ชื่อนักวิจัย: รองศาสตราจารย์ ดร.สุรเทพ เขียวหอม ภาควิชาวิศวกรรมเคมี

E-mail Address: soorathep.k@chula.ac.th

ระยะเวลาโครงการ: 2 ปี

การควบคุมเชิงทำนายแบบจำลองเป็นระเบียบวิธีควบคุมขั้นสูงซึ่งสามารถจัดการระบบหลายตัวแปรซึ่งมี เงื่อนไขบังคับได้ดี แต่ทว่าโดยทั่วไปการควบคุมเชิงทำนายแบบจำลองอาศัยแบบจำลองเชิงเส้นซึ่งไม่ เปลี่ยนแปลงตามเวลานั้นไม่เหมาะสมต่อการควบคุมระบบไม่เชิงเส้นหรือมีความไม่แน่นอน การควบคุมเชิง ทำนายแบบจำลองคงทนได้รับการเสนอเพื่อควบคุมระบบซึ่งมีความไม่แน่นอน ในแต่ละเวลาสุ่มอัตราขยาย ป้อนกลับซึ่งสามารถสร้างเสถียรภาพให้กับระบบวงจรจะกำหนดจากค่าต่ำสุดของตันทุนสมรรถนะที่สภาวะ เลวร้ายที่สุดภายใต้เงื่อนไขบังคับของสัญญาณขาเข้า สัญญาณขาออกและเงื่อนไขเสถียรภาพ แม้ว่าการ ควบคุมเชิงทำนายแบบจำลองคงทนสามารถรับมือกับระบบซึ่งมีความไม่แน่นอนได้ แต่การควบคุมเชิง ทำนายแบบจำลองคงทนนั้นจะใช้ภาระในการคำนวณสูงมากในการใช้งานจริง เพื่อที่จะลดภาระในการ คำนวณลง การควบคุมเชิงทำนายแบบจำลองคงทนเชิงออฟไลน์จึงได้รับความสนใจในการพัฒนา

งานวิจัยนี้ศึกษาวิธีการในการประมาณค่าภายในช่วงซึ่งสามารถใช้ร่วมกับการควบคุมเชิงทำนาย แบบจำลองคงทนเชิงออฟไลน์สำหรับระบบเวลาวิยุตซึ่งพารามิเตอร์มีความไม่แน่นอนแบบโพลีโทป ลำดับ ของอัตราขยายป้อนกลับจะได้จากการแก้ปัญหาการควบคุมแบบออพติมัลหลาย ๆปัญหาแบบออฟไลน์ จากนั้นสำดับของเซตยืนยงทรงเหลี่ยมที่สอดคล้องกับอัตราขยายป้อนกลับจะถูกสร้างขึ้น ในแต่ละเวลาสุ่มจะ ระบุเซตยืนยงขนาดเล็ดที่สุดซึ่งบรรจุสภาวะปัจจุบัน ถ้าเชยยืนยงปัจจุบันเป็นเซตข้างในสุด จะใช้อัตราขยาย ป้อนกลับที่สัมพันธ์กับเซตยืนยงข้างในสุด หากไม่ใช่กรณีดังกล่าว อัตราขยายป้อนกลับซึ่งเปลี่ยนแปลงและ กำหนดโดยการประมาณค่าภายในช่วงแบบเชิงเส้นของค่าอัตราขยายป้อนกลับซึ่งสัมพันธ์กับเซตยืนยง ปัจจุบันและเซตยืนยงลำดับถัดไปจะถูกนำมาใช้ งานวิจัยนี้ศึกษาระเบียบวิธีการประมาณค่าภายในช่วงสอง วิธี ระเบียบวิธีที่นำเสนอจะแสดงในกรณีศึกษาของระบบสองถังและระบบสี่ถัง ผลจากการจำลอง กระบวนการแสดงให้เห็นว่าระเบียบวิธีการประมาณค่าภายในช่วงที่เสนอสามารถปรับปรุงสมรรถนะการ ควบคุมของการควบคุมเชิงทำนายแบบจำลองคงทนเชิงออฟไลน์ได้ในขณะที่ภาระการคำนวณออนไลน์ไม่ เปลี่ยนแปลงมากนัก

คำหลัก: ระบบเวลาวิยุตซึ่งมีความไม่แน่นอนแบบโพลีโทปิค, เซตยืนยงทรงโพลีฮีดรอล, การควบคุมเชิง ทำนายแบบจำลองคงทน, การควบคุมเชิงออฟไลน์, การควบคุมซึ่งอาศัยการประมาณภายในช่วง

Abstract

Project Code: RSA5680044

Project Title: Off-line robust model predictive control for nonlinear large-scale systems

Investigator: Associate Professor Dr. Soorathep Kheawhom

E-mail Address: soorathep.k@chula.ac.th

Project Period: 2 years

Model predictive control (MPC) is an advanced control algorithm which can effectively handle multiple input multiple output (MIMO) processes with constraints. However, a conventional MPC based on an LTI model is often unsuitable to handle nonlinear or uncertain systems. Robust model predictive control (RMPC) has been introduced to control uncertain systems. At each sampling time, a feedback gain that can robustly stabilize the closed-loop system is determined by minimizing the worst-case performance cost subjected to input, output and stability criteria constraints. Though, RMPC can handle uncertain systems, RMPC is computationally prohibitive in practical situations. To overcome an excessive computational cost of RMPC application, a synthesis of off-line RMPC for polytopic uncertain system has been motivated.

This work studies interpolation techniques that can be employed on off-line robust constrained model predictive control for a discrete time-varying system with polytopic parametric uncertainty. A sequence of feedback gains is determined by solving off-line a series of optimal control optimization problems. A sequence of nested corresponding polyhedral invariant set is then constructed. At each sampling time, the smallest invariant set containing the current state is determined. If the current invariant set is the innermost set, the pre-computed gain associated with the innermost set is applied. If otherwise, a feedback gain is variable and determined by a linear interpolation of the pre-computed gains. Two interpolation algorithms are investigated. The proposed algorithms are illustrated with case studies of a two-tank system and a four-tank system. The simulation results showed that the proposed interpolation techniques can improve control performance of off-line robust model predictive control while on-line computation is still tractable.

Keywords: Discrete-time polytopic uncertain system, polyhedral invariant set, robust model predictive control, off-line control, interpolation-based control

Introduction

Model predictive control (MPC) is recognised as an advanced control algorithm which can effectively handle multiple input multiple output (MIMO) processes with constraints (Qin & Badgwell, 2003). Traditionally, MPC is derived by using a linear time invariant (LTI) model. At each sampling time, the algorithm uses an explicit LTI model to solve an optimal control problem, and implements the first element of the optimal input sequence computed. However, the behaviour of real process usually deviates from the linear model used in controller synthesis. A discrepancy between the behaviour of the process and that of the model used leads to deterioration of control performance. Thus, a conventional linear MPC based on an LTI model is often unsuitable to deal with a nonlinear system or a system containing uncertainty.

Robust model predictive control (RMPC) has been introduced to guarantee robustness as well as constraint satisfaction against uncertainty. At each sampling time, a feedback gain that can robustly stabilize the closed-loop system is determined by solving an optimal control problem (Kothare et al., 1996; Schuurmans & Rossiter, 2000; Kouvaritakis et al., 2000; Lee & Kouvaritakis, 2002; Bemporad et al., 2003; Veselý et al., 2010; Li & Xi, 2011; Wang, 2012; He et al., 2014).

In Kothare et al. (1996), the optimisation problem involved is formulated as minimisation of the worst-case performance cost subjected to input, output and stability criteria constraints. The stability criteria constraint is derived based on a single Lyapunov function (SLF). An ellipsoidal invariant set containing the current state is constructed to guarantee robust stability. Any states in the invariant set can be driven to the origin by using the feedback gain computed.

Several approaches have been introduced in order to improve control performance of RMPC. RMPC algorithms based on a parameter dependent Lyapunov function (PDLF) have been proposed (Cuzzola et al., 2002; Mao, 2003). The idea of using PDLF was further extended to the case of LPV systems (Wada et al., 2006) where a scheduling parameter is considered in controller synthesis. However, the number of decision variables and constraints involved in an associated optimisation problem drastically increases. Thus, an application of these algorithms is limited to relatively slow dynamic processes.

RMPC algorithms usually assume that a feedback gain is constant throughout an infinite horizon(Kothare et al., 1996). Thus, one way to improve control performance is to introduce a sequence of free control inputs to the control law (Schuurmans & Rossiter, 2000; Casavola et al., 2002; Bumroongsri & Kheawhom, 2012b). Unfortunately, more on-line computational time is required to calculate these free control inputs.

Though, RMPC can handle polytopic uncertain system, RMPC is computationally prohibitive in practical situations. To overcome an excessive computational cost of RMPC application, a synthesis of off-line RMPC for polytopic uncertain system has been motivated (Nguyen et al., 2012; Wan & Kothare, 2003; Angeli et al., 2008).

In Nguyen et al. (2012), an explicit solution of multi-parametric optimisation

problem was used to construct a control law that is a piecewise affine feedback defined over a polyhedral partition of the state space. In Wan & Kothare (2003), on-line computational time was reduced by pre-computing off-line a sequence of feedback gains corresponding to a sequence of ellipsoidal invariant sets. At each sampling time, a feedback gain applied to the process is calculated by linear interpolation between the pre-computed feedback gains. This strategy was further extended by using nominal performance cost as proposed in Ding et al. (2007).

An off-line robust model predictive control (RMPC) for LPV system was introduced in Bumroongsri & Kheawhom (2012a). This algorithm used the algorithm proposed in Wada et al. (2006) to compute a sequence of feedback gains in off-line fashion. A sequence of corresponding ellipsoidal invariant sets is also off-line pre-computed. At each sampling time, the smallest ellipsoid containing the current state is determined. A feedback gain is obtained by linear interpolation between the pre-computed feedback gains. As the interpolation technique used does not require solving any optimisation problems, the computational burden is very small.

Though a polyhedral invariant set has some advantages over an ellipsoidal invariant set such as better handling of asymmetric constraints and enlargement of domain of attraction, an ellipsoidal invariant set is usually used in RMPC formulation due to its relatively low on-line computational burden. In recent years, an off-line RMPC algorithm based on polyhedral invariant set has been developed in Bumroongsri & Kheawhom (2012c). A sequence of polyhedral invariant sets corresponding to a sequence of pre-computed feedback gains is constructed off-line by using the algorithm proposed in Pluymers et al. (2005a). At each sampling time, the smallest polyhedral invariant set containing the current state is determined. The corresponding feedback gain is then implemented to the process without interpolation of the pre-computed feedback gains. This algorithm provided a larger stabilisable region than off-line RMPC (Wan & Kothare, 2003). However, a spiking effect of control input caused by a switching of feedback gains was observed. Therefore, the algorithm requires constructing a large number of polyhedral invariant sets in order to reduce the spiking effect as well as to improve control performance. Consequently, large data storage is required. Later, an interpolation technique for polyhedral invariant sets was introduced to off-line RMPC for polytopic uncertain systems in order to improve control performance (Bumroongsri & Kheawhom, 2013). The interpolation algorithm could significantly improve control performance and eliminate the spiking effect of control input.

An interpolation-based MPC using polyhedral invariant set was proposed in Rossiter et al. (2004). The algorithm used decomposition variables and solved on-line optimisation on performance index subjected to constraint set. The paper highlighted the potential benefits of using interpolation to generate predictive control algorithm and to enlarge a stabilisable region. However, the technique proposed was only developed for an LTI system.

In Nguyen et al. (2013), an interpolated vertex control for a linear timevarying discrete-time system was introduced. The algorithm uses variable decomposition and convex interpolation between vertex control law and local linear feedback control law. At each sampling time, the algorithm solves linear programming problems on variable decomposition as well as vertex control action. This algorithm has advantages in terms of size of stabilisable region.

In this work, two interpolation techniques, employed on off-line robust model predictive control (RMPC) based on polyhedral invariant set, were investigated. The proposed algorithms are not based on variable decomposition. In the first technique, the parameter used in the interpolation is minimized subjected to constraint set. In the second technique, the parameter used in the interpolation is obtained by minimizing constraint violation of the adjacent smaller invariant set subjected to constraint set. The paper is organized as follows. The background of RMPC as well as interpolation techniques used in off-line RMPC were introduced in this section. Description of the system and control problem is then presented. RMPC and polyhedral invariant set construction are described. Then, the proposed interpolation based algorithms are presented. Implementation of the algorithms proposed is illustrated.

Notation

For a matrix A, A^T denotes its transpose, A^{-1} denotes its inverse. I denotes an identity matrix. For a state vector x, x_k denotes a state measured at time k, x_{k+i} denotes a state at prediction time k+i predicted at time k. y_k and u_k denote an output and a control input at real time k, respectively. The symbol * denotes the corresponding transpose of a lower block part of symmetric matrices.

Problem description

In this work, a discrete-time linear time-varying (LTV) system with polytopic parametric uncertainty as shown in (1) is taken into account:

$$x_{k+1} = A_k x_k + B_k u_k$$

$$y_k = C_k x_k$$
(1)

where $x_k \in R^{n_x}$ is a state vector that can be accurately measured or estimated. $u_k \in R^{n_u}$ is a control input vector, and $y_k \in R^{n_y}$ is a control output vector. A system matrix A_k , a control matrix B_k , and an output matrix C_k are assumed to be within a polytope:

$$[A_k, B_k, C_k] \in Co\{[A_1, B_1, C_1], ..., [A_l, B_l, C_l], ..., [A_L, B_L, C_L]\}.$$

Co denotes a convex hull with $[A_l, B_l, C_l]$ uncertain vertices. Any $[A_k, B_k, C_k]$ within the polytope is a convex combination of all vertices such that:

$$[A_k, B_k, C_k] = \sum_{l=1}^{L} \lambda_{l,k} [A_l, B_l, C_l]$$
$$\sum_{l=1}^{L} \lambda_{l,k} = 1$$

where $0 \le \lambda_{l,k} \le 1$ is an uncertain parameter vector.

The aim is to find a state feedback control law:

$$u_k = K_k x_k \tag{2}$$

that can stabilize the system and achieve the minimum worst case performance cost defined as in (3) while satisfying input, output and state constraints as in (4-6):

$$\min_{u_{k+i}} \max_{[A,B,C] \in \Omega} \sum_{i=0}^{\infty} \begin{bmatrix} x_{k+i} \\ u_{k+i} \end{bmatrix}^T \begin{bmatrix} \Theta & 0 \\ 0 & R \end{bmatrix} \begin{bmatrix} x_{k+i} \\ u_{k+i} \end{bmatrix}$$
 (3)

$$s.t.u_{h,\min} \le u_{h,k+i} \le u_{h,\max}, h = 1, ..., n_u$$
 (4)

$$y_{r,\min} \le y_{r,k+i} \le y_{r,\max}, r = 1, ..., n_y$$
 (5)

$$x_{s,\min} \le x_{s,k+i} \le x_{s,\max}, s = 1, ..., n_x$$
 (6)

where Θ and R are weighting matrices of states and control inputs, respectively.

Robust model predictive control and polyhedral invariant set

An on-line robust model predictive control (RMPC) for a system with polytopic uncertainty was introduced by Kothare et al. (1996). An optimal control problem solved in each sampling time is shown in (7-11):

$$\min_{\gamma \mid YO} \gamma \tag{7}$$

$$s.t. \begin{bmatrix} 1 & * \\ x_k & Q \end{bmatrix} \ge 0 \tag{8}$$

$$\begin{bmatrix} Q & * & * & * & * \\ A_l Q + B_l Y & Q & * & * \\ \Theta^{\frac{1}{2}} Q & 0 & \gamma I & * \\ R^{\frac{1}{2}} Y & 0 & 0 & \gamma I \end{bmatrix} \ge 0, \forall l = 1, ..., L$$
 (9)

$$\begin{bmatrix} X & * \\ Y^T & Q \end{bmatrix} \ge 0, X_{hh} \le u_{h,\text{max}}^2, h = 1, ..., n_u$$
 (10)

$$\begin{bmatrix} X & * \\ Y^T & Q \end{bmatrix} \ge 0, X_{hh} \le u_{h,\text{max}}^2, h = 1, ..., n_u$$

$$\begin{bmatrix} S & * \\ (A_lQ + B_lY)^T C^T & Q \end{bmatrix} \ge 0, \forall l = 1, ..., L$$

$$S_{rr} \le y_{r,\text{max}}^2, r = 1, ..., n_y$$
(11)

where Q > 0 is a symmetrical matrix.

The problem presented in (7-11) is a convex optimisation problem with linear matrix inequalities (LMI). By solving this problem, a state feedback control law $u_k = Kx_k$ with a feedback gain $K = YQ^{-1}$ that can stabilize the system while satisfying input and output constraints, is obtained. A proof of this algorithm can be found in Kothare et al. (1996).

At each sampling time, the algorithm constructs an ellipsoidal invariant set $S = \{x | x^T Q^{-1}x \leq 1\}$ to guarantee stability of the closed loop system. The advantage of using an ellipsoidal set lies in the fact that the constraints involved can be expressed in an LMI form.

By giving a feedback gain K that can stabilize the system, the polyhedral invariant set $S = \{x | Mx \le d\}$ with largest domain of attraction can be constructed using the following procedure (Pluymers et al., 2005b).

Procedure 1

- 1. Set i = 0; $M_i = [I, -I, C_1, -C_1, \dots, C_l, -C_l, \dots, C_L, -C_L, K, -K]^T$; $d_i = [x_{\text{max}}, -x_{\text{min}}, y_{\text{max}}, -y_{\text{min}}, \dots, y_{\text{max}}, -y_{\text{min}}, \dots, y_{\text{max}}, -y_{\text{min}}, u_{\text{max}}, -y_{\text{min}}, u_{\text{max}}, -u_{\text{min}}]^T; S_i = \{x | M_i x \le d_i\}.$
- 2. Set i = i + 1; $M_i = [M_{i-1}, M_{i-1}[A_1 + B_1K], \ldots, M_{i-1}[A_l + B_lK], \ldots, M_{i-1}[A_L + B_LK]]^T$; $d_i = [d_{i-1}, d_{i-1}, \ldots, d_{i-1}, \ldots, d_{i-1}]^T$; $S_i = [d_{i-1}, d_{i-1}, \ldots, d_{i-1}, \ldots, d_{i-1}]^T$ $\{x|M_ix\leq d_i\}$, and eliminate redundant inequalities from the polytope S_i .
- 3. If $S_i \neq S_{i-1}$ then repeat step 2, if otherwise stop the algorithm and $S = \{x | M_i x \le d_i\}.$

Theorem 1. For an LTV system as shown in (1), given the control law $u_k = Kx_k$ with a state feedback gain $K = YQ^{-1}$ provided by solving the optimisation problem presented in (7-11), the polyhedral set $S = \{x | Mx \le d\}$ constructed by using Procedure 1 provides a set of states whereby the system will evolve to the origin without input and output constraints violation.

Proof. The feedback gain K used in the construction of the polyhedral invariant set is obtained by solving convex optimisation problem with LMI constraints as shown in (7-11). The satisfaction of (9) for a state feedback gain K ensures that:

$$[[A_l + B_l K] x_k]^T \gamma Q^{-1} [[A_l + B_l K] x_k] - x_k^T \gamma Q^{-1} x_k \le -[x_k^T \Theta x_k + u_k^T R u_k], l = 1, ..., L.(12)$$

Thus, $V_k = x_k^T \gamma Q^{-1} x_k$ is a strictly decreasing Lyapunov function and the closed-loop system is robustly stabilized by the state feedback gain K.

By following Procedure 1, state, output and input constraints at time step $k+i, i=0,...,i_{\max}$ are repeatedly added to define a polyhedral invariant set $S_i = \{x|M_ix \leq d_i\}$, and all redundant constraints are removed. There must exist a finite index $i=i_{\max}$ such that $M_i=M_{i+1}$ because of the contraction as the feedback gain K is able to ensure robust stability and constraint satisfaction of the system. Hence, a set of initial states $S=\{x|Mx\leq d\}$ is constructed such that all predicted states remain inside S and approach to the origin without constraint violation. Moreover, the polyhedral invariant set constructed is never an empty set because the feedback gain K given is a stabilisable gain.

Off-line RMPC and the proposed interpolation algorithms

In this section, off-line RMPC and the proposed interpolation algorithms are described. An off-line RMPC consists of off-line and on-line calculations. The purpose of the off-line calculation is to generate a sequence of feedback gains, and a sequence of nested polyhedral invariant sets. The off-line calculation used in this work is identical to the off-line RMPC proposed in Bumroongsri & Kheawhom (2012c). The purpose of the on-line calculation is to determine a variable feedback gain applied to the process at each sampling time.

Off-line calculation

• Choose a sequence of states $x_m, m = 1, ..., m_{\text{max}}$ where x_{m+1} is closer to the origin than x_m . For each x_m solve the optimisation problem in (7-10) by replacing x_k with x_m in order to obtain a corresponding feedback gain:

$$K_m = Y_m Q_m^{-1}. (13)$$

In addition, x_m is chosen such that $\epsilon_{m+1}^{-1} \subset \epsilon_m^{-1}$ where $\epsilon_m = \{x | x^T Q_m^{-1} x \le 1\}$. Moreover, for each $m \ne m_{\max}$, there must exist a matrix P > 0 satisfying:

$$P - [A_l + B_l K_m]^T P[A_l + B_l K_m] > 0, l = 1, ..., L$$
(14)

$$P - [A_l + B_l K_{m+1}]^T P[A_l + B_l K_{m+1}] > 0, l = 1, ..., L$$
(15)

to assure robust stability satisfaction of a feedback gain $K = \lambda K_m + (1-\lambda) K_{m+1}$, $0 \le \lambda \le 1$ which is a convex combination between K_m and K_{m+1} .

Each feedback gain K_m is derived based on the minimisation of the upper bound of infinite horizon worst-case performance. The output constraint in (11) is relaxed in order to enlarge the domain of attraction. The input, output and state constraints are properly handled during the polyhedral invariant set construction in the next step.

• For each feedback gain $K_m = Y_m Q_m^{-1}, m = 1, ..., m_{\text{max}}$ as previously calculated, the corresponding polyhedral invariant set $S_m = \{x | M_m x \leq d_m\}$ is constructed by using Procedure 1.

The existence of a common Lyapunov function P in (14) and (15) depends on the difference between x_m and x_{m+1} . (14) and (15) can be satisfied by appropriately selecting x_m and x_{m+1} . For example, x_m and x_{m+1} should be close enough so that Q_m^{-1} can be used as a common Lyapunov function P between K_m and K_{m+1} . In such case, (15) becomes:

$$Q_m^{-1} - [A_l + B_l K_{m+1}]^T Q_m^{-1} [A_l + B_l K_{m+1}] > 0, l = 1, ..., L$$
(16)

which defines the limit of K_{m+1} .

On-line calculation

In the on-line calculation, a feedback gain applied at each sampling time is determined. In Bumroongsri & Kheawhom (2012c), at each sampling time, the smallest invariant set that can embed a measured state is determined, and a corresponding feedback gain is then implemented. In this work, a feedback gain at each sampling time is variable and computed using an interpolation technique.

Algorithm 1

The feedback gain implemented is computed by linear interpolation between the pre-computed feedback gains. At each sampling time, the current state x_k is measured and the smallest polyhedral invariant set $S_m = \{x | M_m x \le d_m\}$ containing the current state is determined.

If $x_k \in S_m$ and $x_k \notin S_{m+1}, \forall m \leq m_{\max} - 1$, a variable feedback gain $K_k = \lambda_k K_m + (1 - \lambda_k) K_{m+1}$ can be obtained by solving the optimisation problem in (17-21):

$$\lim_{\lambda_k} \lambda_k \tag{17}$$

s.t.
$$M_m[A_l + B_l K_k] x_k - d_m \le [0, 0, ..., 0]^T, l = 1, ..., L$$
 (18)

$$u_{\min} \le K_k x_k \le u_{\max} \tag{19}$$

$$K_k = \lambda_k K_m + (1 - \lambda_k) K_{m+1} \tag{20}$$

$$0 \le \lambda_k \le 1. \tag{21}$$

If otherwise, $x_k \in S_{m_{\text{max}}}$, the constant feedback gain $K_{m_{\text{max}}}$ is applied.

The optimisation problem involved is formulated as linear programming and the number of constraints involved is linearly dependent on the number of vertices of the uncertain polytope.

Algorithm 2

The feedback gain implemented is computed by linear interpolation between the pre-computed feedback gains to minimize largest constraint violation to the adjacent smaller invariant set in one step prediction. At each sampling time, the current state x_k is measured and the smallest polyhedral invariant set $S_m = \{x | M_m x \le d_m\}$ containing the current state is determined.

If $x_k \in S_m$ and $x_k \notin S_{m+1}, \forall m \leq m_{\text{max}} - 1$, a feedback gain $K_k = \lambda_k K_m + (1 - \lambda_k) K_{m+1}$ can be obtained by solving the problem in (22-27):

$$\min_{\gamma_k \lambda_k} \gamma_k \tag{22}$$

s.t.
$$M_m[A_l + B_l K_k] x_k - d_m \le [0, 0, ..., 0]^T, l = 1, ..., L$$
 (23)

$$M_{m+1}[A_l + B_l K_k] x_k - d_{m+1} \le [\gamma_k, \gamma_k, ..., \gamma_k]^T, l = 1, ..., L$$
 (24)

$$u_{\min} \le K_k x_k \le u_{\max} \tag{25}$$

$$K_k = \lambda_k K_m + (1 - \lambda_k) K_{m+1} \tag{26}$$

$$0 \le \lambda_k \le 1. \tag{27}$$

If otherwise, $x_k \in S_{m_{\text{max}}}$, the constant feedback gain $K_{m_{\text{max}}}$ is applied.

The optimisation problem involved is formulated as linear programming and the number of constraints involved is linearly dependent on the number of vertices of the uncertain polytope.

Theorem 2. For an LTV system as shown in (1), given an initial state $x_k \in S_m$, the control law, provided by Algorithms 1 and 2, assures robust stability to the closed-loop system while satisfying input, output and state constraints.

Proof. As (14) and (15) are satisfied, a common Lyapunov function $V_k = x_k^T P$ x_k ensures that a feedback gain of $K_k = \lambda_k K_m + (1 - \lambda_k) K_{m+1}$, $0 \le \lambda_k \le 1$, which is a convex combination of K_m and K_{m+1} , is a stabilisable gain.

In solving the problem in (17-21), (20) and (21) restrict K_k to be a convex combination. The input constraint is guaranteed by (19). The state and output constraints are satisfied by forcing a one step prediction state x_{k+1} to remain inside S_m as in (18). Thus, an initial state x_k evolves closer to the origin by passing S_{m+1} , S_{m+2} , ..., and $S_{m_{\text{max}}}$. A state inside $S_{m_{\text{max}}}$ is then driven to the origin by the constant feedback gain $K_{m_{\text{max}}}$ because $S_{m_{\text{max}}}$ is satisfied with Theorem 1. Thus, Algorithm 1 assures robust stability to the closed-loop system with input, output and state constraints satisfaction.

In solving the problem in (22-27), (26) and (27) restrict K_k to be a convex combination. The input constraint is guaranteed by (25). The state and output constraints are satisfied by forcing a one step prediction state x_{k+1} to remain inside S_m as in (23). Thus, an initial state x_k evolves closer to the origin by passing S_{m+1} , S_{m+2} , ..., and $S_{m_{\max}}$. A state inside $S_{m_{\max}}$ is then driven to the origin by the constant feedback gain $K_{m_{\max}}$ because $S_{m_{\max}}$ is satisfied with Theorem 1. Thus, Algorithm 2 assures robust stability to the closed-loop system with input, output and state constraints satisfaction.

Case study

In this section, examples are presented to illustrate the proposed interpolation algorithms. The latter are compared with on-line RMPC proposed in Kothare et al. (1996), off-line RMPC algorithm proposed in Bumroongsri & Kheawhom (2012c) and interpolated vertex control proposed in Nguyen et al. (2013). Numerical simulation was performed in 2.3 GHz Intel Core i-5 with 16 GB RAM, using SDPT3(Tütüncü et al., 2003) and YALMIP (Löfberg, 2004) within Matlab R2011b environment.

Two-tank system

Application of a two-tank system which is similar to the system considered in Dlapa (2007) was considered. Spherical tanks with radius 0.5 m are connected as shown in Fig. 1. An outflow from each tank depends on its current liquid level as $F_1 = 1.6971\sqrt{h_1}$ and $F_2 = 1.6971\sqrt{h_2}$. The system is modelled as (28-29):

$$\frac{dh_1}{dt} = -\frac{1.6971\sqrt{h_1}}{\pi h_1 - \pi h_1^2} + \frac{F_i}{\pi h_1 - \pi h_1^2}$$
 (28)

$$\frac{dh_2}{dt} = \frac{1.6971\sqrt{h_1}}{\pi h_2 - \pi h_2^2} - \frac{1.6971\sqrt{h_2}}{\pi h_2 - \pi h_2^2}$$
 (29)

where h_1 is a liquid level of tank 1, h_2 is a liquid level in tank 2 and F_i is an inlet flow rate.

 $\bar{h}_1 = h_1 - h_{1,eq}$, $\bar{h}_2 = h_2 - h_{2,eq}$ and $\bar{F}_i = F_i - F_{i,eq}$ are defined. Subscript eq denotes a corresponding variable at equilibrium condition, $h_{1,eq} = 50$ cm, $h_{2,eq} = 50$ cm, and $F_{i,eq} = 1.2$ m³/hr.

The objective is to regulate \bar{h}_1 and \bar{h}_2 to the origin by manipulating \bar{F}_i . An input constraint of $-0.5 \leq \bar{F}_i \leq 0.5$ m³/hr is symmetric. In addition, output constraints of $-0.45 \leq \bar{h}_1 \leq 0.45$ and $-0.45 \leq \bar{h}_2 \leq 0.45$ are also symmetric. It was assumed that the maximum values of following terms including $1.6971/(\pi h_1^{1.5} - \pi h_1^{2.5}) -1.6971/(\pi h_{1,eq}^{1.5} - \pi h_{1,eq}^{2.5})$, $1/(\pi h_1 - \pi h_1^2) -1/(\pi h_{1,eq} - \pi h_{1,eq}^2)$, $1.6971/(\pi h_1^{0.5} (\pi h_2 - \pi h_2^2) -1.6971/(\pi h_{1,eq}^{0.5} (\pi h_{2,eq} - \pi h_{2,eq}^2))$ and $1.6971/(\pi h_2^{0.5} - \pi h_2^{0.5}) -1.6971/(\pi h_2^{0.5} - \pi h_2^{0.5})$ are small enough to be neglected. Thus, the system can be described in terms of deviation variables as in (30-31):

$$\frac{d\bar{h}_1}{dt} = -\frac{1.6971}{\pi h_1^{1.5} - \pi h_1^{2.5}} \bar{h}_1 + \frac{1}{\pi h_1 - \pi h_1^2} \bar{F}_i \tag{30}$$

$$\frac{d\bar{h}_2}{dt} = \frac{1.6971}{\pi h_2 h_1^{0.5} - \pi h_2^2 h_1^{0.5}} \bar{h}_1 - \frac{1.6971}{\pi h_2^{1.5} - \pi h_2^{2.5}} \bar{h}_2.$$
(31)

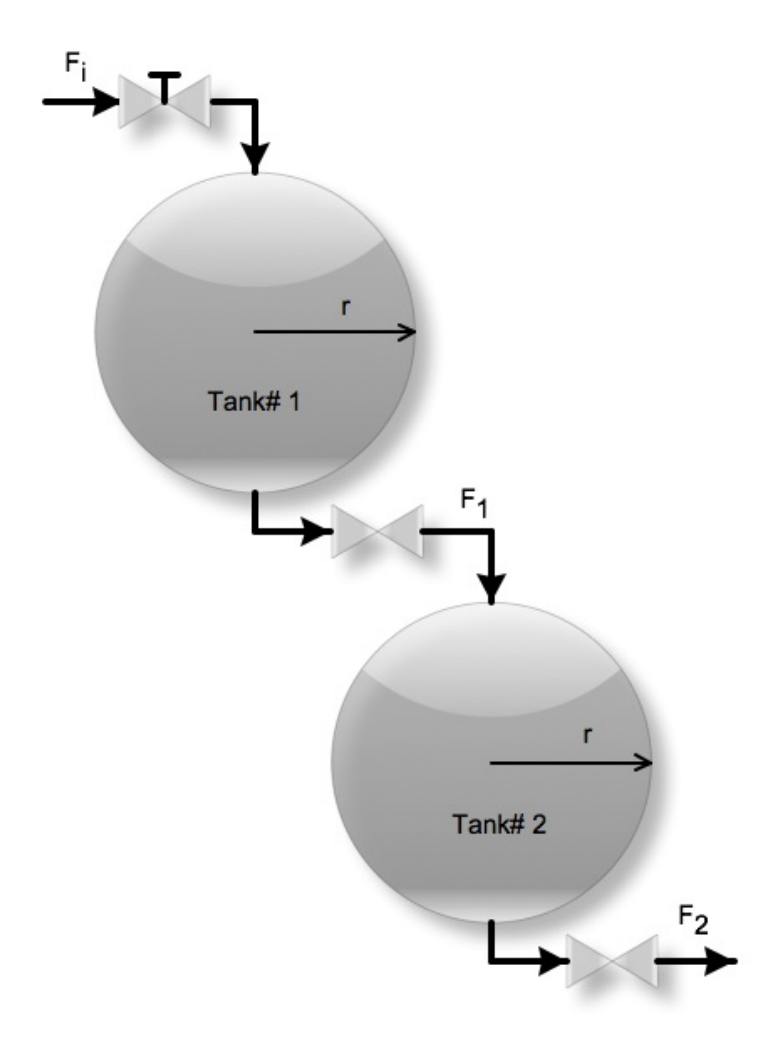


Figure 1: Two-tank system considered in case study 1.

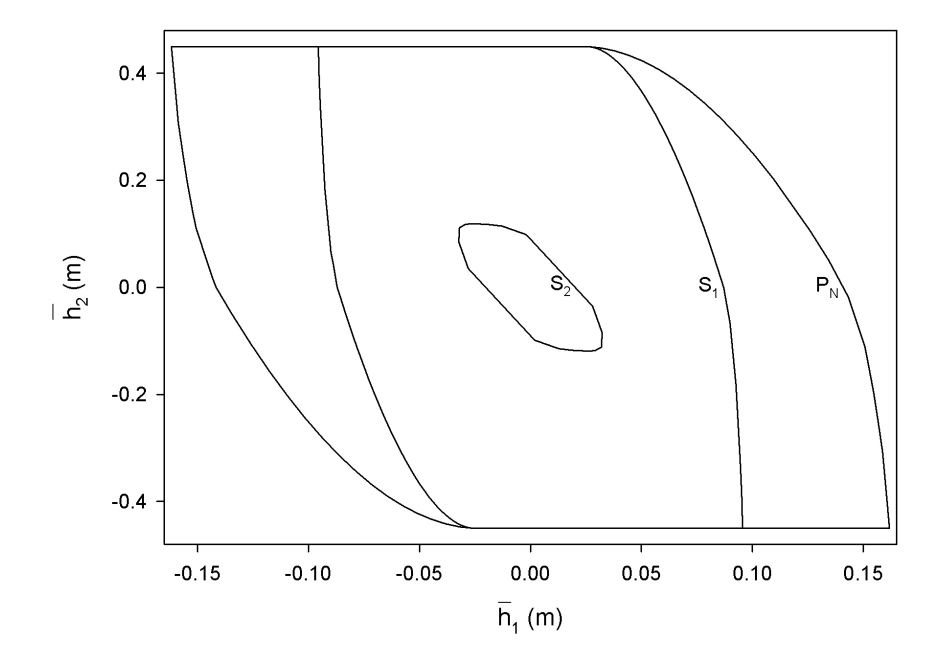


Figure 2: Invariant sets generated in case study 1.

By rearranging (30-31) all 16 vertices of the uncertainty polytope, the system is represented by the following differential inclusion:

$$\begin{bmatrix} \bar{h}_1 \\ \bar{h}_2 \end{bmatrix} \in \sum_{l=1}^{16} \lambda_l (A_l \begin{bmatrix} \bar{h}_1 \\ \bar{h}_2 \end{bmatrix} + B_l \bar{F}_i)$$
 (32)

where $\sum_{l=1}^{16} \lambda_l = 1$, and $0 \le \lambda_l \le 1$.

A discrete-time model is obtained by discretisation of (32) using Euler first-order approximation with a sampling period of 30 s. The said model is omitted here for brevity. Tuning parameters are $\Theta = [[0,0],[0,1]]^T$ and R = 0.01.

States of $[\bar{h}_1, \bar{h}_2]^T = [0.45, 0.45]^T$ and $[0.01, 0.01]^T$ were used to generate feedback gains and to construct polyhedral invariant sets $(S_1 \text{ and } S_2)$ using the algorithms described previously. Figure 2 shows the polyhedral invariant sets constructed. An initial state $x \in S_1$ can be stabilized by off-line RMPC (Bumroongsri & Kheawhom, 2012c) as well as the algorithms proposed. P_N is a maximal robustly controlled invariant set projected from S_2 . An initial state $x \in P_N$ can be stabilized by interpolated vertex control (Nguyen et al., 2013). This algorithm provided the largest stabilisable region.

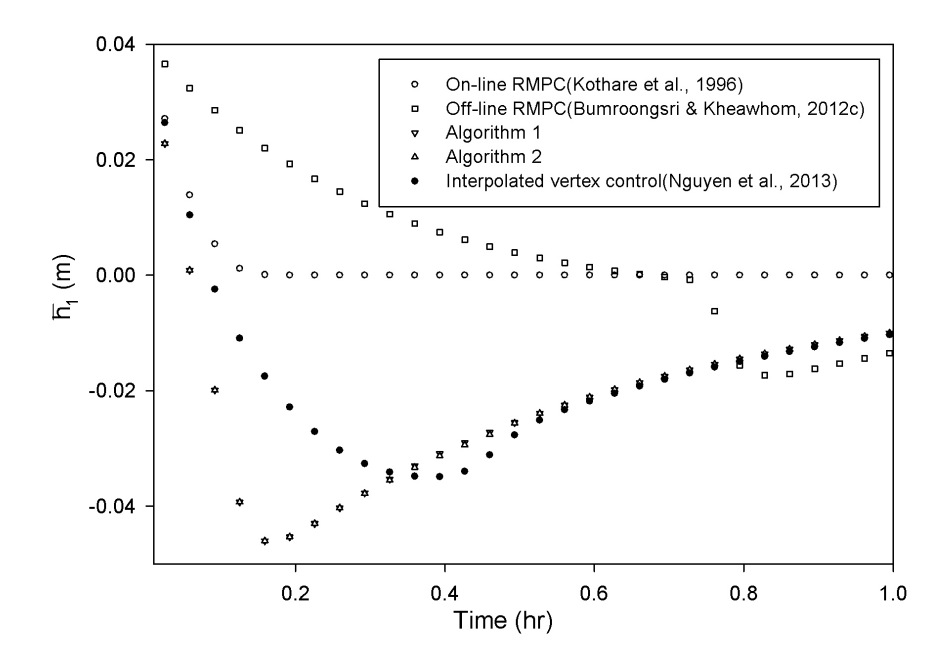


Figure 3: Regulated state (\bar{h}_1) profiles for case study 1.

The system was regulated from an initial state of $[\bar{h}_1, \bar{h}_2]^T = [0.04, 0.3]^T$ to the origin. The chosen initial state belongs to the stabilisable region of all algorithms. Profiles of regulated state $(\bar{h}_1 \text{ and } \bar{h}_2)$ are shown in Figs. 3 and 4. All algorithms could drive the initial state to the origin without violation of input and state constraints. As the tuning parameters of $\Theta = [[0,0],[0,1]]^T$ and R = 0.01 are concerned, only control input \bar{F}_i and state \bar{h}_2 contributed to the performance cost. The settling times of on-line RMPC (Kothare et al., 1996) and off-line RMPC (Bumroongsri & Kheawhom, 2012c) were about 2.0 hrs. In comparison, the proposed algorithms could drive the system to the origin in about 1.2 hrs. which is faster than on-line RMPC (Kothare et al., 1996) and off-line RMPC (Bumroongsri & Kheawhom, 2012c). Interpolated vertex control (Nguyen et al., 2013) is faster than on-line RMPC (Kothare et al., 1996) and off-line RMPC (Bumroongsri & Kheawhom, 2012c) but slightly slower than the proposed algorithms.

Figure 5 shows control input \bar{F}_i profiles. A spiking effect of control input was noticed in off-line RMPC (Bumroongsri & Kheawhom, 2012c). The spiking effect is caused by the switching of the feedback control law. Algorithms 1 and 2 produced similar responses and control input \bar{F}_i profiles. The control input profiles of Algorithm 1 and 2 saturated between 0 to to 0.15 hr. Control input saturation was then repealed when states move closer to the origin. In on-

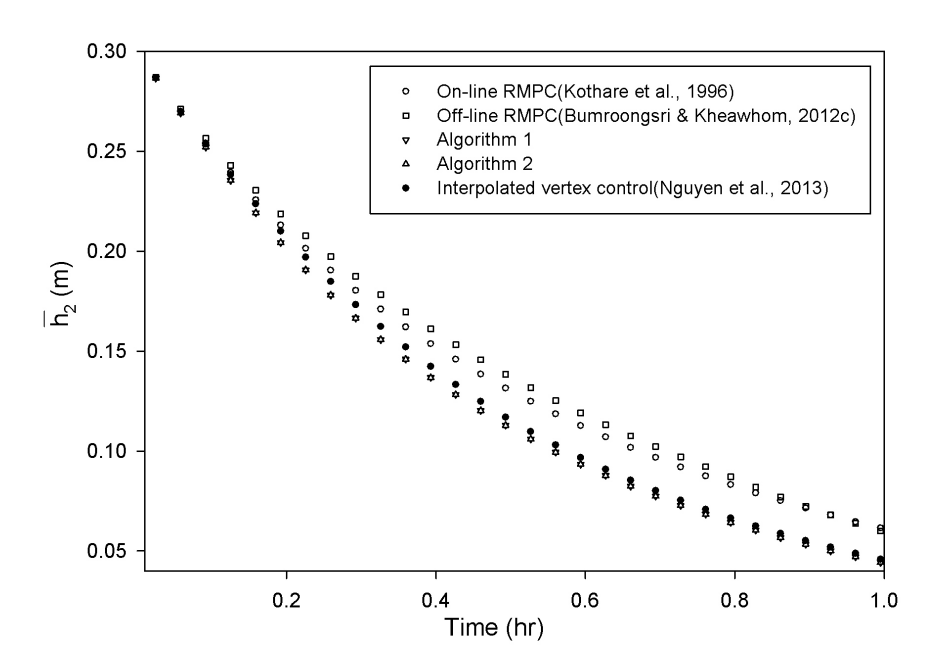


Figure 4: Regulated state (\bar{h}_2) profiles for case study 1.

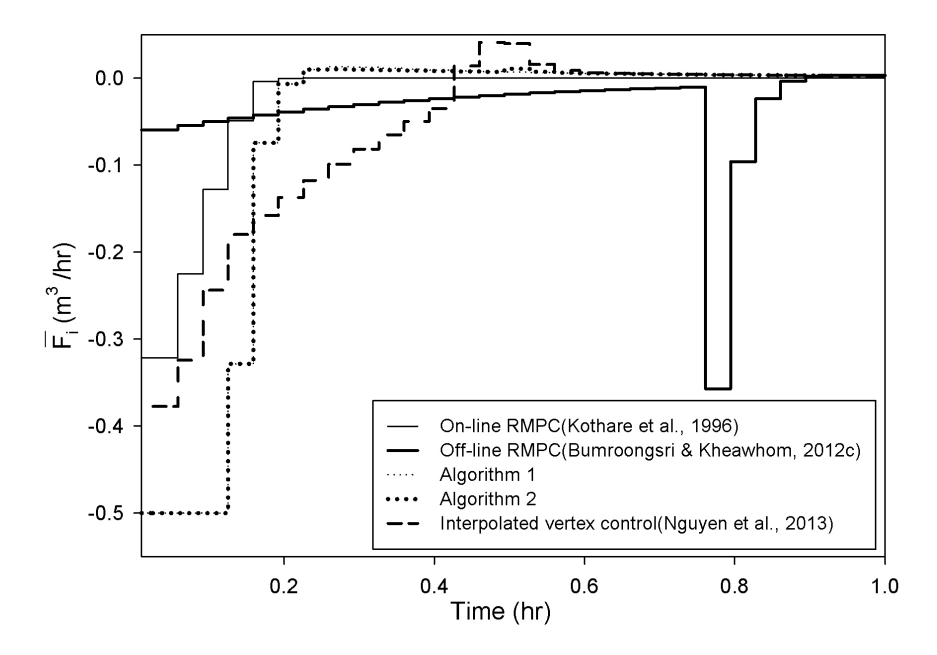


Figure 5: Control input \bar{F}_i profiles for case study 1.

line RMPC (Kothare et al., 1996), off-line RMPC (Bumroongsri & Kheawhom, 2012c) and interpolated vertex control (Nguyen et al., 2013), control input saturation was not observed.

Figure 6 shows the cumulative performance cost. Control performance of on-line RMPC (Kothare et al., 1996) was better than that of off-line RMPC (Bumroongsri & Kheawhom, 2012c) because on-line RMPC solves the optimisation problem on-line and updates a feedback gain more frequently. Both on-line RMPC (Kothare et al., 1996) and off-line RMPC (Bumroongsri & Kheawhom, 2012c) obtain a feedback gain based on the assumption that the feedback gain remains constant throughout an infinite horizon. Saturation at one step in the horizon requires a small gain for all steps in the horizon. Thus, control performance deteriorates when input saturation occurs. Implementation of interpolation algorithms proposed can improve control performance. Though the proposed algorithms are also derived based on a constant feedback gain assumption, at each sampling time, the proposed algorithms obtain a variable feedback gain by solving a simple optimisation problem. Therefore, the proposed algorithms provided better control performance than on-line RMPC (Kothare et al., 1996) and off-line RMPC (Bumroongsri & Kheawhom, 2012c). Control performance of interpolated vertex control (Nguyen et al., 2013) was also better than that of on-line RMPC (Kothare et al., 1996) and off-line RMPC (Bumroongsri & Kheawhom, 2012c). However, control performance of interpolated

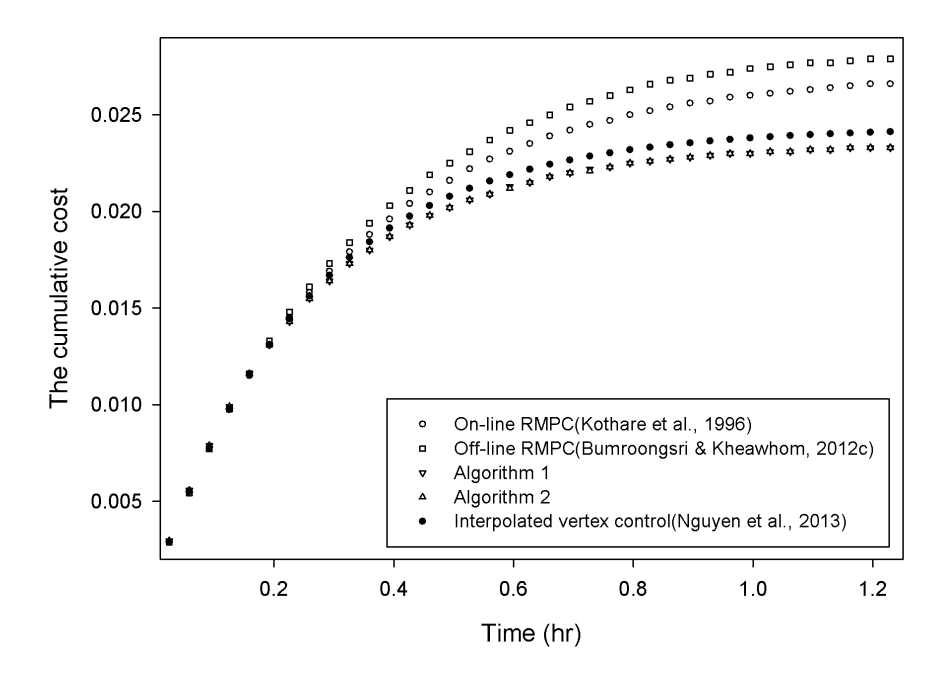


Figure 6: Cumulative cost for case study 1.

vertex control (Nguyen et al., 2013) was slightly lower than that of the proposed algorithms.

Table 1 shows the on-line computational cost of each algorithm. For all off-line RMPC algorithms, most computational burdens are moved off-line so on-line computation is tractable. Off-line RMPC(Bumroongsri & Kheawhom, 2012c) does not solve optimisation problems on-line. Thus, this algorithm is very fast. An optimisation problem involved in both Algorithms 1 and 2 is linear programming and the number of constraints involved is linearly dependent on the number of vertices of the uncertain polytope and size of the polyhedral invariant sets involved. The number of constraints involved in Algorithm 1 is smaller than that of Algorithm 2. The online computational time of interpolation vertex control (Nguyen et al., 2013) was comparable with the proposed algorithms. At each sampling time, this algorithm requires solving linear programming problems on variable decomposition as well as vertex control action.

Four-tank system

In this case study, simulation of a four-tank system which is similar to the system considered in Johansson (2000) was considered. A schematic diagram of

Table 1: On-line computational time required in case study 1.

| Algorithm | On-line computational time |
|--|----------------------------|
| On-line RMPC(Kothare et al., 1996) | 2.232 s |
| Off-line RMPC(Bumroongsri & Kheawhom, 2012c) | < 0.001 s |
| Algorithm 1 | 0.004 s |
| Algorithm 2 | $0.005~\mathrm{s}$ |
| Interpolated vertex control(Nguyen et al., 2013) | $0.007 \mathrm{\ s}$ |

this system is shown in Fig. 7. The system is described by (33-36):

$$\frac{dh_1}{dt} = -5.91\sqrt{h_1} + 5.91\sqrt{h_3} + 0.74F_1 \tag{33}$$

$$\frac{dh_2}{dt} = -5.91\sqrt{h_2} + 5.91\sqrt{h_4} + 0.74F_2 \tag{34}$$

$$\frac{dh_1}{dt} = -5.91\sqrt{h_1} + 5.91\sqrt{h_3} + 0.74F_1$$

$$\frac{dh_2}{dt} = -5.91\sqrt{h_2} + 5.91\sqrt{h_4} + 0.74F_2$$

$$\frac{dh_3}{dt} = -5.91\sqrt{h_3} + 1.73F_2$$
(35)

$$\frac{dh_4}{dt} = -5.91\sqrt{h_4} + 1.73F_1 \tag{36}$$

where h_i is a liquid level of tank i, i = 1, 2, 3, 4, and F_1 and F_2 are inlet flow rates.

Let $h_i = h_i - h_{i,eq}$, i = 1, 2, 3, 4 and $\bar{F}_i = F_i - F_{i,eq}$, i = 1, 2. Subscript eq denotes a corresponding variable at equilibrium condition, $h_{1,eq} = 14.98$ cm; $h_{2,eq} = 14.98$ cm; $h_{3,eq} = 7.34$ cm; $h_{4,eq} = 7.34$ cm and $F_{i,eq} = 9.25$ m³/hr, i = 1, 2.

The objective is to regulate \bar{h}_i , i = 1, 2, 3, 4 to the origin by manipulating \bar{F}_1 and \bar{F}_2 . The input constraints of $-9.25 \leq \bar{F}_1 \leq 9.25$ m³/hr and $-9.25 \le F_2 \le 9.25 \text{ m}^3/\text{hr}$ are symmetric. In contrast, output constraints of $-13.98 \le \bar{h}_1 \le 35.02 \text{ cm}, -13.98 \le \bar{h}_2 \le 35.02 \text{ cm}, -6.34 \le \bar{h}_3 \le 42.66 \text{ cm},$ and $-6.34 \le \bar{h}_4 \le 42.66$ cm are asymmetric.

By rewriting (33-36) in deviation form and rearranging all uncertain vertices, the system is written in differential inclusion form as follows:

$$[\dot{\bar{h}}_1, \dot{\bar{h}}_2, \dot{\bar{h}}_3, \dot{\bar{h}}_4]^T \in \sum_{l=1}^{16} \lambda_l [A_l[\bar{h}_1, \bar{h}_2, \bar{h}_3, \bar{h}_4]^T + B_l[\bar{F}_1, \bar{F}_2]^T]. \tag{37}$$

A discrete-time model is obtained by discretisation of (37) using Euler firstorder approximation with a sampling period of 0.1 min. The said model is omitted here for brevity. Tuning parameters are $R = [[0.01, 0], [0, 0.01]]^T$ and $\Theta = [[1,0,0,0],[0,1,0,0],[0,0,0,0],[0,0,0,0]]^T$. It should be noted that only

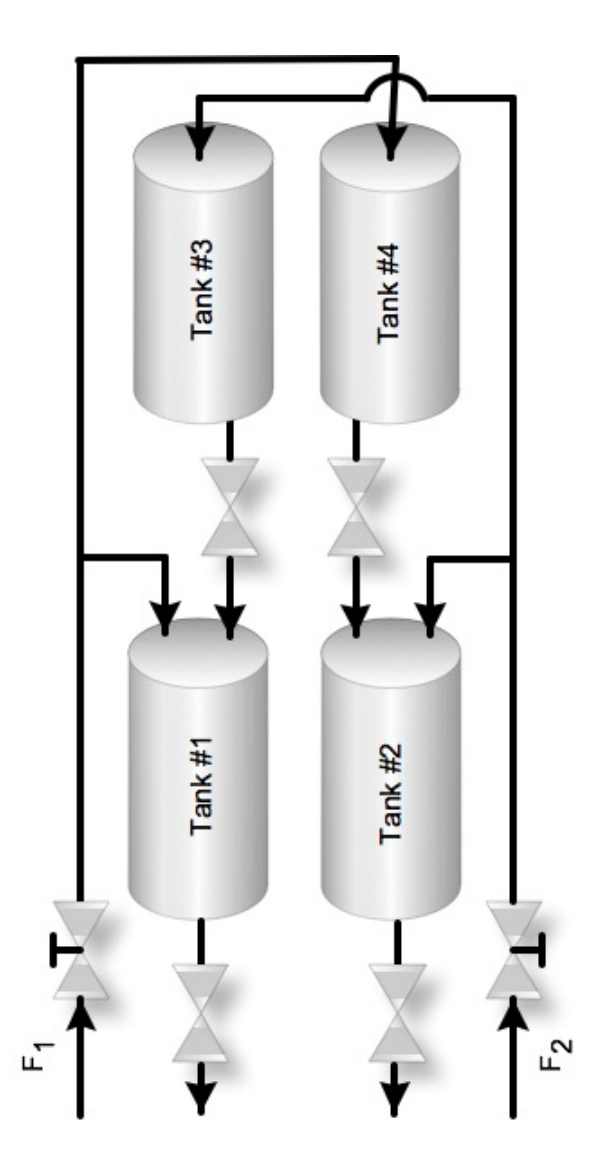


Figure 7: Four-tank system considered in case study 2.

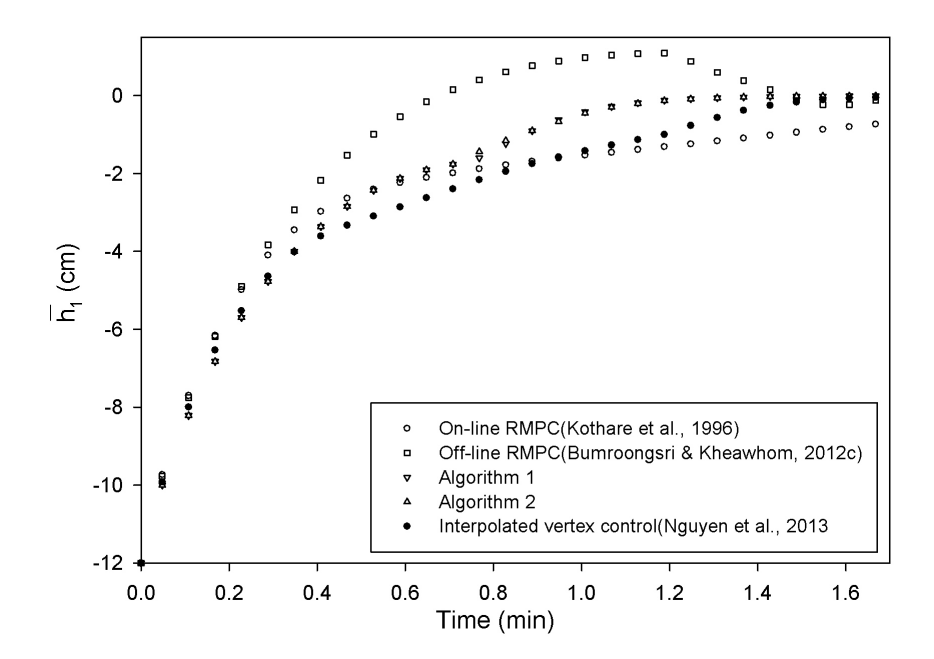


Figure 8: Regulated state (\bar{h}_1) profiles for case study 2.

states \bar{h}_1 and \bar{h}_2 and control inputs \bar{F}_1 and \bar{F}_2 contributed to the performance cost.

A sequence of six polyhedral invariant sets with associated feedback gains were generated by using the following states, $[13.5, 13.5, 6.3, 6.3]^T$, $[4.0, 4.0, 2.0, 2.0]^T$, $[2.5, 2.5, 1.0, 1.0]^T$, $[1.0, 1.0, 0.5, 0.5]^T$, $[0.2, 0.2, 0.1, 0.1]^T$ and $[0.05, 0.05, 0.01, 0.01]^T$. A maximal robustly controlled invariant set projected from the innermost invariant set was also constructed for interpolated vertex control (Nguyen et al., 2013). Interpolated vertex control (Nguyen et al., 2013) provided the largest stabilisable region. The system was regulated from an initial state of $[\bar{h}_1, \bar{h}_2, \bar{h}_3, \bar{h}_4]^T = [-12.0, 12.0, 10.0, 10.0]^T$ that belongs to the stabilisable region of all algorithms, to the origin.

Figures 8 and 9 show profiles of regulated states \bar{h}_1 and \bar{h}_2 , respectively. Figures 10 and 11 show profiles of control inputs \bar{F}_1 and \bar{F}_2 , respectively. All algorithms could drive the initial state to the origin without violation of input and state constraints. The settling times of on-line RMPC (Kothare et al., 1996) and off-line RMPC (Bumroongsri & Kheawhom, 2012c) were about 4.0 mins. In comparison, the proposed algorithms could drive the system to the origin in about 1.8 mins. On-line RMPC(Kothare et al., 1996) and off-line RMPC (Bumroongsri & Kheawhom, 2012c) provided slower responses than in-

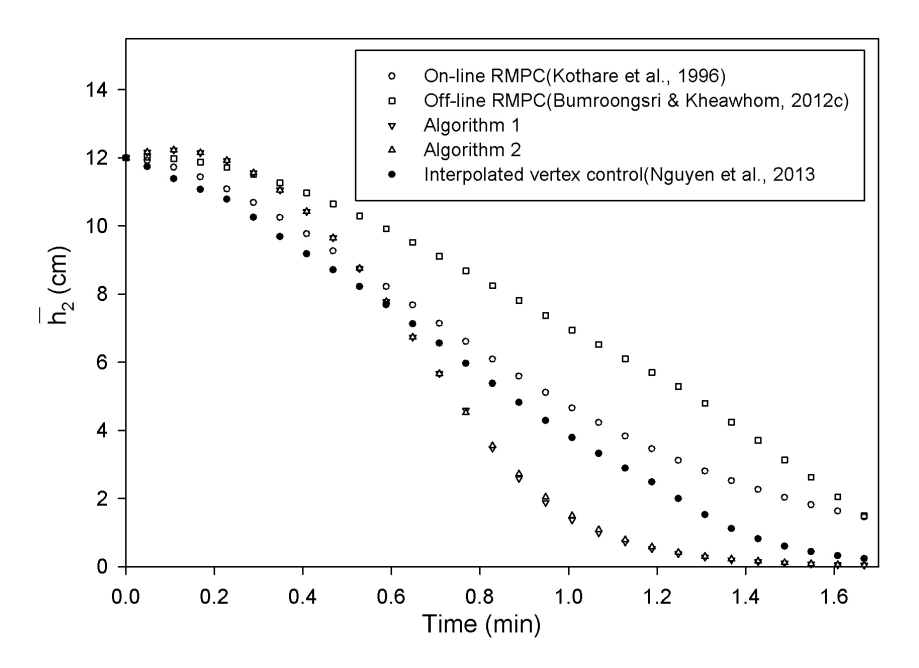


Figure 9: Regulated state (\bar{h}_2) profiles for case study 2.

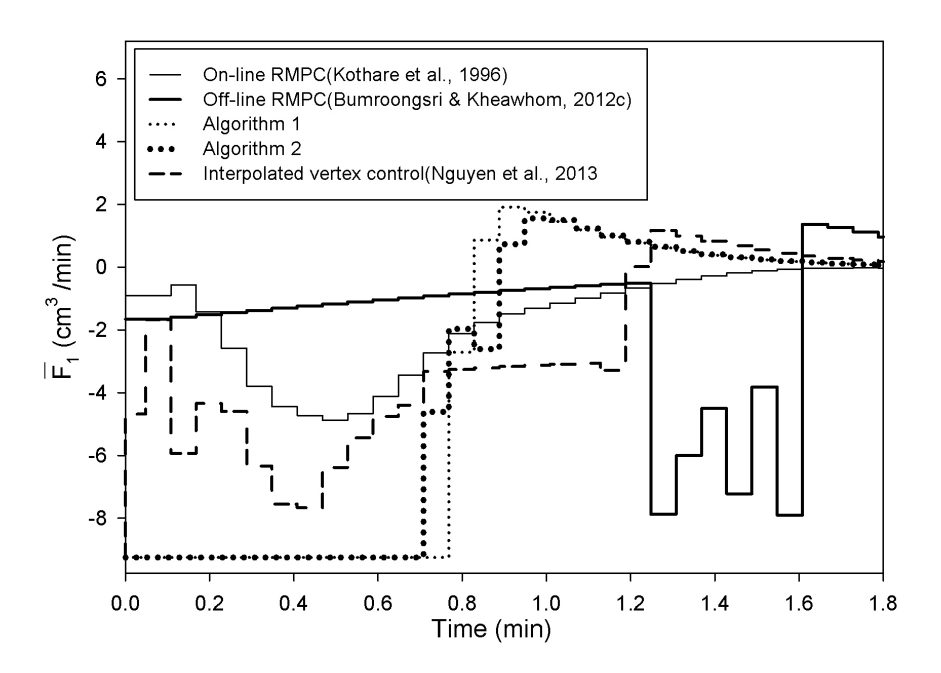


Figure 10: Control input \bar{F}_1 profiles for case study 2.

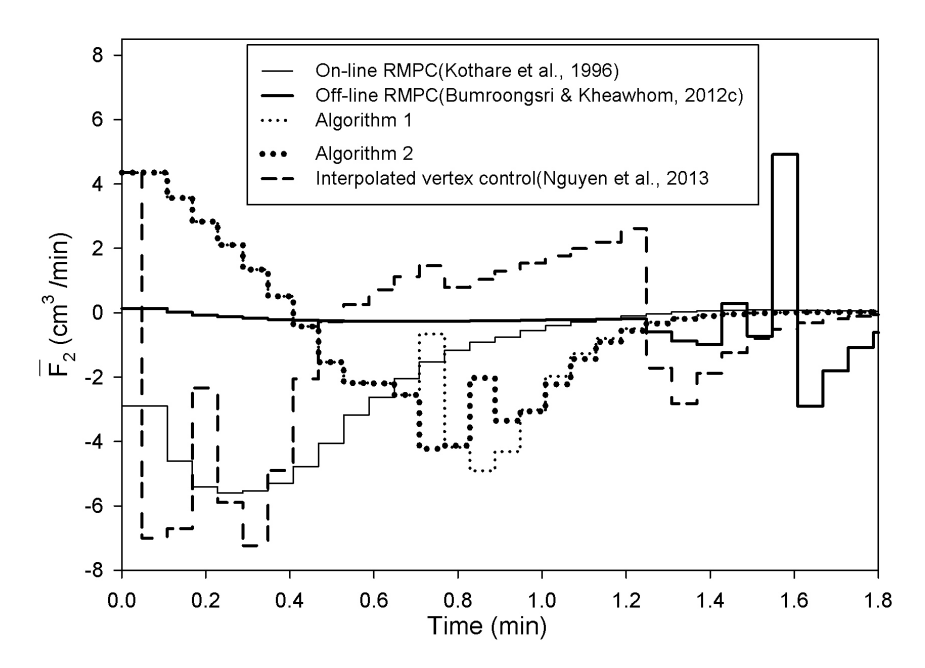


Figure 11: Control input \bar{F}_2 profiles for case study 2.

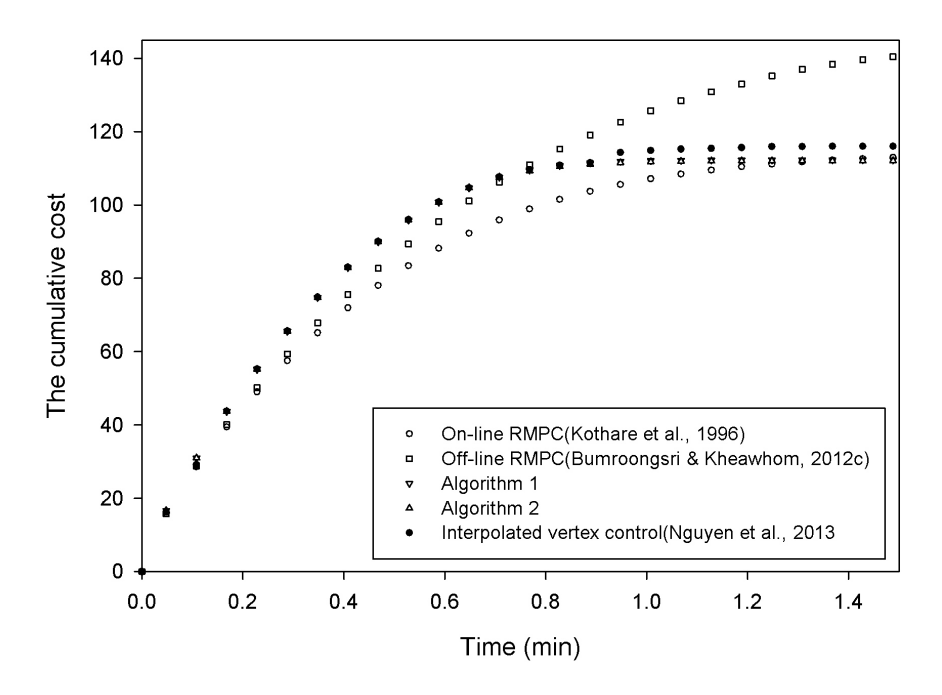


Figure 12: Cumulative cost for case study 2.

terpolated vertex control (Nguyen et al., 2013) and the proposed algorithms. Interpolated vertex control (Nguyen et al., 2013) is slightly slower than the proposed algorithms. Both Algorithms 1 and 2 produced similar responses. There was a difference between Algorithm 1 and Algorithm 2 in control input \bar{F}_1 and \bar{F}_2 profiles. Saturation of control input \bar{F}_1 was observed in Algorithms 1 and 2 from 0 to 0.75 min. A spiking effect of control input which is caused by the switching of feedback control gains, was noticed in off-line RMPC (Bumroongsri & Kheawhom, 2012c).

Figure 12 shows the cumulative performance cost. The cumulative cost of Algorithms 1 and 2 were lower than those of on-line RMPC(Kothare et al., 1996), off-line RMPC(Bumroongsri & Kheawhom, 2012c) and interpolated vertex control (Nguyen et al., 2013). Control performance of Algorithm 1 was slightly better than that of Algorithm 2.

Table 2 shows the on-line computational cost of each algorithm. Although, on-line computational time of Algorithms 1 and 2 were higher than that of off-line RMPC(Bumroongsri & Kheawhom, 2012c), the proposed algorithms were much faster than on-line RMPC(Kothare et al., 1996). The online computational time of interpolation vertex control (Nguyen et al., 2013) was comparable with the proposed algorithms. Computational times required in this case study

Table 2: On-line computational time required in case study 2.

| Algorithm | On-line computational time |
|--|----------------------------|
| On-line RMPC(Kothare et al., 1996) | 14.639 s |
| Off-line RMPC(Bumroongsri & Kheawhom, 2012c) | < 0.001 s |
| Algorithm 1 | $0.012 \; \mathrm{s}$ |
| Algorithm 2 | $0.018 \; \mathrm{s}$ |
| Interpolated vertex control(Nguyen et al., 2013) | $0.024 \mathrm{\ s}$ |

were larger than those of case study 1 because the number of vertices of the uncertain polytope and the size of the polyhedral invariant set involved in case study 2 were larger than those of case study 1.

Conclusion

In this paper, implementation of interpolation algorithms on RMPC of polytopic uncertain discrete-time systems was studied. Control algorithms employed an off-line solution of an optimal control optimisation problem to determine a feedback gain. A sequence of nested polyhedral invariant sets associated with each feedback gain pre-computed was constructed. At each sampling time, the smallest invariant set which contained the current state was identified. If the current invariant set is the innermost set, the pre-computed feedback gain associated with the innermost set is applied to the process. If otherwise, a feedback gain is variable and determined by linear interpolation which is a convex combination of the pre-computed feedback gains associated with the current invariant set and the adjacent smaller invariant set. Two interpolation algorithms were proposed. Further, two case studies were used to illustrate the applicability of the algorithms proposed. An optimisation problem involved in the proposed algorithms was linear programming, and the number of constraints involved was linearly dependent on the number of vertices of the uncertain polytope and the size of the polyhedral invariant set involved. The number of constraints involved in Algorithm 1 was smaller than that of Algorithm 2. The simulation results showed that the proposed algorithms yielded better control performance than existing RMPC algorithms while on-line computation was still tractable.

Future perspective

In this work, the interpolation based control algorithms was designed for a linear system because of two reasons. First, computation of an invariant set for a linear system is much more easy than that of a non-linear system. Second, for the recursive feasibility and asymptotic stability proof of the interpolation based control scheme, the linearity of the system and the convexity of the feasible region shows important advantages.

For the class of nonlinear models, the analysis and control design is significantly more difficult. There is no constructive procedure for computing the feasible invariant sets for non-linear systems. In addition, these sets are generally non-convex. Though, the interpolation principle is held, the practical computation of the level sets and the associated vertex control will not be straightforward. If the linear assumptions are relaxed but a certain structure is preserved, an invariant set for a certain class of homogeneous non-linear system can be efficiently computed.

References

Angeli, D., Casavola, A., Franzé, G. & Mosca, E. (2008) An ellipsoidal off-line MPC scheme for uncertain polytopic discrete-time systems. *Automatica*, **44**, 3113–3119.

- Bemporad, A., Borrelli, F. & Morari, M. (2003) Minmax control of constrained uncertain discrete-time linear systems. *IEEE Transactions on Automatic Control*, **48**, 1600–1606.
- Bumroongsri, P. & Kheawhom, S. (2012a) An ellipsoidal off-line model predictive control strategy for linear parameter varying systems with applications in chemical processes. *Syst. Control Lett.*, **61**, 435–442.
- Bumroongsri, P. & Kheawhom, S. (2012b) MPC for LPV systems based on parameter-dependent Lyapunov function with perturbation on control input strategy. *Engineering Journal*, **16**, 61–72.
- Bumroongsri, P. & Kheawhom, S. (2012c) An off-line robust MPC algorithm for uncertain polytopic discrete-time systems using polyhedral invariant sets. J. Process Contr., 22, 975–983.
- Bumroongsri, P. & Kheawhom, S. (2013) An Interpolation-based Robust MPC Algorithm Using Polyhedral Invariant sets. In *Proceedings of the 2013 European Control Conference (ECC)*, pages 3161–3166.
- Casavola, A., Famularo, D. & Franzé, G. (2002) A feedback min-max MPC algorithm for LPV systems subject to bounded rates of change of parameters. *IEEE T. Automat. Contr.*, **47**, 1147–1152.
- Cuzzola, F., Geromel, J. & Morari, M. (2002) An improved approach for constrained robust model predictive control. *Automatica*, **38**, 1183–1189.
- Ding, B., Xi, Y., Cychowski, M. & O'Mahony, T. (2007) Improving off-line approach to robust MPC based-on nominal performance cost. *Automatica*, 43, 158–163.
- Dlapa, M. (2007) Decoupled Control of Two Tank System via Algebraic μ-Synthesis. In *Proceedings of the 15th Mediterranean Conference on Control and Automation*.
- He, D., Huang, H. & Chen, Q. (2014) Stabilizing model predictive control of time-varying non-linear systems using linear matrix inequalities. *IMA Journal of Mathematical Control and Information*, pages 1–15.
- Johansson, K. (2000) The Quadruple-Tank Process: A Multivariable Laboratory Process with an Adjustable Zero. *IEEE Transactions on Control Systems Technology*, **8**, 456–465.
- Kothare, M., Balakrishnan, V. & Morari, M. (1996) Robust constrained model predictive control using linear matrix inequalities. *Automatica*, **32**, 1361–1379.
- Kouvaritakis, B., Rossiter, J. & Schuurmans, J. (2000) Efficient robust predictive control. *IEEE Transactions on Automatic Control*, **45**, 1545–1549.
- Lee, Y. & Kouvaritakis, B. (2002) Superposition in efficient robust constrained predictive control. *Automatica*, **38**, 875–878.

- Li, D. & Xi, Y. (2011) Constrained feedback robust model predictive control for polytopic uncertain systems with time delays. *International Journal of Systems Science*, **42**, 1651–1660.
- Löfberg, J. (2004) YALMIP: A toolbox for modeling and optimization in MAT-LAB. In *Proc. IEEE international symposium on computer aided control systems design*, pages 284–289.
- Mao, W. (2003) Robust stabilization of uncertain time-varying discrete systems and comments on "an improved approach for constrained robust model predictive control". *Automatica*, **39**, 1109–1112.
- Nguyen, H., Gutman, P., Olaru, S. & Hovd, M. (2013) Implicit improved vertex control for uncertain, time-varying linear discrete-time systems with state and control constraints. *Automatica*, **49**, 2754–2759.
- Nguyen, H., Olaru, S. & Hovd, M. (2012) A patchy approximation of explicit model predictive control. *Int. J. Control*, **85**, 1929–1941.
- Pluymers, P., Rossiter, J., Suykens, J. & Moore, B. (2005a) The efficient computation of polyhedral invariant sets for linear systems with polytopic uncertainty. In *Proc. of the American Control Conference*, pages 804–809.
- Pluymers, P., Rossiter, J., Suykens, J. & Moore, B. (2005b) Interpolation Based MPC for LPV Systems using Polyhedral Invariant Sets. In *Proc. of the American Control Conference*, pages 810–815.
- Qin, S. & Badgwell, T. (2003) A survey of industrial model predictive control technology. *Control Engineering Practice*, **11**, 733–764.
- Rossiter, J., Kouvaritakis, B. & Bacic, M. (2004) Interpolation based computationally efficient predictive control. *Int. J. Control*, **77**, 290–301.
- Schuurmans, J. & Rossiter, J. (2000) Robust predictive control using tight sets of predicted states. *IEE P.-Contr. Theor. Ap.*, **147**, 13–18.
- Tütüncü, R., Toh, K. & Todd, M. (2003) Solving semidefinite-quadratic-linear programs using SDPT3. *Math. Prog. Series B*, **95**, 189–217.
- Veselý, V., Rosinová, D. & Foltin, M. (2010) Robust model predictive control design with input constraints. *ISA Transactions*, **49**, 114–120.
- Wada, N., Saito, K. & Saeki, M. (2006) Model predictive control for linear parameter varying systems using parameter dependent lyapunov function. *IEEE T. Circuits Syst.*, 53, 1446–1450.
- Wan, Z. & Kothare, M. (2003) An efficient off-line formulation of robust model predictive control using linear matrix inequalities. *Automatica*, **39**, 837–846.
- Wang, C. (2012) Robust model predictive control by iterative optimisation for polytopic uncertain systems. *International Journal of Systems Science*, **43**, 1656–1663.

Publication list

- 1. Kheawhom, S., Bumroongsri, P., Interpolation techniques for robust constrained model predictive control based on polyhedral invariant set, 2016, IMA Journal of Mathematical Control and Information, DOI: 10.1093/imamci/dnv057, in press. [IF=0.75]
- 2. Bumroongsri, P., Kheawhom, S., An off-Line Formulation of Tube-Based Robust MPC Using Polyhedral Invariant Sets, 2016, Chemical Engineering Communications, 203, 6, 736-745.

 [IF=1.104]
- 3. Srirachat, W., Wongsawa, T., Sunsandee, N., Pancharoen, U., Kheawhom, S., Phase equilibrium for ternary liquid systems of water + di-(2-ethylhexyl)phosphoric acid + organic diluents: Thermodynamic study, 2015, Fluid Phase Equilibria, 401, 34-47. [IF=2.241]
- 4. Kheawhom, S., Bumroongsri, P. Modeling of a small-scale biomass updraft gasifier, 2014, Chemical Engineering Transactions, 37, 217-222. [SCOPUS]
- 5. Bumroongsri, P., Kheawhom, S. Interpolation-based off-line robust MPC for uncertain polytopic discrete-time systems, 2014, Engineering Journal, 18, 1, 87-104. [SCOPUS]
- 6. Kheawhom, S., Bumroongsri, P. Robust distributed framework of interpolation-based control for polytopic uncertain systems, 19th International Conference on Methods and Models in Automation and Robotics, MMAR 2014, Miedzyzdroje, Poland, 2-5 September 2014. [SCOPUS]
- 7. Kheawhom, S., Bumroongsri, P. Interpolation-based robust constrained model predictive output feedback control, 22nd Mediterranean Conference on Control and Automation, MED 2014; University of Palermo, Palermo, Italy, 16-19 June 2014. [SCOPUS]
- 8. Kheawhom, S., Bumroongsri, P. Robust MPC based on polyhedral invariant sets for LPV systems, 2013, IFAC Proceedings Volumes (IFAC-PapersOnline), 10, 355-360. [SCOPUS]
- 9. Bumroongsri, P., Kheawhom, S. Interpolation-based Off-line MPC for LPV systems, 2013, IFAC Proceedings Volumes (IFAC-PapersOnline), 10, 81-86. [SCOPUS]

IMA Journal of Mathematical Control and Information (2015) Page 1 of 19 doi:10.1093/imamci/dnv057

Interpolation techniques for robust constrained model predictive control based on polyhedral invariant set

SOORATHEP KHEAWHOM*

Computational Process Engineering, Department of Chemical Engineering, Faculty of Engineering, Chulalongkorn University, Bangkok 10330, Thailand *Corresponding author. Email: soorathep.k@chula.ac.th

AND

PORNCHAI BUMROONGSRI

Department of Chemical Engineering, Faculty of Engineering, Mahidol University, Nakhon Pathom 73170, Thailand

[Received on 19 May 2015; revised on 6 August 2015; accepted on 19 September 2015]

This work studies interpolation techniques that can be employed on off-line robust constrained model predictive control (MPC) for a discrete time-varying system with polytopic parametric uncertainty. A sequence of feedback gains is determined by solving off-line a series of optimal control optimization problems. A sequence of nested corresponding polyhedral invariant set is then constructed. At each sampling time, the smallest invariant set containing the current state is determined. If the current invariant set is the innermost set, the pre-computed gain associated with the innermost set is applied. If otherwise, a feedback gain is variable and determined by a linear interpolation of the pre-computed gains. Two interpolation algorithms are investigated. The proposed algorithms are illustrated with case studies of a two-tank system and a four-tank system. The simulation results showed that the proposed interpolation techniques can improve control performance of off-line robust MPC while on-line computation is still tractable.

Keywords: discrete-time polytopic uncertain system; polyhedral invariant set; robust model predictive control; interpolation-based control.

1. Introduction

Model predictive control (MPC) is recognized as an advanced control algorithm which can effectively handle multiple input multiple output processes with constraints (Qin & Badgwell, 2003). Traditionally, MPC is derived by using a linear time invariant (LTI) model. At each sampling time, the algorithm uses an explicit LTI model to solve an optimal control problem, and implements the first element of the optimal input sequence computed. However, the behaviour of real process usually deviates from the linear model used in controller synthesis. A discrepancy between the behaviour of the process and that of the model used leads to deterioration of control performance. Thus, a conventional linear MPC based on an LTI model is often unsuitable to deal with a non-linear system or a system containing uncertainty.

Robust MPC (RMPC) has been introduced to guarantee robustness as well as constraint satisfaction against uncertainty. At each sampling time, a feedback gain that can robustly stabilize the closed-loop system is determined by solving an optimal control problem (Kothare *et al.*, 1996; Kouvaritakis *et al.*,

2000; Schuurmans & Rossiter, 2000; Lee & Kouvaritakis, 2002; Bemporad *et al.*, 2003; Veselý *et al.*, 2010; Li & Xi, 2011; Wang, 2012; He *et al.*, 2014).

In Kothare *et al.* (1996), the optimization problem involved is formulated as minimization of the worst-case performance cost subjected to input, output and stability criteria constraints. The stability criteria constraint is derived based on a single Lyapunov function. An ellipsoidal invariant set containing the current state is constructed to guarantee robust stability. Any states in the invariant set can be driven to the origin by using the feedback gain computed.

Several approaches have been introduced in order to improve control performance of RMPC. RMPC algorithms based on a parameter-dependent Lyapunov function (PDLF) have been proposed (Cuzzola et al., 2002; Mao, 2003). The idea of using PDLF was further extended to the case of LPV systems (Wada et al., 2006) where a scheduling parameter is considered in controller synthesis. However, the number of decision variables and constraints involved in an associated optimization problem drastically increases. Thus, an application of these algorithms is limited to relatively slow dynamic processes.

RMPC algorithms usually assume that a feedback gain is constant throughout an infinite horizon (Kothare *et al.*, 1996). Thus, one way to improve control performance is to introduce a sequence of free control inputs to the control law (Schuurmans & Rossiter, 2000; Casavola *et al.*, 2002; Bumroongsri & Kheawhom, 2012b). Unfortunately, more on-line computational time is required to calculate these free control inputs.

Though, RMPC can handle polytopic uncertain system, RMPC is computationally prohibitive in practical situations. To overcome an excessive computational cost of RMPC application, a synthesis of off-line RMPC for polytopic uncertain system has been motivated (Wan & Kothare, 2003; Angeli *et al.*, 2008; Nguyen *et al.*, 2012).

In Nguyen *et al.* (2012), an explicit solution of multi-parametric optimization problem was used to construct a control law that is a piecewise affine feedback defined over a polyhedral partition of the state space. In Wan & Kothare (2003), on-line computational time was reduced by pre-computing offline a sequence of feedback gains corresponding to a sequence of ellipsoidal invariant sets. At each sampling time, a feedback gain applied to the process is calculated by linear interpolation between the pre-computed feedback gains. This strategy was further extended by using nominal performance cost as proposed in Ding *et al.* (2007).

An off-line RMPC for LPV system was introduced in Bumroongsri & Kheawhom (2012a). This algorithm used the algorithm proposed in Wada et al. (2006) to compute a sequence of feedback gains in off-line fashion. A sequence of corresponding ellipsoidal invariant sets is also off-line pre-computed. At each sampling time, the smallest ellipsoid containing the current state is determined. A feedback gain is obtained by linear interpolation between the pre-computed feedback gains. As the interpolation technique used does not require solving any optimization problems, the computational burden is very small.

Though a polyhedral invariant set has some advantages over an ellipsoidal invariant set such as better handling of asymmetric constraints and enlargement of domain of attraction, an ellipsoidal invariant set is usually used in RMPC formulation due to its relatively low on-line computational burden. In recent years, an off-line RMPC algorithm based on polyhedral invariant set has been developed in Bumroongsri & Kheawhom (2012c). A sequence of polyhedral invariant sets corresponding to a sequence of pre-computed feedback gains is constructed off-line by using the algorithm proposed in Pluymers *et al.* (2005a). At each sampling time, the smallest polyhedral invariant set containing the current state is determined. The corresponding feedback gain is then implemented to the process without interpolation of the pre-computed feedback gains. This algorithm provided a larger stabilizable region than off-line RMPC (Wan & Kothare, 2003). However, a spiking effect of control input caused by a

switching of feedback gains was observed. Therefore, the algorithm requires constructing a large number of polyhedral invariant sets in order to reduce the spiking effect as well as to improve control performance. Consequently, large data storage is required. Later, an interpolation technique for polyhedral invariant sets was introduced to off-line RMPC for polytopic uncertain systems in order to improve control performance (Bumroongsri & Kheawhom, 2013). The interpolation algorithm could significantly improve control performance and eliminate the spiking effect of control input.

An interpolation-based MPC using polyhedral invariant set was proposed in Rossiter *et al.* (2004). The algorithm used decomposition variables and solved on-line optimization on performance index subjected to constraint set. The paper highlighted the potential benefits of using interpolation to generate predictive control algorithm and to enlarge a stabilizable region. However, the technique proposed was only developed for an LTI system.

In Nguyen *et al.* (2013), an interpolated vertex control for a linear time-varying (LTV) discrete-time system was introduced. The algorithm uses variable decomposition and convex interpolation between vertex control law and local linear feedback control law. At each sampling time, the algorithm solves linear programming problems on variable decomposition as well as vertex control action. This algorithm has advantages in terms of size of stabilizable region.

In this paper, two interpolation techniques, employed on off-line RMPC based on polyhedral invariant set, were investigated. The proposed algorithms are not based on variable decomposition. In the first technique, the parameter used in the interpolation is minimized subjected to constraint set. In the second technique, the parameter used in the interpolation is obtained by minimizing constraint violation of the adjacent smaller invariant set subjected to constraint set. The paper is organized as follows. In Section 1, the background of RMPC as well as interpolation techniques used in off-line RMPC were introduced. In Section 2, description of the system and control problem is presented. In Section 3, RMPC and polyhedral invariant set construction are described. In Section 4, the proposed control algorithms are presented. In Section 5, implementation of the algorithms proposed is illustrated. In the final section, the paper is concluded.

Notation

For a matrix A, A^{\top} denotes its transpose, A^{-1} denotes its inverse. I denotes an identity matrix. For a state vector x, x_k denotes a state measured at time k, x_{k+i} denotes a state at prediction time k+i predicted at time k, y_k and u_k denote an output and a control input at real time k, respectively. The symbol * denotes the corresponding transpose of a lower block part of symmetric matrices.

2. Problem description

In this work, a discrete-time LTV system with polytopic parametric uncertainty as shown in (2.1) is taken into account:

$$x_{k+1} = A_k x_k + B_k u_k$$

$$y_k = C_k x_k$$
(2.1)

where $x_k \in R^{n_x}$ is a state vector that can be accurately measured or estimated. $u_k \in R^{n_u}$ is a control input vector, and $y_k \in R^{n_y}$ is a control output vector. A system matrix A_k , a control matrix B_k and an output matrix C_k are assumed to be within a polytope:

$$[A_k, B_k, C_k] \in Co\{[A_1, B_1, C_1], \dots, [A_l, B_l, C_l], \dots, [A_L, B_L, C_L]\}.$$

Co denotes a convex hull with $[A_l, B_l, C_l]$ uncertain vertices. Any $[A_k, B_k, C_k]$ within the polytope is a convex combination of all vertices such that

$$[A_k, B_k, C_k] = \sum_{l=1}^{L} \lambda_{l,k} [A_l, B_l, C_l]$$
$$\sum_{l=1}^{L} \lambda_{l,k} = 1$$

where $0 \le \lambda_{l,k} \le 1$ is an uncertain parameter vector.

The aim is to find a state feedback control law:

$$u_k = K_k x_k \tag{2.2}$$

that can stabilize the system and achieve the minimum worst-case performance cost defined as in (2.3) while satisfying input, output and state constraints as in (2.4-2.6):

$$\min_{u_{k+i}} \max_{[A,B,C] \in \Omega} \quad \sum_{i=0}^{\infty} \begin{bmatrix} x_{k+i} \\ u_{k+i} \end{bmatrix}^{\top} \begin{bmatrix} \Theta & 0 \\ 0 & R \end{bmatrix} \begin{bmatrix} x_{k+i} \\ u_{k+i} \end{bmatrix}$$
(2.3)

s.t.
$$u_{h,\min} \le u_{h,k+i} \le u_{h,\max}, \quad h = 1, \dots, n_u$$
 (2.4)

$$y_{r,\min} \leqslant y_{r,k+i} \leqslant y_{r,\max}, \quad r = 1, \dots, n_{y}$$

$$(2.5)$$

$$x_{s,\min} \leqslant x_{s,k+i} \leqslant x_{s,\max}, \quad s = 1, \dots, n_x \tag{2.6}$$

where Θ and R are weighting matrices of states and control inputs, respectively.

3. RMPC and polyhedral invariant set

An on-line RMPC for a system with polytopic uncertainty was introduced by Kothare *et al.* (1996). An optimal control problem solved in each sampling time is shown in (3.1–3.5):

$$\min_{\gamma, \gamma, Q} \gamma \tag{3.1}$$

s.t.
$$\begin{vmatrix} 1 & * \\ x_k & Q \end{vmatrix} \geqslant 0$$
 (3.2)

$$\begin{bmatrix} Q & * & * & * \\ A_{l}Q + B_{l}Y & Q & * & * \\ \Theta^{1/2}Q & 0 & \gamma I & * \\ R^{1/2}Y & 0 & 0 & \gamma I \end{bmatrix} \geqslant 0 \quad \forall l = 1, \dots, L$$
(3.3)

$$\begin{bmatrix} X & * \\ Y^{\top} & Q \end{bmatrix} \geqslant 0, \quad X_{hh} \leqslant u_{h,\text{max}}^2, \quad h = 1, \dots, n_u$$
 (3.4)

$$\begin{bmatrix} S & * \\ (A_l Q + B_l Y)^\top C^\top & Q \end{bmatrix} \geqslant 0 \quad \forall l = 1, \dots, L$$

$$S_{rr} \leqslant y_{r,\text{max}}^2, \quad r = 1, \dots, n_y$$
(3.5)

where Q > 0 is a symmetrical matrix.

The problem presented in (3.1–3.5) is a convex optimization problem with linear matrix inequalities (LMI). By solving this problem, a state feedback control law $u_k = Kx_k$ with a feedback gain $K = YQ^{-1}$ that can stabilize the system while satisfying input and output constraints, is obtained. A proof of this algorithm can be found in Kothare *et al.* (1996).

At each sampling time, the algorithm constructs an ellipsoidal invariant set $S = \{x | x^{\top} Q^{-1} x \le 1\}$ to guarantee stability of the closed loop system. The advantage of using an ellipsoidal set lies in the fact that the constraints involved can be expressed in an LMI form.

By giving a feedback gain K that can stabilize the system, the polyhedral invariant set $S = \{x | Mx \le d\}$ with largest domain of attraction can be constructed using the following procedure (Pluymers *et al.*, 2005b).

Procedure 1:

(1) Set
$$i = 0$$
; $M_i = [I, -I, C_1, -C_1, \dots, C_l, -C_l, \dots, C_L, -C_L, K, -K]^\top$; $d_i = [x_{\text{max}}, -x_{\text{min}}, y_{\text{max}}, -y_{\text{min}}, \dots, y_{\text{max}}, -y_{\text{min}}, u_{\text{max}}, -u_{\text{min}}]^\top$; $S_i = \{x | M_i x \leq d_i\}$.

- (2) Set i = i + 1; $M_i = [M_{i-1}, M_{i-1}[A_1 + B_1K], \dots, M_{i-1}[A_l + B_lK], \dots, M_{i-1}[A_L + B_LK]]^\top$; $d_i = [d_{i-1}, d_{i-1}, \dots, d_{i-1}, \dots, d_{i-1}]^\top$; $S_i = \{x | M_i x \le d_i\}$, and eliminate redundant inequalities from the polytope S_i .
- (3) If $S_i \neq S_{i-1}$, then repeat Step 2, if otherwise stop the algorithm and $S = \{x \mid M_i x \leq d_i\}$.

THEOREM 3.1 For an LTV system as shown in (2.1), given the control law $u_k = Kx_k$ with a state feedback gain $K = YQ^{-1}$ provided by solving the optimization problem presented in (3.1–3.5), the polyhedral set $S = \{x \mid Mx \le d\}$ constructed by using Procedure 1 provides a set of states whereby the system will evolve to the origin without input and output constraints violation.

Proof. The feedback gain K used in the construction of the polyhedral invariant set is obtained by solving convex optimization problem with LMI constraints as shown in (3.1–3.5). The satisfaction of (3.3) for a state feedback gain K ensures that

$$[[A_l + B_l K] x_k]^{\top} \gamma Q^{-1} [[A_l + B_l K] x_k] - x_k^{\top} \gamma Q^{-1} x_k \leqslant -[x_k^{\top} \Theta x_k + u_k^{\top} R u_k], \quad l = 1, \dots, L.$$

Thus, $V_k = x_k^{\top} \gamma Q^{-1} x_k$ is a strictly decreasing Lyapunov function and the closed-loop system is robustly stabilized by the state feedback gain K.

By following Procedure 1, state, output and input constraints at time step k+i, $i=0,\ldots,i_{\max}$ are repeatedly added to define a polyhedral invariant set $S_i=\{x\mid M_ix\leqslant d_i\}$, and all redundant constraints are removed. There must exist a finite index $i=i_{\max}$ such that $M_i=M_{i+1}$ because of the contraction as the feedback gain K is able to ensure robust stability and constraint satisfaction of the system. Hence, a set of initial states $S=\{x\mid Mx\leqslant d\}$ is constructed such that all predicted states remain inside S and approach to the origin without constraint violation. Moreover, the polyhedral invariant set constructed is never an empty set because the feedback gain K given is a stabilizable gain.

4. Off-line RMPC and the proposed interpolation algorithms

In this section, off-line RMPC and the proposed interpolation algorithms are described. An off-line RMPC consists of off-line and on-line calculations. The purpose of the off-line calculation is to generate a sequence of feedback gains, and a sequence of nested polyhedral invariant sets. The off-line calculation used in this work is identical to the off-line RMPC proposed in Bumroongsri & Kheawhom (2012c). The purpose of the on-line calculation is to determine a variable feedback gain applied to the process at each sampling time.

4.1 Off-line calculation

• Choose a sequence of states x_m , $m = 1, ..., m_{\text{max}}$ where x_{m+1} is closer to the origin than x_m . For each x_m solve the optimization problem in (3.1–3.4) by replacing x_k with x_m in order to obtain a corresponding feedback gain:

$$K_m = Y_m Q_m^{-1}.$$

In addition, x_m is chosen such that $\epsilon_{m+1}^{-1} \subset \epsilon_m^{-1}$ where $\epsilon_m = \{x \mid x^\top Q_m^{-1} x \leq 1\}$. Moreover, for each $m \neq m_{\text{max}}$, there must exist a matrix P > 0 satisfying:

$$P - [A_l + B_l K_m]^{\mathsf{T}} P[A_l + B_l K_m] > 0, \quad l = 1, \dots, L$$
 (4.1)

$$P - [A_l + B_l K_{m+1}]^{\top} P[A_l + B_l K_{m+1}] > 0, \quad l = 1, \dots, L$$
(4.2)

to assure robust stability satisfaction of a feedback gain $K = \lambda K_m + (1 - \lambda)K_{m+1}$, $0 \le \lambda \le 1$ which is a convex combination between K_m and K_{m+1} .

Each feedback gain K_m is derived based on the minimization of the upper bound of infinite horizon worst-case performance. The output constraint in (3.5) is relaxed in order to enlarge the domain of attraction. The input, output and state constraints are properly handled during the polyhedral invariant set construction in the next step.

• For each feedback gain $K_m = Y_m Q_m^{-1}$, $m = 1, ..., m_{\text{max}}$ as previously calculated, the corresponding polyhedral invariant set $S_m = \{x \mid M_m x \leq d_m\}$ is constructed by using Procedure 1.

The existence of a common Lyapunov function P in (4.1) and (4.2) depends on the difference between x_m and x_{m+1} . (4.1) and (4.2) can be satisfied by appropriately selecting x_m and x_{m+1} . For example, x_m and x_{m+1} should be close enough so that Q_m^{-1} can be used as a common Lyapunov function P between K_m and K_{m+1} . In such case, (4.2) becomes

$$Q_m^{-1} - [A_l + B_l K_{m+1}]^{\top} Q_m^{-1} [A_l + B_l K_{m+1}] > 0, \quad l = 1, \dots, L$$

which defines the limit of K_{m+1} .

4.2 On-line calculation

In the on-line calculation, a feedback gain applied at each sampling time is determined. In Bumroongsri & Kheawhom (2012c), at each sampling time, the smallest invariant set that can embed a measured state is determined, and a corresponding feedback gain is then implemented. In this work, a feedback gain at each sampling time is variable and computed using an interpolation technique.

4.2.1 Algorithm 1 The feedback gain implemented is computed by linear interpolation between the pre-computed feedback gains. At each sampling time, the current state x_k is measured and the smallest polyhedral invariant set $S_m = \{x \mid M_m x \leq d_m\}$ containing the current state is determined.

If $x_k \in S_m$ and $x_k \notin S_{m+1}$, $\forall m \le m_{\text{max}} - 1$, a variable feedback gain $K_k = \lambda_k K_m + (1 - \lambda_k) K_{m+1}$ can be obtained by solving the optimization problem in (4.3-4.7):

$$\min_{\lambda_k} \quad \lambda_k \tag{4.3}$$

s.t.
$$M_m[A_l + B_l K_k] x_k - d_m \leq [0, 0, \dots, 0]^\top, \quad l = 1, \dots, L$$
 (4.4)

$$u_{\min} \leqslant K_k x_k \leqslant u_{\max} \tag{4.5}$$

$$K_k = \lambda_k K_m + (1 - \lambda_k) K_{m+1} \tag{4.6}$$

$$0 \leqslant \lambda_k \leqslant 1. \tag{4.7}$$

If otherwise, $x_k \in S_{m_{\text{max}}}$, the constant feedback gain $K_{m_{\text{max}}}$ is applied.

The optimization problem involved is formulated as linear programming and the number of constraints involved is linearly dependent on the number of vertices of the uncertain polytope.

4.2.2 Algorithm 2 The feedback gain implemented is computed by linear interpolation between the pre-computed feedback gains to minimize largest constraint violation to the adjacent smaller invariant set in one step prediction. At each sampling time, the current state x_k is measured and the smallest polyhedral invariant set $S_m = \{x \mid M_m x \leq d_m\}$ containing the current state is determined.

If $x_k \in S_m$ and $x_k \notin S_{m+1}$, $\forall m \le m_{\text{max}} - 1$, a feedback gain $K_k = \lambda_k K_m + (1 - \lambda_k) K_{m+1}$ can be obtained by solving the problem in (4.8–4.13):

$$\min_{\gamma_k \lambda_k} \quad \gamma_k \tag{4.8}$$

s.t.
$$M_m[A_l + B_l K_k] x_k - d_m \leq [0, 0, \dots, 0]^\top, \quad l = 1, \dots, L$$
 (4.9)

$$M_{m+1}[A_l + B_l K_k] x_k - d_{m+1} \leq [\gamma_k, \gamma_k, \dots, \gamma_k]^\top, \quad l = 1, \dots, L$$
 (4.10)

$$u_{\min} \leqslant K_k x_k \leqslant u_{\max} \tag{4.11}$$

$$K_k = \lambda_k K_m + (1 - \lambda_k) K_{m+1} \tag{4.12}$$

$$0 \leqslant \lambda_k \leqslant 1. \tag{4.13}$$

If otherwise, $x_k \in S_{m_{\text{max}}}$, the constant feedback gain $K_{m_{\text{max}}}$ is applied.

The optimization problem involved is formulated as linear programming and the number of constraints involved is linearly dependent on the number of vertices of the uncertain polytope.

THEOREM 4.1 For an LTV system as shown in (2.1), given an initial state $x_k \in S_m$, the control law, provided by Algorithms 1 and 2, assures robust stability to the closed-loop system while satisfying input, output and state constraints.

Proof. As (4.1) and (4.2) are satisfied, a common Lyapunov function $V_k = x_k^\top P x_k$ ensures that a feedback gain of $K_k = \lambda_k K_m + (1 - \lambda_k) K_{m+1}$, $0 \le \lambda_k \le 1$, which is a convex combination of K_m and K_{m+1} , is a stabilizable gain.

In solving the problem in (4.3-4.7), (4.6) and (4.7) restrict K_k to be a convex combination. The input constraint is guaranteed by (4.5). The state and output constraints are satisfied by forcing a one step prediction state x_{k+1} to remain inside S_m as in (4.4). Thus, an initial state x_k evolves closer to the origin by passing $S_{m+1}, S_{m+2}, \ldots, S_{m_{\max}}$. A state inside $S_{m_{\max}}$ is then driven to the origin by the constant feedback gain $K_{m_{\max}}$ because $S_{m_{\max}}$ is satisfied with Theorem 3.1. Thus, Algorithm 1 assures robust stability to the closed-loop system with input, output and state constraints satisfaction.

In solving the problem in (4.8-4.13), (4.12) and (4.13) restrict K_k to be a convex combination. The input constraint is guaranteed by (4.11). The state and output constraints are satisfied by forcing a one step prediction state x_{k+1} to remain inside S_m as in (4.9). Thus, an initial state x_k evolves closer to the origin by passing $S_{m+1}, S_{m+2}, \ldots, S_{m_{\max}}$. A state inside $S_{m_{\max}}$ is then driven to the origin by the constant feedback gain $K_{m_{\max}}$ because $S_{m_{\max}}$ is satisfied with Theorem 3.1. Thus, Algorithm 2 assures robust stability to the closed-loop system with input, output and state constraints satisfaction.

5. Case study

In this section, examples are presented to illustrate the proposed interpolation algorithms. The latter are compared with on-line RMPC proposed in Kothare *et al.* (1996), off-line RMPC algorithm proposed in Bumroongsri & Kheawhom (2012c) and interpolated vertex control proposed in Nguyen *et al.* (2013). Numerical simulation was performed in 2.3 GHz Intel Core i-5 with 16 GB RAM, using SDPT3 (Tütüncü *et al.*, 2003) and YALMIP (Löfberg, 2004) within Matlab R2011b environment.

5.1 Two-tank system

Application of a two-tank system which is similar to the system considered in Dlapa (2007) was considered. Spherical tanks with radius 0.5 m are connected as shown in Fig. 1. An outflow from each tank depends on its current liquid level as $F_1 = 1.6971\sqrt{h_1}$ and $F_2 = 1.6971\sqrt{h_2}$. The system is modelled as (5.1) and (5.2):

$$\frac{\mathrm{d}h_1}{\mathrm{d}t} = -\frac{1.6971\sqrt{h_1}}{\pi h_1 - \pi h_1^2} + \frac{F_i}{\pi h_1 - \pi h_1^2}$$
 (5.1)

$$\frac{\mathrm{d}h_2}{\mathrm{d}t} = \frac{1.6971\sqrt{h_1}}{\pi h_2 - \pi h_2^2} - \frac{1.6971\sqrt{h_2}}{\pi h_2 - \pi h_2^2}$$
 (5.2)

where h_1 is a liquid level of tank 1, h_2 is a liquid level in tank 2 and F_i is an inlet flow rate.

 $h_1 = h_1 - h_{1,eq}$, $h_2 = h_2 - h_{2,eq}$ and $\bar{F}_i = F_i - F_{i,eq}$ are defined. Subscript eq denotes a corresponding variable at equilibrium condition, $h_{1,eq} = 50$ cm, $h_{2,eq} = 50$ cm and $F_{i,eq} = 1.2$ m³/h.

The objective is to regulate \bar{h}_1 and \bar{h}_2 to the origin by manipulating \bar{F}_i . An input constraint of $-0.5 \leqslant \bar{F}_i \leqslant 0.5 \, \text{m}^3/\text{h}$ is symmetric. In addition, output constraints of $-0.45 \leqslant \bar{h}_1 \leqslant 0.45$ and $-0.45 \leqslant \bar{h}_2 \leqslant 0.45$ are also symmetric. It was assumed that the maximum values of following terms including $1.6971/(\pi h_1^{1.5} - \pi h_2^{2.5}) - 1.6971(\pi h_{1,\text{eq}}^{1.5} - \pi h_{1,\text{eq}}^{2.5})$, $1/(\pi h_1 - \pi h_1^2) - 1/(\pi h_{1,\text{eq}} - \pi h_{1,\text{eq}}^2)$, $1.6971/h_1^{0.5}(\pi h_2 - \pi h_2^2) - 1.6971/h_{1,\text{eq}}^{0.5}(\pi h_{2,\text{eq}} - \pi h_{2,\text{eq}}^2)$ and $1.6971/(\pi h_2^{1.5} - \pi h_2^{2.5}) - 1.6971/(\pi h_{2,\text{eq}}^{1.5} - \pi h_{2,\text{eq}}^{2.5})$ are small enough to be neglected. Thus, the system can be described

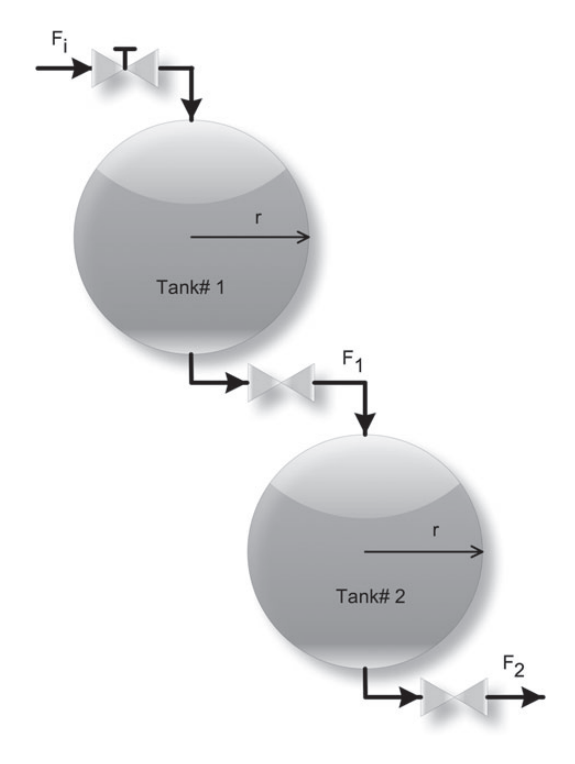


Fig. 1. Two-tank system considered in case study 1.

in terms of deviation variables as in (5.3) and (5.4):

$$\frac{\mathrm{d}\bar{h}_1}{\mathrm{d}t} = -\frac{1.6971}{\pi h_1^{1.5} - \pi h_1^{2.5}} \bar{h}_1 + \frac{1}{\pi h_1 - \pi h_1^2} \bar{F}_i \tag{5.3}$$

$$\frac{\mathrm{d}\bar{h}_2}{\mathrm{d}t} = \frac{1.6971}{\pi h_2 h_1^{0.5} - \pi h_2^2 h_1^{0.5}} \bar{h}_1 - \frac{1.6971}{\pi h_2^{1.5} - \pi h_2^{2.5}} \bar{h}_2. \tag{5.4}$$

By rearranging (5.3) and (5.4) all 16 vertices of the uncertainty polytope, the system is represented by the following differential inclusion:

$$\begin{bmatrix} \dot{\bar{h}}_1 \\ \dot{\bar{h}}_2 \end{bmatrix} \in \sum_{l=1}^{16} \lambda_l \left(A_l \begin{bmatrix} \bar{h}_1 \\ \bar{h}_2 \end{bmatrix} + B_l \bar{F}_i \right)$$
 (5.5)

where $\sum_{l=1}^{16} \lambda_l = 1$, and $0 \le \lambda_l \le 1$.

A discrete-time model is obtained by discretization of (5.5) using Euler first-order approximation with a sampling period of 30 s. The said model is omitted here for brevity. Tuning parameters are $\Theta = [[0,0],[0,1]]^{\top}$ and R = 0.01.

States of $[\bar{h}_1, \bar{h}_2]^{\top} = [0.45, 0.45]^{\top}$ and $[0.01, 0.01]^{\top}$ were used to generate feedback gains and to construct polyhedral invariant sets $(S_1 \text{ and } S_2)$ using the algorithms described previously. Figure 2 shows

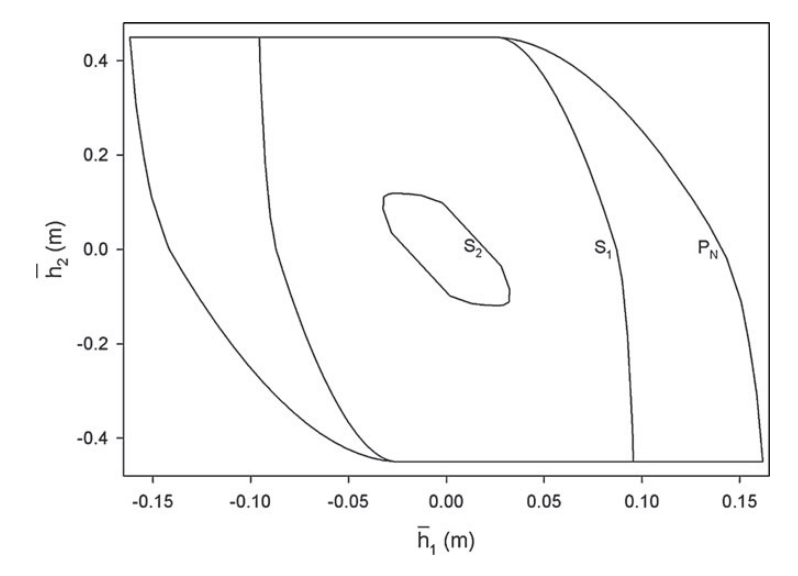


Fig. 2. Invariant sets generated in case study 1.

the polyhedral invariant sets constructed. An initial state $x \in S_1$ can be stabilized by off-line RMPC (Bumroongsri & Kheawhom, 2012c) as well as the algorithms proposed. P_N is a maximal robustly controlled invariant set projected from S_2 . An initial state $x \in P_N$ can be stabilized by interpolated vertex control (Nguyen *et al.*, 2013). This algorithm provided the largest stabilizable region.

The system was regulated from an initial state of $[\bar{h}_1, \bar{h}_2]^{\top} = [0.04, 0.3]^{\top}$ to the origin. The chosen initial state belongs to the stabilizable region of all algorithms. Profiles of regulated state $(\bar{h}_1 \text{ and } \bar{h}_2)$ are shown in Figs 3 and 4. All algorithms could drive the initial state to the origin without violation of input and state constraints. As the tuning parameters of $\Theta = [[0,0],[0,1]]^{\top}$ and R = 0.01 are concerned, only control input \bar{F}_i and state \bar{h}_2 contributed to the performance cost. The settling times of on-line RMPC (Kothare *et al.*, 1996) and off-line RMPC (Bumroongsri & Kheawhom, 2012c) were ~2 hr. In comparison, the proposed algorithms could drive the system to the origin in ~1.2 hr. which is faster than on-line RMPC (Kothare *et al.*, 1996) and off-line RMPC (Bumroongsri & Kheawhom, 2012c). Interpolated vertex control (Nguyen *et al.*, 2013) is faster than on-line RMPC (Kothare *et al.*, 1996) and off-line RMPC (Bumroongsri & Kheawhom, 2012c) but slightly slower than the proposed algorithms.

Figure 5 shows control input \bar{F}_i profiles. A spiking effect of control input was noticed in off-line RMPC (Bumroongsri & Kheawhom, 2012c). The spiking effect is caused by the switching of the feedback control law. Algorithms 1 and 2 produced similar responses and control input \bar{F}_i profiles. The control input profiles of Algorithms 1 and 2 saturated between 0 and 0.15 hr. Control input saturation was then repealed when states move closer to the origin. In on-line RMPC (Kothare *et al.*, 1996), off-line RMPC (Bumroongsri & Kheawhom, 2012c) and interpolated vertex control (Nguyen *et al.*, 2013), control input saturation was not observed.

Figure 6 shows the cumulative performance cost. Control performance of on-line RMPC (Kothare *et al.*, 1996) was better than that of off-line RMPC (Bumroongsri & Kheawhom, 2012c) because online RMPC solves the optimization problem on-line and updates a feedback gain more frequently. Both on-line RMPC (Kothare *et al.*, 1996) and off-line RMPC (Bumroongsri & Kheawhom, 2012c) obtain a feedback gain based on the assumption that the feedback gain remains constant throughout an infinite

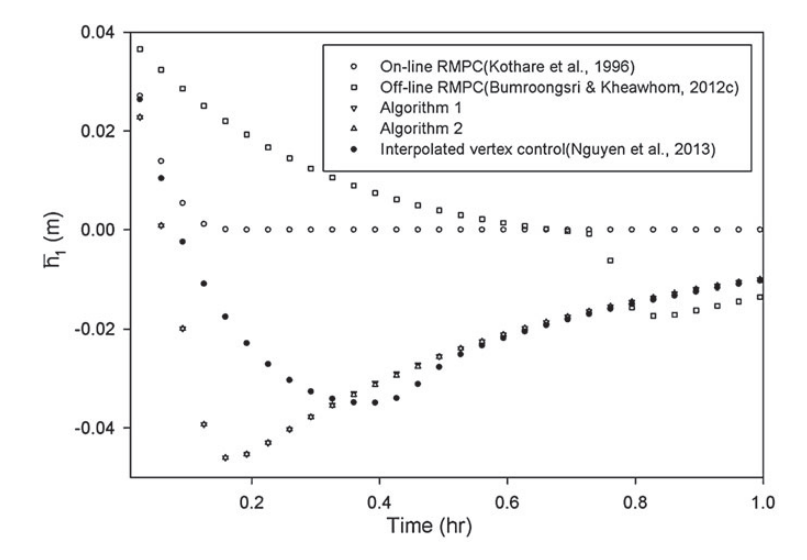


Fig. 3. Regulated state (\bar{h}_1) profiles for case study 1.

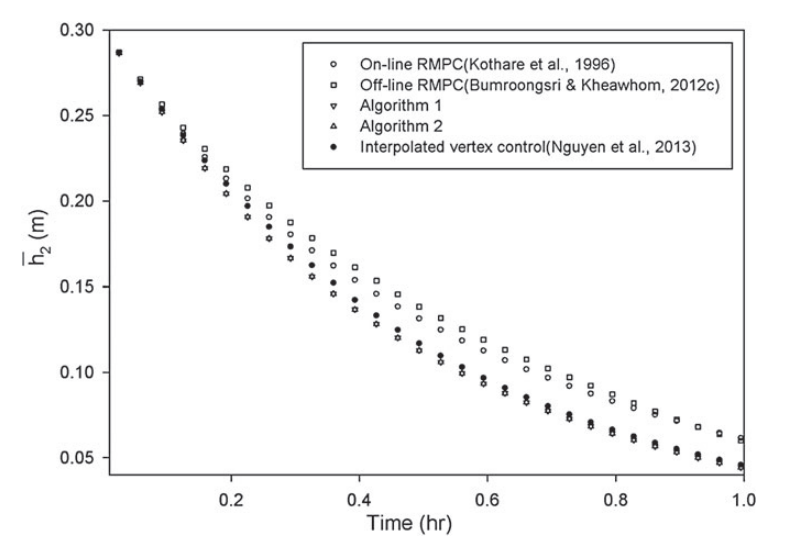


Fig. 4. Regulated state (\bar{h}_2) profiles for case study 1.

horizon. Saturation at one step in the horizon requires a small gain for all steps in the horizon. Thus, control performance deteriorates when input saturation occurs. Implementation of interpolation algorithms proposed can improve control performance. Though the proposed algorithms are also derived based on a constant feedback gain assumption, at each sampling time, the proposed algorithms obtain a variable feedback gain by solving a simple optimization problem. Therefore, the proposed algorithms provided better control performance than on-line RMPC (Kothare *et al.*, 1996) and off-line RMPC (Bumroongsri & Kheawhom, 2012c). Control performance of interpolated vertex control (Nguyen *et al.*, 2013) was

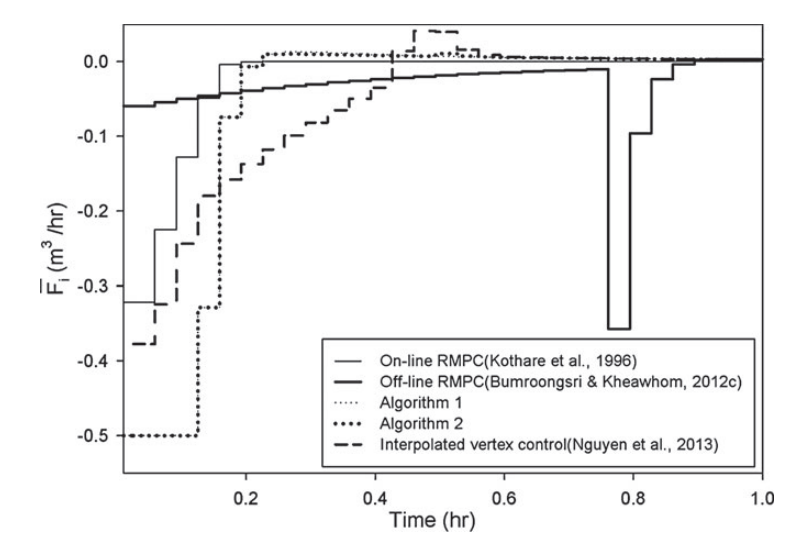


Fig. 5. Control input \bar{F}_i profiles for case study 1.

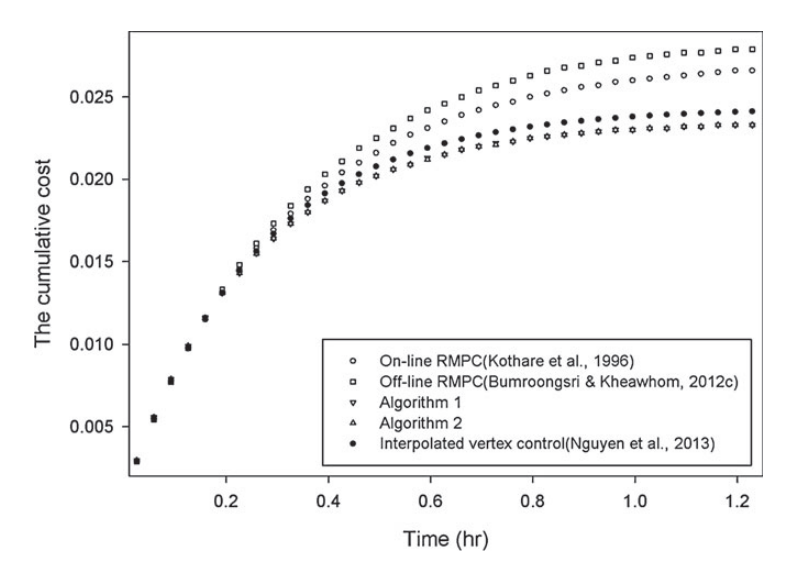


Fig. 6. Cumulative cost for case study 1.

also better than that of on-line RMPC (Kothare *et al.*, 1996) and off-line RMPC (Bumroongsri & Kheawhom, 2012c). However, control performance of interpolated vertex control (Nguyen *et al.*, 2013) was slightly lower than that of the proposed algorithms.

Table 1 shows the on-line computational cost of each algorithm. For all off-line RMPC algorithms, most computational burdens are moved off-line so on-line computation is tractable. Off-line RMPC (Bumroongsri & Kheawhom, 2012c) does not solve optimization problems on-line. Thus, this algorithm is very fast. An optimization problem involved in both Algorithms 1 and 2 is linear programming and

| Algorithm | On-line computational time (s) |
|---|--------------------------------|
| On-line RMPC (Kothare et al., 1996) | 2.232 |
| Off-line RMPC (Bumroongsri & Kheawhom, 2012c) | < 0.001 |
| Algorithm 1 | 0.004 |
| Algorithm 2 | 0.005 |
| Interpolated vertex control (Nguyen et al., 2013) | 0.007 |

Table 1 On-line computational time required in case study 1

the number of constraints involved is linearly dependent on the number of vertices of the uncertain polytope and size of the polyhedral invariant sets involved. The number of constraints involved in Algorithm 1 is smaller than that of Algorithm 2. The on-line computational time of interpolation vertex control (Nguyen *et al.*, 2013) was comparable with the proposed algorithms. At each sampling time, this algorithm requires solving linear programming problems on variable decomposition as well as vertex control action.

5.2 Four-tank system

In this case study, simulation of a four-tank system which is similar to the system considered in Johansson (2000) was considered. A schematic diagram of this system is shown in Fig. 7. The system is described by (5.6–5.9):

$$\frac{\mathrm{d}h_1}{\mathrm{d}t} = -5.91\sqrt{h_1} + 5.91\sqrt{h_3} + 0.74F_1 \tag{5.6}$$

$$\frac{\mathrm{d}h_2}{\mathrm{d}t} = -5.91\sqrt{h_2} + 5.91\sqrt{h_4} + 0.74F_2 \tag{5.7}$$

$$\frac{\mathrm{d}h_3}{\mathrm{d}t} = -5.91\sqrt{h_3} + 1.73F_2 \tag{5.8}$$

$$\frac{\mathrm{d}h_4}{\mathrm{d}t} = -5.91\sqrt{h_4} + 1.73F_1\tag{5.9}$$

where h_i is a liquid level of tank i, i = 1, 2, 3, 4, and F_1 and F_2 are inlet flow rates.

Let $\bar{h}_i = h_i - h_{i,eq}$, i = 1, 2, 3, 4 and $\bar{F}_i = F_i - F_{i,eq}$, i = 1, 2. Subscript eq denotes a corresponding variable at equilibrium condition, $h_{1,eq} = 14.98$ cm; $h_{2,eq} = 14.98$ cm; $h_{3,eq} = 7.34$ cm; $h_{4,eq} = 7.34$ cm and $F_{i,eq} = 9.25$ m³/hr, i = 1, 2.

The objective is to regulate \bar{h}_i , i=1, 2, 3, 4 to the origin by manipulating \bar{F}_1 and \bar{F}_2 . The input constraints of $-9.25 \leqslant \bar{F}_1 \leqslant 9.25$ m³/hr and $-9.25 \leqslant \bar{F}_2 \leqslant 9.25$ m³/hr are symmetric. In contrast, output constraints of $-13.98 \leqslant \bar{h}_1 \leqslant 35.02$ cm, $-13.98 \leqslant \bar{h}_2 \leqslant 35.02$ cm, $-6.34 \leqslant \bar{h}_3 \leqslant 42.66$ cm and $-6.34 \leqslant \bar{h}_4 \leqslant 42.66$ cm are asymmetric.

By rewriting (5.6–5.9) in deviation form and rearranging all uncertain vertices, the system is written in differential inclusion form as follows:

$$\left[\dot{\bar{h}}_{1}, \dot{\bar{h}}_{2}, \dot{\bar{h}}_{3}, \dot{\bar{h}}_{4}\right]^{\top} \in \sum_{l=1}^{16} \lambda_{l} \left[A_{l} \left[\bar{h}_{1}, \bar{h}_{2}, \bar{h}_{3}, \bar{h}_{4}\right]^{\top} + B_{l} \left[\bar{F}_{1}, \bar{F}_{2}\right]^{\top}\right]. \tag{5.10}$$

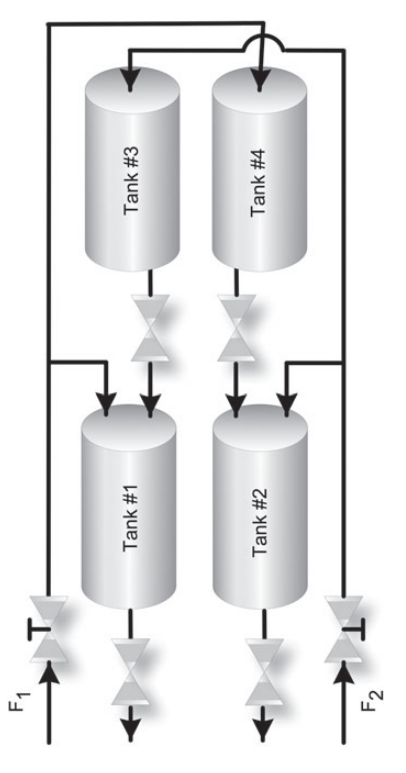


Fig. 7. Four-tank system considered in case study 2.

A discrete-time model is obtained by discretization of (5.10) using Euler first-order approximation with a sampling period of 0.1 min. The said model is omitted here for brevity. Tuning parameters are $R = [[0.01, 0], [0, 0.01]]^{T}$ and $\Theta = [[1, 0, 0, 0], [0, 1, 0, 0], [0, 0, 0, 0], [0, 0, 0, 0]]^{T}$. It should be noted that only states \bar{h}_1 and \bar{h}_2 and control inputs \bar{F}_1 and \bar{F}_2 contributed to the performance cost.

A sequence of six polyhedral invariant sets with associated feedback gains were generated by using the following states, $[13.5, 13.5, 6.3, 6.3]^{\top}$, $[4.0, 4.0, 2.0, 2.0]^{\top}$, $[2.5, 2.5, 1.0, 1.0]^{\top}$, $[1.0, 1.0, 0.5, 0.5]^{\top}$, $[0.2, 0.2, 0.1, 0.1]^{\top}$ and $[0.05, 0.05, 0.01, 0.01]^{\top}$. A maximal robustly controlled invariant set projected from the innermost invariant set was also constructed for interpolated vertex control (Nguyen *et al.*, 2013). Interpolated vertex control (Nguyen *et al.*, 2013) provided the largest stabilizable region. The system was regulated from an initial state of $[\bar{h}_1, \bar{h}_2, \bar{h}_3, \bar{h}_4]^{\top} = [-12.0, 12.0, 10.0, 10.0]^{\top}$ that belongs to the stabilizable region of all algorithms, to the origin.

Figures 8 and 9 show profiles of regulated states \bar{h}_1 and \bar{h}_2 , respectively. Figures 10 and 11 show profiles of control inputs \bar{F}_1 and \bar{F}_2 , respectively. All algorithms could drive the initial state to the origin without violation of input and state constraints. The settling times of on-line RMPC (Kothare *et al.*, 1996) and off-line RMPC (Bumroongsri & Kheawhom, 2012c) were ~4.0 min. In comparison, the proposed algorithms could drive the system to the origin in ~1.8 min. On-line RMPC (Kothare *et al.*, 1996) and off-line RMPC (Bumroongsri & Kheawhom, 2012c) provided slower responses than interpolated vertex control (Nguyen *et al.*, 2013) and the proposed algorithms. Interpolated vertex control (Nguyen *et al.*, 2013) is slightly slower than the proposed algorithms. Both Algorithms 1 and 2 produced similar

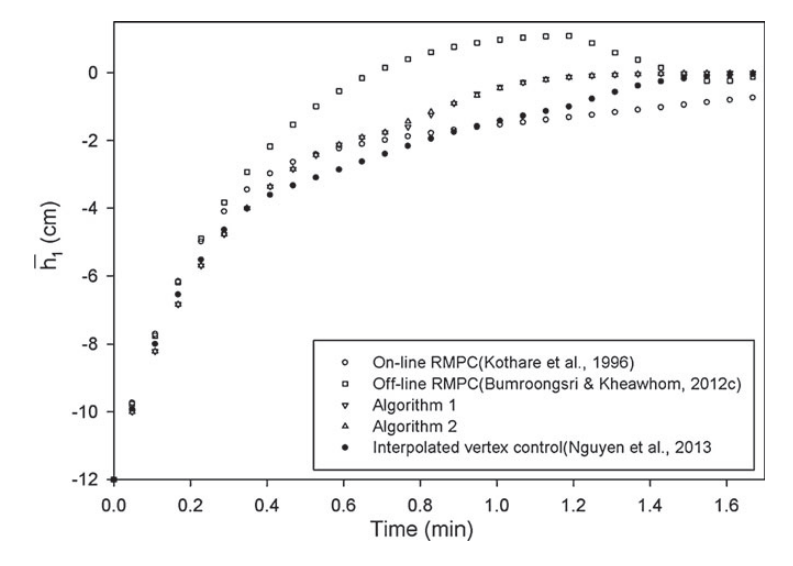


Fig. 8. Regulated state (\bar{h}_1) profiles for case study 2.

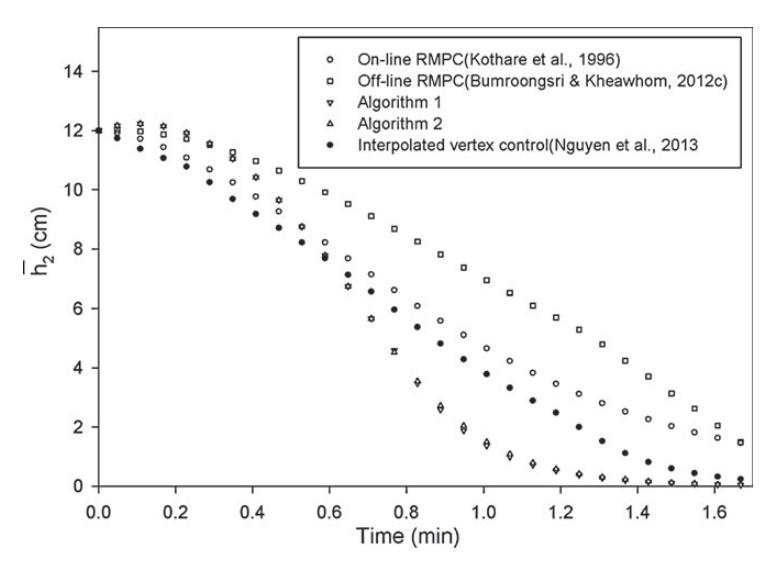


Fig. 9. Regulated state (\bar{h}_2) profiles for case study 2.

responses. There was a difference between Algorithms 1 and 2 in control input \bar{F}_1 and \bar{F}_2 profiles. Saturation of control input \bar{F}_1 was observed in Algorithms 1 and 2 from 0 to 0.75 min. A spiking effect of control input, which is caused by the switching of feedback control gains, was noticed in off-line RMPC (Bumroongsri & Kheawhom, 2012c).

Figure 12 shows the cumulative performance cost. The cumulative cost of Algorithms 1 and 2 were lower than those of on-line RMPC (Kothare *et al.*, 1996), off-line RMPC (Bumroongsri & Kheawhom,

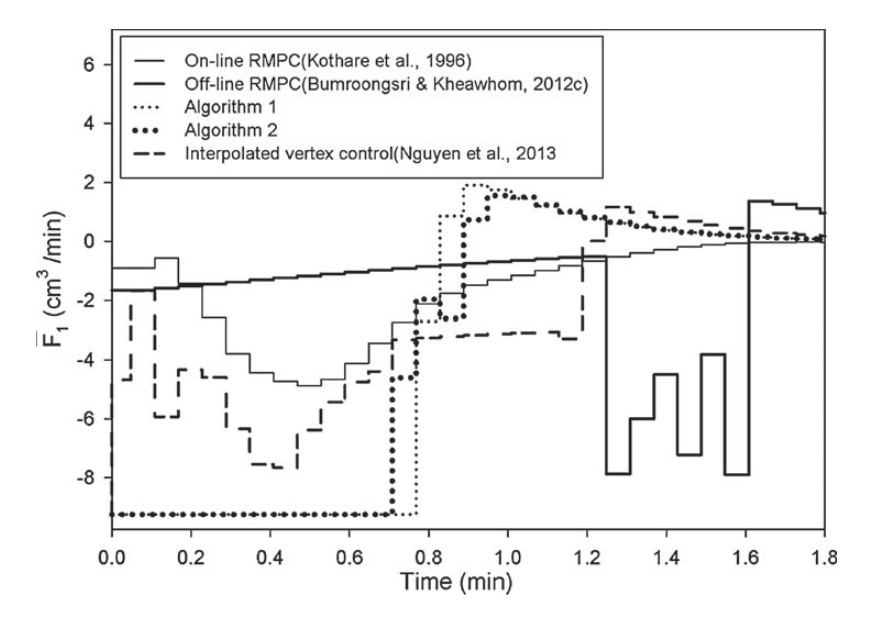


Fig. 10. Control input \bar{F}_1 profiles for case study 2.

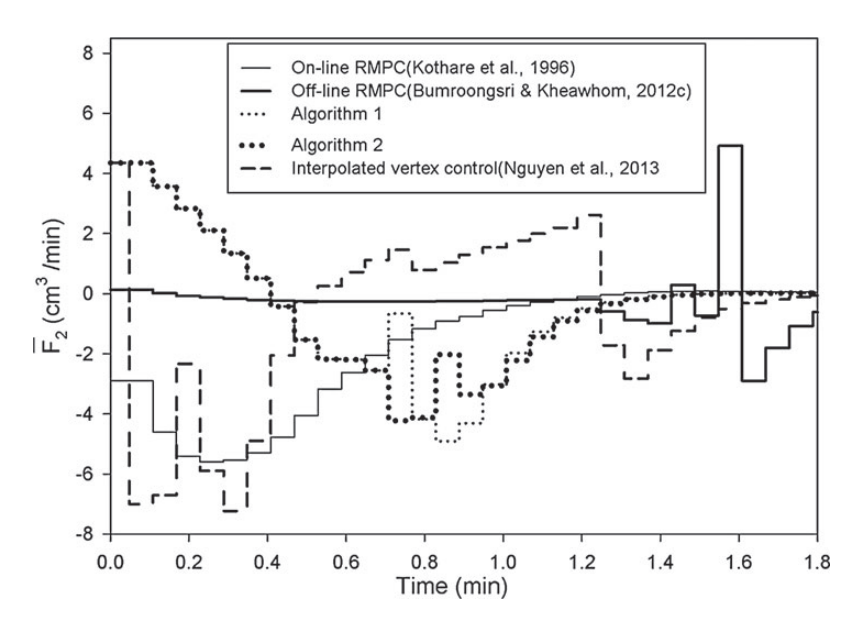


Fig. 11. Control input \bar{F}_2 profiles for case study 2.

2012c) and interpolated vertex control (Nguyen *et al.*, 2013). Control performance of Algorithm 1 was slightly better than that of Algorithm 2.

Table 2 shows the on-line computational cost of each algorithm. Although, on-line computational time of Algorithms 1 and 2 were higher than that of off-line RMPC (Bumroongsri & Kheawhom,

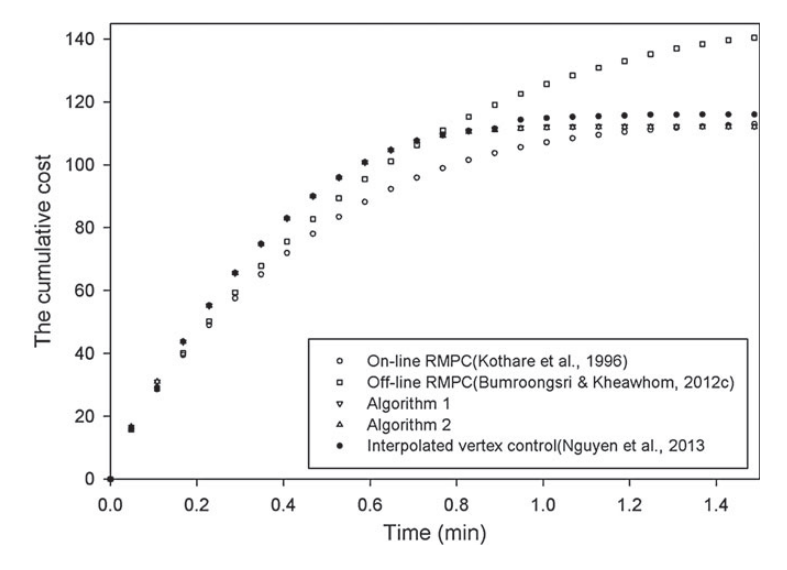


Fig. 12. Cumulative cost for case study 2.

Table 2 On-line computational time required in case study 2

| Algorithm | On-line computational time (s) |
|---|--------------------------------|
| On-line RMPC (Kothare et al., 1996) | 14.639 |
| Off-line RMPC (Bumroongsri & Kheawhom, 2012c) | < 0.001 |
| Algorithm 1 | 0.012 |
| Algorithm 2 | 0.018 |
| Interpolated vertex control (Nguyen et al., 2013) | 0.024 |

2012c), the proposed algorithms were much faster than on-line RMPC (Kothare *et al.*, 1996). The on-line computational time of interpolation vertex control (Nguyen *et al.*, 2013) was comparable with the proposed algorithms. Computational times required in this case study were larger than those of case study 1 because the number of vertices of the uncertain polytope and the size of the polyhedral invariant set involved in case study 2 were larger than those of case study 1.

6. Conclusion

In this paper, implementation of interpolation algorithms on RMPC of polytopic uncertain discrete-time systems was studied. Control algorithms employed an off-line solution of an optimal control optimization problem to determine a feedback gain. A sequence of nested polyhedral invariant sets associated with each feedback gain pre-computed was constructed. At each sampling time, the smallest invariant set which contained the current state was identified. If the current invariant set is the innermost set, the pre-computed feedback gain associated with the innermost set is applied to the process. If otherwise, a feedback gain is variable and determined by linear interpolation which is a convex combination of the pre-computed feedback gains associated with the current invariant set and the adjacent smaller invariant set. Two interpolation algorithms were proposed. Furthermore, two case studies were used to illustrate

the applicability of the algorithms proposed. An optimization problem involved in the proposed algorithms was linear programming, and the number of constraints involved was linearly dependent on the number of vertices of the uncertain polytope and the size of the polyhedral invariant set involved. The number of constraints involved in Algorithm 1 was smaller than that of Algorithm 2. The simulation results showed that the proposed algorithms yielded better control performance than existing RMPC algorithms while on-line computation was still tractable.

Funding

This work was supported by Rajadapisek Sompoj Fund, Chulalongkorn University Centenary Academic Development Project, The Commission on Higher Education of Thailand and the Thailand Research Fund (RSA5680044, RES5741121076).

REFERENCES

- ANGELI, D., CASAVOLA, A., FRANZÉ, G. & MOSCA, E. (2008) An ellipsoidal off-line MPC scheme for uncertain polytopic discrete-time systems. *Automatica*, **44**, 3113–3119.
- Bemporad, A., Borrelli, F. & Morari, M. (2003) Min-max control of constrained uncertain discrete-time linear systems. *IEEE Trans. Automat. Control*, **48**, 1600–1606.
- Bumroongsri, P. & Kheawhom, S. (2012a) An ellipsoidal off-line model predictive control strategy for linear parameter varying systems with applications in chemical processes. *Syst. Control Lett.*, **61**, 435–442.
- Bumroongsri, P. & Kheawhom, S. (2012b) MPC for LPV systems based on parameter-dependent Lyapunov function with perturbation on control input strategy. *Eng. J.*, **16**, 61–72.
- Bumroongsri, P. & Kheawhom, S. (2012c) An off-line robust MPC algorithm for uncertain polytopic discrete-time systems using polyhedral invariant sets. *J. Process Control*, **22**, 975–983.
- Bumroongsri, P. & Kheawhom, S. (2013) An interpolation-based robust MPC algorithm using polyhedral invariant sets. *Proceedings of the 2013 European Control Conference (ECC)*, pp. 3161–3166.
- CASAVOLA, A., FAMULARO, D. & FRANZÉ, G. (2002) A feedback min-max MPC algorithm for LPV systems subject to bounded rates of change of parameters. *IEEE Trans. Automat. Control*, **47**, 1147–1152.
- CUZZOLA, F., GEROMEL, J. & MORARI, M. (2002) An improved approach for constrained robust model predictive control. Automatica, 38, 1183–1189.
- DING, B., XI, Y., CYCHOWSKI, M. & O'MAHONY, T. (2007) Improving off-line approach to robust MPC based-on nominal performance cost. *Automatica*, **43**, 158–163.
- DLAPA, M. (2007) Decoupled control of two tank system via algebraic μ-synthesis. *Proceedings of the 15th Mediterranean Conference on Control and Automation*.
- HE, D., HUANG, H. & CHEN, Q. (2014) Stabilizing model predictive control of time-varying non-linear systems using linear matrix inequalities. *IMA J. Math. Control Inf.*, 1–15.
- JOHANSSON, K. (2000) The quadruple-tank process: a multivariable laboratory process with an adjustable zero. *IEEE Trans. Control Syst. Technol.*, **8**, 456–465.
- KOTHARE, M., BALAKRISHNAN, V. & MORARI, M. (1996) Robust constrained model predictive control using linear matrix inequalities. *Automatica*, **32**, 1361–1379.
- KOUVARITAKIS, B., ROSSITER, J. & SCHUURMANS, J. (2000) Efficient robust predictive control. *IEEE Trans. Automat. Control*, **45**, 1545–1549.
- LEE, Y. & KOUVARITAKIS, B. (2002) Superposition in efficient robust constrained predictive control. *Automatica*, **38**, 875–878.
- Li, D. & Xi, Y. (2011) Constrained feedback robust model predictive control for polytopic uncertain systems with time delays. *Int. J. Syst. Sci.*, **42**, 1651–1660.
- Löfberg, J. (2004) YALMIP: a toolbox for modeling and optimization in MATLAB. *Proceedings of IEEE International Symposium on Computer Aided Control Systems Design*, pp, 284–289.

- MAO, W. (2003) Robust stabilization of uncertain time-varying discrete systems and comments on 'an improved approach for constrained robust model predictive control'. *Automatica*, **39**, 1109–1112.
- NGUYEN, H., GUTMAN, P., OLARU, S. & HOVD, M. (2013) Implicit improved vertex control for uncertain, time-varying linear discrete-time systems with state and control constraints. *Automatica*, **49**, 2754–2759.
- NGUYEN, H., OLARU, S. & HOVD, M. (2012) A patchy approximation of explicit model predictive control. Int. J. Control, 85, 1929–1941.
- PLUYMERS, P., ROSSITER, J., SUYKENS, J. & MOORE, B. (2005a) The efficient computation of polyhedral invariant sets for linear systems with polytopic uncertainty. *Proceedings of the American Control Conference*, pp. 804–809.
- PLUYMERS, P., ROSSITER, J., SUYKENS, J. & MOORE, B. (2005b) Interpolation based MPC for LPV systems using polyhedral invariant sets. *Proceedings of the American Control Conference*, pp. 810–815.
- QIN, S. & BADGWELL, T. (2003) A survey of industrial model predictive control technology. *Control Eng. Practice*, 11, 733–764.
- ROSSITER, J., KOUVARITAKIS, B. & BACIC, M. (2004) Interpolation based computationally efficient predictive control. *Int. J. Control*, 77, 290–301.
- Schuurmans, J. & Rossiter, J. (2000) Robust predictive control using tight sets of predicted states. *IEE Proc. Control Theory Appl.*, **147**, 13–18.
- TÜTÜNCÜ, R., ТОН, K. & TODD, M. (2003) Solving semidefinite-quadratic-linear programs using SDPT3. *Math. Prog. Ser. B*, **95**, 189–217.
- Veselý, V., Rosinová, D. & Foltin, M. (2010) Robust model predictive control design with input constraints. *ISA Trans.*, **49**, 114–120.
- WADA, N., SAITO, K. & SAEKI, M. (2006) Model predictive control for linear parameter varying systems using parameter dependent lyapunov function. *IEEE T. Circuits Syst.*, **53**, 1446–1450.
- WAN, Z. & KOTHARE, M. (2003) An efficient off-line formulation of robust model predictive control using linear matrix inequalities. *Automatica*, **39**, 837–846.
- WANG, C. (2012) Robust model predictive control by iterative optimisation for polytopic uncertain systems. *Int. J. Syst. Sci.*, **43**, 1656–1663.



Chemical Engineering Communications



Date: 11 April 2016, At: 19:58

ISSN: 0098-6445 (Print) 1563-5201 (Online) Journal homepage: http://www.tandfonline.com/loi/gcec20

An Off-Line Formulation of Tube-Based Robust MPC Using Polyhedral Invariant Sets

Pornchai Bumroongsri & Soorathep Kheawhom

To cite this article: Pornchai Bumroongsri & Soorathep Kheawhom (2016) An Off-Line Formulation of Tube-Based Robust MPC Using Polyhedral Invariant Sets, Chemical Engineering Communications, 203:6, 736-745, DOI: 10.1080/00986445.2015.1089402

To link to this article: http://dx.doi.org/10.1080/00986445.2015.1089402

| | Accepted author version posted online: 17 Sep 2015. |
|-----------|---|
| | Submit your article to this journal 🗗 |
| ılıl | Article views: 53 |
| a a | View related articles 🗷 |
| CrossMark | View Crossmark data 🗗 |

Full Terms & Conditions of access and use can be found at http://www.tandfonline.com/action/journalInformation?journalCode=gcec20

ISSN: 0098-6445 print/1563-5201 online DOI: 10.1080/00986445.2015.1089402



An Off-Line Formulation of Tube-Based Robust MPC Using Polyhedral Invariant Sets

PORNCHAI BUMROONGSRI1 and SOORATHEP KHEAWHOM2

¹Department of Chemical Engineering, Mahidol University, Nakhon Pathom, Thailand

In this paper, an off-line formulation of tube-based robust model predictive control (MPC) using polyhedral invariant sets is proposed. A novel feature is the fact that no optimal control problem needs to be solved at each sampling time. Moreover, the proposed tube-based robust MPC algorithm can deal with the linear time-varying (LTV) system with bounded disturbance. The simulation results show that the state at each time step is restricted to lie within a tube whose center is the state of the nominal LTV system that converges to the origin. Finally, the state is kept within a tube whose center is at the origin, so robust stability is guaranteed. Satisfaction of the state and control constraints is guaranteed by employing tighter constraint sets for the nominal LTV system.

Keywords: Bounded disturbance; Linear time-varying system; Robust stability; Tube-based robust MPC

Introduction

Tube-based robust model predictive control (MPC) is an advanced control algorithm that can deal with model uncertainty. The basic idea of tube-based robust MPC is to maintain a state trajectory of an uncertain system inside a sequence of tubes (Rawlings and Mayne, 2009). Tube-based robust MPC is motivated by the fact that a real state trajectory differs from a state trajectory of a nominal system due to uncertainty (Mayne and Langson, 2001). Chisci et al. (2001) developed a tube-based robust model predictive controller for the linear time-invariant (LTI) system subject to bounded disturbance. The control law has the form u = Kx + c, where K is obtained by solving an unconstrained linear quadratic regulator (LQR) problem, x is the state, and c is the vanishing input, that is, $c_i = 0$ for $i \ge \text{control horizon}$. The objective is to drive the state of an uncertain system to a terminal set while using c as little as possible. Constraint fulfillment is guaranteed by replacing the original constraints with more stringent ones. A larger control horizon implies better control performance at the price of a higher computational load, so a suitable trade-off is required. Langson et al. (2004) proposed tube-based robust MPC employing the time-varying control inputs instead of the LTI control law. A sequence of time-varying control inputs is obtained by solving an optimal control problem subject to the additional constraint sets in order to guarantee robust stability. Since

Address correspondence to P. Bumroongsri, Department of Chemical Engineering, Mahidol University, Nakhon Pathom, Thailand. E-mail: pornchai.bum@mahidol.ac.th

Color versions of one or more of the figures in the article can be found online at www.tandfonline.com/gcec.

the control inputs are time-varying, the proposed MPC algorithm can achieve better control performance than the conventional tube-based MPC algorithm using the LTI control law. The price to be paid is the computational complexity that increases with the prediction horizon.

Mayne et al. (2005) established robust exponential stability of the disturbance invariant set for the LTI system with bounded disturbance. The optimal control problem solved at each sampling time includes the initial state of the nominal model as a decision variable. The result is that the value function is zero in the disturbance invariant set so robust exponential stability of the disturbance invariant set can be established. The control law has the form $u = K(x - \bar{x}) +$ \bar{u} , where \bar{x} and \bar{u} are the state and control inputs of the nominal system, respectively. Higher online computational time is required because the optimal control problem with increased decision variable has to be solved at each sampling time. In the case when the state of the LTI system with bounded disturbance is not exactly known, tube-based robust MPC can be implemented based on the observer state as proposed by Mayne et al. (2006). A simple Luenberger observer is employed to estimate the state. The state estimation and control errors at each time step are bounded by minimal robust positively invariant sets. Hence, the actual and observer states are restricted to lie within tubes whose center is the state of the nominal system. The control law has the form $u = K(\hat{x} - \bar{x}) + \bar{u}$, where \hat{x} is the observer state. The controller is based on the observer state so the state \bar{x} and control input \bar{u} of the nominal system are subject to tighter constraint sets than the case when the state is exactly known. In Mayne et al. (2009), this idea is extended to the case when the initial state estimation error does not lie

²Department of Chemical Engineering, Chulalongkorn University, Bangkok, Thailand

in the minimal robust positively invariant set but it lies in the time-varying set that converges to the minimal robust positively invariant set. In this case, higher online computational time is required because the time-varying set is computed online.

Tube-based robust MPC for tracking of LTI system with bounded disturbance was presented by Limon et al. (2010). The artificial steady variables are introduced as the decision variables in the optimal control problem. If the target is unreachable, the system will be steered to the neighborhood of the artificial target. The proposed MPC algorithm is suitable for the system whose target is significantly changed. However, the main drawback is that the proposed MPC algorithm requires high online computational time because some of the decision variables and constraints are introduced to the optimal control problem. Gonzalez et al. (2011) proposed tube-based robust MPC for tracking of linear time-varying (LTV) system subject to bounded disturbance. The proposed MPC algorithm requires an additional assumption that the time-varying parameter at each step within the prediction horizon is known a priori. Then, a reachable set at each time step is calculated instead of a disturbance invariant set in order to reduce the conservativeness. Although the conservativeness is reduced, the computational problem is more severe because both optimal control problem and reachable set are computed online.

In this paper, an off-line formulation of tube-based robust MPC using polyhedral invariant sets is proposed. The main contributions are that: (i) we propose tube-based robust MPC that solves all of the optimal control problems off-line. so no optimal control problem needs to be solved online; (ii) the proposed tube-based robust MPC algorithm can deal with LTV system subject to bounded disturbance. Unlike Gonzalez et al. (2011), the proposed algorithm does not require an additional assumption that the time-varying parameter at each step within the prediction horizon is known a priori. This article is organized as follows. The backgrounds of the conventional tube-based robust MPC are described in Backgrounds of Conventional Tube-Based Robust MPC section. In An Off-Line Formulation of Tube-Based Robust MPC Using Polyhedral Invariant Sets section, off-line tube-based robust MPC is proposed. In Illustrative Example section, the simulation results are presented. The conclusions are then drawn in Conclusions section.

Nomenclature

Given two subsets X and Y of \mathbb{R}^n , Minkowski set addition and set difference are defined, respectively, by $X \oplus Y$: = $\{x+y|x\in X,\ y\in Y\}$ and $X\ominus Y$: = $\{x|x\oplus Y\subseteq X\}$. The distance of a point $x\in\mathbb{R}^n$ from a set $Y\subseteq\mathbb{R}^n$ is denoted by $d(x,\ Y)$: = $\inf\{|x-y||y\in Y\}$ where $|\cdot|$ denotes the Euclidean norm. The distance of a point $x\in\mathbb{R}^n$ from a point $y\in\mathbb{R}^n$ is denoted by $d(x,\ y)$: = |x-y|. For a matrix A, A>0 means that A is a positive-definite matrix and A<0 means that A is a negative-definite matrix. The spectral radius of a matrix A is denoted by $\rho(A)$. Conv $\{\cdot\}$ denotes the convex hull of the elements in $\{\cdot\}$.

Backgrounds of Conventional Tube-Based Robust MPC

In this section, some relevant backgrounds for the conventional tube-based robust MPC are presented. Consider the following discrete-time LTI system with disturbance

$$x^+ = Ax + Bu + w \tag{1}$$

where $x \in \mathbb{R}^n$ is the state, $u \in \mathbb{R}^m$ is the control input, $w \in \mathbb{R}^n$ is the bounded disturbance, and $x^+ \in \mathbb{R}^n$ is the successor state. The system is subject to the state constraint $x \in \mathbb{X}$ and the control constraint $u \in \mathbb{U}$, where $\mathbb{X} \subset \mathbb{R}^n$ and $\mathbb{U} \subset \mathbb{R}^m$ are compact, convex, and each set contains the origin as an interior point. The disturbance is bounded, that is, $w \in \mathbb{W}$ where $\mathbb{W} \subset \mathbb{R}^n$ is compact, convex, and contains the origin as an interior point. The objective is to robustly stabilize the system in Equation (1). The presence of a persistent disturbance w means it is not possible to regulate the state x to the origin. The best that can be hoped for is to regulate the state to a neighborhood of the origin.

Let the nominal system be defined by

$$\bar{x}^+ = A\bar{x} + B\bar{u} \tag{2}$$

where $\bar{x} \in \mathbb{R}^n$ and $\bar{u} \in \mathbb{R}^m$ are the state and control inputs of the nominal system, respectively. The predicted nominal state trajectory and control sequence when the initial state is \bar{x}_0 are denoted by $\bar{\mathbf{x}} := \{\bar{x}_0, \bar{x}_1, \dots, \bar{x}_N\}$ and $\bar{\mathbf{u}} := \{\bar{u}_0, \bar{u}_1, \dots, \bar{u}_{N-1}\}$, respectively, where N is the prediction horizon. Consider the following equation which is the difference between Equations (1) and (2)

$$x^{+} - \bar{x}^{+} = A(x - \bar{x}) + B(u - \bar{u}) + w \tag{3}$$

In order to counteract the effect of disturbance, the control law $u = K(x - \bar{x}) + \bar{u}$ is employed, where K is the disturbance rejection gain. The system in Equation (3) is rewritten as

$$x^{+} - \bar{x}^{+} = (A + BK)(x - \bar{x}) + w \tag{4}$$

We will bound $x^+ - \bar{x}^+$ by a robust positively invariant set Z. The definition of Z for the LTI system with disturbance is as follows:

Definition 1. The set $Z \subset \mathbb{R}^n$ is a robust positively invariant set of the LTI system with disturbance $x^+ = Ax + w$, if $AZ \oplus \mathbb{W} \subseteq Z$ for $\forall x \in Z$ and $\forall w \in \mathbb{W}$.

For the system in Equation (4), it is clear that if K is chosen such that $\rho(A+BK)<1$, we can bound $x^+ - \bar{x}^+$ by a robust positively invariant set Z satisfying $(A+BK)Z \oplus \mathbb{W} \subseteq Z$ for $\forall (x-\bar{x}) \in Z$ and $\forall w \in \mathbb{W}$. It is desirable that Z be as small as possible. The minimal Z can be calculated as (Kolmanovsky and Gilbert, 1998):

$$Z = \bigoplus_{i=0}^{\infty} (A + BK)^{i} \mathbb{W} = \mathbb{W} \oplus (A + BK)$$
$$\mathbb{W} \oplus (A + BK)^{2} \mathbb{W} \oplus (A + BK)^{3} \mathbb{W} \oplus \dots$$
(5)

If (A + BK) is nilpotent with index s, that is, $(A + BK)^s = 0$, then Z in Equation (5) can be finitely determined. In the case when (A + BK) is not nilpotent, Z in Equation (5) can be approximated by using the method in Raković (2005) and Raković et al. (2005).

Since $x^+ - \bar{x}^+$ is bounded by Z, we can control the nominal system $\bar{x}^+ = A\bar{x} + B\bar{u}$ in such a way that LTI system with disturbance $x^+ = Ax + Bu + w$ satisfies the original state and control constraints $x \in \mathbb{X}$ and $u \in \mathbb{U}$, respectively. To achieve this, the tighter constraint sets for the nominal system are employed $\bar{x}_i \in \mathbb{X} \ominus Z$, $\bar{u}_i \in \mathbb{U} \ominus KZ$ for $i \in \{0, \ldots, N-1\}$. In order to ensure stability, an additional terminal constraint is employed $\bar{x}_N \in \overline{X}_f \subset \mathbb{X} \ominus Z$ where \bar{X}_f is the terminal constraint set. The cost function for a trajectory of the nominal system $\bar{x}^+ = A\bar{x} + B\bar{u}$ is

$$V_N(\bar{\mathbf{x}}_0, \bar{\mathbf{u}}) := \sum_{i=0}^{N-1} l(\bar{\mathbf{x}}_i, \bar{\mathbf{u}}_i) + V_f(\bar{\mathbf{x}}_N)$$
 (6)

where $l(\bar{x}_i, \bar{u}_i) := \frac{1}{2} [\bar{x}_i^T Q \bar{x}_i + \bar{u}_i^T R \bar{u}_i]$ is the stage cost; $V_f(\bar{x}_N) := \frac{1}{2} \bar{x}_N^T P \bar{x}_N$ is the terminal cost; Q, R, and P are the positive definite weighting matrices. The terminal constraint set and the terminal cost must satisfy the following usual assumptions (Mayne et al., 2000):

Assumption 1. $(A + BK)\bar{X}_f \subset \bar{X}_f, \bar{X}_f \subset \mathbb{X} \ominus Z, K\overline{X}_f \subset \mathbb{U} \ominus ; KZ.$

Assumption 2.
$$V_f((A+BK)\bar{x}) + l(\bar{x},K\bar{x}) \leq V_f(\bar{x}), \forall \bar{x} \in \bar{X}_f$$
.

In summary, at each sampling time the state x is measured and the following optimization problem is solved online:

$$\min_{\bar{\mathbf{x}}_0,\bar{\mathbf{u}}} V_N(\bar{\mathbf{x}}_0,\bar{\mathbf{u}}) \tag{7}$$

such that
$$x \in \bar{x}_0 \oplus Z$$
 (8)

$$\bar{\mathbf{x}}_{i+1} = A\bar{\mathbf{x}}_i + B\bar{\mathbf{u}}_i, \ i \in \{0, \dots, N-1\}$$
 (9)

$$\bar{x}_i \in \mathbb{X} \ominus Z, \bar{u}_i \in \mathbb{U} \ominus KZ, i \in \{0, \dots, N-1\}$$
 (10)

$$\bar{\mathbf{x}}_N \in \overline{X}_f$$
 (11)

Then, the control law $u = K(x - \bar{x}) + \bar{u}$, $\bar{x} = \bar{x}_0$, $\bar{u} = \bar{u}_0$ is implemented to the process.

An Off-Line Formulation of Tube-Based Robust MPC Using Polyhedral Invariant Sets

It is seen that the conventional tube-based robust MPC in Backgrounds of Conventional Tube-Based Robust MPC section does not include a time-varying parameter in the problem formulation. Moreover, the optimal control problem must be solved at each sampling time. In this section, an off-line formulation of tube-based robust MPC is presented. No optimal control problem needs to be solved online. Additionally, the time-varying parameter is included in the problem formulation. Consider the following

discrete-time LTV system with disturbance

$$x^{+} = A^{\lambda}x + B^{\lambda}u + w \tag{12}$$

The descriptions for the state $x \in \mathbb{X}$, the control input $u \in \mathbb{U}$, and the disturbance $w \in \mathbb{W}$ are the same as in Backgrounds of Conventional Tube-Based Robust MPC section. The only difference is that, in this case, the matrices A^{λ} and B^{λ} are not constant but they vary with the time-varying parameter λ . The time-varying parameter λ can be measured at each sampling time but its future values are uncertain. We make the following assumption:

Assumption 3. $[A^{\lambda}B^{\lambda}] \in \text{Conv}\{[A_jB_j], \forall j \in 1, 2, ..., L\}$, where $[A_jB_j]$ are vertices of the convex hull and L is the number of vertices of the convex hull. The pair $[A_j B_j]$ is controllable.

Let the nominal LTV system be defined by

$$x'^{+} = A^{\lambda}x' + B^{\lambda}u' \tag{13}$$

where $x' \in \mathbb{R}^n$ and $u' \in \mathbb{R}^m$ are the state and control inputs of the nominal LTV system, respectively. The predicted state trajectory and control sequence when the initial state is x'_0 are denoted by $\mathbf{x}' := \{x'_0, x'_1, \dots, x'_N\}$ and $\mathbf{u}' := \{u'_0, u'_1, \dots, u'_{N-1}\}$, respectively. Consider the following equation which is the difference between the systems in Equations (12) and (13):

$$x^{+} - x'^{+} = A^{\lambda}(x - x') + B^{\lambda}(u - u') + w \tag{14}$$

In order to counteract the effect of disturbance, the control law u = K(x - x') + u' is employed where K is the disturbance rejection gain. The system in Equation (14) is rewritten as

$$x^{+} - x'^{+} = (A^{\lambda} + B^{\lambda}K)(x - x') + w \tag{15}$$

We will bound $x^+ - x'^+$ by a robust positively invariant set Z. The definition of Z for the LTV system with disturbance is as follows:

Definition 2. The set $Z \subset \mathbb{R}^n$ is a robust positively invariant set of the LTV system with disturbance $x^+ = A^{\lambda}x + w$, if $A^{\lambda}Z \oplus \mathbb{W} \subseteq Z$ for $\forall x \in Z, \forall w \in \mathbb{W}$, and $\forall A^{\lambda} \in \text{Conv}\{A_j, \forall j \in 1, 2, ..., L\}$.

For the system in Equation (15), it is clear that if K satisfies $(A_j + B_j K)^T P(A_j + B_j K) - P < 0$, $\forall j \in \{1, ..., L\}$ where P is a Lyapunov matrix, then $(A^{\lambda} + B^{\lambda} K)^T P(A^{\lambda} + B^{\lambda} K) - P < 0$, $\forall [A^{\lambda} B^{\lambda}] \in \text{Conv}\{[A_j B_j], \forall j \in 1, 2, ..., L\}$ and we can bound $x^+ - x'^+$ by a robust positively invariant set Z satisfying $(A^{\lambda} + B^{\lambda} K)Z \oplus \mathbb{W} \subseteq Z$ for $\forall (x - x') \in Z$, $\forall w \in \mathbb{W}$ and $\forall [A^{\lambda} B^{\lambda}] \in \text{Conv}\{[A_j B_j], \forall j \in 1, 2, ..., L\}$. It is desirable that Z be as small as possible. Unlike Equation (5), in the case of the LTI system with disturbance, the minimal Z of the LTV system with disturbance is $Z = \bigoplus_{i=0}^{\infty} (A^{\lambda} + B^{\lambda} K)^i$ \mathbb{W} . Since $[A^{\lambda} B^{\lambda}] \in \text{Conv}\{[A_j B_j], \forall j \in 1, 2, ..., L\}$, the minimal

Z of the LTV system with disturbance can be calculated as

$$Z = \mathbb{W} \oplus \operatorname{Conv}\{(A_j + B_j K) \mathbb{W}, \forall j \in 1, 2, \dots, L\}$$

$$\oplus \operatorname{Conv}\{(A_j + B_j K)(A_l + B_l K), \mathbb{W} \forall j, l \in 1, 2, \dots, L\}$$

$$\oplus \{\operatorname{Conv}(A_j + B_j K)(A_l + B_l K)(A_m + B_m K)$$

$$\mathbb{W}, \forall j, l, m \in 1, 2, \dots, L\} \oplus \dots$$
(16)

Defining $F_s := \bigoplus_{i=0}^{s-1} (A^{\lambda} + B^{\lambda}K)^i \mathbb{W}$, F_s can be properly scaled for some finite integer s to obtain the outer approximation of Z in Equation (16). Since we can bound $x^+ - x^{\prime +}$ by Z, the following proposition can be established:

Proposition 1. If $x \in x' \oplus Z$ and u = K(x - x') + u', then $x^+ \in x'^+ \oplus Z$ for $\forall w \in \mathbb{W}$ and $\forall [A^{\lambda}B^{\lambda}] \in \text{Conv}\{[A_jB_j], \forall j \in \{1, 2, ..., L\}.$

Proposition 1 states that the control law u = K(x - x') + u'keeps the state x of the LTV system with disturbance $x^{+} = A^{\lambda}x + B^{\lambda}u + w$ close to the state x' of the nominal LTV system $x'^{+} = A^{\lambda}x' + B^{\lambda}u'$. It is clear that if we can regulate x' to the origin, then x must be regulated to a robust positively invariant set Z whose center is at the origin. An off-line robust MPC algorithm for the nominal LTV system $x'^{+} = A^{\lambda}x' + B^{\lambda}u'$ has been developed by Bumroongsri and Kheawhom (2012). The problem of regulating the state x'to the origin has been considered. In this approach, a sequence of stabilizing feedback gains F corresponding to a sequence of polyhedral invariant sets P_i , $i = \{1, ..., N_p\}$, where $N_{\rm p}$ is the number of polyhedral invariant sets, is precomputed off-line by solving the optimal control problems subject to LMI constraints (Boyd and Vandenberghe, 2004). At each sampling time, the state x' is measured and the smallest P containing x' is determined. Then, we set the real-time stabilizing feedback gain F equal to F and apply the control law u' = Fx' to the process. The control law u' = Fx' minimizes the following cost function:

$$V_{\infty}(x_0', \mathbf{u}') := \max_{[A^{\lambda}B^{\lambda}] \in \operatorname{Conv}\{[A_jB_j], \forall j \in 1, 2, \dots, L\}} \sum_{i=0}^{\infty} x_i'^T$$

$$Qx_i' + (Fx_i')^T R(Fx_i') \tag{17}$$

where x'_i is the state of the nominal LTV system at prediction time i and Q and R are the positive-definite weighting matrices. Additionally, the control law u' = Fx' ensures that the Lyapunov function $V(x') := {x'}^T Px'$ is a strictly decreasing function satisfying

$$V(x'^{+}) - V(x') \le -x'^{T} Q x' - (Fx')^{T} R(Fx'), \, \forall [A^{\lambda} B^{\lambda}] \in \text{Conv}\{[A_{j} B_{j}], \, \forall j \in 1, 2, \dots, L\}$$
(18)

where P is a Lyapunov matrix. At each sampling time, although the future values of the time-varying parameter λ in the prediction horizon (which is the infinite horizon in this case) are unknown, the satisfaction of Equation (18) for the stabilizing feedback gain F ensures that the time-varying set of all future states $R_{i+1} = (A^{\lambda} + B^{\lambda}F)R_i$, $R_o = \{x_0'\}$, converges to the origin $d(0, R_{i+1}) \rightarrow 0$, $\forall [A^{\lambda}B^{\lambda}] \in \text{Conv}$

 $\{[A_jB_j], \forall j \in 1, 2, \dots, L\}$. Hence, robust stability of the nominal LTV system $x'^+ = (A^{\lambda} + B^{\lambda}F)x'$ is guaranteed. In order to guarantee satisfaction of the original state and control constraints, $x \in \mathbb{X}$ and $u \in \mathbb{U}$, we must employ tighter constraint sets for the nominal LTV system, that is, $x' \in \mathbb{X} \ominus \mathbb{Z}$ and $Fx' \in \mathbb{U} \ominus K\mathbb{Z}$. The control law u = K(x - x') + u' is now rewritten as u = K(x - x') + Fx'. An important consequence is the following result:

Proposition 2 If $x \in x' \oplus Z$, $x' \in \mathbb{X} \ominus Z$, and $Fx' \in \mathbb{U} \ominus KZ$, then the control law u = K(x - x') + Fx' of the LTV system with disturbance $x^+ = A^{\lambda}x + B^{\lambda}u + w$ ensures satisfaction of the original constraints $x \in \mathbb{X}$, $u \in \mathbb{U}$ for $\forall w \in \mathbb{W}$ and $\forall [A^{\lambda}B^{\lambda}] \in \text{Conv}\{[A_{j}B_{j}], \forall j \in 1, 2, \dots, L\}$.

Proposition 2 states that the control law u = K(x - x') + Fx' ensures satisfaction of the original state and control constraints. In summary, off-line tube-based robust MPC for LTV system with disturbance $x^+ = A^{\lambda}x + B^{\lambda}u + w$ can be formulated as follows:

Off-line:

Step 1: Calculate the disturbance rejection gain K satisfying $(A_j + B_j K)^T P(A_j + B_j K) - P < 0$, $\forall j \in \{1, ..., L\}$. Then, calculate a tube Z in Equation (16).

Step 2: Calculate a sequence of stabilizing feedback gains F_i and the corresponding sequence of polyhedral invariant sets P_i , $i = \{1, ..., N_p\}$ using the method in Bumroongsri and Kheawhom (2012) with tighter constraint sets for the nominal LTV system, that is, $x' \in \mathbb{X} \ominus Z$ and $Fx' \in \mathbb{U} \ominus KZ$.

Online:

At the first sampling time (t=0): Measure the state x and the time-varying parameter λ . Find the smallest polyhedral invariant set P_i containing the measured state x, set $F=F_i$ and apply the control law u=Fx to the process. Then, calculate x'^+ from $x'^+=(A^\lambda+B^\lambda F)x$. (Note that at the first sampling time, x=x' so the control law u=K(x-x')+Fx' is reduced to u=Fx.)

At each sampling time (t > 0): Measure the state x and the time-varying parameter λ . Find the smallest polyhedral invariant set P_i containing x' (which is calculated from the previous step), set $F = F_i$, and apply the control law u = K(x - x') + Fx' to the process. Then, calculate x'^+ from $x'^+ = (A^{\lambda} + B^{\lambda}F)x'$.

Theorem 1. The proposed tube-based MPC algorithm steers any initial state x of the system $x^+ = A^{\lambda}x + B^{\lambda}u + w$ in a sequence of polyhedral invariant sets P_i , $i = \{1, ..., N_p\}$ to a robust positively invariant set Z whose center is at the origin and thereafter maintains the state in Z for $\forall w \in \mathbb{W}$ and $\forall [A^{\lambda}B^{\lambda}] \in \text{Conv}\{[A_jB_j], \forall j \in 1, 2, ..., L\}.$

Proof. Consider the following difference equation between $x^+ = A^{\lambda}x + B^{\lambda}u + w$ and $x'^+ = A^{\lambda}x' + B^{\lambda}u'$, where u = K(x - x') + Fx' and u' = Fx',

$$x^{+} - x'^{+} = (A^{\lambda} + B^{\lambda}K)(x - x') + w$$
 (19)

The disturbance rejection gain K satisfies $(A_1 + B_1K)^T$ $P(A_1 + B_1K) - P < 0$, $\forall j \in \{1, ..., L\}$ so $x^+ - x'^+$ is bounded by a robust positively invariant set Z, that is, $x^+ \in x'^+ \oplus Z$. Since the stabilizing feedback gain F ensures that the Lyapunov function is a strictly decreasing function satisfying Equation (18), the state x'^+ must converge to the origin $d(x'^+, 0) \to 0$. Since $x^+ \in x'^+ \oplus Z$, x^+ must converge to a tube Z whose center is at the origin $d(x^+, Z) \to 0$. Finally, the disturbance rejection controller u = Kx keeps the state within a tube Z whose center is at the origin.

Corollary 1. The state of the LTV system with disturbance $x^+ = A^{\lambda}x + B^{\lambda}u + w$ at each time step is restricted to lie within a tube whose center is the state of the nominal LTV system $x'^+ = A^{\lambda} x' + B^{\lambda}u'$.

Remark 1. For any initial state x contained in the first polyhedral invariant set P_1 (which is largest in the sequence of P_i , $i = \{1, ..., N_p\}$), there exists a control law that is able to steer the state to a tube Z whose center is at the origin by satisfying all state and control constraints $x \in \mathbb{X}$, $u \in \mathbb{U}$ for $\forall w \in \mathbb{W}$ and $\forall [A^{\lambda}B^{\lambda}] \in \text{Conv}\{[A_j \ B_j], \forall j \in 1, 2, ..., L\}$. Hence, the region of attraction for the proposed MPC algorithm is P_1 .

Illustrative Example

Example 1. Consider the following LTV system with bounded disturbance

$$x^{+} = \begin{bmatrix} 1 & 1 \\ 0 & \lambda \end{bmatrix} x + \begin{bmatrix} 0.5 \\ 1 \end{bmatrix} u + w \tag{20}$$

The state $x \in \mathbb{X}$, where \mathbb{X} : = $\{x \in \mathbb{R}^2 | [0 \ 1] x \le 2\}$; the control $u \in \mathbb{U}$, where \mathbb{U} : = $\{u \in ||u| \le 1\}$; the disturbance $w \in \mathbb{W}$, where $\mathbb{W} := \{w \in \mathbb{R}^2 | [-0.1 - 0.1^T \le w \le [0.10.1^T]\}$; and the time-varying parameter $\lambda \in \mathbb{L}$, where $\mathbb{L} := \{\lambda \in \mathbb{R} | 0.9 \le \lambda \le 1.1\}$. The weighting matrices in the cost function (Equation (17)) are given as Q = I and R = 0.01. The following nominal LTV system:

$$x'^{+} = \begin{bmatrix} 1 & 1 \\ 0 & \lambda \end{bmatrix} x' + \begin{bmatrix} 0.5 \\ 1 \end{bmatrix} u' \tag{21}$$

is subject to tighter state and control constraints, that is, $x' \in \mathbb{X} \ominus Z$ and $u' \in \mathbb{U} \ominus KZ$. The disturbance rejection gain K = [-0.66 - 1.33] satisfies $(A_j + B_jK)^T P(A_j + B_jK) - P < 0$, $\forall j \in \{1,2\}$. The difference equation between Equations (20) and (21) can be written as

$$x^{+} - x'^{+} = \begin{bmatrix} 1 & 1 \\ 0 & \lambda \end{bmatrix} (x - x') + \begin{bmatrix} 0.5 \\ 1 \end{bmatrix} (u - u') + w$$
 (22)

The closed-loop system is simulated using the initial state $x = x' = [-5 - 2]^T$. The time-varying parameter λ and the disturbance w are varied as $\lambda = 1 + 0.1\sin(4k)$ and

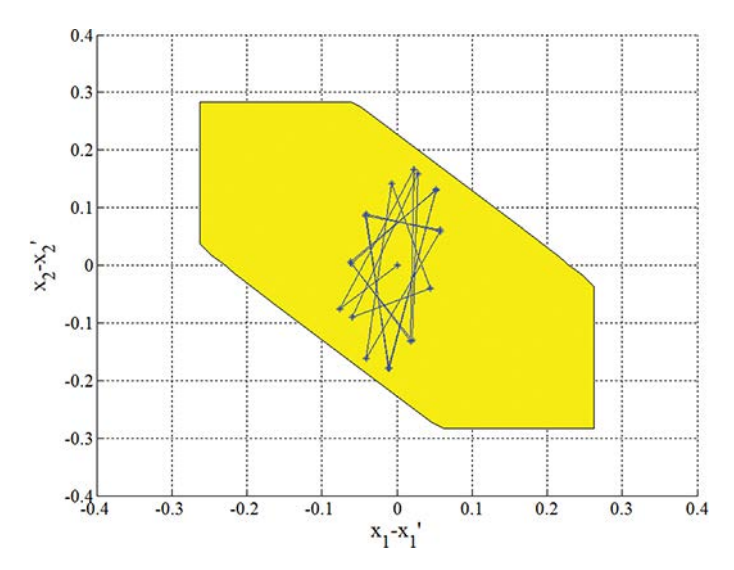


Fig. 1. The robust positively invariant set Z precomputed off-line. The set Z is shown in yellow.

 $w = [0.1 \sin(4k)0.1 \sin(4k)]^T$, respectively, where $k \in \{1, ..., 19\}$ is the simulation horizon.

Figure 1 shows a robust positively invariant set Z precomputed off-line. The set Z is shown in yellow. The blue line represents the trajectory of the difference Equation (22). Starting from the origin, it is seen that the trajectory of the difference equation is restricted to lie within the set Z.

Figure 2 shows a sequence of 10 polyhedral invariant sets P_i , $i \in \{1, ..., 10\}$ precomputed off-line. In this example, only 10 polyhedral invariant sets are precomputed because P_i are almost constant for i > 10. The red line represents the trajectory of the nominal LTV system (Equation (21)). Starting from the initial point $x = x' = [-5 - 2]^T$, the state of the nominal LTV system at each time step is restricted to lie within a sequence of 10 polyhedral invariant sets P_i , $i \in \{1, ..., 10\}$ precomputed off-line. Finally, the state of the nominal LTV system converges to the origin.

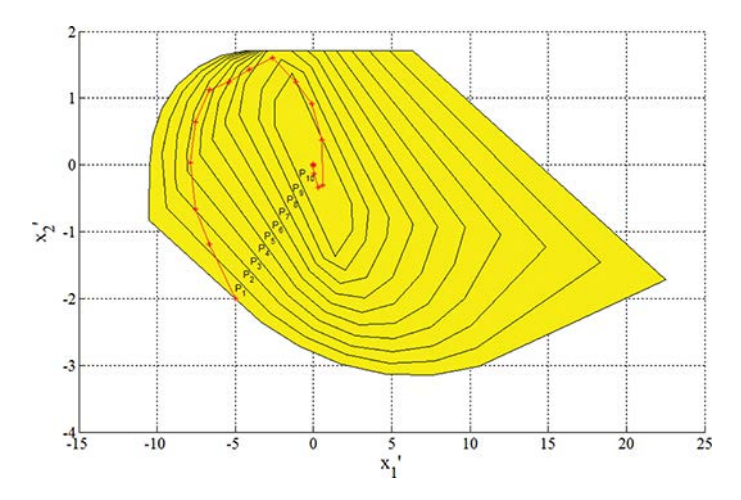


Fig. 2. A sequence of 10 polyhedral invariant sets P_i , $i \in \{1, ..., 10\}$ precomputed off-line. The polyhedral invariant sets are shown in yellow.

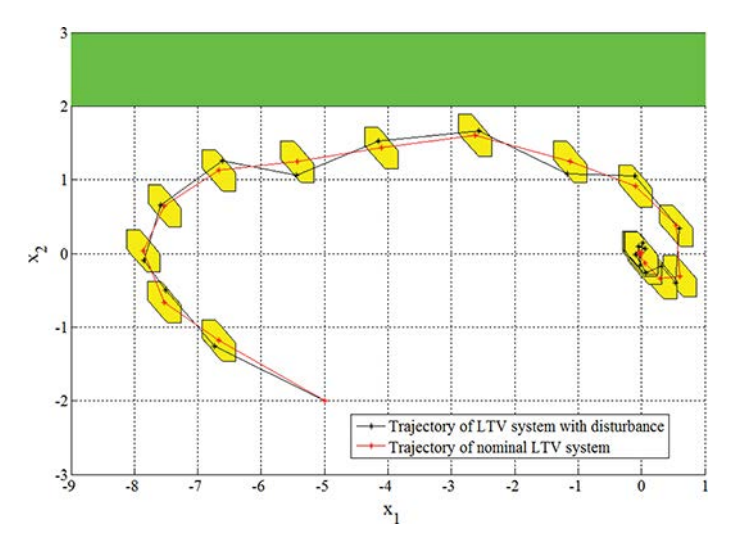


Fig. 3. The trajectory of the system when $\lambda = 1 + 0.1\sin(4k)$ and $w = [0.1\sin(4k)\ 0.1\sin(4k)]^T$. The infeasible region of state con-

The trajectory of the LTV system with disturbance (Equation (20)) is shown in Figure 3. The region shown in green is the infeasible region of the state constraint $X: = \{x \in \mathbb{R}^2 | [0\ 1]x \le 2\}$. The red line corresponds to the trajectory of the nominal LTV system (Equation (21)). The cross-section of a tube Z precomputed off-line is shown in yellow. It is seen that the state of the LTV system with disturbance at each time step is restricted to lie within a tube Z whose center is the state of the nominal LTV system that converges to the origin. Finally, the state of the LTV system with disturbance is kept within a tube Z whose center is at the origin.

Figure 4 shows the control input as a function of sampling time. The region shown in yellow is $U \ominus KZ$. The red line corresponds to the control input of the nominal LTV system (Equation (21)). The black line corresponds to the control input of the LTV system with disturbance (Equation (20)). It can be observed that the control input of the

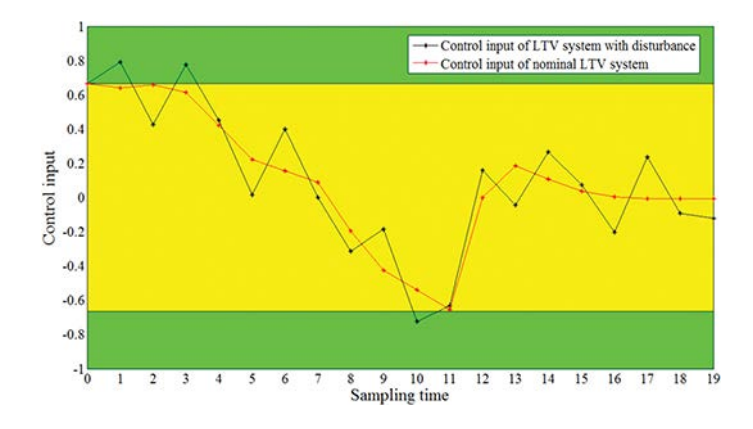


Fig. 4. The control input satisfying the input constraint U: = $\{u \in \mathbb{R} \mid |u| \le 1\}$. The tightened input constraint $U \ominus KZ$ is shown in yellow. The original input constraint U is shown in green.

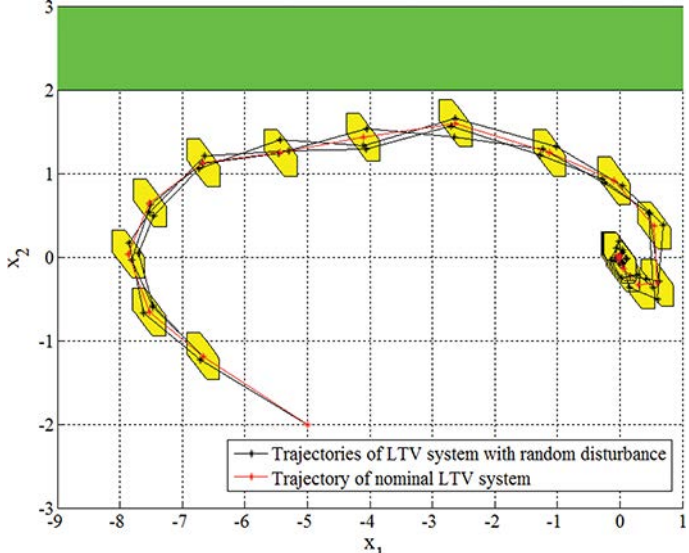


Fig. 5. The trajectories of the system when $\lambda = 1 + 0.1\sin(4k)$ and w are randomly time-varying. The infeasible region of state constraint is shown in green. The cross-section of tube is shown in yellow.

nominal LTV system is restricted to lie within the region $\mathbb{U} \ominus KZ$ so that the control input of the LTV system with disturbance satisfies the control constraint $\mathbb{U} := \{u \in ||u| < 1\}$.

Figure 5 shows the trajectories of the LTV system with disturbance (Equation (20)) when the disturbance $w \in W$ is randomly time-varying. At each time step, the states of the LTV system with random disturbance lie within a tube Z whose center is the state of the nominal LTV system that converges to the origin.

Example 2. In this example, the proposed algorithm is applied to a non-isothermal continuous stirred tank reactor (CSTR) in which an irreversible exothermic reaction $A \rightarrow B$ takes place. The dimensionless modeling equations of this CSTR can be written as (Silva and Kwong, 1999; Nagrath et al., 2002)

$$\frac{dx_1}{d\tau} = q(x_{1f} - x_1) - \varphi x_1 \exp\left(\frac{x_2}{1 + \frac{x_2}{\gamma}}\right) + w_1 \qquad (23)$$

$$\frac{dx_2}{d\tau} = q(x_{2f} - x_2) - \delta(x_2 - x_3) + \beta \varphi x_1 \exp\left(\frac{x_2}{1 + \frac{x_2}{\gamma}}\right) + w_2$$
(24)

$$\frac{dx_3}{d\tau} = \delta_1[q_c(x_{3f} - x_3) + \delta\delta_2(x_2 - x_3)] + w_3$$
 (25)

where x_1 is the dimensionless concentration of reactant A, x_2 is the dimensionless reactor temperature, and x_3 is the dimensionless cooling jacket temperature. The manipulated variable is the dimensionless coolant flow rate q_c . The disturbances acting on the system are w_1 , w_2 , and w_3 . By linearizing

and discretizing Equation (23) to Equation (25) with a sampling period ΔT , the following discrete-time state space model is obtained:

no disturbances (CSTR containing only time-varying parameter). It can be observed that the trajectory of the uncertain CSTR with disturbances lies in a sequence of tubes

$$\begin{bmatrix}
\bar{x}_{1}(k+1) \\
\bar{x}_{2}(k+1) \\
\bar{x}_{3}(k+1)
\end{bmatrix}$$

$$= \begin{bmatrix}
1 + \Delta T[-q - \varphi \kappa(x_{2S})] & -\Delta T \left[\frac{\varphi x_{1S} \kappa(x_{2S})}{(1 + \frac{x_{2S}}{\gamma})^{2}} \right] & 0 \\
\Delta T[\beta \varphi \kappa(x_{2S})] & 1 + \Delta T \left[-q - \delta + \frac{\beta \varphi \kappa(x_{2S}) x_{1S}}{(1 + \frac{x_{2S}}{\gamma})^{2}} \right] & \Delta T \delta \\
0 & \Delta T \delta \delta_{1} \delta_{2} & 1 - \Delta T[\delta_{1} q_{cS} + \delta \delta_{1} \delta_{2}]
\end{bmatrix}$$

$$\begin{bmatrix}
\bar{x}_{1}(k) \\
\bar{x}_{2}(k) \\
\bar{x}_{3}(k)
\end{bmatrix}$$

$$+ \begin{bmatrix}
0 \\
0 \\
\Delta T \delta_{1}[x_{3f} - x_{3S}]
\end{bmatrix} \bar{q}_{c}(k) + \Delta T \begin{bmatrix}
1 & 0 & 0 \\
0 & 1 & 0 \\
0 & 0 & 1
\end{bmatrix} \begin{bmatrix}
\bar{w}_{1}(k) \\
\bar{w}_{2}(k) \\
\bar{w}_{3}(k)
\end{bmatrix}$$

$$(26)$$

where $\bar{x}_1(k)=x_1(k)-x_{1S},\ \bar{x}_2(k)=x_2(k)-x_{2S},\ \bar{x}_3(k)=x_3(k)-x_{3S},\ \bar{q}_c(k)=q_c(k)-q_{cS},\ \bar{w}_1(k)=w_1(k)-w_{1S},\ \bar{w}_2(k)=w_2(k)-w_{2S},\ \bar{w}_3(k)=w_3(k)-w_{3S},\ \text{and}\ \kappa(x_{2S})=\exp\left(x_{2S}/1+\frac{x_{2S}}{\gamma}\right).$ The model parameter values are shown in Table I. The Damkohler number ϕ is considered to be uncertain and its value is randomly time-varying between $\phi_{\min}=0.0648$ and $\phi_{\max}=0.0792$. The disturbances $\bar{w}_1(k),\ \bar{w}_2(k),\ \text{and}\ \bar{w}_3(k)$ are randomly time-varying between -0.01 and 0.01. The constraints are $|\bar{x}_1(k)|\leq 0.5$ and $|\bar{q}_c(k)|\leq 1.0$. The weighting matrices in the cost function in Equation (17) are Q=I and R=0.1. The objective is to regulate the state from $(\bar{x}_1(0),\bar{x}_2(0),\bar{x}_3(0))=(0,5,0)$ to the neighborhood of the origin by manipulating $\bar{q}_c(k)$.

Figure 6 shows a sequence of four polyhedral invariant sets P, $i \in \{1, ..., 4\}$ precomputed off-line. Figure 7 shows the trajectory of the uncertain CSTR. The black line is the trajectory of the uncertain CSTR with disturbances (CSTR containing both time-varying parameter and disturbances). The red line is the trajectory of the uncertain CSTR with

Table I. The model parameter values in Example 2

| Parameter | Value | Parameter | Value |
|----------------|-----------------|-------------------------------|-------|
| \overline{q} | 1.0 | δ | 0.3 |
| x_{1f} | 1.0 | β | 8.0 |
| φ | 0.0648 - 0.0792 | $\overset{\cdot}{\delta}_{1}$ | 10 |
| γ | 20 | χ_{3f} | -1.0 |
| x_{2f} | 0.0 | δ_2^{-3} | 1.0 |
| x_{1S} | 0.8933 | w_{1S} | 0.0 |
| x_{2S} | 0.5193 | w_{2S} | 0.0 |
| x_{3S} | -0.5950 | w_{3S} | 0.0 |
| q_{cS} | 1.65 | | |

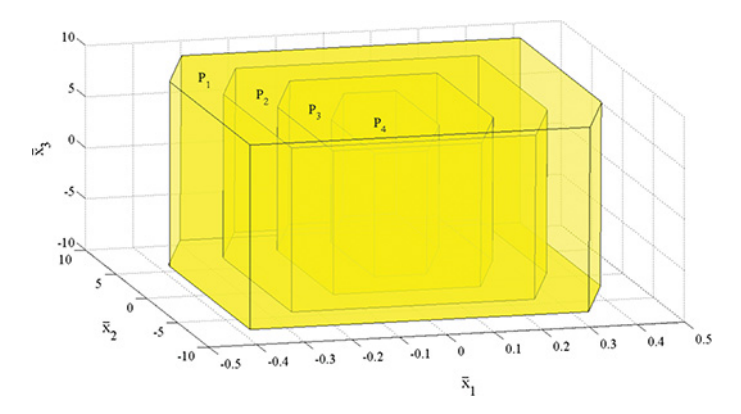


Fig. 6. A sequence of four polyhedral invariant sets P_i , $i \in \{1, ..., 4\}$ precomputed off-line. The polyhedral invariant sets are shown in yellow.

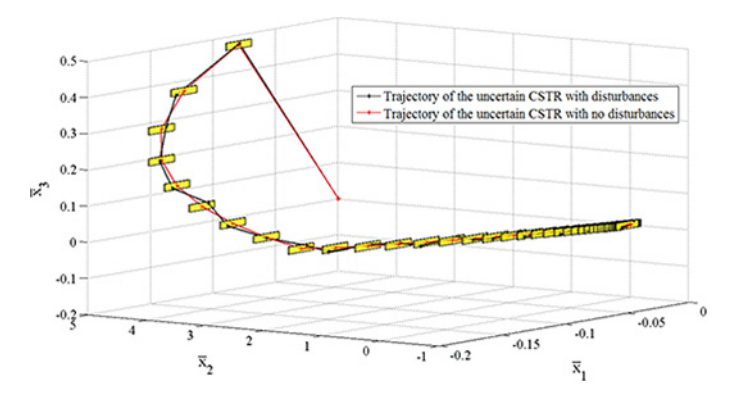


Figure 7. The trajectory of the uncertain CSTR. The cross-section of tube is shown in yellow.

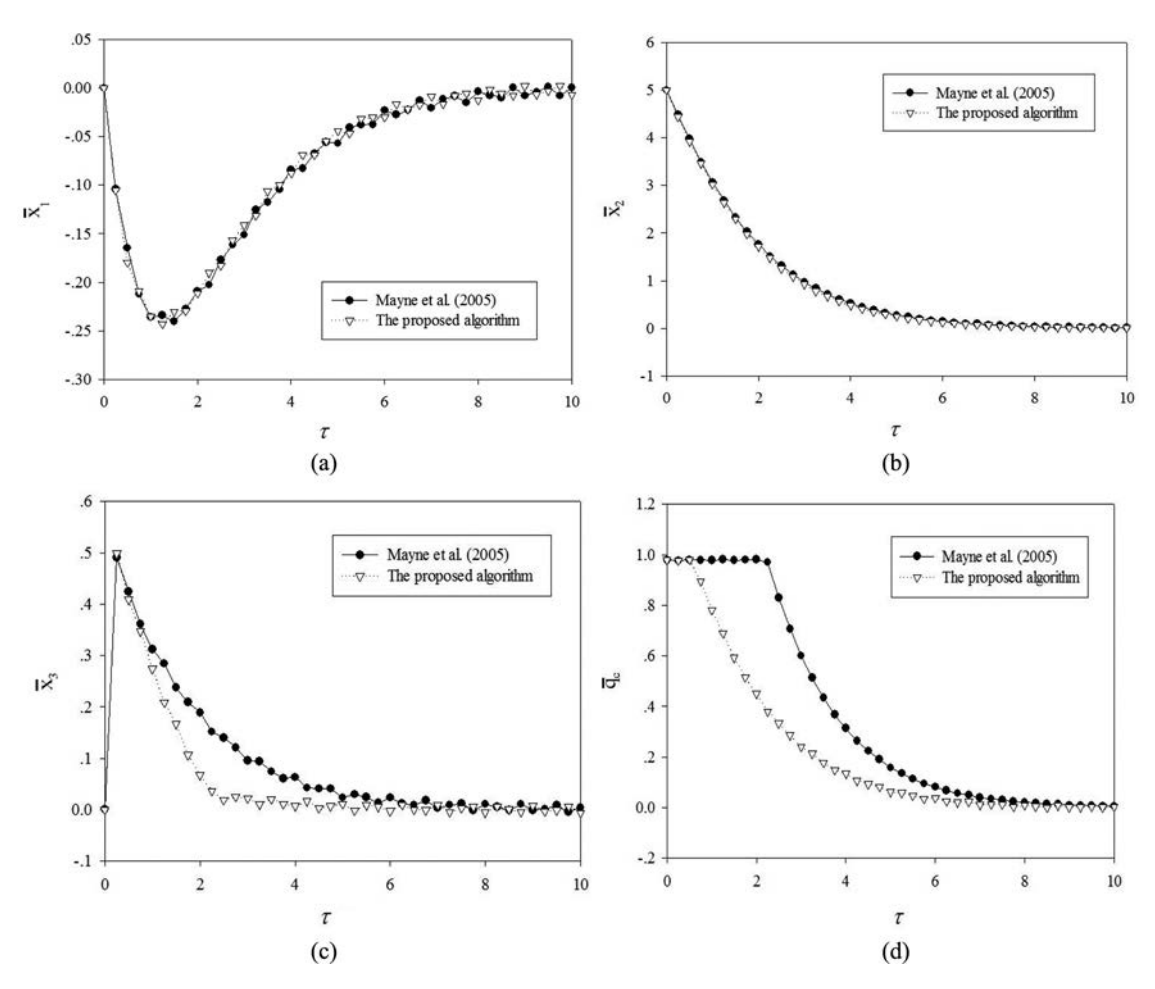


Fig. 8. The control performance (a) dimensionless concentration of reactant A; (b) dimensionless reactor temperature; (c) dimensionless cooling jacket temperature; and (d) dimensionless coolant flow rate.

shown in yellow. Finally, the state of the uncertain CSTR with disturbances is steered to a tube whose center is at the origin.

The proposed algorithm will be compared with tube-based robust MPC algorithm of Mayne et al. (2005) in which the online optimization problem must be solved at each sampling time. In Mayne et al. (2005), only disturbances are included in the controller design so there is a mismatch between the model and the process when the time-varying parameter is present. From Figure 8, it is seen that the proposed algorithm is able to steer the state of the uncertain CSTR with disturbances to the neighborhood of the origin faster than the algorithm of Mayne et al. (2005). Moreover, the proposed algorithm requires significantly less online computational time, as shown in Table II. The

Table II. The online computational time

| Algorithm | Online computational time for each step (s) |
|------------------------|---|
| Mayne et al. (2005) | 0.067 |
| The proposed algorithm | 0.015 |

computations are performed using Intel Core 2 Duo (2.53 GHz), 2 GB RAM.

Conclusions

In this paper, we present an offline tube-based robust MPC algorithm using polyhedral invariant sets. All of the optimal control problems are solved off-line so no optimal control problem needs to be solved online. The simulation results show that the state at each time step of the LTV system with disturbance is restricted to lie within a tube whose center is the state of the nominal LTV system that converges to the origin. Hence, the state of the LTV system with disturbance converges to a tube whose center is at the origin. Robust stability and satisfaction of the state and control constraints are guaranteed. In future work, the proposed algorithm can be extended to the nonlinear system with bounded disturbance.

Funding

This research project is supported by Mahidol University and Thailand Research Fund (TRF).

| Nomenclati | ure |
|--|--|
| X | state |
| и | input |
| c | vanishing input |
| $ar{m{\mathcal{X}}}$ | state of nominal system |
| \hat{x} | observer state |
| \bar{u} | input of nominal system |
| N | prediction horizon |
| K | disturbance rejection gain |
| Z | robust positively invariant set |
| W | disturbance |
| $ar{	extbf{X}}_{\!f}$ | terminal constraint set |
| $\stackrel{\circ}{Q}_R$ | state weighting matrix |
| | input weighting matrix |
| λ_{\parallel} | time-varying parameter |
| x' | state of nominal LTV system |
| u' | input of nominal LTV system |
| P | Lyapunov matrix |
| P_{i} | polyhedral invariant set i |
| $\vec{F_i}$ | stabilizing feedback gain corresponding |
| | to P_i |
| F | real-time stabilizing feedback gain |
| V(x') | Lyapunov function of variable x' |
| Example 1 | |
| X_{1} | state 1 of LTV system with disturbance |
| x_2 | state 2 of LTV system with disturbance |
| $\begin{matrix} x \\ x_1^2 \end{matrix}$ | state 1 of nominal LTV system |
| x_2' | state 2 of nominal LTV system |
| u | input of LTV system with disturbance |
| u' | input of nominal LTV system |
| Example 2 | |
| X_{1} | dimensionless concentration of reactant A |
| $\chi_{_{2}}^{^{1}}$ | dimensionless reactor temperature |
| $\chi_{_{_{3}}}^{^{2}}$ | dimensionless cooling jacket temperature |
| q° | dimensionless reactor feed-flow rate |
| $q_{_{ m c}}$ | dimensionless coolant flow rate |
| W_{i} | disturbance variable i |
| $\bar{x}_i(k)$ | deviation form of state i at time k |
| $\mathcal{X}_{_{iS}}$ | equilibrium point of state i |
| $\mathcal{X}_{_{\mathrm{1f}}}$ | dimensionless reactor feed concentration |
| $\mathcal{X}^{}_{\mathrm{2f}}$ | dimensionless reactor feed temperature |
| $\mathcal{X}^{}_{ m 3f}$ | dimensionless cooling jacket feed |
| 0 | temperature |
| β | dimensionless heat of reaction |
| $\stackrel{\gamma}{\delta}$ | dimensionless activation energy |
| 0 | dimensionless heat transfer coefficient |
| $\delta_{_1}$ | dimensionless volume ratio of reactor to |
| S | cooling jacket |
| $\delta_{_2}$ | dimensionless density × heat capacity ratio |
| ϕ | reactor to cooling jacket Damkohler number |
| φ τ | dimensionless time |
| | |
| Mathematic | |
| $X \oplus Y$ | Minkowski set addition between X and Y |
| $X\ominus Y$ | Minkowski set difference between X and Y |

| d(x, Y) | distance of a point x from a set Y |
|----------------------------------|--|
| d(x, y) | distance of a point x from a point y |
| - | Euclidean norm |
| A > 0 | A is a positive-definite matrix |
| A < 0 | A is a negative-definite matrix |
| $\rho(A)$ | spectral radius of a matrix A |
| $\widehat{\text{Conv}}\{\cdot\}$ | convex hull of the elements in $\{\cdot\}$ |
| Abbreviatio | one |
| | /IIS |
| MPC | model predictive control |
| MPC LTI | |
| LTI | model predictive control linear time-invariant |
| | model predictive control linear time-invariant linear quadratic regulator |
| LTI LQR | model predictive control linear time-invariant |
| LTI LQR LTV | model predictive control linear time-invariant linear quadratic regulator linear time-varying |

References

Boyd, S., and Vandenberghe, L. (2004). *Convex Optimization*, Cambridge University Press, Cambridge.

Bumroongsri, P., and Kheawhom, S. (2012). An off-line robust MPC algorithm for uncertain polytopic discrete-time systems using polyhedral invariant sets, *J. Process Control*, 22, 975–983. doi:10.1016/j.jprocont.2012.05.002

Chisci, L., Rossiter, J. A., and Zappa, G. (2001). Systems with persistent disturbances: Predictive control with restricted constraints, *Automatica*, 37, 1019–1028. doi:10.1016/S0005-1098(01)00051-6

Gonzalez, R., Fiacchini, M., Alamo, T., Guzman, J. L., and Rodriguez, F. (2011). Online robust tube-based MPC for time-varying systems: A practical approach, *Int. J. Control*, 84, 1157–1170. doi:10.1080/00207179.2011.594093

Kolmanovsky, I., and Gilbert, E. G. (1998). Theory and computation of disturbance invariant sets for discrete-time linear systems, *Math. Prob. Eng.*, 4, 317–367. doi:10.1155/S1024123X98000866

Langson, W., Chryssochoos, I., Raković, S. V., and Mayne, D. Q. (2004). Robust model predictive control using tubes, *Automatica*, 40, 125–133. doi:10.1016/j.automatica.2003.08.009

Limon, D., Alvarado, I., Alamo, T., and Camacho, E. F. (2010). Robust tube-based MPC for tracking of constrained linear systems with additive disturbances, J. Process Control, 20, 248–260. doi:10.1016/j.jprocont.2009.11.007

Mayne, D. Q., Rawlings, J. B., Rao, C. V., and Scokaert, P. O. M. (2000). Constrained model predictive control: stability and optimality, *Automatica*, 36, 789–814. doi:10.1016/S0005-1098(99) 00214-9

Mayne, D. Q., Seron, M. M., and Raković, S. V. (2005). Robust model predictive control of constrained linear systems with bounded disturbances, *Automatica*, 41, 219–224. doi:10.1016/j.automatica. 2004.08.019

Mayne, D. Q., Raković, S. V., Findeisen, R., and Allgower, F. (2006).
Robust output feedback model predictive control of constrained linear systems, *Automatica*, 42, 1217–1222. doi:10.1016/j.automatica. 2006.03.005

Mayne, D. Q., Raković, S. V., Findeisen, R., and Allgower, F. (2009).
Robust output feedback model predictive control of constrained linear systems: Time varying case, *Automatica*, 45, 2082–2087.
doi:10.1016/j.automatica.2009.05.009

Mayne, D. Q., and Langson, W. (2001). Robustifying model predictive control of constrained linear systems, *Electron. Lett.*, **37**, 1422–1423. doi:10.1049/el:20010951

Nagrath, D., Prasad, V., and Bequette, B. W. (2002). A model predictive formulation for control of open-loop unstable cascade

- systems, Chem. Eng. Sci., **57**, 365–378. doi:10.1016/S0009-2509(01) 00398-0
- Raković, S. V. (2005). Robust Control of Constrained Discrete Time Systems: Characterization and Implementation, Imperial College London, London.
- Raković, S. V., Kerrigan, E. C., Kouramas, K. I., and Mayne, D. Q. (2005). Invariant approximations of the minimal robust positively
- invariant set, *IEEE Trans. Autom. Control*, **50**, 406–410. doi:10.1109/TAC.2005.843854
- Rawlings, J. B., and Mayne, D. Q. (2009). *Model Predictive Control: Theory and Design*, Nob Hill Publishing, Wisconsin.
- Silva, R. G., and Kwong, W. H. (1999). Nonlinear model predictive control of chemical processes, *Braz. J. Chem. Eng.*, **16**, 83–99. doi:10.1590/S0104-66321999000100008

FISEVIER

Contents lists available at ScienceDirect

Fluid Phase Equilibria

journal homepage: www.elsevier.com/locate/fluid



Phase equilibrium for ternary liquid systems of water + di-(2-ethylhexyl)phosphoric acid + organic diluents: Thermodynamic study



Wanchalerm Srirachat ^a, Thidarat Wongsawa ^a, Niti Sunsandee ^b, Ura Pancharoen ^{a,*}, Soorathep Kheawhom ^{a,**}

ARTICLE INFO

Article history: Received 21 February 2015 Received in revised form 6 May 2015 Accepted 10 May 2015 Available online 15 May 2015

Keywords:
Phase equilibrium
Ternary liquid systems
Di-(2-ethylhexyl)phosphoric acid
Organic diluents
Thermodynamics

ABSTRACT

The influences of temperature on equilibrium solubility for the ternary liquid systems of water+di-(2-ethylhexyl)phosphoric acid+organic diluents were investigated by cloud point titration at T=303.2–333.2 K and atmospheric pressure. Various organic diluents having different dielectric constants of kerosene (n/a), n-heptane (1.9), chlorobenzene (5.6) and 1-octanol (10.3) were designated to observe the polar influence on the solubility. All ternary systems exhibited the type II behavior, and their solubility increased with the polarity and studied temperatures. The tie-line data for each ternary liquid system were also studied and correlated by the Bachman plots. Moreover, the experimental solubility of water in the organic phases were predicted using the modified Apelblat equation, and the results were validated by the relative average deviation (RAD) as shown in a range of 0.01–4.09%. The dissolution thermodynamics of water in the organic phases were studied using the van't Hoff model in order to determine its enthalpy ($\Delta H_{\rm d}$), entropy ($\Delta S_{\rm d}$) and Gibbs energy ($\Delta G_{\rm d}$). The results indicated that the dissolution of water in the organic phases was endothermic and a non-spontaneous process and driven by entropy.

© 2015 Elsevier B.V. All rights reserved.

1. Introduction

Solubility data of the ternary liquid systems have a fundamental and important role in industry [1,2]. Such data are used to develop and design the separation processes for economic [3] and environmental issues [4]. Based on the above aspects, many ternary liquid systems have been studied by varying the temperature and type of organic diluents; their results present different solubility behaviors [5–8]. This is because the solubility depends on the chemical structures, polarity and temperatures of the components used [9,10]. The mutual solubility of extractant, organic diluent and water is also important in the separation processes since it can change the separation efficiency [3,11]. Thus, their solubility is primarily considered as an essential factor for selecting a suitable organic diluent.

Di-(2-ethylhexyl)phosphoric acid extractant has been widely used for the separation of metal ions [12,13]. However, the molecule of this extractant is composed of the polar functional

groups of P=O and P—OH [14] that interact with the molecule of water. Darvishi et al. [15] reported that the solubility of water in the organic phase was increased in the similar trend with the concentration of di-(2-ethylhexyl)phosphoric acid. In addition, the quantity of water in the organic phase was varied according to the dielectric constants of organic diluents and the temperatures [16–18]. For these purposes, the temperature dependence is of interest to study the solubility of di-(2-ethylhexyl)phosphoric acid, organic diluent and water.

Models of thermodynamics are also important in the design of separation processes. Their application has been used to predict the thermodynamic properties of components in the ternary liquid systems. For example, the modified Apelblat equation has a reliability that can determine the temperature-dependent solubility [19–21]. Furthermore, the van't Hoff model has been widely used to obtain the thermodynamic parameters such as enthalpy and entropy [22–24]. The results from the van't Hoff model can describe the relationship between the thermodynamic properties and the dissolution processes.

The main purpose of this work is to provide solubility data and thermodynamic properties. Ternary liquid systems of water+di-(2-ethylhexyl)phosphoric acid+organic diluents were carried out by cloud point titration [25–28] at the temperatures of 303.2–

^a Department of Chemical Engineering, Faculty of Engineering, Chulalongkorn University, Patumwan, Bangkok 10330, Thailand

^b Government Pharmaceutical Organization, Ratchathewi, Bangkok 10400, Thailand

^{*} Corresponding author. Tel.: +66 2 2186891; fax: +66 2 2186877.

^{**} Corresponding author. Tel.: +66 2 2186893; fax: +66 2 2186877.

E-mail addresses: ura.p@chula.ac.th (U. Pancharoen), soorathep.k@chula.ac.th (S. Kheawhom).

Nomenclature

A,B The parameters of the Bachman correlation

a, b, c The constant parameters in the correlated modified Apelblat model

RAD Relative average deviation m_i Mass of component i (g)

 M_i Molecular weight of component i (g/mol)

T Absolute temperature (K) T_{fus} Fusion temperature R^2 Coefficient of determination R Gas constant (J/mol K) W_i Mass fraction of component i

 w_{ij} Mass fraction of component i in the j phase

 x_i Mole fraction of component i

 $\begin{array}{lll} \Delta H_{\rm d} & \text{Molar enthalpy of dissolution (kJ/mol)} \\ \Delta S_{\rm d} & \text{Molar entropy of dissolution (kJ/mol)} \\ \Delta G_{\rm d} & \text{Molar Gibbs energy of dissolution (kJ/mol)} \\ \Delta H_{\rm fus} & \text{Molar enthalpy of fusion (kJ/mol)} \\ \Delta S_{\rm fus} & \text{Molar entropy of fusion (kJ/mol)} \end{array}$

 ΔS_{fus} Molar entropy of fusion (kJ/mol) R Gas constant (8.314 J/mol K) N The number of experiment points

Subscripts

i Indices for all components (1–3)

j Indices for all phases (1–3)

Greek letters

 δ Hansen solubility parameter (Pa^{1/2})

 σ Standard deviation

333.2 K and the atmospheric pressure. The organic diluents having different dielectric constants of kerosene, *n*-heptane, chlorobenzene and 1-octanol were used in all experiments. The equilibrium solubility was investigated and focused on the influences of polarity and temperature. Tie-line data were determined and correlated with the data from the Bachman equation. Thereafter,

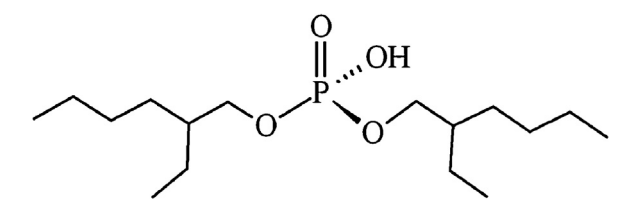


Fig. 1. The structure of di-2(ethylhexyl) phosphoric acid [9].

Table 1The properties of the pure components used in this work.

Properties Di-(2-ethylhexyl)phosphoric acid Kerosene n-Heptane Chlorobenzene 1-Octanol Water CAS no. 298-07-7 64742-47-8 142-82-5 108-90-7 111-87-5 7732-18-5 Chemical $C_{16}H_{35}O_4P$ H_2O $C_6 - C_{16}$ C_7H_{16} C₆H₅Cl $C_8H_{17}O$ formula molecular weights (g/mol) 322.43 143ª 100.20 112.56 130.23 18.02 Purity $\geq 98.0^{b}$ ≥99.0 ≥99.5 ≥99.0 100 (wt%) 192^d 5 69^d 10.30^d Dielectric constant (pF/m) n/a n/a 80 10^e

^a Molar mass of kerosene (ExxsolTM D40 fluid) reported by Ref. [30].

^b Aromatic content (0.00–2.0 wt%) of kerosene (ExxsolTM D40 fluid) reported by Ref. [30].

Is the purity of each component as obtained by its individual data sheet from the manufacturing supplier.

 $^{
m d}$ Dielectric constant values at the temperature of 20 $^{\circ}$ C as reported by Ref. [31].

^e Dielectric constant values at the temperature of 20°C as reported by Ref. [32].

the solubility of water in the organic phases was predicted using the modified Apelblat equation and its results were validated by the RAD values. The thermodynamic parameters of enthalpy, entropy and Gibbs energy were obtained using the van't Hoff model to study the relationship between the thermodynamic properties and the dissolution of water in the organic phases.

2. Experimental

2.1. Chemicals

Di-(2-ethylhexyl)phosphoric acid – its chemical structure was as shown in Fig. 1 – and 1-octanol were supplied by Merck. n-Heptane and chlorobenzene were purchased from RCI Labscan. Kerosene (ExxsolTM D40 fluid) was supplied by ExxonMobil. All compounds were used without further purification and kept in a light brown bottle containing dried molecular sieves. Then, the bottle was tightly sealed to protect the contamination of water. The composition of water in the organic diluents and di-(2-ethylhexyl) phosphoric acid was determined by the Karl Fischer titration and the oven evaporator [29], and found to be 0.001 wt% and 0.002 wt%, respectively. More details of the components are listed in Table 1. Distilled water was used throughout the experiments.

2.2. Apparatus and procedure

Equilibrium solubility for each ternary liquid system was determined by the cloud point titration as shown in Fig. 2. The weights of all components were obtained by an analytical precision electronic balance (Sartorius, model 11222-46) with an uncertainty of 0.0001 g. The temperatures of the systems were controlled by a water jacket that was heated using a digital hotplate stirrer (DAIHAN, MSH-20D) and checked by a precision Pt-100 thermocouple with an accuracy of $\pm 0.1 \, \text{K}$. Moreover, an accurate thermometer was immersed into the systems for controlling their temperature. The binary mixtures of the given compositions of di-(2-ethylhexyl)phosphoric acid and organic diluents were added into the closed cell and then put in the water jacket. Both liquid components were agitated by the magnetic stirrers at 200 rpm. Thereafter, the mixtures were titrated with water in a precision syringe until they became turbid. The end point of titration was achieved when the mixtures remained turbid for 15 min. During this time, the closed cell was agitated periodically to observe the turbidity. These procedures were used to obtain the solubility of the organic phase. The solubility of the aqueous phase was determined using the binary mixtures of di-(2-ethylhexyl)phosphoric acid and water and operated in the same manner. The organic diluents were added for titration. Moreover, the solubility for binary liquid systems of (water + di-(2-ethylhexyl)phosphoric acid) and (water+organic diluents) was investigated until the

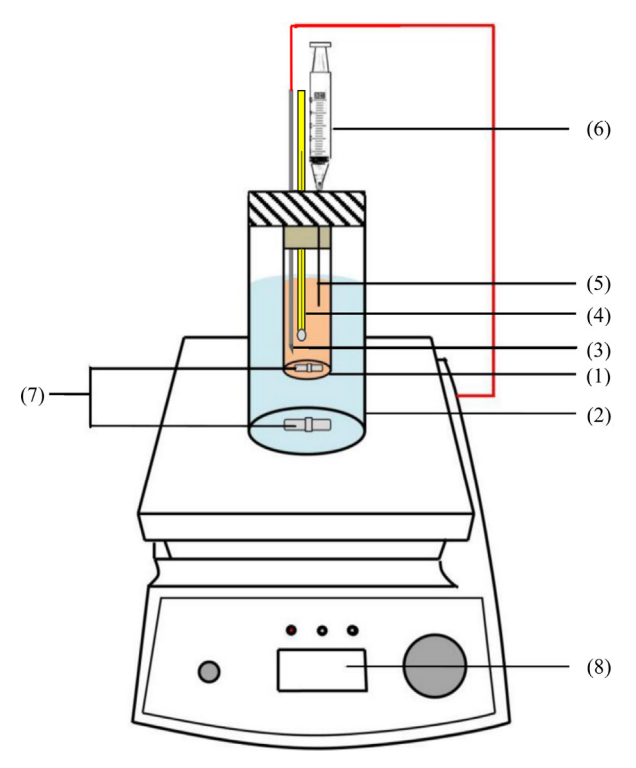


Fig. 2. Schematic diagram of the liquid-liquid equilibrium apparatus: (1) equilibrium cell surrounded by water (2) water jacket (3) Pt-100 probe with feedback controller (4) glass thermometer (5) syringe needle (6) syringe (7) magnetic bars and (8) digital hotplate magnetic stirrer.

samples became turbid. All samples were measured three times, and the uncertainty of their compositions was ± 0.027 wt%.

The tie-line data were obtained from the ternary mixtures at equilibrium. More water was added in the mixtures until they transformed from homogeneous phase to heterogeneous one. Thereafter, the mixtures were agitated vigorously at 500 rpm for 30 min and then centrifuged by Stanhope-Seta (model 9000) at 1500 rpm for 3 h to complete the separation of both phases. During centrifuge, the temperatures of the mixtures were controlled and presented the uncertainty of $\pm 1.0 \, \text{K}$. The organic phase was carefully withdrawn from the top layer of the closed cell by syringe and then weighed. The composition of water in the organic phase was determined by the Karl Fischer titration (Metrohm, model 759 KF) together with the oven evaporator that had the uncertainty of 0.0021 wt% [29]. After this step, the composition of di-(2ethylhexyl)phosphoric acid was weighed to obtain its composition. The composition of the organic diluent was obtained by the mass balance equation that followed on the compositions of water and di-(2-ethylhexyl)phosphoric acid. The remaining aqueous phase was also weighed, and the compositions of the components were calculated by the mass balance equation as based on the compositions in the organic phase. All measurements were repeated three times.

2.3. Analysis

The organic phase in the vial was weighed and then tightly capped with an aluminum seal for analysis by the Karl Fischer titration (756 KF Coulometer, Metrohm) together with the oven evaporator at the setting temperature of 473 K. This operation resulted in the evaporation of the water and the organic diluent into the titration cell; only water was titrated by the iodine solution (I₂) to obtain its composition. Thereafter, di-(2-ethylhexyl) phosphoric acid which remained in the vial was weighed to

Table 2 Equilibrium solubility data in form of mass percentage $(%w_i)$ for the ternary liquid systems of water (1)+di-(2-ethylhexyl)phosphoric acid (2)+organic diluents (3) at the temperatures of 303.2–333.2 K and the pressure of 0.1 MPa.^a

| Kerosene n-Heptane | | Chlorobe | enzene | 1-Octan | ol | | |
|--------------------|-----------------|----------------|------------------|----------------|-----------------|-----------------|------------------|
| %w ₁ | %w ₂ | ${w_1}$ | %w ₂ | ${w_1}$ | %w ₂ | %w ₁ | %w ₂ |
| T=303.2 | - | | | <u>·</u> | | | |
| 0.007 | 0.000 | 0.017 | 0.000 | 0.041 | 0.000 | 4.932 | 0.000 |
| 0.007 | 9.918 | 0.159 | 9.843 | 0.318 | 9.939 | 5.198 | 4.738 |
| 0.162 | 19.829 | 0.133 | 19.776 | 0.795 | 19.971 | 5.161 | 14.999 |
| 0.102 | 29.710 | 0.332 | 29.712 | 1.108 | 29.825 | 5.134 | 24.767 |
| 0.339 | 39.657 | 0.332 | 39.556 | 1.259 | 38.952 | 5.099 | 35.079 |
| 0.339 | 49.644 | 0.424 | 49.767 | 1.735 | 49.049 | 5.047 | 45.341 |
| | | | | | | | |
| 0.409 | 59.605 | 0.703 | 59.325 69.210 | 2.191 | 58.654 | 4.724 | 55.347 |
| 0.369 | 69.584 | 0.742 0.925 | | 2.567 | 67.818 | 4.207 3.641 | 65.711 |
| 0.313 | 79.704 | | 79.059 | 2.608 | 77.644 | | 76.467 86.797 |
| 1.290 | 88.685 | 1.685 | 88.338 | 2.582 2.399 | 87.462 | 3.082 2.399 | |
| 2.399 | 97.601 | 2.399 | 97.601 | 99.951 | 97.601 | | 97.601 |
| 99.998 | 0.000 | 99.997 | 0.000 | | 0.000 | 99.948 | 0.000 |
| 99.990 | 0.010 | 99.990 | 0.010 | 99.990 | 0.010 | 99.990 | 0.010 |
| T=313.2 | K | | | | | | |
| 0.013 | 0.000 | 0.031 | 0.000 | 0.113 | 0.000 | 5.221 | 0.000 |
| 0.128 | 9.878 | 0.239 | 9.663 | 0.435 | 9.827 | 5.481 | 4.524 |
| 0.128 | 19.834 | 0.239 | 19.701 | 0.455 | 19.158 | 5.446 | 14.776 |
| 0.334 | 29.746 | 0.469 | 29.417 | 1.259 | 28.774 | 5.442 | 24.521 |
| 0.420 | 39.669 | 0.564 | 39.355 | 1.459 | 38.619 | 5.398 | 34.864 |
| 0.420 | 49.627 | 0.641 | 49.569 | 1.876 | 48.196 | 5.422 | 44.977 |
| 0.483 | 59.576 | 0.836 | 59.094 | 2.299 | 57.898 | 5.073 | 55.115 |
| 0.439 | 69.618 | 0.898 | 69.305 | 2.654 | 67.515 | 4.543 | 65.399 |
| 0.389 | 79.679 | 1.087 | 78.816 | 2.739 | 77.392 | 3.993 | 76.151 |
| 1.368 | 88.714 | 1.873 | 88.141 | 2.682 | 87.383 | 3.348 | 86.411 |
| 2.483 | 97.517 | 2.483 | 97.517 | 2.483 | 97.517 | 2.483 | 97.517 |
| 99.996 | 0.000 | 99.995 | 0.000 | 99.929 | 0.000 | 99.935 | 0.000 |
| 99.984 | 0.000 | 99.984 | 0.000 | 99.984 | 0.000 | 99.984 | 0.000 |
| 33.304 | 0.010 | 33.304 | 0.010 | 33.304 | 0.010 | 33.304 | 0.010 |
| T = 323.2 | .K | | | | | | |
| 0.019 | 0.000 | 0.048 | 0.000 | 0.192 | 0.000 | 5.337 | 0.000 |
| 0.166 | 9.871 | 0.383 | 9.699 | 0.521 | 9.570 | 5.579 | 4.429 |
| 0.293 | 19.783 | 0.523 | 19.399 | 0.976 | 19.051 | 5.625 | 14.630 |
| 0.416 | 29.716 | 0.631 | 29.456 | 1.419 | 28.617 | 5.680 | 24.265 |
| 0.542 | 39.517 | 0.771 | 39.274 | 1.586 | 38.469 | 5.645 | 34.623 |
| 0.544 | 49.512 | 0.866 | 49.323 | 1.996 | 48.069 | 5.606 | 44.736 |
| 0.560 | 59.479 | 1.021 | 59.116 | 2.407 | 57.669 | 5.298 | 54.874 |
| 0.519 | 69.533 | 1.057 | 69.339 | 2.755 | 67.336 | 4.815 | 65.109 |
| 0.469 | 79.603 | 1.252 | 78.664 | 2.846 | 77.222 | 4.231 | 75.885 |
| 1.450 | 88.617 | 2.077 | 87.937 | 2.786 | 87.295 | 3.564 | 86.317 |
| 2.521 | 97,479 | 2.521 | 97.479 | 2.521 | 97.479 | 2.521 | 97.479 |
| 99.995 | 0.000 | 99.994 | 0.000 | 99.903 | 0.000 | 99.911 | 0.000 |
| 99.982 | 0.018 | 99.982 | 0.018 | 99.982 | 0.018 | 99.982 | 0.018 |
| | | | | | | | |
| T = 333.2 | K | | | | | | |
| 0.025 | 0.00 | 0.069 | 0.00 | 0.271 | 0.00 | 5.625 | 0.00 |
| 0.218 | 9.842 | 0.519 | 9.507 | 0.636 | 9.416 | 5.865 | 4.078 |
| 0.357 | 19.759 | 0.685 | 19.364 | 1.121 | 18.933 | 5.889 | 14.352 |
| 0.470 | 29.666 | 0.821 | 29.579 | 1.591 | 28.449 | 5.968 | 24.014 |
| 0.648 | 39.450 | 0.958 | 38.994 | 1.766 | 38.289 | 5.946 | 34.417 |
| 0.642 | 49.397 | 1.061 | 49.228 | 2.173 | 47.874 | 5.825 | 44.781 |
| 0.636 | 59.465 | 1.265 | 58.675 | 2.586 | 57.476 | 5.486 | 54.639 |
| 0.600 | 69.436 | 1.256 | 68.618 | 2.895 | 67.197 | 5.096 | 64.866 |
| 0.539 | 79.509 | 1.478 | 78.424 | 2.971 | 77.089 | 4.513 | 75.608 |
| 1.534 | 88.515 | 2.334 | 87.906 | 2.897 | 87.169 | 3.786 | 86.342 |
| 2.577 | 97.423 | 2.577 | 97.423 | 2.577 | 97.423 | 2.577 | 97.423 |
| 99.993 | 0.000 | 99.991 | 0.000 | 99.888 | 0.000 | 99.894 | 0.000 |
| 99.980 | 0.010 | 99.980 | 0.010 | 99.980 | 0.010 | 99.980 | 0.010 |
| | | | | | | | |

determine its composition. The composition of the organic diluent was determined by the mass balance equation after knowing the compositions of water and di-(2-ethylhexyl)phosphoric acid.

2.4. Reliability of experimental results

According to NIST, the standard uncertainties, as expressed in the respective footnote tables, were used to confirm the reliability of the experimental results and were calculated based on Eqs. (1)

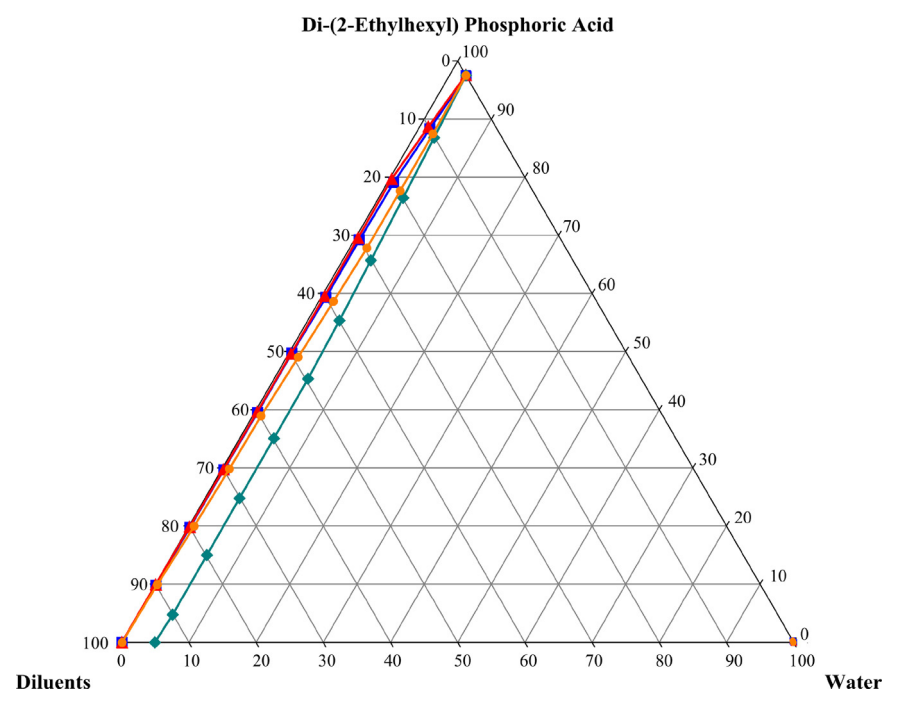


Fig. 3. The solubility curves for the ternary liquid systems of water (1) + di-(2-ethylhexyl)phosphoric acid (2) + organic diluents (3) (———= n-heptane; ————= kerosene; ————= 1-octanol and ————= chlorobenzene) at the temperature of 303.2 K and the pressure of 0.1 MPa.

and (2) [33] as follows:

$$u(x_i) = \left(\frac{1}{n(n-1)} \sum_{k=1}^{n} (X_{i,k} - \overline{X}_i)^2\right)^{1/2}$$
 (1)

$$x_i = \overline{X}_i = \frac{1}{n} \sum_{k=1}^n X_{i,k} \tag{2}$$

where n is the number of independent observation, $X_{i,k}$ is the input quantity as obtained under the same conditions of measurement and $k = 1, 2, \ldots, n$.

3. Results and discussion

3.1. Liquid-liquid equilibrium solubility and tie-line data

The equilibrium solubility data for the ternary liquid systems of water + di-(2-ethylhexyl) phosphoricacid + organic diluents at

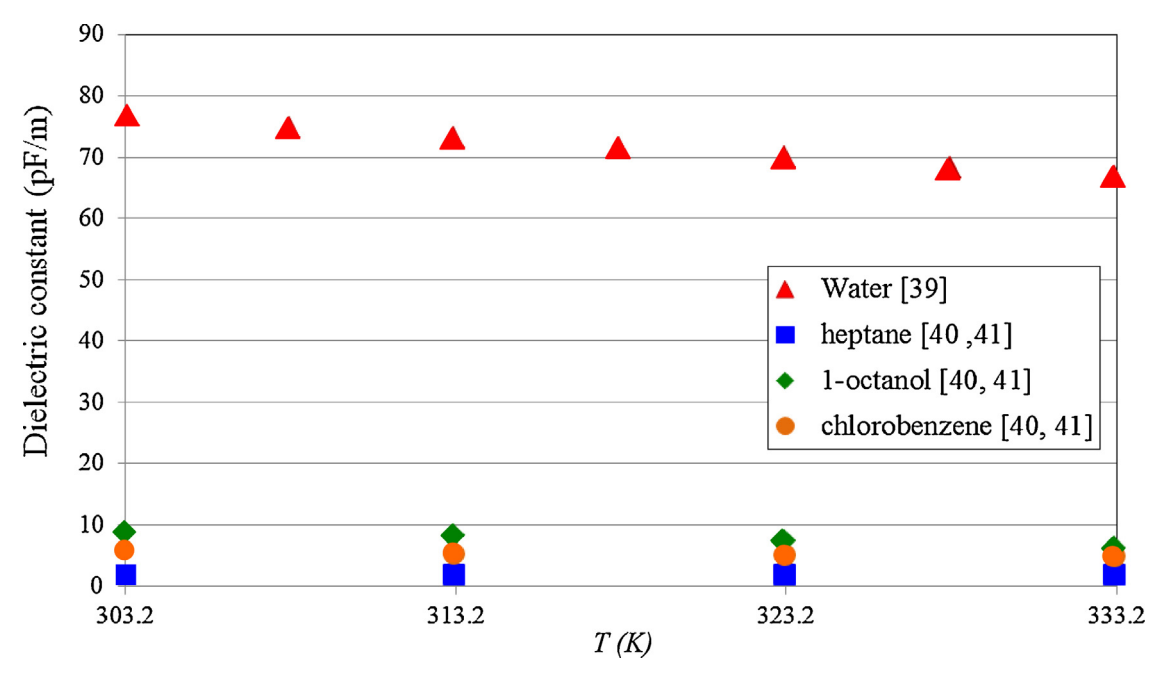


Fig. 4. The dielectric constants of organic diluents and water at the temperatures of 303.2–333.2 K.

Table 3The equilibrium tie-line data in term of mass percentage (w_i) for the binary liquid systems of (water + di-(2-ethylhexyl)phosphoric acid) and (water + organic diluents) at the temperatures of 303.2–333.2 K and the pressure of 0.1 MPa (comparison between this work and the literature).

| Binary system | T (K) | Aqueous pha | se | Organic phase | |
|--|-------|-----------------|--------------------------------|------------------------------|-----------------|
| | | %w ₁ | %w ₂ , literature | %w ₁ , literature | %w ₂ |
| Water (1) + di-(2-ethylhexyl)phosphoric acid (2) | 303.2 | 99.990 | 0.010, 0.028 [46] ^b | 2.399, 2.4 [47] | 97.601 |
| | 313.2 | 99.984 | 0.016, n/a | 2.483, n/a | 97.517 |
| | 323.2 | 99.982 | 0.018, n/a | 2.521, n/a | 97.479 |
| | 333.2 | 99.980 | 0.020, n/a | 2.577, n/a | 97.423 |
| Water (1)+kerosene (2) | 303.2 | 99.998 | 0.002, n/a | 0.007, 0.003 [10] | 99.993 |
| | 313.2 | 99.996 | 0.004, n/a | 0.013, <i>n</i> / <i>a</i> | 99.987 |
| | 323.2 | 99.995 | 0.005, n/a | 0.019, n/a | 99.981 |
| | 333.2 | 99.993 | 0.007, <i>n</i> / <i>a</i> | 0.025, <i>n</i> / <i>a</i> | 99.975 |
| Water $(1) + n$ -heptane (2) | 303.2 | 99.997 | 0.003, n/a | 0.017, 0.014 [48] | 99.983 |
| | 313.2 | 99.995 | 0.005, n/a | 0.031, 0.013 [49] | 99.969 |
| | 323.2 | 99.994 | 0.006, n/a | 0.048, 0.025 [50] | 99.952 |
| | 333.2 | 99.991 | 0.009, n/a | 0.069, n/a | 99.931 |
| Water (1) + chlorobenzene (2) | 303.2 | 99.951 | 0.049, 0.054 [51] | 0.041, 0.049 [51] | 99.959 |
| | 313.2 | 99.929 | 0.071, 0.068 [51] | 0.113, 0.074 [51] | 99.887 |
| | 323.2 | 99.903 | 0.097, 0.088 [51] | 0.192, 0.108 [51] | 99.808 |
| | 333.2 | 99.888 | 0.112, 0.116 [51] | 0.271, 0.115 [51] | 99.729 |
| Water (1)+1-octanol (2) | 303.2 | 99.948 | 0.052, 0.064 [52] | 4.932, 4.937 [52] | 95.068 |
| | 313.2 | 99.935 | 0.065, 0.065 [52] | 5.221, 5.075 [52] | 94.779 |
| | 323.2 | 99.911 | 0.089, 0.105 [52] | 5.337, 5.256 [52] | 94.663 |
| | 333.2 | 99.894 | 0.106, 0.088 [52] | 5.625, 5.462 [52] | 94.375 |

^a Standard uncertainties, u; $u(\%w_i) = 0.027$, u(T) = 1.0 K and u(p) = 10 kPa.

b Is solubility at pH 3.0.

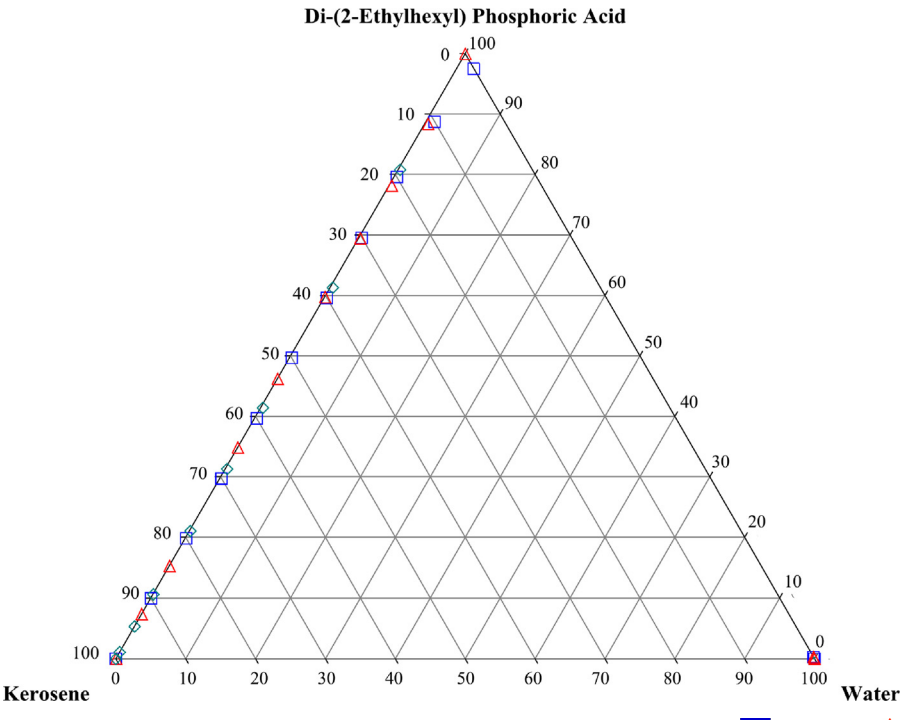


Fig. 5. Comparison of solubility for the ternary systems of water (1) + di-(2-ethylhexyl)phosphoric acid (2) + kerosene (3) (= this work; = ref. [45] and = ref. [15]) at the temperature of 303.2 K and the pressure of 0.1 MPa.

T = 303.2–333.2 K and the atmospheric pressure (0.1 MPa) are listed in Table 2. The solubility curves for these ternary liquid systems at the temperature of 303.2 K are examined in Fig. 3. From this figure, only one liquid pair of (di-(2-ethylhexyl)phosphoric acid + organic diluents) was completely soluble and two liquid pairs of (di-(2-ethylhexyl)phosphoric acid + water) and (water + organic diluents) were partially soluble. This demonstrated that all ternary systems

exhibited type II behavior according to Treybal's classification [34]. As regards other temperatures studied, the solubility curves showed a similar type of behavior. In addition, the areas of two-phase region in this figure decreased in the following order of organic diluents: kerosene > n-heptane > chlorobenzene > 1-octanol. This indicated that water was most soluble in 1-octanol that resulted from its strongest polarity [35–37]. An increase in

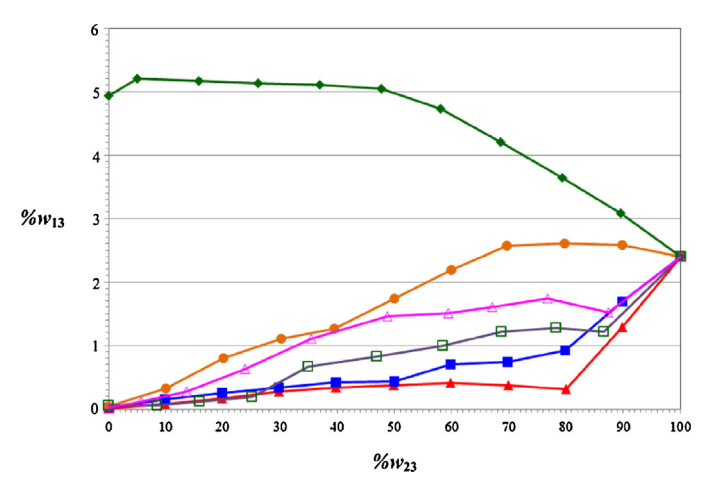


Fig. 6. The operating line of water solubility in organic phases ($%w_{13}$) consisting of di-(2-ethylhexyl)phosphoric acid in organic diluents ($%w_{23}$) at the various concentrations (- = - n-heptane; - = echlorobenzene; - = chloroform [45]) at the temperature of 303.2 K and the pressure of 0.1 MPa.

Table 4 The Hansen solubility parameter (δ) of the pure components at T = 303.2 K.

| Components | Hansen solubility parameter (Pa ^{1/2}) | $\Delta \delta_1$ | $\Delta \delta_2$ |
|--|---|-------------------|-------------------|
| Di-(2-ethylhexyl)phosphoric acid (monomeric) | 18.02 ^a | 29.8 | 0.00 |
| Water | 47.82 ^b | 0.00 | 29.8 |
| Kerosene | >15.90 ^b | <31.92 | < 2.12 |
| n-Heptane | 15.20 ^b | 32.62 | 2.82 |
| Chlorobenzene | 19.61 ^b | 28.21 | 1.59 |
| 1-Octanol | 20.87 ^b | 26.95 | 2.85 |

 $[\]varDelta \delta_1 = |\delta_{water} - \delta_{diluent, extractant}| \ \ \text{and} \ \ \Delta \delta_2 = |\delta_{extractant} - \delta_{diluent, water}|.$

dielectric constants of organic diluents led to an increase in the solubility of water in the organic phases [38]. This is because the dielectric constant presents the capacity of organic diluent to produce a dipole force for interaction with water [39]. Moreover, for each organic diluent the solubility of water in the organic phase increased with temperature. It could be explained by the two points of view. Firstly, the increment of temperature caused to the increase in heat in the aqueous and organic phases which resulted in the easier moving of water into the organic phase. In the case of second point, the increment of temperature conduced to the weaker force of hydrogen bonding in the water molecule that made it easier to dissolve in the organic phase [40-41]. Furthermore, the second point could be supported by the variation of dielectric constants with temperatures as shown in Fig. 4 [42-44]. From this figure, the dielectric constants of organic diluents slightly decreased when the temperatures increased, but in the case of water this value obviously decreased. According to the high temperature, these tendencies resulted in the close values between organic diluents and water that attained to the greater solubility of water in the organic phases. Since the solubility of solute in the solvent phase strongly depended on the difference between their polarities, the smaller difference of polarities resulted in the great solubility. Thus, the solubility of solute in the solvent phase increased when the temperature increased.

The equilibrium solubility data for the binary liquid systems of (water+di-(2-ethylhexyl)phosphoric acid) and (water+organic diluents) were also presented in Table 3, and the results were compared with the literature. Moreover, the equilibrium solubility data for the ternary liquid system of (water+di-(2-ethylhexyl) phosphoric acid+kerosene) were also compared with the previous work as shown in Fig. 5. Furthermore, the operating lines plotting between w_{23} and w_{13} for each organic diluent in this work and the literature were also provided for the collection of data as shown in Fig. 6.

The Hansen solubility parameter (δ) was also studied to ensure the solubility results of the ternary liquid systems. This parameter

Table 5The experimental tie-line data for water (1)+di-(2-ethylhexyl)phosphoric acid (2)+organic diluents (3) at the temperatures of 303.2–333.2 K and the pressure of 0.1 MPa.

| Organic phase | Aqueous phase | | | Slope | | |
|---------------|-----------------|-----------------|-----------------|-----------------|-----------------|-------|
| | %w ₁ | %w ₂ | %w ₃ | %w ₁ | %w ₂ | %w₃ |
| Kerosene | | | | | | |
| T = 303.2 K | | | | | | |
| 0.080 | 9.969 | 89.952 | 99.950 | 0.048 | 0.002 | 0.110 |
| 0.279 | 29.842 | 69.879 | 99.879 | 0.116 | 0.005 | 0.425 |
| 0.410 | 59.744 | 39.846 | 99.787 | 0.211 | 0.002 | 1.494 |
| 1.327 | 88.873 | 9.801 | 99.714 | 0.282 | 0.004 | 9.043 |
| T=313.2 K | | | | | | |
| 0.131 | 9.926 | 89.943 | 99.946 | 0.051 | 0.003 | 0.110 |
| 0.336 | 29.788 | 69.876 | 99.880 | 0.118 | 0.002 | 0.425 |
| 0.486 | 59.662 | 39.852 | 99.784 | 0.214 | 0.002 | 1.492 |
| 1.377 | 88.794 | 9.830 | 99.713 | 0.285 | 0.002 | 9.004 |
| T=323,2 K | | | | | | |
| 0.168 | 9.895 | 89.938 | 99.943 | 0.054 | 0.003 | 0.109 |
| 0.418 | 29.721 | 69.861 | 99.879 | 0.118 | 0.003 | 0.424 |
| 0.564 | 59.568 | 39.868 | 99.757 | 0.239 | 0.004 | 1.488 |
| 1.468 | 88.687 | 9.846 | 99.699 | 0.297 | 0.004 | 8.983 |
| T=333.2 K | | | | | | |
| 0.221 | 9.843 | 89.936 | 99.938 | 0.058 | 0.004 | 0.109 |
| 0.474 | 29.672 | 69.854 | 99.880 | 0.116 | 0.004 | 0.423 |
| 0.639 | 59.463 | 39.899 | 99.736 | 0.259 | 0.005 | 1.484 |
| 1.546 | 88.544 | 9.910 | 99.698 | 0.297 | 0.005 | 8.905 |
| n-Heptane | | | | | | |
| T = 303.2 K | | | | | | |
| 0.182 | 10.094 | 89.724 | 99.947 | 0.051 | 0.002 | 0.112 |

^a The total solubility parameters as reported by Ref. [56].

^b The total solubility parameters as reported by Ref. [57].

Table 5 (Continued)

| Organic phase | Aqueous phase | | | Slope | | |
|----------------------|------------------|------------------|--------------------|----------------|-----------------|-------------|
| | %w ₁ | %w ₂ | %w ₃ | ${w_1}$ | %w ₂ | %w₃ |
| 0.342 | 29.980 | 69.678 | 99.882 | 0.117 | 0.001 | 0.42 |
| 0.727 | 59.842 | 39.431 | 99.786 | 0.213 | 0.001 | 1.51 |
| 1.744 | 88.711 | 9.545 | 99.715 | 0.284 | 0.001 | 9.26 |
| | | | | | | |
| T = 313.2 K 0.252 | 10.015 | 89.733 | 99.947 | 0.051 | 0.002 | 0.11 |
| | | | | | | 0.11 |
| 0.476 | 29.862 | 69.662 | 99.882 | 0.116 | 0.002 | |
| 0.845 | 59.671 | 39.485 | 99.786 | 0.213 | 0.001 | 1.50 |
| 1.895 | 88.417 | 9.688 | 99.715 | 0.282 | 0.003 | 9.09 |
| T=323.2 K | | | | | | |
| 0.391 | 9.919 | 89.691 | 99.947 | 0.049 | 0.004 | 0.11 |
| 0.638 | 29.676 | 69.687 | 99.881 | 0.116 | 0.003 | 0.43 |
| 1.029 | 59.436 | 39.534 | 99.786 | 0.213 | 0.001 | 1.49 |
| 2.092 | 88.020 | 9.889 | 99.717 | 0.282 | 0.001 | 8.8 |
| T 222 2 V | | | | | | |
| T=333.2 K | 0.014 | 00.650 | 00.045 | 0.050 | 0.000 | 0.44 |
| 0.533 | 9.814 | 89.653 | 99.947 | 0.050 | 0.003 | 0.10 |
| 0.821 | 29.362 | 69.817 | 99.882 | 0.116 | 0.002 | 0.4 |
| 1.272 | 59.153 | 39.575 | 99.786 | 0.213 | 0.001 | 1.48 |
| 2.302 | 87.514 | 10.184 | 99.718 | 0.281 | 0.001 | 8.5 |
| Chlorobenzene | | | | | | |
| T = 303.2 K | | | | | | |
| 0.341 | 10.286 | 89.374 | 99.908 | 0.053 | 0.039 | 0.1 |
| 1.098 | 29.101 | 69.801 | 99.872 | 0.095 | 0.033 | 0.4 |
| 2.183 | 58.199 | 39.619 | 99.838 | 0.136 | 0.026 | 1.40 |
| 2.594 | 87.580 | 9.827 | 99.768 | 0.221 | 0.011 | 8.9 |
| | | | | | | |
| Γ=313.2 K | 10.102 | 00.261 | 00.000 | 0.000 | 0.041 | 0.11 |
| 0.457 | 10.183 | 89.361 | 99.899 | 0.060 | 0.041 | 0.1 |
| 1.264 | 28.907 | 69.829 | 99.856 | 0.099 | 0.044 | 0.4 |
| 2.325 | 57.997 | 39.678 | 99.806 | 0.143 | 0.051 | 1.40 |
| 2.695 | 87.448 | 9.857 | 99.749 | 0.198 | 0.053 | 8.90 |
| T=323.2 K | | | | | | |
| 0.556 | 10.063 | 89.381 | 99.885 | 0.068 | 0.048 | 0.11 |
| 1.427 | 28.690 | 69.883 | 99.842 | 0.105 | 0.054 | 0.40 |
| 2.434 | 57.820 | 39.747 | 99.787 | 0.154 | 0.060 | 1.45 |
| 2.787 | 87.308 | 9.905 | 99.736 | 0.201 | 0.063 | 8.8 |
| | | | | | | |
| T = 333.2 K | | | | | | |
| 0.675 | 9.983 | 89.342 | 99.877 | 0.072 | 0.051 | 0.11 |
| 1.601 | 28.450 | 69.949 | 99.834 | 0.108 | 0.058 | 0.4 |
| 2.611 | 57.547 | 39.842 | 99.775 | 0.163 | 0.063 | 1.44 |
| 2.897 | 87.144 | 9.959 | 99.719 | 0.212 | 0.069 | 8.7 |
| 1-Octanol | | | | | | |
| T = 303.2 K | | | | | | |
| 5.203 | 4.679 | 90.118 | 99.900 | 0.059 | 0.041 | 0.0 |
| 5.152 | 24.763 | 70.085 | 99.869 | 0.097 | 0.034 | 0.3 |
| 4.750 | 55.179 | 40.071 | 99.819 | 0.156 | 0.025 | 1.3 |
| 3.087 | 86.886 | 10.028 | 99.755 | 0.130 | 0.023 | 8.6 |
| 5.007 | 00.000 | 10.020 | 33.733 | 0.254 | 0.011 | 0.0 |
| T = 313.2 K | | | | | | |
| 5.488 | 4.337 | 90.175 | 99.900 | 0.045 | 0.055 | 0.0 |
| 5.467 | 24.319 | 70.214 | 99.871 | 0.081 | 0.048 | 0.3 |
| 5.105 | 54.710 | 40.184 | 99.828 | 0.137 | 0.035 | 1.3 |
| 3.359 | 86.483 | 10.158 | 99.760 | 0.224 | 0.016 | 8.5 |
| Т=323.2 K | | | | | | |
| 1 = 323.2 K 5.582 | 4.148 | 90.270 | 99.892 | 0.027 | 0.081 | 0.0 |
| | | | | | | |
| 5.698 | 23.999 | 70.304 | 99.870 | 0.056 | 0.074 | 0.3 |
| 5.327 3.576 | 54.382 86.163 | 40.292 10.261 | 99.832 99.764 | 0.111 0.207 | 0.057 0.029 | 1.3- 8.4 |
| 5.570 | 00.103 | 10.201 | 33.7U 4 | 0.207 | 0.025 | 0.4 |
| T = 333.2 K | | | | | | |
| 5.869 | 3.812 | 90.319 | 99.884 | 0.015 | 0.101 | 0.0 |
| 5.974 | 23.703 | 70.323 | 99.867 | 0.042 | 0.091 | 0.3 |
| 5.517 | 54.086 | 40.397 | 99.830 | 0.097 | 0.073 | 1.3 |
| 3.835 | 85.858 | 10.306 | 99.767 | 0.194 | 0.039 | 8.3 |

^a Standard uncertainties, u; $u(%w_i) = 0.027$, u(T) = 1.0 K and u(p) = 10 kPa.

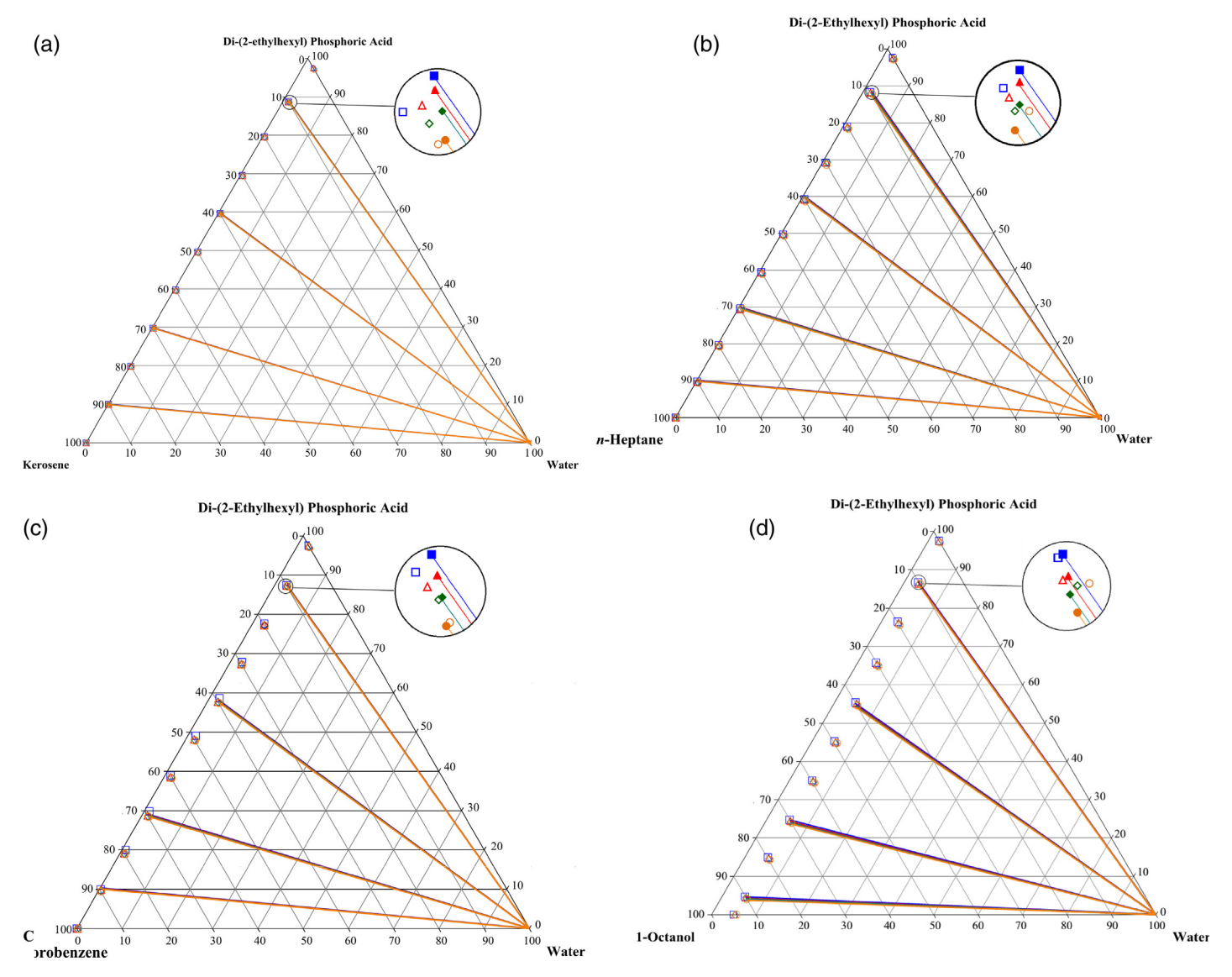


Fig. 7. (a) The solubility curves and the tie-lines for the ternary liquid system of water (1)+di-(2-ethylhexyl)phosphoric acid (2)+kerosene (3) at the different temperatures of (fx2=303.2 K, fx3=313.2 K, fx4=323.2 K and fx5=333.2 K) and the pressure of 0.1 MPa. (b). The solubility curves and the tie-lines for the ternary liquid system of water (1)+di-(2-ethylhexyl)phosphoric acid (2)+*n*-heptane (3) at the different temperatures of (fx2=303.2 K, fx3=313.2 K, fx4=323.2 K and fx5=333.2 K) and the pressure of 0.1 MPa. (c) The solubility curves and the tie-lines for the ternary liquid system of water (1)+di-(2-ethylhexyl)phosphoric acid (2)+chlorobenzene (3) at the different temperatures of (fx2=303.2 K, fx3=313.2 K, fx4=323.2 K and fx5=333.2 K) and the pressure of 0.1 MPa. (d) The solubility curves and the tie-lines for the ternary liquid system of water (1)+di-(2-ethylhexyl)phosphoric acid (2)+1-octanol (3) at the different temperatures of (fx2=303.2 K, fx3=313.2 K, fx4=323.2 K and fx5=333.2 K) and the pressure of 0.1 MPa.

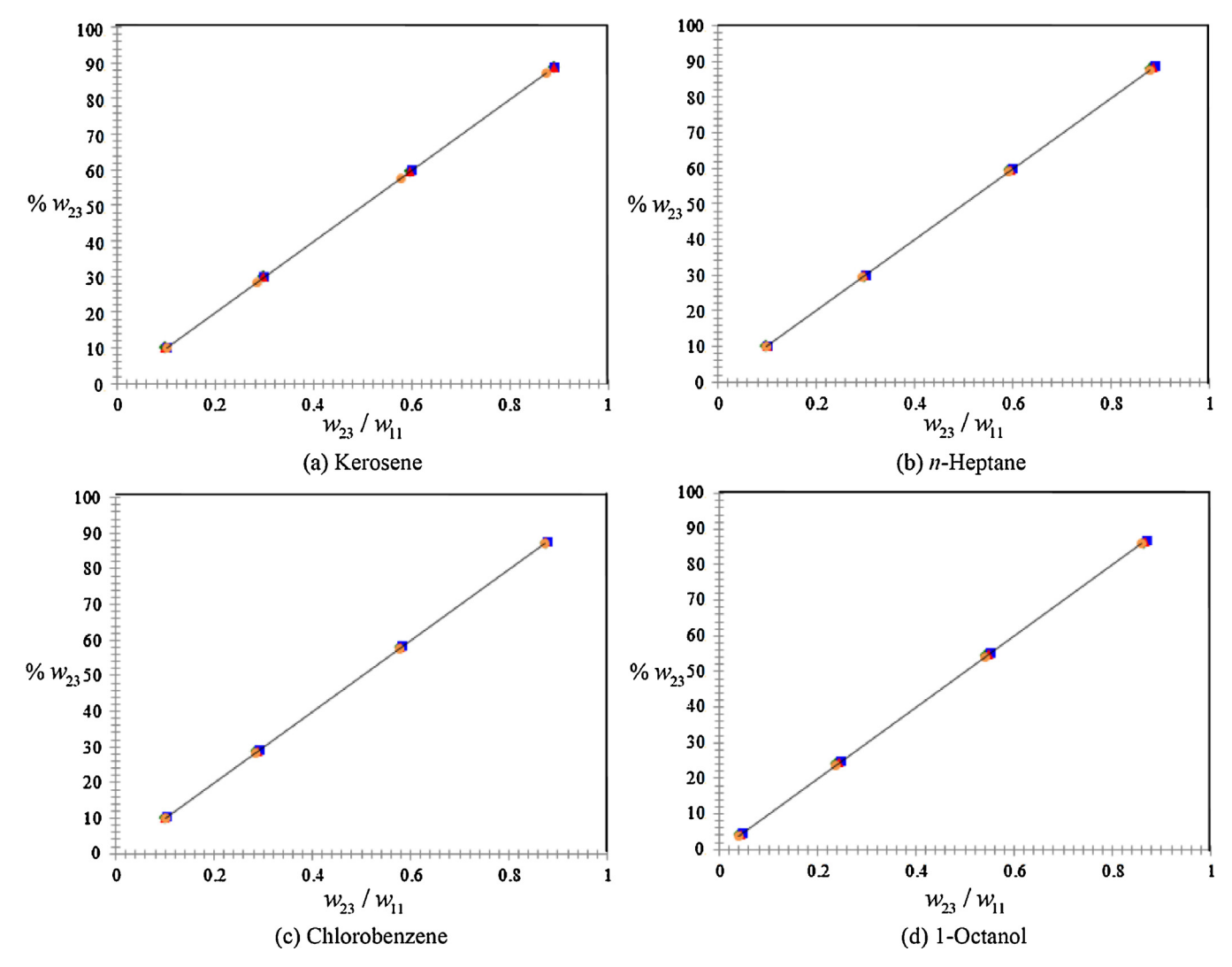


Fig. 8. Bachman correlations for the ternary liquid systems of water (1)+di-(2-ethylhexyl)phosphoric acid (2)+organic diluents (3): (a) kerosene (b) *n*-heptane (c) chlorobenzene and (d) 1-octanol at the different temperatures of (fx2 = 303.2 K, fx3 = 313.2 K, fx4 = 323.2 K and fx5 = 333.2 K) and the pressure of 0.1 MPa.

Table 6Bachman parameters for the ternary liquid systems of water (1)+di-(2-ethylhexyl) phosphoric acid (2)+organic diluents (3) and their standard deviation of error.

| Organic diluents | T (K) | Α | В | σ |
|------------------|-------|--------|----------|---------|
| Kerosene | 303.2 | 0.0441 | 99.68508 | 0.01876 |
| | 313.2 | 0.0453 | 99.67567 | 0.01897 |
| | 323.2 | 0.0461 | 99.66221 | 0.01828 |
| | 333.2 | 0.0449 | 99.65814 | 0.01643 |
| n-Heptane | 303.2 | 0.0448 | 99.68123 | 0.01918 |
| - | 313.2 | 0.0445 | 99.68176 | 0.01916 |
| | 323.2 | 0.0435 | 99.68434 | 0.01995 |
| | 333.2 | 0.0428 | 99.68570 | 0.02042 |
| Chlorobenzene | 303.2 | 0.0284 | 99.74181 | 0.02369 |
| | 313.2 | 0.0293 | 99.72841 | 0.02268 |
| | 323.2 | 0.0284 | 99.71483 | 0.02184 |
| | 333.2 | 0.0302 | 99.69724 | 0.01900 |
| 1-Octanol | 303.2 | 0.0213 | 99.74638 | 0.02757 |
| | 313.2 | 0.0206 | 99.75288 | 0.03282 |
| | 323.2 | 0.0193 | 99.75828 | 0.03857 |
| | 333.2 | 0.0176 | 99.76217 | 0.04067 |

was concerned with dispersion force, intermolecular force and hydrogen bonds between the solute and the solvent molecules [53].

The differences of the Hansen solubility parameters between water and each organic diluent/di-(2-ethylhexyl)phosphoric acid $(\Delta \delta_1)$ and the differences of these between di-(2-ethylhexyl) phosphoric acid and each organic diluent/water ($\Delta \delta_2$) were calculated as shown in Table 4. The results showed the highest value of $\Delta \delta_1$ for 1-octanol and its lowest value for kerosene. This indicated that water was better soluble in 1-octanol than in kerosene as corresponded to the above results. Moreover, the lowest value of $\Delta \delta_2$ appeared in the case of chlorobenzene. In other words, di-(2-ethylhexyl)phosphoric acid was most soluble in chlorobenzene. Since the intermolecular forces of organic diluents were strongly depended on their polarity as follows: 1-octanol> chlorobenzene > n-heptane \approx kerosene. Thus, chlorobenzene broke its intermolecular forces easier than 1-octanol for renew interaction with di-(2-ethylhexyl)phosphoric acid, and provided the higher stability of solvation than n-heptane and kerosene. In order to select the suitable organic diluent for use in the separation processes, the solubility results of each organic diluent were considered by concerning the loss of organic phase into the

Table 7The modified Apelblat parameters for each organic diluent and their RAD values.

| | %w ₂₃ | | | | | | | | | | | |
|----------|------------------|---------|---------|---------|---------|---------|---------|---------|---------|---------|---------|--|
| | 0 | 10 | 20 | 30 | 40 | 50 | 60 | 70 | 80 | 90 | 100 | |
| Kerosene | 2 | | | | | | | | | | | |
| а | 1054.6 | 750.70 | 175.29 | 1.14 | -70.72 | -25.75 | 56.65 | 91.37 | 18.79 | -8.86 | -142.60 | |
| b | -53778 | -38421 | -10616 | -1675.6 | 1416.1 | -380.95 | -3984.2 | -5495.5 | -1982.2 | -71.67 | 6382.1 | |
| c | -154.80 | -110.05 | -25.26 | 0.15 | 10.99 | 4.18 | -8.13 | -13.31 | -2.61 | 1.29 | 21.07 | |
| %RAD | 1.85 | 2.74 | 0.67 | 1.06 | 0.92 | 0.18 | 0.15 | 0.16 | 0.12 | 0.01 | 0.27 | |
| n-Hepta | ne | | | | | | | | | | | |
| а | 485.46 | -81.00 | 192.62 | 135.69 | -5.26 | 399.96 | -167.63 | 48.80 | -14.53 | -41.92 | -151.84 | |
| b | -27074 | 293.77 | -12066 | -9046.7 | -2131.7 | -21355 | 6208.1 | -3773.9 | -591.88 | 1158.9 | 6815.9 | |
| c | -70.54 | 13.19 | -27.47 | -19.18 | 1.55 | -58.25 | 25.27 | -6.82 | 2.49 | 6.39 | 22.43 | |
| %RAD | 0.85 | 1.90 | 0.64 | 0.24 | 1.05 | 0.82 | 0.25 | 0.26 | 0.33 | 0.16 | 0.31 | |
| Chlorobe | enzene | | | | | | | | | | | |
| а | 1989.2 | 370.51 | -203.26 | -12.79 | 135.68 | -15.97 | -53.44 | -39.66 | 10.54 | -9.23 | -108.37 | |
| b | -99109 | -19460 | 8545.9 | -394.67 | -7295.8 | 157.93 | 2088.9 | 1555.6 | -815.05 | 147.71 | 4746.7 | |
| С | -291.87 | -54.22 | 30.19 | 2.08 | -19.89 | 2.40 | 7.89 | 5.81 | -1.59 | 1.32 | 16.02 | |
| %RAD | 4.09 | 1.51 | 0.25 | 0.028 | 0.75 | 0.24 | 0.24 | 0.11 | 0.099 | 0.009 | 0.14 | |
| 1-Octano | ol | | | | | | | | | | | |
| а | 40.70 | 39.00 | 27.26 | 20.16 | 11.15 | 71.24 | 66.28 | 35.34 | 62.91 | 34.59 | -104.95 | |
| b | -2222.9 | -2108.6 | -1573.3 | -1266.9 | -842.74 | -3642.7 | -3419.1 | -2043.8 | -3389.5 | -2061.5 | 4580.1 | |
| с | -6.03 | -5.79 | -4.04 | -2.97 | -1.63 | -10.53 | -9.79 | -5.17 | -9.23 | -5.05 | 15.52 | |
| %RAD | 0.41 | 0.40 | 0.20 | 0.14 | 0.12 | 0.29 | 0.15 | 0.12 | 0.27 | 0.12 | 0.12 | |

aqueous phase [54]. Thus, the organic diluent with low solubility in water should be selected [55]. From the results, chlorobenzene and 1-octanol were not recommended although they were highly soluble with di-(2-ethylhexyl)phosphoric acid.

The tie-line data of the ternary liquid systems for each temperature were listed in Table 5 and also plotted in Fig. 7(a) to (d). The slopes (S) of all tie-lines were calculated as shown in Eq. (3) and their values are reported in Table 5. From this table, the slope values slightly decreased when the temperatures increased. The decrease in slope values indicates the decrease in di-(2-ethylhexyl)phosphoric acid composition in the organic phase and it increased in the aqueous phase. This is because the slope of the tie-lines expresses its composition in the organic and aqueous phases. The increase in di-(2-ethylhexyl)phosphoric acid composition in the aqueous phase was resulted from the decrease in polarity of water until closing to the polarity of di-(2-ethylhexyl) phosphoric acid.

$$S = \frac{w_{23} - w_{21}}{w_{33} - w_{31}} \tag{3}$$

where w_{21} and w_{23} are the mass percentages of di-(2-ethylhexyl) phosphoric acid in the aqueous and organic phases, and w_{31} and w_{33} are the mass percentages of organic diluent in the aqueous and organic phases, respectively.

The Bachman equation was also applied to align with the experimental tie-line data, and its equation was shown below [58]:

$$w_{23} = A + B\left(\frac{w_{23}}{w_{11}}\right) \tag{4}$$

where w_{11} and w_{23} are the mass percentages of water and di-(2-ethylhexyl)phosphoric acid in the aqueous and organic phases, respectively. A and B are the parameters in the Bachman equation.

The plots between w_{23} and w_{23}/w_{11} for each organic diluent and studied temperature are presented in Fig. 8 to observe their linearity and obtain the Bachman parameters of A and B. From these figures, the graphs showed good linearity where R^2 approached to 1.0000. The Bachman parameters of A and B were obtained from the interceptions and slopes of graphs, respectively. Their values are shown in Table 6. In addition, the standard

deviations of error (σ) between calculated and experimental results were also determined and reported in this table. The small values of standard deviations of error indicated the accuracy of the experimental tie-line results

3.2. The correlation of solubility data by the modified Apelblat equation

The modified Apelblat equation was applied to predict the solubility of the solid component in the organic phase [36]. Furthermore, Marche et al. [59] used this model to predict the solubility of n-alkanes (C6–C8) in water. In this work, the modified Apelblat equation was used to predict the solubility of water in the organic phases by varying the temperatures. Moreover, mole fraction of water (x_1) was obtained as shown in Eq. (5) for use in the modified Apelblat equation:

$$x_1 = \frac{m_1/M_1}{m_1/M_1 + m_2/M_2 + m_3/M_3} \tag{5}$$

where m_1 , m_2 , m_3 and M_1 , M_2 , M_3 are the masses and molecular weights of water, di-(2-ethylhexyl)phosphoric acid and organic diluent, respectively.

The relationship between solubility and temperature for any organic diluents could be described by the modified Apelblat equation as follows [60,61]:

$$\ln(x_1) = a + \frac{b}{T/K} + c\ln(T/K) \tag{6}$$

where a, b and c are the modified Apelblat parameters as obtained by the experimental solubility data and T is the absolute temperature (K).

The correlation of calculated and experimental results was shown by the relative average deviation (RAD) as defined below:

$$RAD = \frac{1}{N} \sum_{i=1}^{n} \left| \frac{x_{i,exp} - x_{i,cal}}{x_{i,exp}} \right|$$
 (7)

where N is the number of experimental points and $x_{i,\text{exp}}$ and $x_{i,\text{cal}}$ are the experimental and calculated solubility values, respectively.

The modified Apelblat parameters of *a*, *b* and *c* together with the RAD values are listed in Table 7. From this table, the calculated and

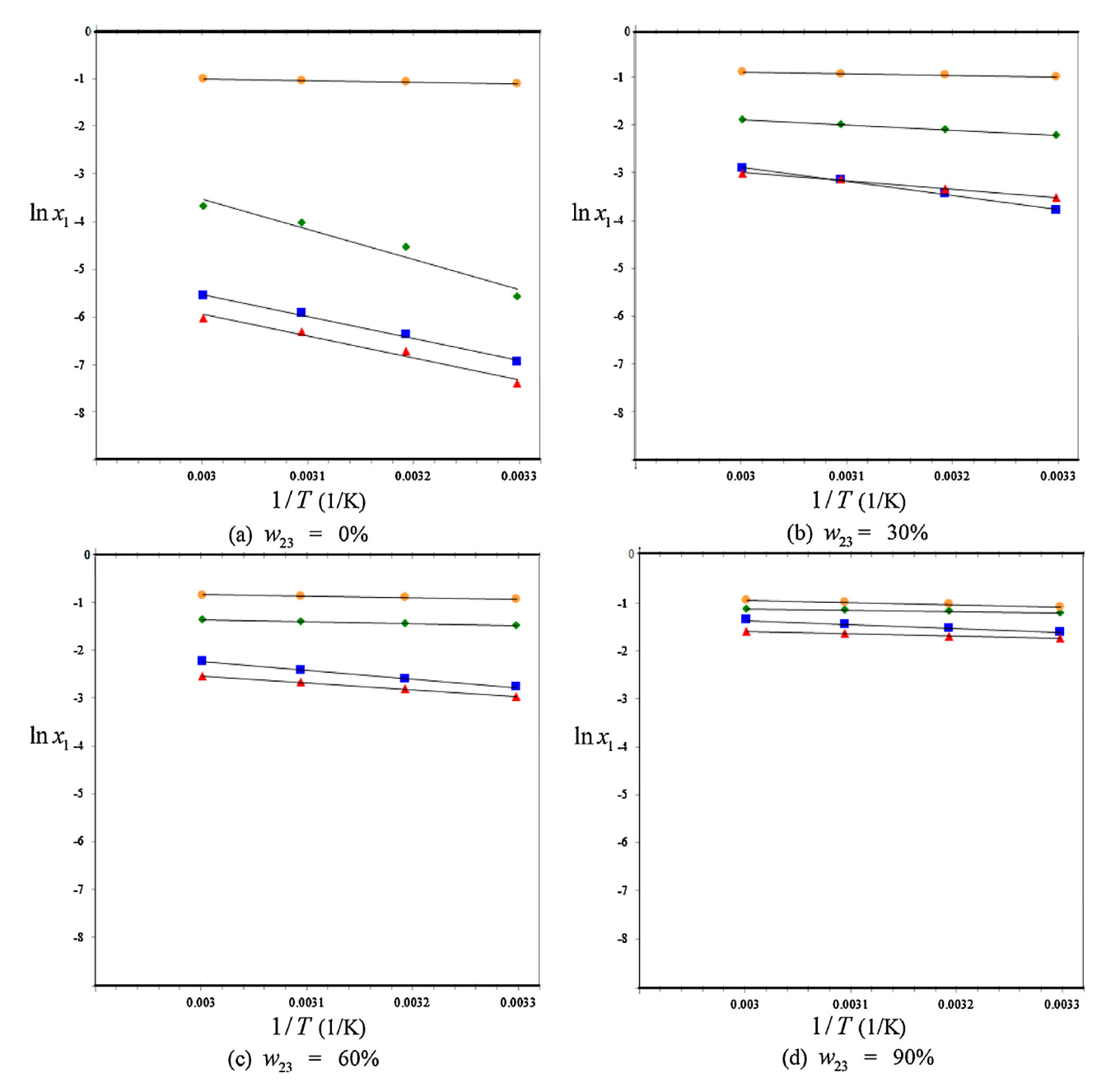


Fig. 9. The van't Hoff plots of $\ln x_1$ versus 1/T for the different organic diluents (fx2 = n-heptane, fx3 = kerosene, fx4 = 1-octanol and fx5 = chlorobenzene).

experimental results showed a good correlation as confirmed by the RAD values in the range of 0.01–4.09%. The results demonstrated that the modified Apelblat equation had the reliability to describe the relationship of solubility and temperature for any organic diluents.

3.3. The thermodynamic parameters for dissolution of water in the organic phases

The dissolution of water in each organic phase by varying the temperatures was considered by the van't Hoff equation to determine their thermodynamic parameters of enthalpy and entropy. The equation was shown below as follows [62]:

$$\ln x_1 = \frac{\Delta H_{\text{fus}}}{R} \left(\frac{1}{T_{\text{fus}}} - \frac{1}{T} \right) = -\frac{\Delta H_{\text{fus}}}{RT} + \frac{\Delta S_{\text{fus}}}{R}$$
 (8)

where x_1 is the mole fraction of water in the organic phase, $T_{\rm fus}$ is the fusion temperature (melting point) of the water, T is the organic temperature (K), $\Delta H_{\rm fus}$ is the molar fusion enthalpy of water (kJ/mol), $\Delta S_{\rm fus}$ is the molar fusion entropy of water (kJ/mol) and R is the gas constant (=8.314J/mol K).

The molar enthalpy ($\Delta H_{\rm fus}$) and molar entropy ($\Delta S_{\rm fus}$) were accounted for replacing $\Delta H_{\rm fus}$ by the dissolution enthalpy ($\Delta H_{\rm d}$) and $\Delta S_{\rm fus}$ by the dissolution entropy ($\Delta S_{\rm d}$) as shown in Eq. (9) [63]:

$$\ln x_1 = -\frac{\Delta H_d}{RT} + \frac{\Delta S_d}{R} \tag{9}$$

From Eq. (9), $\ln x_1$ was plotted with 1/T by varying the compositions of di-(2-ethylhexyl)phosphoric acid in the organic phase. The results are shown in Figs. 9(a)–(d). The linearity of these plots was observed, and ΔH_d and ΔS_d were determined by the slopes and interceptions of the graphs, respectively. Their values are presented in Table 8 and the linearity of the graphs was also

Table 8 The dissolution enthalpy (ΔH_d , kJ/mol) and the dissolution entropy (ΔS_d , J/mol K) for the dissolution of water in the organic phases.

| | %w ₂₃ | | | | | | | | | | |
|---------------------|------------------|--------|--------|--------|--------|--------|--------|--------|--------|--------|--------|
| | 0 | 10 | 20 | 30 | 40 | 50 | 60 | 70 | 80 | 90 | 100 |
| Kerosei | ne | | | | | | | | | | |
| $\Delta H_{ m d}$ | 38.00 | 28.12 | 21.69 | 14.70 | 17.56 | 14.27 | 11.65 | 10.53 | 9.57 | 4.00 | 1.37 |
| $\Delta S_{ m d}$ | 64.56 | 52.68 | 37.68 | 19.26 | 30.74 | 21.18 | 13.81 | 11.40 | 9.64 | -1.22 | -5.32 |
| R^2 | 0.9715 | 0.9786 | 0.9950 | 0.9922 | 0.9970 | 0.9999 | 0.9987 | 0.9966 | 0.9998 | 0.9999 | 0.9792 |
| n-Hept | ane | | | | | | | | | | |
| $\Delta H_{\rm cl}$ | 38.67 | 33.09 | 27.89 | 24.52 | 22.16 | 23.77 | 15.16 | 13.31 | 11.38 | 7.19 | 1.37 |
| $\Delta S_{\rm d}$ | 70.11 | 70.40 | 57.65 | 49.55 | 44.39 | 50.99 | 26.87 | 22.30 | 18.65 | 10.30 | -5.31 |
| R^2 | 0.9938 | 0.9955 | 0.9967 | 0.9987 | 0.9969 | 0.9865 | 0.9957 | 0.9995 | 0.9985 | 0.9974 | 0.9690 |
| Chlorol | oenzene | | | | | | | | | | |
| $\Delta H_{ m cl}$ | 52.42 | 18.21 | 8.73 | 8.78 | 7.91 | 4.95 | 3.40 | 2.40 | 2.54 | 2.26 | 1.40 |
| $\Delta S_{\rm d}$ | 127.90 | 31.35 | 7.37 | 10.59 | 9.16 | 2.02 | -1.11 | -2.97 | -1.92 | -2.47 | -5.23 |
| R^2 | 0.9509 | 0.9874 | 0.9806 | 0.9999 | 0.9999 | 0.9949 | 0.9790 | 0.9847 | 0.9988 | 0.9994 | 0.9591 |
| 1-Octai | nol | | | | | | | | | | |
| $\Delta H_{ m d}$ | 2.42 | 2.10 | 2.34 | 2.64 | 2.66 | 2.41 | 2.54 | 3.30 | 3.73 | 3.77 | 1.39 |
| $\Delta S_{\rm d}$ | -1.24 | -1.84 | -0.81 | 0.44 | 0.75 | 0.23 | 0.66 | 2.87 | 3.95 | 3.56 | -5.26 |
| R^2 | 0.9760 | 0.9701 | 0.9929 | 0.9975 | 0.9985 | 0.9736 | 0.9764 | 0.9963 | 0.9912 | 0.9972 | 0.9729 |

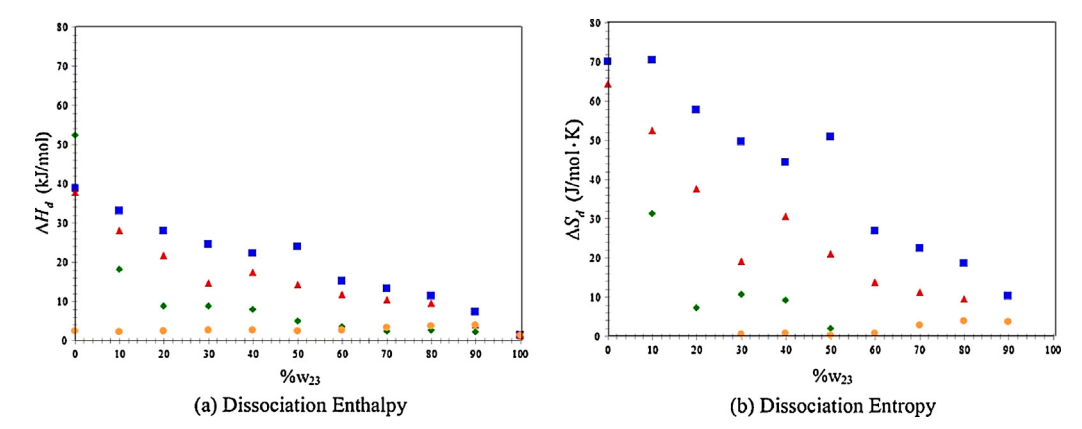


Fig. 10. The dissociation enthalpy (a) and the dissociation entropy (b) for the dissociation of water in the organic phases versus the mass percentages of di-(2-ethylhexyl) phosphoric acid in the different organic diluents (fx2 = *n*-heptane; fx3 = kerosene; fx4 = 1-octanol and fx5 = chlorobenzene).

expressed by R^2 . From this table, the positive values of $\Delta H_{\rm d}$ and $\Delta S_{\rm d}$ indicated that the dissolution of water in all organic phases was endothermic and driven by the entropy.

In addition, the plots between $\Delta H_{\rm d}$ or $\Delta S_{\rm d}$ values and the compositions of di-(2-ethylhexyl)phosphoric acid in the organic phases are presented in Fig. 10(a) and (b). Both values decreased when the compositions of di-(2-ethylhexyl)phosphoric acid increased. The decrease in dissolution enthalpy meant that the dissolution of water in the organic phases required little energy for use in the process. For dissolution entropy, the decrease of its results demonstrated the order of dissolution process [64].

The Gibbs energy $(\Delta H_{\rm d})$ of water solubility in the organic phase for each organic diluent and studied temperature was also determined from Eqs. (10) and (11) [65] and used the $\Delta H_{\rm d}$ and $\Delta S_{\rm d}$ values in Table 9 for calculation:

$$\Delta G_{\rm d} = \Delta H_{\rm d} - T \Delta S_{\rm d} \tag{10}$$

$$\Delta G_{\rm d} = -RT \ln x_1 \tag{11}$$

The plots of $\Delta G_{\rm d}$ and $\ln x_1$ for each organic diluent and studied temperature are presented in Fig. 11. Gibbs energy decreased when the solubility of water in the organic phases increased. The Gibbs energy values are also listed in Table 9 and their positive values

Table 9 The Gibbs energy (ΔG_d) for water solubility in the organic phases.

| T(K) | $\Delta G_{\rm d}$ (kJ/mol) | | | | | | | | | | |
|-----------|-----------------------------|-------|-------|------|------|------|------|------|------|------|------|
| | %w ₂₃ | | | | | | | | | | |
| | 0 | 10 | 20 | 30 | 40 | 50 | 60 | 70 | 80 | 90 | 100 |
| | Kerosene | | | | | | | | | | |
| 303.2 | 18.65 | 12.30 | 10.31 | 8.87 | 8.24 | 7.84 | 7.48 | 7.10 | 6.65 | 4.37 | 2.92 |
| 313.2 | 17.51 | 11.40 | 9.86 | 8.69 | 7.97 | 7.64 | 7.32 | 6.94 | 6.54 | 4.38 | 3.00 |
| 323.2 | 16.96 | 11.07 | 9.45 | 8.40 | 7.57 | 7.41 | 7.18 | 6.83 | 6.45 | 4.40 | 2.99 |
| 333.2 | 16.72 | 10.67 | 9.20 | 8.33 | 7.34 | 7.21 | 7.07 | 6.76 | 6.36 | 4.41 | 2.95 |
| | n-Heptane | | | | | | | | | | |
| 303.2 | 17.52 | 11.75 | 10.46 | 9.53 | 8.71 | 8.40 | 6.98 | 6.56 | 5.72 | 4.05 | 2.92 |
| 313.2 | 16.59 | 11.10 | 9.80 | 8.97 | 8.28 | 8.58 | 6.79 | 6.31 | 5.53 | 3.97 | 3.00 |
| 323.2 | 15.93 | 10.21 | 9.19 | 8.48 | 7.74 | 7.97 | 6.50 | 6.10 | 5.38 | 3.87 | 2.99 |
| 333.2 | 15.42 | 9.70 | 8.75 | 8.05 | 7.41 | 7.14 | 6.17 | 5.88 | 5.15 | 3.74 | 2.95 |
| | Chlorobenzene | | | | | | | | | | |
| 303.2 | 14.06 | 8.78 | 6.45 | 5.56 | 5.16 | 4.33 | 3.72 | 3.29 | 3.13 | 3.01 | 2.94 |
| 313.2 | 11.84 | 8.28 | 6.47 | 5.46 | 5.00 | 4.32 | 3.76 | 3.34 | 3.14 | 3.04 | 2.99 |
| 323.2 | 10.81 | 8.08 | 6.38 | 5.35 | 4.97 | 4.32 | 3.78 | 3.37 | 3.17 | 3.06 | 2.99 |
| 333.2 | 10.21 | 7.81 | 6.23 | 5.25 | 4.87 | 4.26 | 3.75 | 3.38 | 3.19 | 3.08 | 2.95 |
| 1-Octanol | | | | | | | | | | | |
| 303.2 | 2.80 | 2.67 | 2.59 | 2.51 | 2.43 | 2.35 | 2.36 | 2.44 | 2.55 | 2.70 | 2.94 |
| 313.2 | 2.79 | 2.66 | 2.59 | 2.50 | 2.42 | 2.31 | 2.32 | 2.39 | 2.48 | 2.65 | 2.99 |
| 323.2 | 2.84 | 2.72 | 2.61 | 2.51 | 2.42 | 2.33 | 2.32 | 2.37 | 2.46 | 2.62 | 2.99 |
| 333.2 | 2.83 | 2.71 | 2.61 | 2.50 | 2.41 | 2.34 | 2.34 | 2.35 | 2.43 | 2.59 | 2.95 |

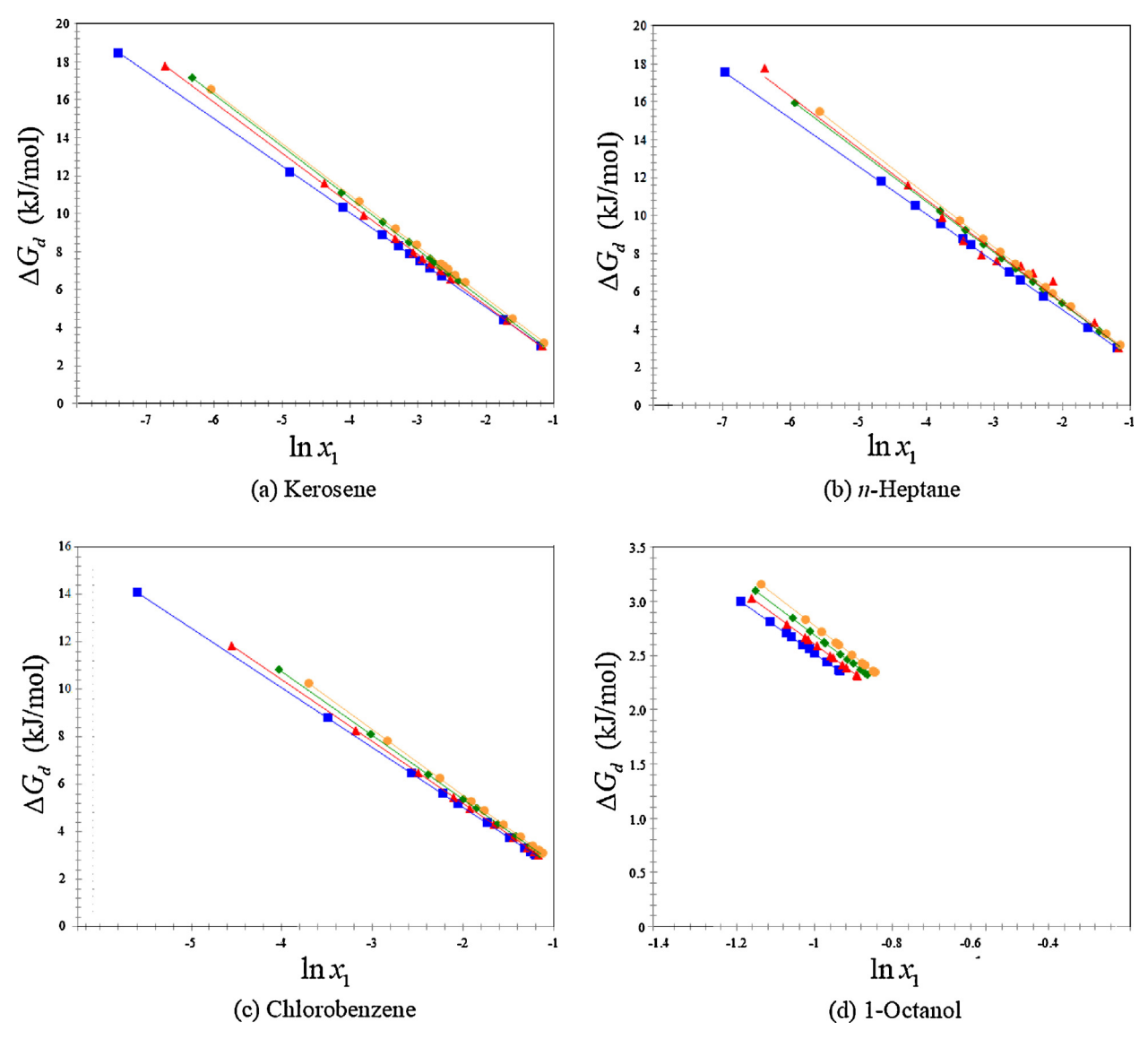


Fig. 11. The Gibbs energy for the dissociation of water in the organic phases versus its solubility in term of logarithm at the different temperatures (fx2 = 303.2 K, fx3 = 313.2 K, fx4 = 323.2 K and fx5 = 333.2 K) and the pressure of 0.1 MPa.

demonstrated that the dissociation of water in the organic phases was a non-spontaneous process.

4. Conclusion

The equilibrium solubility for the ternary systems of water + di-(2-ethylhexyl)phosphoric acid+organic diluents (kerosene, nheptane, chlorobenzene and 1-octanol) exhibited type II behavior at the temperature of 303.2-333.2 K and the pressure of 0.1 MPa. Solubility increased when the polarity of organic diluents and the temperatures increased. The solubility of water in the organic phases simultaneously increased. When the temperature increased, the slopes of tie-lines decreased which indicated the decrease in composition of di-(2-ethylhexyl)phosphoric acid in the organic phases and its solubility in the aqueous phases. The solubility of water in the organic phases was calculated by the modified Apelblat equation which showed a good correlation with the experimental results as confirmed by the RAD values of 0.01-4.09%. The thermodynamic parameters of enthalpy, entropy and Gibbs energy were calculated using the van't Hoff model. Their positive values demonstrated that the dissociation of water in the organic phases was endothermic and a non-spontaneous process and driven by the entropy. Based on the important role of solubility and temperature for the separation processes, kerosene was found to be the most suitable organic diluent in this work and should be further recommended.

Acknowledgements

The authors gratefully acknowledge the financial support by the National Research University Project, Office of Higher Education Commission (WCU-041-EN-57), as well as the Thailand Research Fund (RSA5680044) and Chulalongkorn University. Sincere thanks also go to Asst. Prof. Dr. Kadisit Nootong for his kind support.

Appendix A. Supplementary data

Supplementary data associated with this article can be found, in the online version, at http://dx.doi.org/10.1016/j.fluid.2015.05.017.

References

- [1] H.G. Gilani, M. Ganji, S. Fallahi, Appl. Math. Modell. 36 (2012) 4096–4105.
- [2] H.G. Gilani, A.G. Gilani, M. Sangashekan, J. Chem. Thermodyn. 58 (2013) .

- [3] J. Rydberg, M. Cox, C. Musikas, R.G. Choppin, Solvent Extraction Principals and Practices, second ed., Marcel Dekker, New York, 2004.
- [4] T.M. Letcher, Thermodynamics, Solubility and Environmental Issues, Elsevier, 2007.
- [5] M.T. Zafarani-Moattar, P. Jafari, Fluid Phase Equilib. 353 (2013) 50-60.
- [6] A. Cháfer, J. Torre, E. Lladosa, J.B. Montón, Fluid Phase Equilib. 377 (2014) 38–44.
- [7] B.E. García-Flores, D.N. Justo-García, M.A. Aquino-Olivos, F. García-Sánchez, Fluid Phase Equilib. 385 (2015) 166–174.
- [8] E.J. González, P.F. Requejo, Á. Domínguez, E.A. Macedo, Fluid Phase Equilib. 360 (2013) 416–422.
- [9] F. Principe, G.P. Demopoulos, Hydrometallurgy 68 (2003) 115-124.
- [10] Y. Meguro, S. Iso, T. Sasaki, Z. Yoshida, Anal. Chem. 70 (1998) 774-779.
- [11] D.L. Wise, Remediation of Hazardous Waste Contaminated Soils, CRC Press, 1994, pp. 755.
- [12] G. Owusu, Hydrometallurgy 47 (1998) 202–215.
- [13] T. Sato, J. Inorg. Nucl. Chem. 24 (1962) 699–706.
- [14] T. Bin, Z. Zheng, L. GuangSheng, W. JiaDing, Sci. China Ser. B 51 (2008) 887–892.
- [15] D. Darvishi, D.F. Haghshenas, S. Etemadi, E.K. Alamdari, S.K. Sadrnezhaad, Hydrometallurgy 88 (2007) 92–97.
- [16] I.G. Garcia, A.C. Perez, F.C. Calero, J. Chem. Eng. Data 33 (4) (1988) 468-472.
- [17] C. Ye, J. Mol. Liq. 186 (2013) 39-43.
- [18] C.Y. Cheng, Hydrometallurgy 56 (2000) 369-386.
- [19] L. Wang, T. Lv, J. Mol. Liq. 181 (2013) 29-33.
- [20] N. Sunsandee, M. Hronec, M. Stolcova, N. Leepipatpiboon, U. Pancharoen, J. Mol. Liq. 180 (2013) 252–259.
- [21] G. Yang, Y. Huang, G. Nan, H. Chen, A. Zeng, X. Bian, J. Mol. Liq. 180 (2013) 160–163.
- [22] Z. Meng, Y. Hu, Y. Kai, W. Yang, Z. Cao, F. Shen, Fluid Phase Equilib. 352 (2013)
- [23] W. Liu, L. Xu, Y. Li, T. Luo, G. Liu, Thermochim. Acta 544 (2012) 89-94.
- [24] T.L. Chester, J.W. Coym, J. Chromatogr. A 1003 (2003) 101-111.
- [25] T. Wongsawa, M. Hronec, U. Pancharoen, S. Phatanasri, Fluid Phase Equilib. 379 (2014) 10–18.
- [26] M.-J. Lee, Y.-C. Kuo, P.-J. Lien, H.-M. Lin, Open Thermodyn. J. 4 (2010) 122–128.
- [27] X. Zhang, C. Jian, J. Chem. Eng. Data 57 (2012) 142-147.
- [28] M. Rogošiæ, M. Bakula, M. Upan, Chem. Biochem. Eng. Q. 26 (2012) 155-162.
- [29] W. Larsson, J. Jalbert, R. Gilbert, A. Cedergren, Anal Chem. 75 (2003) 1227–1232.
- [30] United States Environmental Protection Agency, Exemptions from the Requirement of a Tolerance for Petroleum Hydrocarbons, EPA, Washington, D.C, 2006.
- [31] David R. Lide, CRC Handbook of Chemistry and Physics, eighty fourth ed., CRC Press, 2003–2004.
- [32] Landolt-Börnstein, New Series, Static Dielectric Constants of Pure Liquids and Binary Liquid Mixtures, Springer-Verlag, Heidelberg, 1991.
- [33] B.N. Taylor, C.E. Kuyatt, NIST Technical Note 1297, National Institute of Standards and Technology (NIST), 1994, pp. 1–20.

- [34] R.E. Treybal, Mass-Transfer Operations, McGraw-Hill Book Company, Inc., USA, 1987
- [35] J.E. Ricci, T.W. Davis, J. Am. Chem. Soc. 62 (1940) 407–413.
- [36] A. Jouyban, J. Pharm. Sci. 11 (2008) 32-58.
- [37] K. Wongkaew, U. Pancharoen, S. Phatanasri, N. Leepipatpiboon, A.W. Lothongkum, J. Ind. Eng. Chem. 21 (2015) 212–220.
- [38] R.M. Stephenson, J. Stuart, M. Tabak, J. Chem. Eng. Data 29 (1984) 287-290.
- [39] M. Valiskó, D. Boda, Condens. Matter Phys. 8 (2005) 357–376.
- [40] J.N. Spencer, E.A. Robinson, H.D. Schreiber, J. Phys. Chem. 75 (1971) 2219–2222.
- [41] R.C. Dougherty, J. Chem. Phys. 109 (1998) 7372-7378.
- [42] C.G. Malmberg, A.A. Maryott, J. Res. Natl. Stand. 56 (1956) 1-8.
- [43] C. Wohlfarth, Static Dielectric Constants of Pure Liquids and Binary Liquid Mixtures, Landolt-Börnstein, Springer-Verlag, Berlin, 1991.
- [44] K.N. Marsh, Recommended Reference Materials for the Realization of Physicochemical Properties, Blackwell Scientific Publications, Oxford, 1987.
- [45] T. Wongsawa, N. Sunsandee, A.W. Lothongkum, U. Pancharoen, S. Phatanasri, Fluid Phase Equilib. 388 (2015) 22–30.
- [46] M.A. Azam, S. Alam, F.I. Khan, J. Chem. Eng. IEB 25 (2010) 18-21.
- [47] Heavy Water Board, India, TOPS 99 Product Data Sheet (2014).
- [48] B.A. Englin, A.F. Plate, V.M. Tugolukov, M.A. Pryanishnikova, Khim. Tekhnol. Topl. Masel. 10 (1965) 42.
- [49] H.-J. Bittrich, H. Gedan, G. Feix, Z. Phys. Chem. (Leipzig) 260 (1979) 1009.
- [50] B.A. Englin, A.F. Plate, V.M. Tugolukov, M.A. Pryanishnikova, Khim. Tekhnol. Topl. Masel. 10 (1965) 42.
- [51] IUPAC, Solubility Data Series: Halogenated Benzenes, Toluenes and Phenol with Water, 20, IUPAC, 1985, pp. 153–185.
- [52] B.E. Lang, J. Chem. Eng. Data 57 (2012) 2221-2226.
- [53] C. Hansen, The Three Dimensional Solubility Parameter and Solvent Diffusion Coefficient and Their Importance in Surface Coating Formulation, Danish Technical Press, Copenhagen, 1967.
- [54] S. Ramaswamy, H.-J. Huang, B.V. Ramarao, Separation and Purification Technologies in Biorefineries, Wiley, 2013.
- [55] N.P. Cheremisinoff, Industrial Solvents Handbook Revised And Expanded, CRC Press, 2002, pp. 79–80.
- [56] C.F. Baes Jr., B.A. Moyera, G.N. Casea, F.I. Casea, Sep. Sci. Technol. 25 (1990) 1675–1688.
- [57] C. Hansen, Hansen Solubility Parameters: A User's Handbook, second ed., CRC Press, 2007.
- [58] H.G. Gilani, M. Golpour, S.S. Ashraf, Fluid Phase Equilib. 310 (2011) 192-197.
- [59] C. Marche, C. Ferronato, J. Jose, J. Chem. Eng. Data 48 (2003) 967–971.
- [60] A. Apelblat, E. Manzurola, J. Chem. Thermodyn. 29 (1997) 1527-1533.
- [61] A. Apelblat, E. Manzurola, J. Chem. Thermodyn. 31 (1999) 85–91.
- [62] U.K. Deiters, Fluid Phase Equilib. 336 (2012) 22-27.
- [63] L.C. Song, Y. Gao, J.B. Gong, J. Chem. Eng. 56 (2011) 2553–2556.
- [64] N. Nevers, Physical and Chemical Equilibrium for Chemical Engineers, second ed., Wiley, 2012.
- [65] J. Sousa, J. Almeida, A. Ferreira, H. Fachada, I. Fonseca, Fluid Phase Equilib. 303 (2011) 115–119.

A publication of

ADDC

The Italian Association of Chemical Engineering www.aidic.it/cet

VOL. 37, 2014

Guest Editors: Eliseo Ranzi, Katharina Kohse- Höinghaus Copyright © 2014, AIDIC Servizi S.r.I., ISBN 978-88-95608-28-0: ISSN 2283-9216

DOI: 10.3303/CET1437037

Modeling of a Small-scale Biomass Updraft Gasifier

Soorathep Kheawhom*a, Pornchai Bumroongsrib

^aComputational Process Engineering, Department of Chemical Engineering, Faculty of Engineering, Chulalongkorn University, Phayathai Rd., Pathumwan, Bangkok, 10330, Thailand.

^bDepartment of Chemical Engineering, Faculty of Engineering, Mahidol University, Nakhon Pathom, 73170 Thailand. soorathep.k@chula.ac.th

Biomass can be efficiently transformed into valuable gas products via gasification. Gasification converts biomass through partial oxidation into a gaseous mixture, small quantities of char and condensable compounds. In this work, an updraft gasifier is regarded because the updraft gasifier is suitable for wet fuels such as agricultural residues. Moreover, it is the most simple and can be used as a basis for the design and operation of small-scale gasifier. However, due to the high tar content of the gas produced, updraft gasifiers may not effectively be used without comprehensive gas cleaning. To improve an insight on the gasification process, appropriate mathematical models are required. Further, models are useful for gasifier design and operation such as prediction of operation behavior during normal operation, startup, and shutdown. This article presents a one-dimensional mathematical model for the simulation of a smallscale fixed-bed updraft gasifier of rice straw. The model is based on a set of differential equations describing the entire gasification process. The governing equations include conservation of mass and energy, complemented by boundary conditions, constitutive relationships. The main features of the model include homogeneous and heterogeneous combustion and gasification reactions, pyrolysis kinetics and drying, heat and mass transfer in the solid and gas phases as well as between phases. The simulation results were compared with experimental data, and showed good agreement. The model constructed was then used to predict the effects of varying moisture content and air feed temperature. Fuel with higher moisture content of fuel feed lowered the performance of the gasification process. But, higher temperature of air feed resulted in higher performance with lower tar content and more environmentally preferable.

1. Introduction

Renewable energy plays an important role in reducing greenhouse gas emissions resulting from burning fossil fuels. Biomass refers to any organic materials derived from plants or animals. Biomass is one of the renewable energy sources with a great potential to produce energy, in addition to being carbon neutral. It can be converted to gaseous or liquid fuels by thermo-chemical or biochemical processes (Wetterlund et al., 2010).

Biomass gasification is one of few technologies that can potentially generate carbon neutral energy with pollution-free power and also turn agricultural waste into energy (Moghadam et al., 2013). Biomass gasification is a thermo-chemical process that generates producer gas or synthesis gas by partial oxidation of biomass feedstock in fuel-rich conditions in the presence of air, steam, or oxygen.

The advantage of gasification lies on the fact that using the syngas is potentially more efficient than direct combustion of the original fuel because it can be combusted at higher temperature, so that it shifts the thermodynamic upper limit to the efficiency.

Thermo-chemical gasification can be classified on the basis of the gasifying agent, which could be air, steam, or oxygen. Air blown gasification processes usually yield a low heating value gas. Oxygen and steam blown gasification usually yield a higher heating value gas. However, the disadvantage with the oxygen blown or steam injection systems is the high cost for the oxygen or steam production equipment.

Three types of gasifier including fixed or moving bed, fluidized bed, and entrained flow are generally used. For large-scale applications, the most preferred and reliable system is the circulating fluidized bed. In contrast, fixed bed systems are more appropriate for small-scale systems.

The fixed-bed designs are basically updraft or downdraft. In downdraft gasifiers, the fuel and gasification agent flow in the same direction and the gas leaves the reactor near the hottest zone, which makes the tar concentration much lower than in updraft gasifiers. In the other hand, the fuel bed moves downwards and the gasification agent flows from the bottom upwards in updraft gasifiers, As the gas leaves the reactor near the pyrolysis zone, the gas generated in updraft gasifiers has a high content of organic components (tar). The solid carbon in the fuel is almost completely converted into gas and tar. However, updraft gasifiers can be used for wet fuels and are relatively intensive to the fuel size. Updraft gasifiers generally operate with high overall carbon conversion, high thermal efficiency, high residence time of solids, low gas velocity and low ash carry-over. The updraft gasifiers are suitable for small-scale systems. The maximum size of these units is limited to a few MW fuel power because of the problem of maintaining a regular conversion front in a wide fixed bed.

Biomass gasifiers are complex facilities, which makes it difficult to investigate their various operating conditions. The characteristics of biomass greatly influence the performance of a biomass gasifier. A proper understanding of the physical and the chemical properties of biomass feedstock is essential for the design and operation of a biomass gasifier to be reliable. Numerous models for biomass gasifier have been developed. These models can be categorized into two groups: (1) thermodynamic equilibrium models and (2) kinetic models. The thermodynamic equilibrium models, also known as zero-dimensional (0D) models, are widely used among researchers to predict the composition of the produced syngas and the equilibrium temperature by assuming that the chemical reactions reach equilibrium. However, these models cannot provide highly accurate results and also cannot provide the concentration or temperature profiles inside the reactor. Because this approach is independent of the gasifier design, kinetic models, which take into account the reaction kinetics and the transfer phenomena among the phases, onedimensional (1D) biomass gasification models have been developed. These models simulated the variations in the physical and chemical properties along the reactor height by considering the vertical movements. A 1D unsteady mathematical model of updraft wood gasifier was developed and used to simulate the structure of the reaction fronts and the gasification behavior of a laboratory-scale plant (Blasi, 2004). Blasi and Branca (2013) developed a mathematical model of an open-core downdraft gasifier with dual air entry. The reaction front structure varies with percentage and position of secondary air. Thus, char and tar conversion can be improved. Two-dimensional (2D) models have been developed to improve an insight on the effects of the reactor geometry. Wu et al. (2013) developed a 2D computational fluid dynamics (CFD) model for downdraft gasifier with preheated air and steam in order to investigate various operating conditions. Zhang et al. (2011) used 2D CFD model for and updraft gasifier to perform a simulation of municipal solid waste gasification.

In this study, we developed a 1D mathematical model of small-scale updraft biomass gasifier. Rice straw was used as fuel feed. The model developed was validated with experimental data. The mathematical model constructed was then used to investigate the effects of varying moisture content and air feed temperature. The paper is organized as follows. In section 2, principles of biomass gasification are presented. In section 3, experimental setup used to validate the model developed is presented. In section 4, the model development and validation are presented. In sections 5, the effects of various parameters are discussed. In the last section, we conclude the paper.

2. Principles of biomass gasification

Gasification is partial thermal oxidation resulting in a high proportion of gaseous products, small quantities of char, ash and condensable compounds. Steam, air or oxygen is supplied to the reaction as a gasifying agent. The chemistry of biomass gasification is complex and consists of the following stages:

2.1 Drying

In this stage, the moisture content of the biomass is reduced. The typical moisture content of biomass ranges from 5 to 60%. Most gasification systems use dry biomass with moisture content of 10 to 20%. The final drying takes place at about 400 - 500 K after the feed enters the gasifier, where it receives heat from the hot zone downward. This heat dries the feed, which releases water. As the temperature rises, the low-molecular-weight extractives start volatilizing. This process continues until a temperature of approximately 500 K is reached.

2.2 Thermal decomposition

In pyrolysis no external agent is added. The oxygen is largely diminished. The volatile matter in the biomass is reduced. Consequently, hydrocarbon gases are released from the biomass, and the biomass is reduced to solid charcoal. The hydrocarbon gases can condense at a sufficiently low temperature to generate liquid tars.

2.3 Gasification

The gasification step involves chemical reactions among the hydrocarbons in fuel, steam, carbon dioxide, oxygen, and hydrogen in the reactor, as well as chemical reactions among the evolved gases. Char gasification is the most important. The char produced through pyrolysis of biomass is not necessarily pure carbon. It contains a certain amount of hydrocarbon comprising hydrogen and oxygen. Gasification of biomass char involves several reactions between the char and the gasifying mediums. In the absence of oxygen, several reduction reactions occur in the 1100 - 1300 K temperature range. These reactions are mostly endothermic.

2.4 Combustion

Most gasification reactions are endothermic. To provide the required heat of reaction as well as that required for heating, drying, and pyrolysis, a certain amount of exothermic combustion reaction is allowed in a gasifier. Combustion is a reaction between solid carbonized biomass and oxygen in the air, resulting in formation of carbon dioxide. Hydrogen present in the biomass is also oxidized to generate water. A large amount of heat is released with the oxidation of carbon and hydrogen. Combustion reactions are generally faster than gasification reactions under similar conditions.

3. Experimental setup

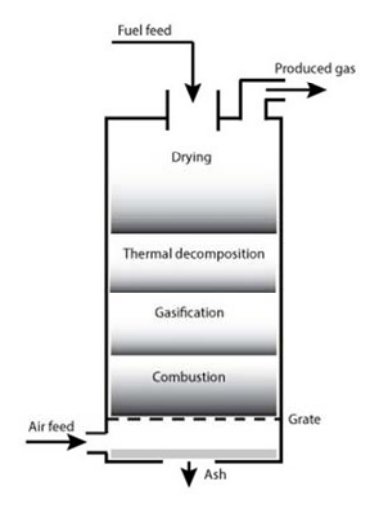
A small-scale updraft biomass gasifier has been devised. Figure 1 shows a schematic diagram of the updraft gasifier used in this work. The reactor is a vertically cylindrical chamber with 0.15 m diameter and 0.6 m height. The fuel feed, rice straw, was introduced from the top of a chamber using a continuous screw feeding system. Gasifying medium (air) was preheated to 313.5 K by an external heater to maintain a stable operation, and fed to the chamber through a grid at the bottom of the chamber. The gas then rose through a bed of descending fuel or ash in the gasifier chamber. The grate stopped biomass/char particles, resulting in a charcoal bed. The temperature of 1500 K was the highest temperature being close to the grate, where oxygen met and burned the char. Hot gas produced by combustion traveled up, providing heat to the endothermic gasification reactions at 1000 to 1200 K, and met pyrolyzing biomass at a lower temperature of 500 to 800 K. Primary tar was produced in this temperature range. The temperatures were measured using thermocouple probes located at the centerline along the height of the reactor in various different reaction zones. The product gas, which was sampled at the outlet, leaved from the top while solids left from the bottom. The feedstock used for this study was rice straw, 0.01 m in diameter, with an average length/diameter ratio of 1 to 2.5. The bulk density of rice straw was 150 kg/m³. The properties of the feedstock are shown in Table 1.

Table 1: Characterization of the feedstock, rice straw.

| Proximate analysis | | | Ultimate analysis | |
|--------------------------------|-------|-------|-------------------|-------|
| Total moisture (%) | 12.00 | C (%) | | 37.48 |
| Ash (%, dry basis) | 12.65 | H (%) | | 4.41 |
| Volatile matter (%, dry basis) | 56.46 | O (%) | | 33.27 |
| Fixed carbon (%, dry basis) | 18.88 | N (%) | | 0.17 |
| | | S (%) | | 0.04 |

4. Model development and validation

Updraft gasifier was modeled by means of the equations of conservation of mass and energy for the solid and gas phases. The model was derived as an unsteady system for a one-dimensional along reactor axis. Fuel was assumed to be the same size and shape with constant porosity, and without intraparticle gradients of temperature. Turbulence in chamber was taken in to account through the correlations for the heat/mass transfer coefficients. In addition, constant pressure along the axis of chamber was considered. The main processes modeled included: (1) moisture evaporation/condensation, (2) finite-rate kinetics of biomass devolatilization to gaseous species, primary tar, and char, (3) primary tar degradation to gaseous species and refractory tar, (4) heterogeneous gasification and combustion of char, (5) combustion of volatile species, (6) steam reforming of methane and refractory tar, (7) finite-rate gas-phase water—gas shift, (8) extra-particle mass transfer resistances, (9) heat and mass transfer across the bed resulting from macroscopic (convection) and molecular (diffusion and conduction) exchanges, (10) absence of thermal equilibrium, (11) solid- and gas-phase heat transfer with the reactor walls, (12) radiative heat transfer through the porous bed, and (13) variable solid and gas flow rates.



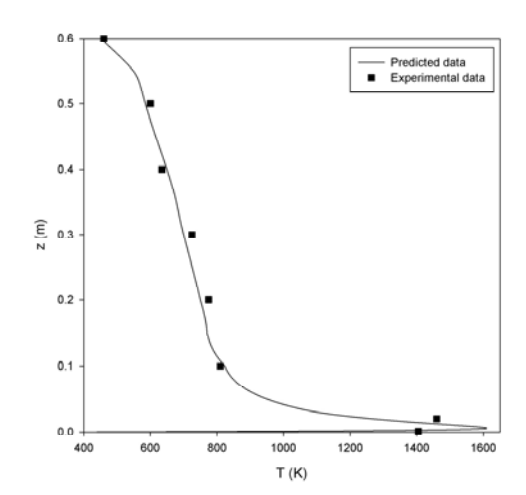


Figure 1: Diagram of an updraft gasifier.

Figure 2: Experimental and predicted temperatures.

The conservation equations are governed based on the work by Blasi (2004) as following equations. Biomass:

$$\frac{\partial}{\partial t} \rho_{\text{biomass}} + \frac{\partial}{\partial z} U_{\text{s}} \rho_{\text{biomass}} = -r_{p_1}$$
(1)

Moisture

$$\frac{\partial}{\partial t} \rho_{\text{moisture}} + \frac{\partial}{\partial z} U_{s} \rho_{\text{moisture}} = -m_{\text{moisture}}$$
 (2)

Gas-phase species:

$$\varepsilon \frac{\partial}{\partial t} \rho_i + \frac{\partial}{\partial z} U_g \rho_i = \frac{\partial}{\partial z} (\varepsilon D_i \rho_g \frac{\partial}{\partial z} Y_i) + M_i \sum_i v_{ij} r_j + v_i r_{p_1} + v_i^* r_{p_2}$$
(3)

Where $i = O_2$, H_2 , CO, CO_2 , CH_4 , $j = c_1-c_6$, g_1-g_3 , wg, sr_1 , sr_2

$$\varepsilon \frac{\partial}{\partial t} \rho_{\text{water}} + \frac{\partial}{\partial z} U_g \rho_{\text{water}} = \frac{\partial}{\partial z} (\varepsilon D_v \rho_g \frac{\partial}{\partial z} Y_{\text{water}}) + M_{\text{water}} \sum_j \nu_{\text{water},j} r_j + \nu_{\text{water}} r_{p_1} + \nu_{\text{water}}^* r_{p_2} + m_{\text{moisture}}$$
(4)

Where $j = c_1-c_5$, g_1-g_3 , wg, sr_1 , sr_2

Vapor-phase primary tar:

$$\varepsilon \frac{\partial \rho_{\text{tar}_{i}}}{\partial t} + \frac{\partial (U_{g}\rho_{\text{tar}_{i}})}{\partial z} = \frac{\partial}{\partial z} (\varepsilon D_{\text{tar}_{i}} \rho_{g} \frac{\partial}{\partial z} Y_{\text{tar}_{i}}) + V_{\text{tar}_{i}} r_{p_{i}} - r_{p_{2}} - M_{\text{tar}_{i}} r_{c_{i}}$$
(5)

Vapor-phase refractory tar:

$$\varepsilon \frac{\partial \rho_{\text{tar}_2}}{\partial t} + \frac{\partial (U_g \rho_{\text{tar}_2})}{\partial z} = \frac{\partial}{\partial z} (\varepsilon D_{\text{tar}_2} \rho_g \frac{\partial}{\partial z} Y_{\text{tar}_2}) + V_{\text{tar}_2} r_{p_2} - M_{\text{tar}_2} r_{c_5} - M_{\text{tar}_2} r_{s_1}$$
(6)

Nitrogen:

$$\rho_{N_2} = \rho_g - \sum_{i \neq N_r} \rho_i \tag{7}$$

Total gas continuity:

$$\varepsilon \frac{\partial}{\partial t} \rho_g + \frac{\partial}{\partial z} U_g \rho_g = \sum_i \sum_j v_{ij} M_i r_j + m_{moisture} + (1 - v_{char}) r_{p_1}$$
(8)

Where $i = O_2$, H_2 , CO, CO_2 , CH_4 , N_2 , H_2O , $j = c_6$, g_1 - g_3 Solid-phase enthalpy:

$$\frac{\partial}{\partial t} \left(\sum_{i} \rho_{i} c_{si} (T_{s} - T_{0}) \right) = \frac{\partial}{\partial z} \left(\lambda_{s}^{*} \frac{\partial T_{s}}{\partial z} \right) + \frac{\partial}{\partial z} \left(U_{s} \sum_{i} \rho_{i} c_{si} (T_{s} - T_{0}) \right) - \sum_{i} r_{j} \Delta H_{j} - h_{sg} A_{p} v_{p} (T_{s} - T_{g}) + \frac{4 h_{sw}}{d} (T_{w} - T_{s}) - m_{moisture} \Lambda$$
(9)

Where i = biomass, char, moisture, $j = c_5$, g_1 - g_3 , p_1 . Gas-phase enthalpy:

$$\frac{\partial}{\partial t} \left(\sum_{i} \rho_{i} c_{gi} (T_{g} - T_{0}) \right) = \frac{\partial}{\partial z} \left(\lambda_{g}^{*} \frac{\partial T_{g}}{\partial z} \right) + \frac{\partial}{\partial z} \left(U_{g} \sum_{i} \rho_{i} c_{gi} (T_{g} - T_{0}) \right) - \sum_{i} r_{j} \Delta H_{j} - h_{gg} A_{p} v_{p} (T_{s} - T_{g}) + \frac{4 h_{gw}}{d} (T_{w} - T_{g})$$

$$(10)$$

Where $i = N_2$, O_2 , H_2 , CO, CO_2 , CH_4 , water, tar_1 , tar_2 , $j = c_1-c_5$, wg, p_2 , sr_1 , sr_2 . Ideal gas law:

$$P = \frac{\rho_g R T_g}{\sum_i M_i Y_i} \tag{11}$$

Where $i = N_2$, O_2 , H_2 , CO, CO_2 , CH_4 , water, tar_1 , tar_2 .

T denotes temperature. U denotes velocity. Y represents mass fraction. D stands for diffusion coefficient. d represents reactor diameter. A_p is particle surface area. m is evaporation rate. M is molecular weight. p is gas phase mass concentration. p is porosity. p is moisture enthalpy. p and p are solid-gas and solid-wall heat transfer coefficients. The subscripts p and p stand for solid, gas and wall, respectively. The reactions p is related to thermal decomposition where the fractions of gas, primary tar and char generated. Primary tar undergoes secondary cracking to produce gases and refractory tar in reaction p. The reaction of steam reforming of refractory tar and methane were taken into account through reactions p and p steam of volatile products including the reactions for primary and refractory tars, methane, carbon monoxide, and hydrogen were modeled in reactions p to p to p the reactions of char were modeled as reaction p and p and p and p and p and p are reactions with corresponding kinetic parameters, as well as moisture evaporation rate and heat and mass transfer coefficients were modeled the same way as in Blasi and Branca (2013), but omitted here for brevity.

At the bottom of reactor (z=0), temperature, velocity, and densities of the feed air were given. The solid was assumed to be at ambient temperature. At the top of the chamber, the fuel feed properties and a convective outflow conditions were assigned. At initial, the gasifier filled with biomass was fed by hot feed air. After a certain time, the feed air temperature was set back to the predefined conditions. The simulation was then performed with selected parameters.

Model validation was performed using experimental data. The moisture content of rice straw used as fuel feed was 12%. The mass flow rate of fuel feed, and feed air were 1.65 and 2.15 kg/h, respectively. Feed air and fuel were preheated to 313.5 K by an external heater to maintain a stable operation. Figure 2 shows the comparison of the predicted and experimental temperature profiles, at the bottom of the reactor, temperature drastically increases from ambient to 1600 K, which is the highest temperature. The temperature predictions were in good agreement with the experimental data. The gas produced at the outlet was about 450 K. Biomass devolatilization occurred at the temperature above 650 K. The rapid rise of the solid temperature approached 1600 K at slightly above the grate resulted from char combustion.

5. Effects of parameters

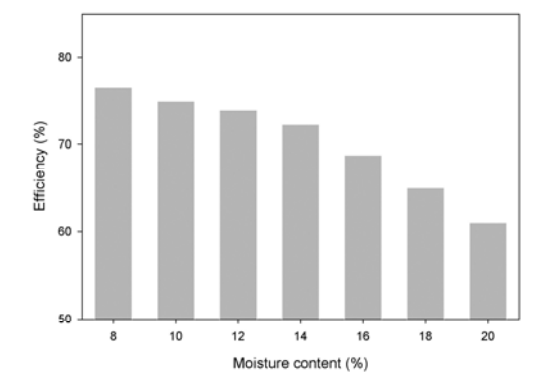
The performance of the gasification process was evaluated based on efficiency term defined as the ratio of the exergy of the syngas to the exergy of the biomass (Ptasinski, 2008).

5.1 The effects of moisture content in fuel feed

The moisture content of fuel feed was varied from 8 to 20 % while keeping the other parameters constant. The performance of the gasifier was directly influenced by the moisture content of fuel feed. Figure 3 shows the performance of gasifer at different moisture contents of fuel feed. The fuel with higher moisture content lowered the performance of the gasification process. Fuel feed with higher moisture content required longer drying zone resulting in a relative decrease in the biomass resident time. In addition, more energy was used to dry biomass, and the temperature inside the chamber decreased.

5.2 The effects and air feed temperature

Air feed temperature was preheated to varying temperatures ranging from 313.5 to 338.5 K while keeping the other parameters constant. Figure 4 shows the performance of gasifer at different air feed temperatures. The higher temperature of air feed resulted in higher performance with lower tar content.



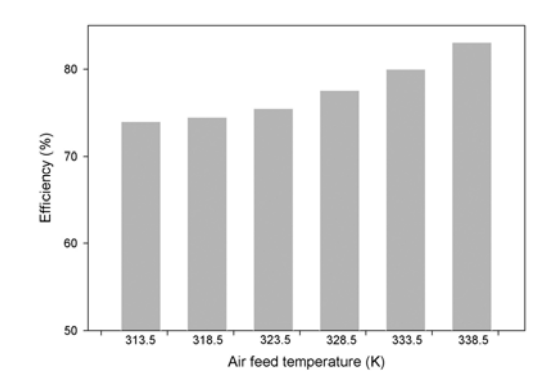


Figure 3: The effect of feed moisture content.

Figure 4: The effect of air feed temperature.

The highest temperature inside the chamber increased as the air feed temperature increased. Because, the hot feed air with higher enthalpy induced an increase of the temperature. The positive impacts of the higher bed temperature were higher chemical reaction rates and enhanced heat transfer. The drying zone was significantly reduced.

6. Conclusions

In this work, a one-dimensional mathematical model for the simulation of a small-scale fixed-bed updraft gasifier has been developed and validated with experimental data of small-scale updraft gasifier of rice straw. Good agreement between the model developed and experimental data has been obtained. The mathematical model constructed was then used to study the effects of varying moisture content and air feed temperature. The fuel with higher moisture content lowered the performance of the gasification process. But, higher temperature of air feed resulted in higher performance with lower tar content and more environmentally preferable.

Acknowledgements

This work was supported by Rajadapisek Sompoj Fund, Chulalongkorn University Centenary Academic Development Project, and The Commission on Higher Education of Thailand, the Thailand Research Fund (TRF).

References

Blasi C., 2004, Modeling Wood Gasification in a Countercurrent Fixed-Bed Reactor, AlChE J., 50, 2306-2319.

Blasi C., Branca C., 2013, Modeling a stratified downdraft wood gasifier with primary and secondary air entry, Fuel, 104, 847-860.

Moghadam R. A., Yusup S., Lam H. L., Al Shoaibi A., Ahmad M., 2013, Hydrogen production from mixture of biomass and polyethylene waste in fluidized bed catalytic steam co-gasification process, Chemical Engineering Transactions, 35, 565-570, DOI: 10.3303/CET1335094.

Ptasinski K., 2008, Thermodynamic efficiency of biomass gasification and biofuels conversion, Biofuels Bioprod Bioref 2, 239-253.

Wetterlund E., Karlsson M., Harvey S., 2010, Biomass gasification integrated with a pulp and paper mill – the need for economic policies promoting biofuels, Chemical Engineering Transactions, 21, 1207-1212, DOI: 10.3303/CET1021202.

Wu Y., Zhang Q., Yang W., Blasiak W., 2013, Two-dimensional computational fluid dynamics simulation of biomass gasification in a downdraft fixed-bed gasifier with highly preheated air and steam, Energy Fuels, 27, 3274-3282.

Zhang Q., Dor L., Yang W., Blasiak W., 2011, Eulerian model for municipal solid waste gasification in a fixed-bed plasma gasification melting reactor, Energy Fuels 25, 4129-4137.

ENGINEERING JOURNAL

Article

Interpolation-based Off-line Robust MPC for Uncertain Polytopic Discrete-time Systems

Pornchai Bumroongsri^{1,a} and Soorathep Kheawhom^{2,b,*}

- ¹ Department of Chemical Engineering, Faculty of Engineering, Mahidol University, Salaya, Nakhon Pathom 73170, Thailand
- 2 Computational Process Engineering, Department of Chemical Engineering, Faculty of Engineering, Chulalongkorn University, Phayathai Rd., Patumwan, Bangkok 10330, Thailand E-mail: apornchai.bum@mahidol.ac.th, bsoorathep.k@chula.ac.th (Corresponding author)

Abstract. In this paper, interpolation-based off-line robust MPC for uncertain polytopic discrete-time systems is presented. Instead of solving an on-line optimization problem at each sampling time to find a state feedback gain, a sequence of state feedback gains is precomputed off-line in order to reduce the on-line computational time. At each sampling time, the real-time state feedback gain is calculated by linear interpolation between the precomputed state feedback gains. Three interpolation techniques are proposed. In the first technique, the smallest ellipsoids containing the measured state are approximated and the corresponding real-time state feedback gain is calculated. In the second technique, the precomputed state feedback gains are interpolated in order to get the largest possible real-time state feedback gain while robust stability is still guaranteed. In the last technique, the real-time state feedback gain is calculated by minimizing the violation of the constraints of the adjacent inner ellipsoids so the real-time state feedback gain calculated has to regulate the state from the current ellipsoids to the adjacent inner ellipsoids as fast as possible. As compared to on-line robust MPC, the proposed techniques can significantly reduce on-line computational time while the same level of control performance is still ensured.

Keywords: Off-line robust MPC, linear interpolation, pre-computed state feedback gains.

ENGINEERING JOURNAL Volume 18 Issue 1

Received 26 March 2013 Accepted 13 June 2013 Published 14 January 2014 Online at http://www.engj.org/ DOI:10.4186/ej.2014.18.1.87

1. Introduction

Model predictive control (MPC) has originated in the industry as an on-line computer control algorithm to solve multivariable control problems. At each sampling instant, MPC uses an explicit process model to solve the optimization problem and only the first computed input is implemented to the process. Although MPC has been successfully implemented to many industrial processes, it is well-known that stability of MPC cannot be guaranteed in the presence of model uncertainty [1]. For this reason, synthesis approaches for robust MPC have been widely investigated [2-6].

On-line robust MPC has been proposed by many researchers. Kothare et al. [2] proposed the algorithm that constructs an invariant ellipsoid containing the measured state at each sampling instant. Any states in this invariant ellipsoid can be driven to the origin by using the stabilizing state feedback gain. Thus, robust stability is guaranteed. The stabilizing state feedback gain is derived by using a single Lyapunov function so a certain degree of conservativeness is obtained. The conservativeness can be reduced by on-line robust MPC formulation using parameter-dependent Lyapunov function as proposed in [3-6]. However, the number of decision variables and constraints also increases. Thus, the algorithms are not suitable for relatively fast dynamic processes. Another approach to reduce the conservativeness is to increase the degrees of freedom in solving the optimization problem by adding a sequence of free control inputs to the state feedback control law [7-11]. By doing so, larger on-line computational time is required to calculate a sequence of free control inputs so the algorithms can only be implemented to slow dynamic processes.

In order to reduce on-line computational time, various researchers have studied off-line robust MPC [12-20]. Wan and Kothare [12] proposed an off-line robust MPC formulation using linear matrix inequalities (LMIs). The on-line computational time is reduced by pre-computing off-line a sequence of state feedback gains corresponding to a sequence of ellipsoidal invariant sets. At each sampling instant, the state is measured and the real-time state feedback gain is calculated by linear interpolation between the precomputed state feedback gains. Although the on-line computational time is significantly reduced, a certain degree of conservativeness is obtained because the algorithm is derived by minimizing the worst-case performance cost. This strategy can be further improved by using the nominal performance cost as proposed by Ding et al. [13]. However, the approach in [13] is restricted to the case of a single Lyapunov function. Another idea is to incorporate the scheduling parameter into off-line MPC formulation. In [14], the sequences of state feedback gains corresponding to the sequences of ellipsoids are pre-computed offline. At each sampling instant, the scheduling parameter is measured and the real-time state feedback gain is calculated by linear interpolation between the pre-computed state feedback gains of each sequence. Off-line robust MPC can also be formulated by using polyhedral invariant sets [15-20] in order to enlarge the size of stabilizable region. Later, an interpolation technique for polyhedral invariant sets was developed to reduce conservativeness and improve the control performances [21].

Recently, Bumroongsri and Kheawhom [22] have developed on-line robust MPC based on nominal performance cost by extending the results of Ding et al. [13] to the case of parameter-dependent Lyapunov function. However, the optimization problem solved at each sampling instant has many decision variables and constraints so its application is rather restricted to relatively slow dynamic processes. This algorithm was then further improved by off-line pre-computing a sequence of state feedback gains corresponding to the sequences of ellipsoidal invariant sets [23].

In this paper, the off-line robust MPC based on nominal performance cost for uncertain polytopic discrete-time systems [23] is further improved by implementing interpolation techniques. Three interpolation techniques are proposed. A sequence of state feedback gains is pre-computed off-line. At each sampling time, the real-time state feedback gain is calculated by linear interpolation between the precomputed state feedback gains. The control performance of each technique is evaluated and compared within an example.

The paper is organized as follows. In section 2, the problem description is presented. In section 3, interpolation-based off-line robust MPC is presented. In section 4, we present an example to illustrate the implementation of the proposed algorithm. Finally, in section 5, we conclude the paper.

2. Problem Description

The model considered here is the following linear time varying (LTV) system with polytopic uncertainty

$$x(k+1) = A(k)x(k) + B(k)u(k)$$

$$y(k) = Cx(k)$$
(1)

where x(k) is the vector of states, u(k) is the vector of control inputs and y(k) is the vector of plant outputs. Moreover, we assume that

$$[A(k), B(k)] \in \Omega, \ \Omega = Co\{[A_1, B_1], [A_2, B_2], ..., [A_L, B_L]\}$$
(2)

where Ω is the polytope, Co denotes convex hull, $[A_j, B_j]$ are the vertices of Ω and L is the number of the vertices of Ω . Any [A(k), B(k)] within the polytope is a linear combination of the vertices such that

$$[A(k), B(k)] = \sum_{j=1}^{L} \lambda_j [A_j, B_j], \sum_{j=1}^{L} \lambda_j = 1, 0 \le \lambda_j \le 1$$
(3)

where $\lambda = [\lambda_1, \lambda_2, ..., \lambda_L]$ is the uncertain parameter vector. The aim of this research is to find the state feedback control law

$$u(k+i/k) = Kx(k+i/k) \tag{4}$$

which stabilizes the system (1) and minimizes the following nominal performance cost

$$\min_{u(k+i/k),\,i\geq 0} J_{n,\infty}(k) \, \min_{u(k+i/k),\,i\geq 0} J_{n,\infty}(k)$$

$$J_{n,\infty}(k) = \sum_{i=0}^{\infty} \begin{bmatrix} \hat{x}(k+i/k) \\ u(k+i/k) \end{bmatrix}^{T} \begin{bmatrix} \Theta & 0 \\ 0 & R \end{bmatrix} \begin{bmatrix} \hat{x}(k+i/k) \\ u(k+i/k) \end{bmatrix}$$
 (5)

where $\hat{x}(k+i/k)$ denotes the predicted nominal state, $\Theta > 0$ and R > 0 are symmetric weighting matrices, subject to input and output constraints

$$|u_h(k+i/k)| \le u_{h,\text{max}}, h = 1, 2, 3, ..., n_u$$
 (6)

$$|y_r(k+i/k)| \le y_{r,\text{max}}, r = 1, 2, 3, ..., n_y$$
 (7)

where n_u is the number of control inputs and n_v is the number of plant outputs.

In [22], the optimization problem (5) is formulated as the convex optimization involving linear matrix inequalities (LMIs). At each sampling time, the state feedback control law which minimizes the upper bound γ_n on the nominal performance cost $J_{n,\infty}(k)$ and asymptotically stabilizes the closed-loop systems

within the ellipsoids $\varepsilon_j = \{x/x^T Q_j^{-1} x \le 1, \forall j = 1, 2, ..., L\}$ is given by $u(k+i/k) = Kx(k+i/k), K = YG^{-1}$ where Y and G are obtained by solving the following problem

$$\min_{\mathbf{Y} \in \mathcal{Q}} \gamma_n$$
 (8)

$$s.t.\begin{bmatrix} 1 & * \\ x(k/k) & Q_j \end{bmatrix} \ge 0, \forall j = 1, 2, \dots, L$$

$$(9)$$

$$\begin{bmatrix} G + G^{T} - Q_{j} & * & * & * \\ \hat{A}G + \hat{B}Y & Q_{l} & * & * \\ \frac{1}{\Theta^{2}G} & 0 & \gamma_{n}I & * \\ \frac{1}{R^{2}Y} & 0 & 0 & \gamma_{n}I \end{bmatrix} \geq 0, \forall j = 1, 2, ..., L, \forall l = 1, 2, ..., L$$

$$(10)$$

$$\begin{bmatrix}
G + G^T - Q_j & * \\
A_j G + B_j Y & Q_l
\end{bmatrix} \ge 0, \forall j = 1, 2, \dots, L, \forall l = 1, 2, \dots, L$$
(11)

$$\begin{bmatrix} X & * \\ Y^{T} & G + G^{T} - Q_{j} \end{bmatrix} \ge 0, \forall j = 1, 2, ..., L, X_{hh} \le u_{h, \max}^{2}, h = 1, 2, ..., n_{u}$$
(12)

$$\begin{bmatrix} S & * \\ (A_j G + B_j Y)^T C^T & G + G^T - Q_j \end{bmatrix} \ge 0, \forall j = 1, 2, ..., L, S_{rr} \le y_{r, \max}^2, r = 1, 2, ..., n_y$$
 (13)

where $[\hat{A}, \hat{B}]$ denotes the nominal model of the plant, the symbol * denotes the corresponding transpose of the lower block part of symmetric matrices, I denotes the identity matrix, X is the diagonal matrix of input constraints and S is the diagonal matrix of output constraints.

Robust stability is guaranteed by the Lyapunov stability constraint (10). For proof details, the reader is referred to [22]. Since the on-line optimization problem contains many decision variables and constraints, the algorithm requires large on-line computational time. Moreover, the number of constraints grows exponentially with the number of vertices of the polytope Q.

3. The Proposed Algorithm

In this section, interpolation-based off-line robust MPC for uncertain polytopic discrete-time systems is presented. The aim is to reduce the on-line computational burdens while the same level of control performance is still ensured. The on-line computational time is reduced by solving off-line the optimization problem (8) to find a sequence of state feedback gain K_i , i = 1, 2, ..., N corresponding to the sequences of ellipsoids $\varepsilon_{i,j} = \left\{x/x^T Q_{i,j}^{-1} x \le 1\right\}$ where i = 1, 2, ..., N is the number of ellipsoids and j = 1, 2, ..., L is the number of vertices of polytope Ω . At each sampling time, the real-time state feedback gain is calculated by linear interpolation between the pre-computed state feedback gains.

3.1. Interpolation-Based Off-Line Robust MPC

Off-line: Choose a sequence of states x_i , i=1,2,...,N. For each x_i , substitute x(k/k) in (9) by x_i and solve the optimization problem (8) to obtain the corresponding state feedback gain $K_i = Y_i G_i^{-1}$ and ellipsoids $\varepsilon_{i,j} = \left\{x/x^T Q_{i,j}^{-1} x \le 1\right\}$, j=1,2,...,L. Note that x_i should be chosen such that $\varepsilon_{i+1,j} \subset \varepsilon_{i,j}$. Moreover, for each $i \ne N$, the following inequality must be satisfied $Q_{i,j}^{-1} - (A_j + B_j K_{i+1})^T Q_{i,j}^{-1} (A_j + B_j K_{i+1}) > 0$, $\forall j=1,2,...,L$

On-line: The real-time state feedback gain is calculated by linear interpolation between the pre-computed state feedback gains. Three interpolation techniques are proposed as follows

Technique 1: The first technique is based on an approximation of the smallest ellipsoids containing the measured state. Instead of solving the optimization problem (8) at each sampling instant, the solution of the optimization problem (8) is approximated by finding the smallest ellipsoids containing the measured state. Then the corresponding real-time state feedback gain can be calculated by linear interpolation between the pre-computed state feedback gains. At each sampling time, when $x(k) \in \mathcal{E}_{i,j}$, $x(k) \notin \mathcal{E}_{i+1,j}$, $\forall j = 1,2,...,L, i \neq N$, the real-time state feedback gain $K(\alpha(k)) = \alpha(k)K_i + (1-\alpha(k))K_{i+1}$ can be calculated from $\alpha(k)$ obtained by solving the following problem.

$$\min \alpha(k)$$
 (14)

s.t.
$$x(k)^{T}(\alpha(k)[Q_{i,j}^{-1}] + (1 - \alpha(k))[Q_{i+1,j}^{-1}])x(k) \le 1, \forall j = 1, 2, ..., L$$
 (15)

$$0 \le \alpha(k) \le 1 \tag{16}$$

It is seen that $\alpha(k) = 0$ and $\alpha(k) = 1$ correspond to the ellipsoids $\varepsilon_{i+1,j}$ and $\varepsilon_{i,j}$, respectively. Thus, the smallest ellipsoids containing the measured state x(k) can be found by minimizing $\alpha(k)$ in (14). Moreover, it is seen that the optimization problem (14) is linear programming and the number of constraints grows only linearly with the number of vertices of the polytope Ω .

Figure 1 shows the graphical representation of the state feedback gain in each prediction horizon. It is seen that the same state feedback gain $K(\alpha(k))$ is implemented throughout the prediction horizon and control horizon. Thus, the state must be restricted to lie in the smallest ellipsoids approximated by (15) and robust stability is guaranteed.

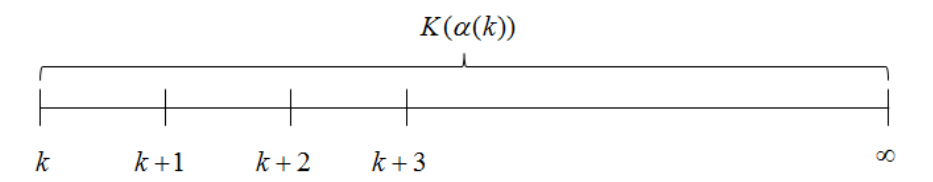


Fig.1. The graphical representation of the state feedback gain in each prediction horizon of technique 1.

Technique 2: In the second technique, the pre-computed state feedback gains K_i , i = 1, 2, ..., N are interpolated in order to get the largest possible real-time state feedback gain. Since the pre-computed state feedback gains are larger as i increases, when the measured state lies between $\varepsilon_{i,j}$ and $\varepsilon_{i+1,j}$, this technique tries to use the value of K_{i+1} as much as possible in the interpolation. This technique can implement larger real-time state feedback gain compared to technique 1 so faster response is obtained. At each sampling time, when $x(k) \in \varepsilon_{i,j}$, $x(k) \notin \varepsilon_{i+1,j}$, $\forall j = 1, 2, ..., L, i \neq N$, the real-time state feedback gain $K(\beta(k)) = \beta(k)K_i + (1 - \beta(k))K_{i+1}$ can be calculated from $\beta(k)$ obtained by solving the following problem.

$$\min \beta(k) \tag{17}$$

s.t.
$$\begin{bmatrix} 1 & ((A_j + B_j K(\beta(k))) x(k))^T \\ (A_j + B_j K(\beta(k))) x(k) & Q_{i,j} \end{bmatrix} \ge 0, j = 1, 2, ..., L$$
 (18)

$$\begin{bmatrix} u_{h,\text{max}}^2 & * \\ (K(\beta(k))x(k))_h & 1 \end{bmatrix} \ge 0 \tag{19}$$

$$0 \le \beta(k) \le 1 \tag{20}$$

 K_{i+1} is always larger than K_i because input and output constraints impose less limit on the state feedback gain as i increases. Thus, the largest possible real-time state feedback gain $K(\beta(k)) = \beta(k)K_i + (1-\beta(k))K_{i+1}$ can be calculated by minimizing $\beta(k)$ in (17). The next predicted state is restricted to lie in the ellipsoidal invariant set by (18) so robust stability is still guaranteed. The input constraint is guaranteed by (19). Note that the output constraint does not need to be incorporated into the problem formulation because the satisfaction of (18) also guarantees output constraint satisfaction. It is seen that the optimization problem (17) is formulated as the convex optimization involving linear matrix inequalities (LMIs) and the number of constraints grows only linearly with the number of vertices of the polytope Ω .

Figure 2 shows the graphical representation of the state feedback gain in each prediction horizon. It is seen that the largest possible real-time state feedback gain $K(\beta(k))$ is only implemented at each sampling time k. At time k+1 and so on, the state feedback gain K_i is implemented. Thus, the state must be restricted to lie in the ellipsoids $\varepsilon_{i,j}$ and robust stability is guaranteed.

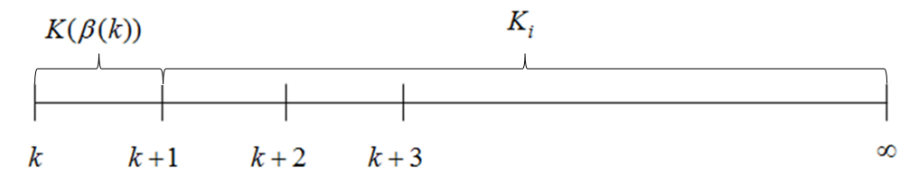


Fig.2. The graphical representation of the state feedback gain in each prediction horizon of technique 2.

Technique 3: In the last technique, the real-time state feedback gain is calculated by minimizing the violation of the constraints of the adjacent inner ellipsoids. When the measured state lies between $\varepsilon_{i,j}$ and

 $\mathcal{E}_{i+1,j}$, the real-time state feedback gain calculated has to drive the state from $\mathcal{E}_{i,j}$ to $\mathcal{E}_{i+1,j}$ as fast as possible in order to minimize the violation of the constraints of $\mathcal{E}_{i+1,j}$. At each sampling time, when $x(k) \in \mathcal{E}_{i,j}$, $x(k) \notin \mathcal{E}_{i+1,j}$, $\forall j = 1,2,...,L$, $i \neq N$, the real-time state feedback gain $K(\delta(k)) = \delta(k)K_i + (1 - \delta(k))K_{i+1}$ can be calculated from $\delta(k)$ obtained by solving the following problem.

$$\min \sigma(k)$$
 (21)

s.t.
$$\begin{bmatrix} 1 + \sigma(k) & ((A_j + B_j K(\delta(k))) x(k))^T \\ (A_j + B_j K(\delta(k))) x(k) & Q_{i+1,j} \end{bmatrix} \ge 0, j = 1, 2, ..., L$$
 (22)

$$\begin{bmatrix} 1 & ((A_j + B_j K(\delta(k))) x(k))^T \\ (A_j + B_j K(\delta(k))) x(k) & Q_{i,j} \end{bmatrix} \ge 0, j = 1, 2, ..., L$$
 (23)

$$\begin{bmatrix} u_{h,\text{max}}^2 & * \\ (K(\beta(k))x(k))_h & 1 \end{bmatrix} \ge 0 \tag{24}$$

$$0 \le \delta(k) \le 1 \tag{25}$$

By applying Schur complement to (22), we obtain $x_j(k+1)^TQ_{i+1,j}^{-1}x_j(k+1) \le 1 + \sigma(k)$ where $x_j(k+1) = (A_j + B_jK(\delta(k)))x(k)$. By minimizing $\sigma(k)$ in (21), the real-time state feedback gain $K(\delta(k)) = \delta(k)K_i + (1-\delta(k))K_{i+1}$ calculated has to regulate the state from the current ellipsoids $\varepsilon_{i,j}$ to the adjacent inner ellipsoids $\varepsilon_{i+1,j}$ as fast as possible. The next predicted state is restricted to lie in the ellipsoidal invariant set by (23) so robust stability is still guaranteed. The input constraint is guaranteed by (24). Note that the output constraint does not need to be incorporated into the problem formulation because the satisfaction of (23) also guarantees output constraint satisfaction. It is seen that the optimization problem (21) is formulated as the convex optimization involving linear matrix inequalities (LMIs) and the number of constraints grows only linearly with the number of vertices of the polytope Ω .

Figure 3 shows the graphical representation of the state feedback gain in each prediction horizon. It is seen that the real-time state feedback gain calculated $K(\delta(k))$ is only implemented at each sampling time k. At time k+1 and so on, the state feedback gain K_i is implemented. Thus, the state must be restricted to lie in the ellipsoids $\varepsilon_{i,j}$ and robust stability is guaranteed.

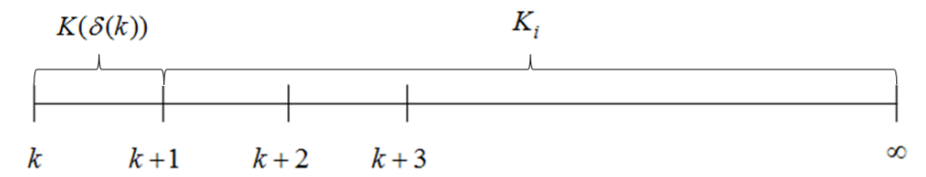


Fig. 3. The graphical representation of the state feedback gain in each prediction horizon of technique 3.

4. Example

We will consider an application of our approach to an angular positioning system [2]. The system consists of an electric motor driving a rotating antenna so that it always points in the direction of a moving object. The motion of the antenna can be described by the following discrete-time equation

$$\begin{bmatrix}
\overline{\theta}(k+1) \\
\overline{\theta}(k+1)
\end{bmatrix} = \begin{bmatrix}
1 & 0.1 \\
0 & 1 - 0.1\omega(k)
\end{bmatrix} \begin{bmatrix}
\overline{\theta}(k) \\
\overline{\theta}(k)
\end{bmatrix} + \begin{bmatrix}
0 \\
0.0787
\end{bmatrix} \overline{u}(k)$$

$$\overline{y}(k) = \begin{bmatrix}
1 & 0
\end{bmatrix} \begin{bmatrix}
\overline{\theta}(k) \\
\overline{\theta}(k)
\end{bmatrix} \\
\overline{\theta}(k)
\end{bmatrix}$$
(26)

where $\overline{\theta}(k)$ is the angular position of the antenna, $\overline{\theta}(k)$ is the angular velocity of the antenna and $\overline{u}(k)$ is the input voltage to the motor. The uncertain parameter $\omega(k)$ is proportional to the coefficient of viscous friction in the rotating parts of the antenna. It is assumed to be arbitrarily time-varying in the range of $0.1 \le \omega(k) \le 10$. Since the uncertain parameter $\omega(k)$ is varied between 0.1 and 10, we conclude that $A(k) \in \Omega$ where Ω is given as follows

$$\Omega = Co \begin{cases} \begin{bmatrix} 1 & 0.1 \\ 0 & 0.99 \end{bmatrix}, \begin{bmatrix} 1 & 0.1 \\ 0 & 0 \end{bmatrix} \end{cases}$$
 (27)

The objective is to regulate $\overline{\theta}$ to the origin by manipulating \overline{u} . The input constraint is $|\overline{u}(k)| \le 2$ volts.

Here $J_{n,\infty}(k)$ is given by (5) with $\Theta = \begin{bmatrix} 1 & 0 \\ 0 & 0 \end{bmatrix}$ and R = 0.00002.

Figure 4 shows two sequences of ellipsoids $\varepsilon_{i,j} = \{x/x^T Q_{i,j}^{-1} x \le 1, i = 1,2,...9, j = 1,2\}$ constructed off-line. Note that the ellipsoids are constructed such that $\varepsilon_{i+1,j} \subset \varepsilon_{i,j}$. In this example, two sequences of ellipsoids are constructed because the polytope Ω has two vertices. Each sequence contains 9 ellipsoids.

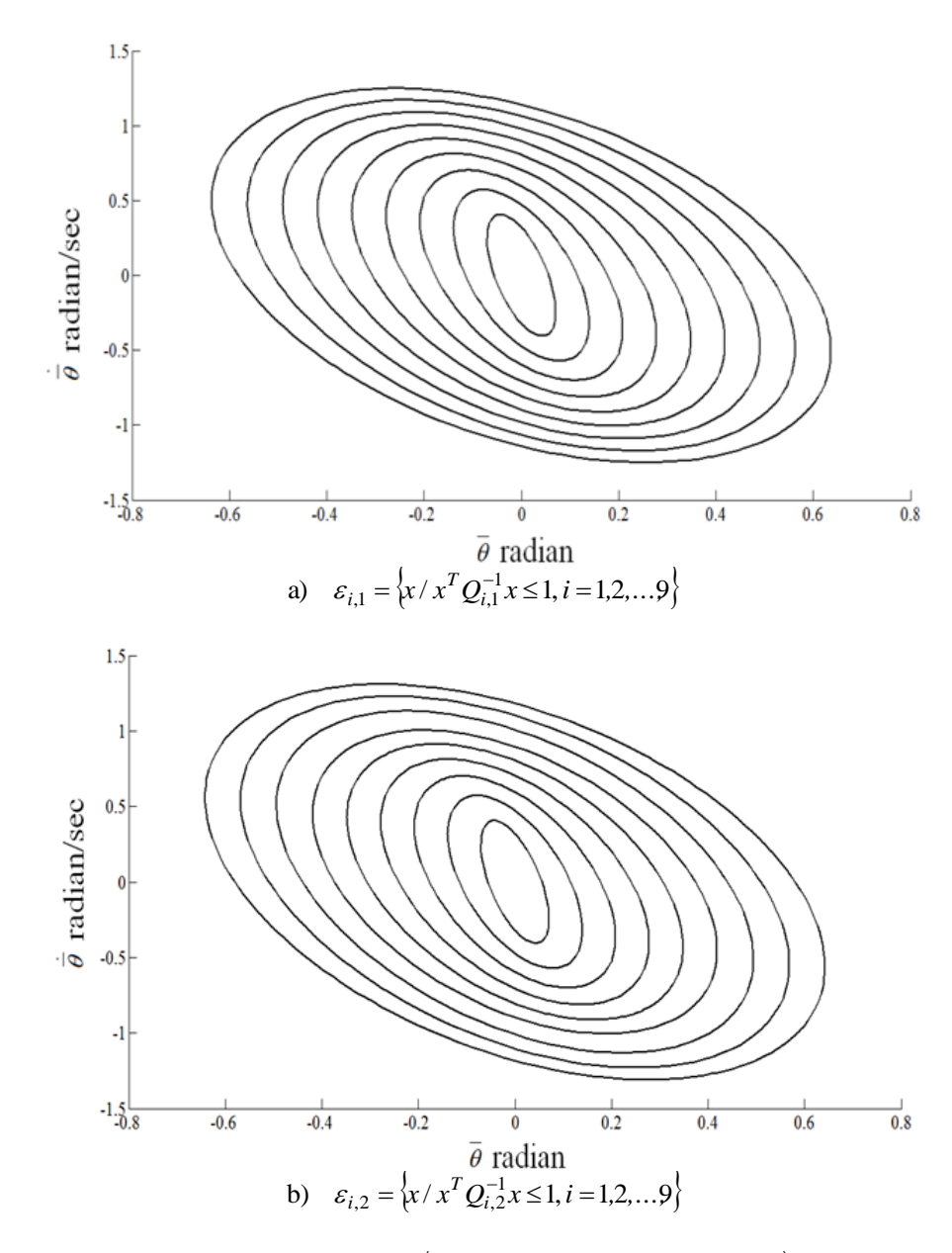


Fig. 4. Two sequences of ellipsoids $\varepsilon_{i,j} = \left\{ x / x^T Q_{i,j}^{-1} x \le 1, i = 1,2,...9, j = 1,2 \right\}$, each sequence has 9 ellipsoids.

Figure 5 shows norm of state feedback gains K_i , i = 1,2,...9. It is seen that norm of K_i increases as i increases. This is due to the fact that input constraint imposes less limit on the state feedback gain as i increases.

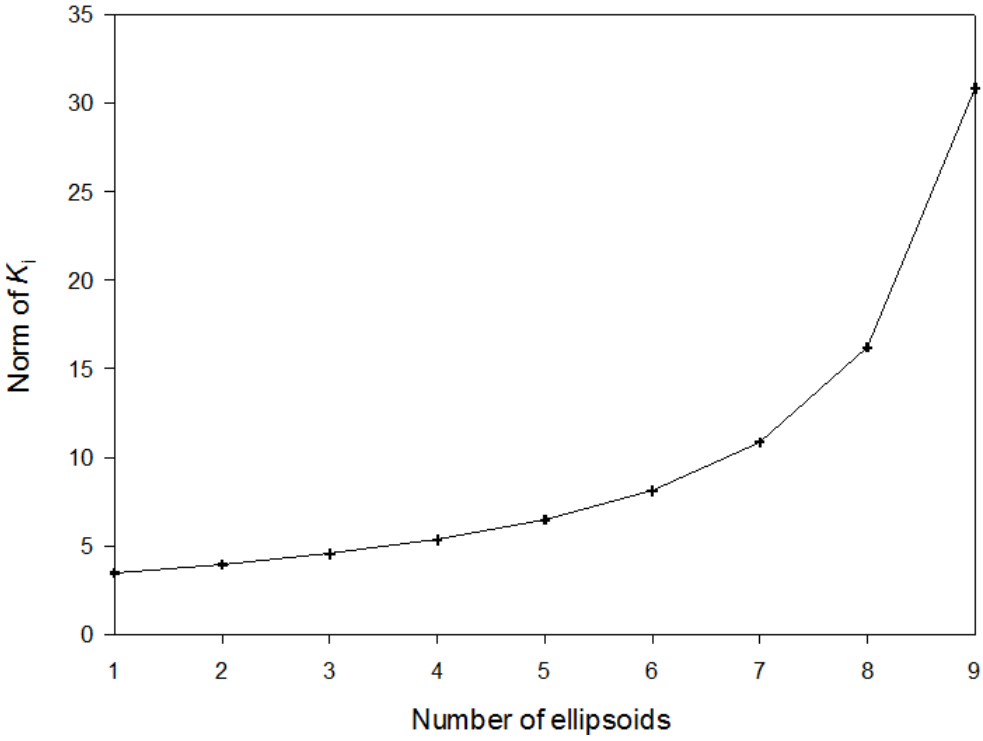


Fig. 5. Norm of state feedback gains K_i , i = 1,2,...9.

Figure 6 shows the closed-loop responses of the system when $\omega(k)$ is randomly time-varying between $0.1 \le \omega(k) \le 10$. As compare to on-line robust MPC [22], technique 1 gives slower response because the real-time state feedback gain and the ellipsoids calculated in technique 1 are only approximations of those calculated by solving on-line optimization problem (8). In comparison, technique 2 and technique 3 give faster responses than technique 1 because they are based on ideas that are completely different from technique 1. In technique 2, the pre-computed state feedback gains are interpolated to get the largest possible real-time state feedback gain so technique 2 tends to make the process responses less sluggish than technique 1. In technique 3, the real-time state feedback gain calculated has to regulate the state from the current ellipsoids $\varepsilon_{i,j}$ to the adjacent inner ellipsoids $\varepsilon_{i+1,j}$ as fast as possible in order to minimize the violation of the constraints of the adjacent inner ellipsoids. For this reason, technique 3 tends to produce faster responses than technique 1.

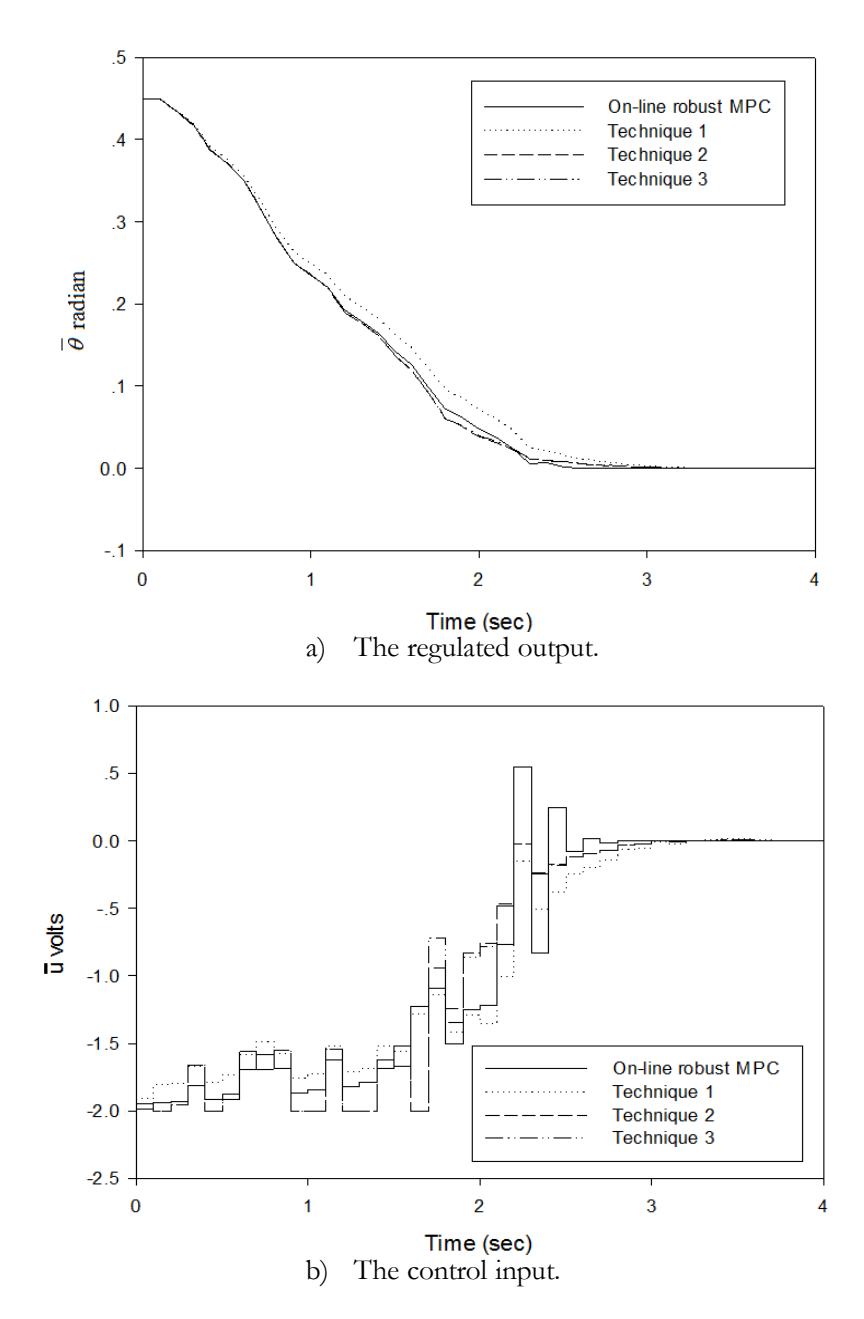


Fig. 6. The closed-loop responses of the system when $\omega(k)$ is randomly time-varying between $0.1 \le \omega(k) \le 10$; a) The regulated output; b) The control input.

Figure 7 shows the state trajectories. It can be observed that the states at each time step of techniques 2 and 3 are closer to the origin that that of technique 1. In this example, techniques 2 and 3 behave almost identically in regulating the states.

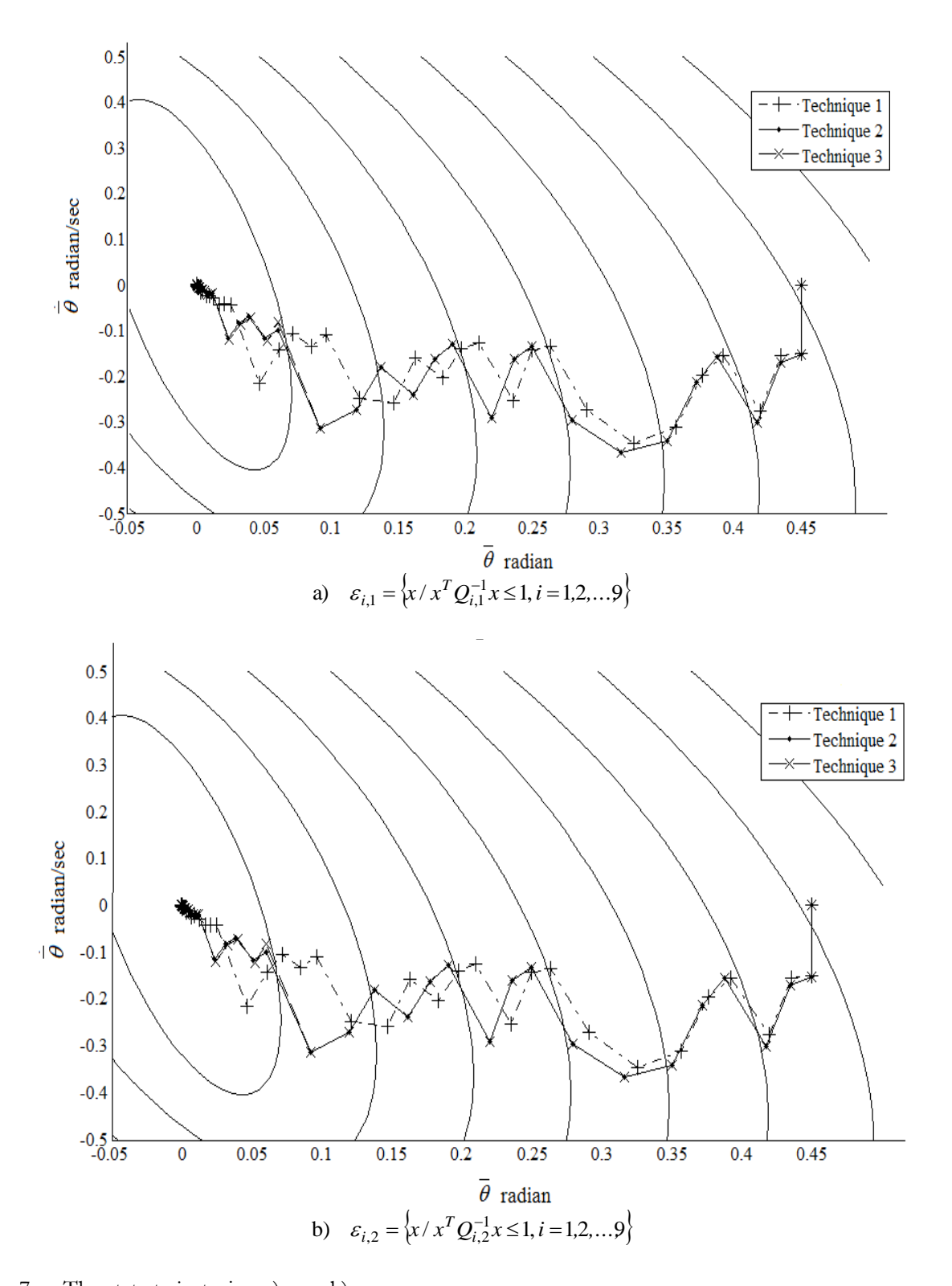


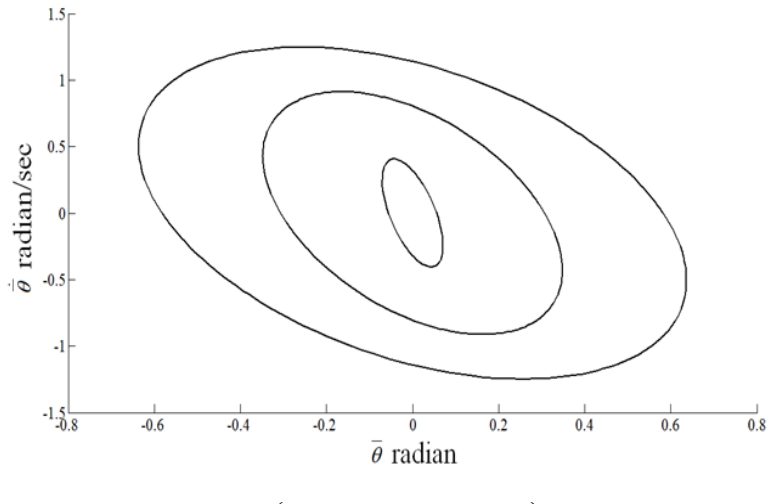
Fig. 7. The state trajectories: a) $\varepsilon_{i,1}$; b) $\varepsilon_{i,2}$.

Table 1 shows the on-line computational time at each sampling instant. By using the proposed techniques, it is seen that the on-line computational time is significantly reduced. Technique 1 gives the smallest on-line computational time because only linear programming is involved in the optimization problem. The numerical simulations have been performed in Intel Core i-5 (2.4GHz), 2 GB RAM, using SeDuMi [24] and YALMIP [25, 26] within Matlab R2008a environment.

Table 1. The on-line computational time at each sampling instant.

| Algorithms | On-line computational time (s) |
|-------------------------|--------------------------------|
| On-line robust MPC [17] | 0.213 |
| Technique 1 | 0.001 |
| Technique 2 | 0.047 |
| Technique 3 | 0.101 |

Next, the effect of the number of ellipsoids constructed off-line is investigated. Figures 8 and 9 show the sequences of ellipsoids when the number of ellipsoids constructed off-line is varied from 9 in Fig. 4 to 3 and 5, respectively. Less computer memory is required as the number of ellipsoids constructed off-line is decreased. Note that in the construction of ellipsoids, the inequality $Q_{i,j}^{-1} - (A_j + B_j K_{i+1})^T Q_{i,l}^{-1} (A_j + B_j K_{i+1}) > 0$, $\forall j = 1,2....L$, $\forall l = 1,2....L$ must be satisfied. This inequality tends to be violated if the number of ellipsoids constructed off-line is too small.



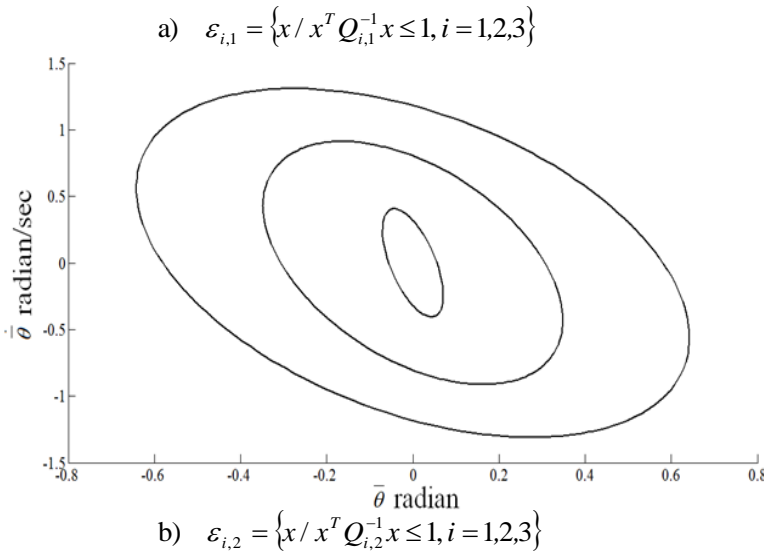


Fig. 8. Two sequences of ellipsoids $\varepsilon_{i,j} = \{x/x^T Q_{i,j}^{-1} x \le 1, i = 1,2,3, j = 1,2\}$, each sequence has 3 ellipsoids.

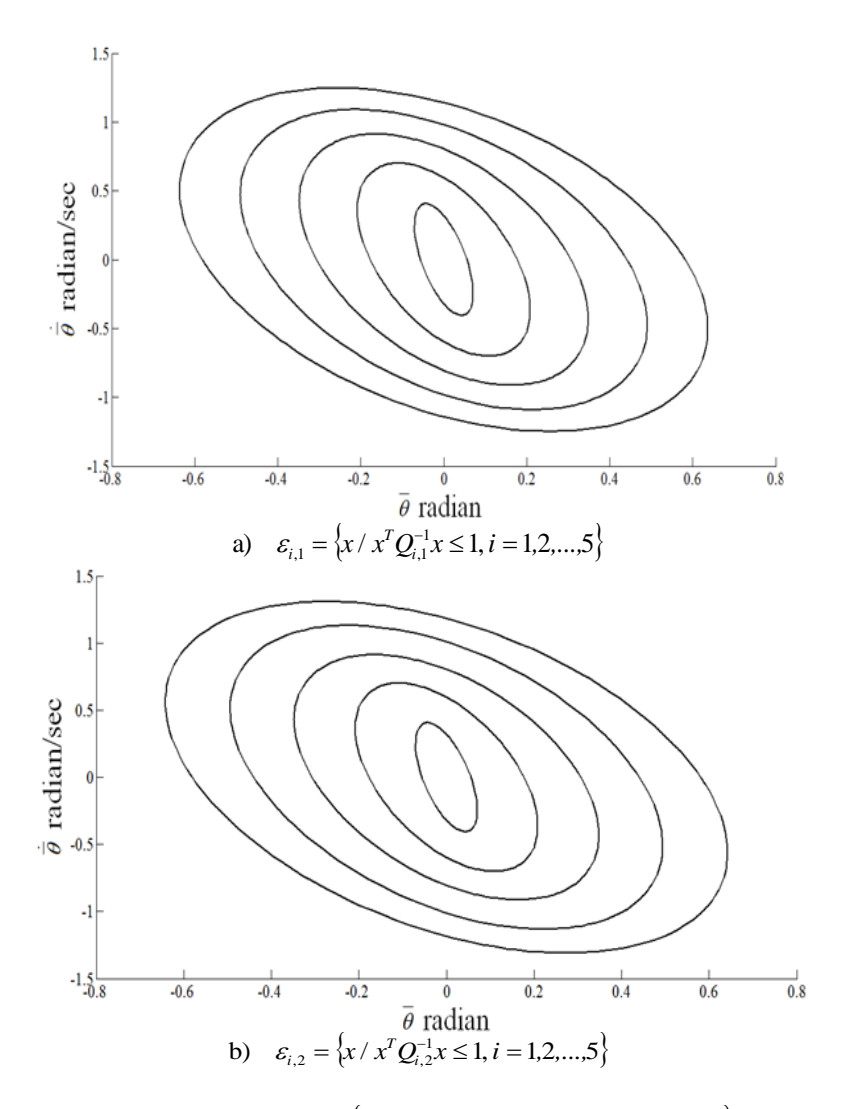


Fig. 9. Two sequences of ellipsoids $\varepsilon_{i,j} = \{x/x^T Q_{i,j}^{-1} x \le 1, i = 1,2,...,5 \ j = 1,2\}$, each sequence has 5 ellipsoids.

Figure 10 shows the closed-loop responses of technique 1 when the number of ellipsoids constructed off-line is varied from 3, 5 and 9. The basic idea of this technique is to approximate the smallest ellipsoids containing the measured state. The approximated ellipsoids become closer to the ellipsoids computed online as the number of ellipsoids constructed off-line is increased. Thus, the control performance of technique 1 becomes closer to on-line robust MPC [22] as the number of ellipsoids constructed off-line is increased.

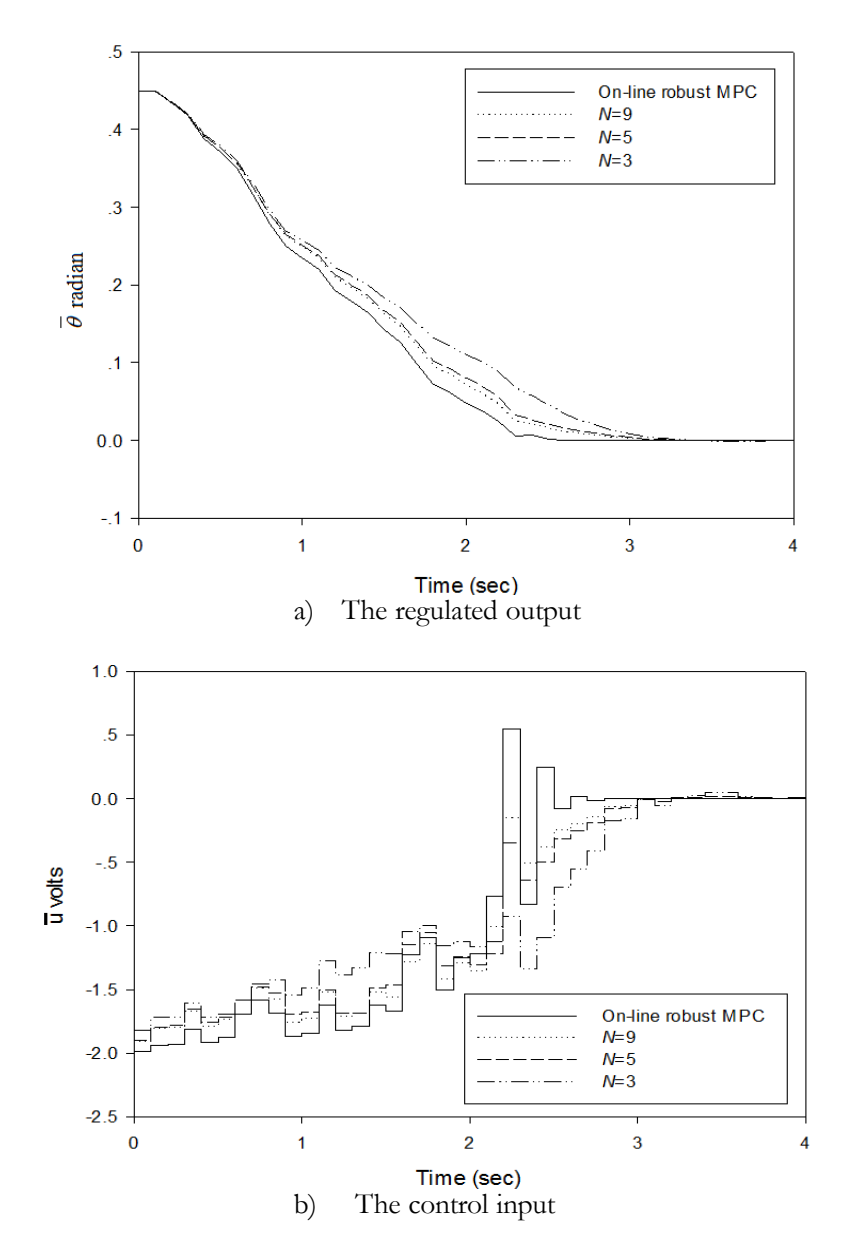


Fig. 10. The closed-loop responses of technique 1 when the number of ellipsoids constructed off-line is varied from 3, 5 and 9; a) The regulated output; b) The control input.

Figure 11 shows the closed-loop responses of technique 2 when the number of ellipsoids constructed off-line is varied from 3, 5 and 9. Since K_{i+1} is larger than K_i as shown in Fig. 5, larger real-time state feedback gain is obtained as the number of ellipsoids is decreased. For this reason, technique 2 tends to produce faster responses as the number of ellipsoids is decreased.

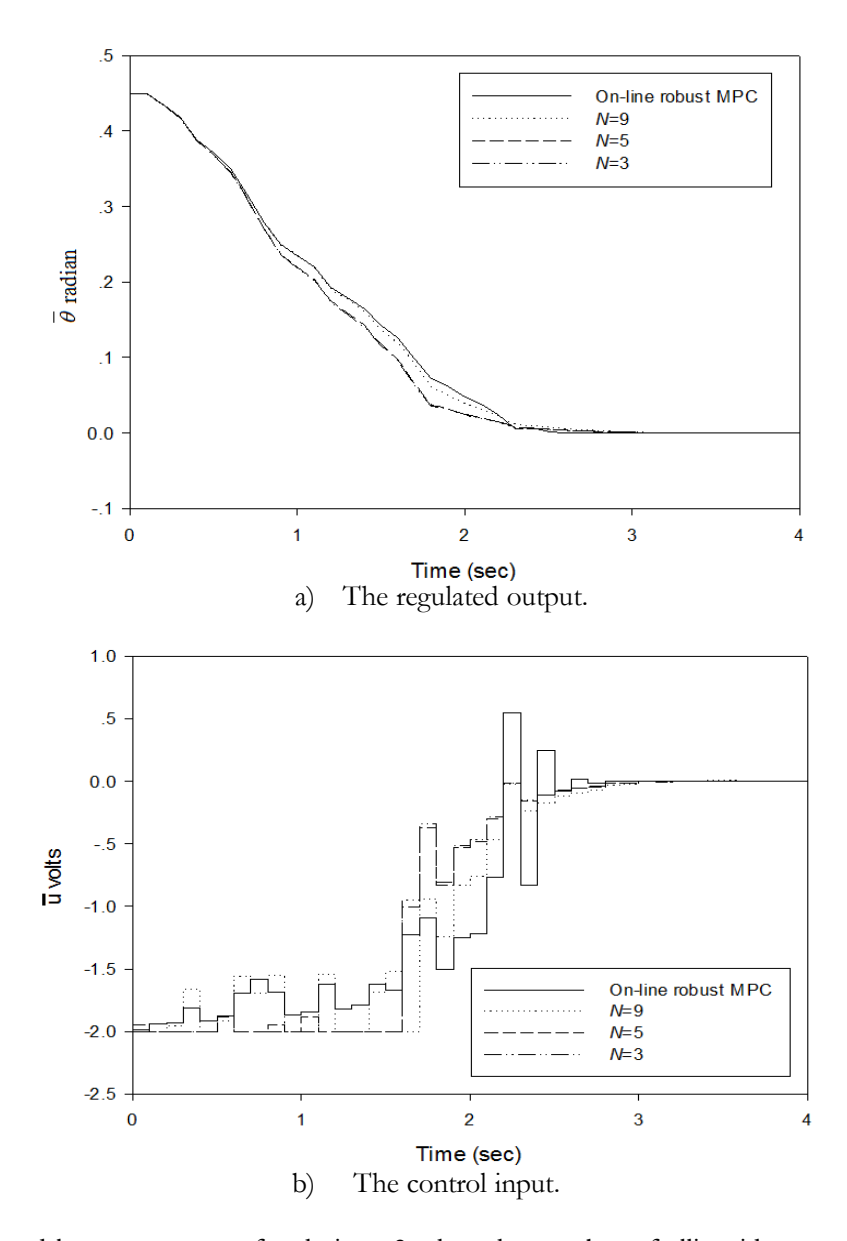


Fig. 11. The closed-loop responses of technique 2 when the number of ellipsoids constructed off-line is varied from 3, 5 and 9; a) The regulated output; b) The control input.

Figure 12 shows the closed-loop responses of technique 3 when the number of ellipsoids constructed off-line is varied from 3, 5 and 9. The real-time state feedback gain calculated has to regulate the state from the current ellipsoids $\varepsilon_{i,j}$ to the adjacent inner ellipsoids $\varepsilon_{i+1,j}$ as fast as possible in order to minimize the violation of the constraints of $\varepsilon_{i+1,j}$. As the number of ellipsoids is decreased, $\varepsilon_{i+1,j}$ are closer to the origin so faster responses are obtained.

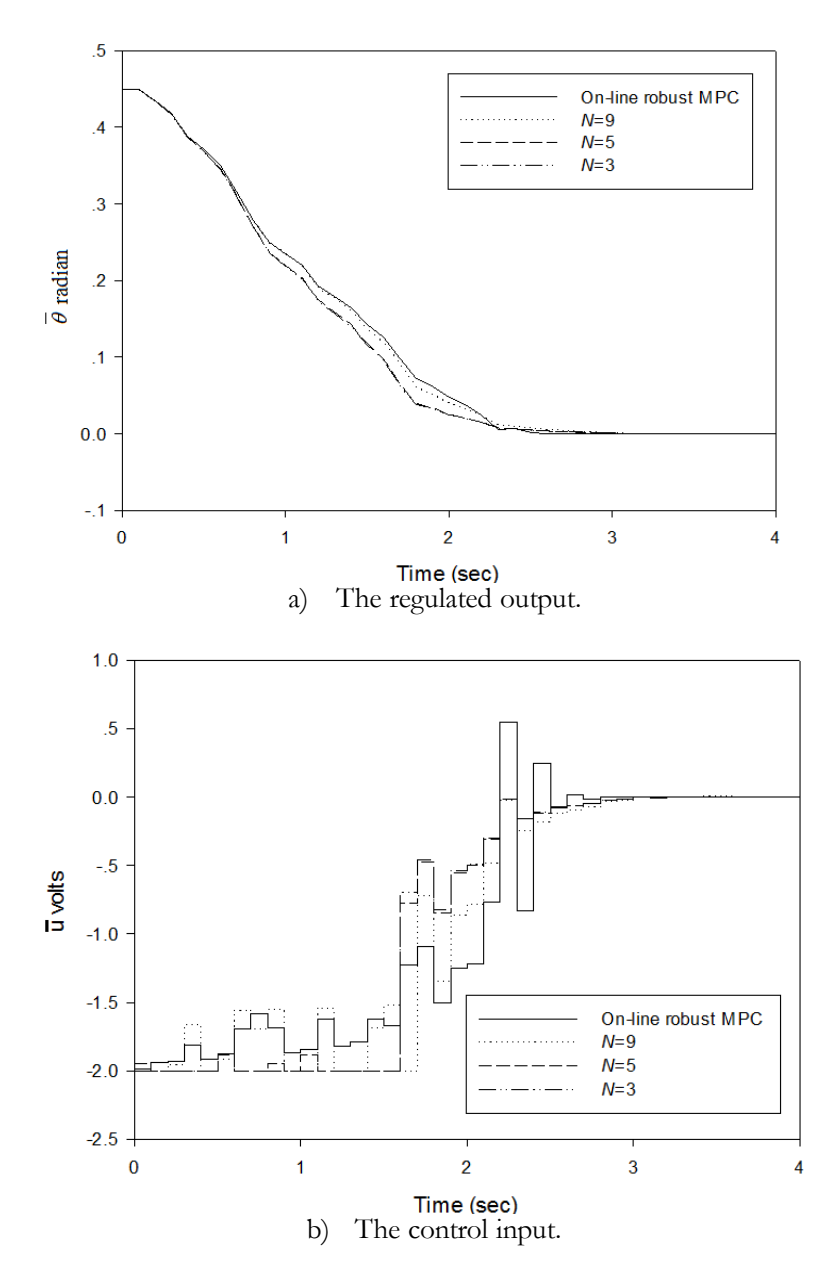


Fig. 12. The closed-loop responses of technique 3 when the number of ellipsoids constructed off-line is varied from 3, 5 and 9: a) The regulated output; b) The control input.

5. Conclusions

This paper presents interpolation-based off-line robust MPC for uncertain polytopic discrete-time systems. The algorithm pre-computes off-line a sequence of state feedback gains corresponding to the sequences of ellipsoids. At each sampling time, the real-time state feedback gain is calculated by linear interpolation between the pre-computed state feedback gains. Three interpolation techniques are proposed. As compared to on-line robust MPC, the on-line computational time is significantly reduced while the same level of control performance is still ensured.

Acknowledgement

This work was supported by Rajadapisek Sompoj Fund, Chulalongkorn University Centenary Academic Development Project, and the Thailand Research Fund (TRF).

References

- [1] M. Morari and J. H. Lee, "Model predictive control: past, present and future," *Comput. Chem. Eng.*, vol. 23, pp. 667-682, 1999.
- [2] M. V. Kothare, V. Balakrishnan, and M. Morari, "Robust constrained model predictive control using linear matrix inequalities," *Automatica*, vol. 32, pp. 1361-1379, 1996.
- [3] F. A. Cuzzola, J. C. Geromel, and M. Morari, "An improved approach for constrained robust model predictive control," *Automatica*, vol. 38, pp. 1183-1189, 2002.
- [4] W. J. Mao, "Robust stabilization of uncertain time-varying discrete systems and comments on "an improved approach for constrained robust model predictive control"," *Automatica*, vol. 39, pp. 1109-1112, 2003.
- [5] T. A. T. Do and D. Banjerdpongchai, "Robust constrained model predictive control for uncertain linear time-varying systems using multiple Lyapunov functions," in *Proceedings of SICE-ICASE International Joint Conference*, Korea, 2006, pp. 908-913.
- [6] N. Wada, K. Saito, and M. Saeki, "Model predictive control for linear parameter varying systems using parameter dependent Lyapunov function," *IEEE T. Circuits Syst.*, vol. 53, pp. 1446-1450, 2006.
- [7] J. Schuurmans and J. A. Rossiter, "Robust predictive control using tight sets of predicted states," *IEE P.-Contr. Theor. Ap.*, vol. 147, pp. 13-18, 2000.
- [8] P. Bumroongsri and S. Kheawhom, "MPC for LPV systems based on parameter-dependent Lyapunov function with perturbation on control input strategy," *Engineering Journal*, vol. 16, pp. 61-72, 2012. doi: 10.4186/ej.2012.16.2.61
- [9] P. Bumroongsri and S. Kheawhom, "MPC for LPV systems using perturbation on control input strategy," *Computer Aided Chemical Engineering*, vol. 31, pp. 350-354, 2012. doi: 10.1016/B978-0-444-59507-2.50062-7
- [10] P. Bumroongsri and S. Kheawhom, "Improving the performance of robust MPC using the perturbation on control input strategy based on nominal performance cost," *Procedia Engineering*, vol. 42, pp. 1027-1037, 2012. doi:10.1016/j.proeng.2012.07.494
- [11] A. Casavola, D. Famularo, and G. Franze, "A feedback min-max MPC algorithm for LPV systems subject to bounded rates of change of parameters," *IEEE T. Automat. Contr.*, vol. 47, pp. 1147-1152, 2002
- [12] Z. Wan and M. V. Kothare, "An efficient off-line formulation of robust model predictive control using linear matrix inequalities," *Automatica*, vol. 39, pp. 837-846, 2003.
- [13] B. Ding, Y. Xi, M. T. Cychowski, and T. O. Mahony, "Improving off-line approach to robust MPC based-on nominal performance cost," *Automatica*, vol. 43, pp. 158-163, 2007.
- [14] P. Bumroongsri and S. Kheawhom, "An ellipsoidal off-line model predictive control strategy for linear parameter varying systems with applications in chemical processes," *Syst. Control Lett.*, vol. 61, pp. 435-442, 2012. doi: 10.1016/j.sysconle.2012.01.003
- [15] P. Bumroongsri and S. Kheawhom, "An off-line robust MPC algorithm for uncertain polytopic discrete-time systems using polyhedral invariant sets," *J. Process Contr.*, vol. 22, pp. 975-983, 2012. doi: 10.1016/j.jprocont.2012.05.002
- [16] P. Bumroongsri and S. Kheawhom, "The polyhedral off-line robust model predictive control strategy for uncertain polytopic discrete-time systems," *IFAC Papersonline Advanced Control of Chemical Processes*, vol. 8, pp. 655-660, 2012. doi: 10.3182/20120710-4-SG-2026.00017
- [17] P. Bumroongsri and S. Kheawhom, "A polyhedral off-line robust MPC strategy for uncertain polytopic discrete-time systems," *Engineering Journal*, vol. 16, pp. 73-89, 2012. doi: 10.4186/ej.2012.16.4
- [18] B. Pluymers, J. A. Rossiter, J. A. K. Suykens, and B. D. Moor, "Interpolation based MPC for LPV systems using polyhedral invariant sets," in *Proceedings of American Control Conference*, vol. 2, 2005, pp. 810-815.
- [19] B. Pluymers, J. A. Rossiter, J. A. K. Suykens, and B. D. Moor, "The efficient computation of polyhedral invariant sets for linear systems with polytopic uncertainty," in Proceedings of American Control Conference, vol. 2, 2005, pp. 804-809.
- [20] J. A. Rossiter, B. Kouvaritakis, and M. Bacic, "Interpolation based computationally efficient predictive control," *Int. J. Control*, vol. 77, pp. 290-301, 2004.
- [21] S. Kheawhom and P. Bumroongsri, "Constrained robust model predictive control based on polyhedral invariant sets by off-line optimization," *Chemical Engineering Transactions*, vol. 32, pp. 1417-1422, 2013. doi: 10.3303/CET1332237

- [22] P. Bumroongsri and S. Kheawhom, "Robust constrained MPC based on nominal performance cost with applications in chemical processes," *Procedia Engineering*, vol. 42, pp. 1561-1571, 2012. doi: 10.1016/j.proeng.2012.07.549
- [23] P. Bumroongsri and S. Kheawhom, "An ellipsoidal off-line robust model predictive control strategy for uncertain polytopic discrete-time systems," *IFAC Papersonline Control Applications of Optimization*, vol. 15, pp. 268-273, 2012. doi: 10.3182/20120913-4-IT-4027.00018
- [24] J. F. Sturm, "Using Sedumi 1.02, a MATLAB toolbox for optimization over symmetric cones," *Optim. Method Softw.*, vol. 11, pp. 625-653, 1999.
- [25] J. Löfberg, "YALMIP: A toolbox for modelling and optimization in MATLAB," in Proceedings of the 2004 IEEE international symposium on computer aided control systems design, Taipei, Taiwan, 2004, pp. 284-289.
- [26] J. Löfberg, "Automatic robust convex programming," Optim. Method Softw., vol. 27, pp. 115-129, 2012.

Robust distributed framework of interpolation-based control for polytopic uncertain systems

Soorathep Kheawhom¹ and Pornchai Bumroongsri²

Abstract—Distributed control is an important framework to handle large-scale systems, however, robust distributed control for polytopic uncertain systems still being a challenge. In this work, we propose a robust distributed framework for interpolation-based control of polytopic uncertain systems. The algorithms proposed consist of both off-line and online computations. The entire system is decomposed into a number of subsystems with smaller number of control inputs. A sequence of nested invariant sets for the entire system, and sequences of state feedback gains corresponding to each subsystem are constructed off-line by minimizing the upper bound of worst-case performance cost in a centralized scheme. The invariant sets constructed are polyhedral sets. At each control iteration, when the state measured lies between any two adjacent invariant sets constructed, a state feedback gain for each subsystem is determined by an interpolation of associated state feedback gains pre-computed. The interpolation problems are based on minimization of a distant from the current state to the adjacent smaller invariant set, solved in a centralized fashion or iteratively solved in a cooperative scheme. Simulation example of quadruple tank system is used to illustrate the algorithms proposed. The cooperative algorithm is capable of inheriting the properties of centralized control scheme but requires lower computational burdens.

I. INTRODUCTION

Model predictive control (MPC) is known as an effective control algorithm to deal with multiple input-multiple output processes with constraints on process variables [1]. Conventional MPC is based on a linear model. To guarantee satisfaction on robustness against model uncertainty, robust model predictive control (RMPC) has been introduced [2]. The goal is to calculate a state feedback gain that robustly stabilizes the closed-loop system. The state feedback gain is derived by minimizing the worst-case performance cost. At each sampling instant, an invariant ellipsoid containing the current state measured is constructed to guarantee robust stability. Since the entire optimization problem is solved online, the algorithm usually requires high on-line computational time. Therefore, its application is rather restricted to the relatively slow dynamic processes. For this reason, the synthesis approaches for off-line RMPC have been widely investigated. An off-line formulation of RMPC using LMI was developed [3]. A sequence of state feedback gains corresponding to a sequence of ellipsoidal invariant sets is

¹Soorathep Kheawhom is with Computational Process Engineering, Department of Chemical Engineering, Faculty of Engineering, Chulalongkorn University, Bangkok 10330 Thailand soorathep.k@chula.ac.th, corresponding author

²Pornchai Bumroongsri is with Department of Chemical Engineering, Faculty of Engineering, Mahidol University, Nakhon Pathom 73170 Thailand pornchai.bum@mahidol.ac.th

computed off-line. At each sampling instant, a smallest ellipsoidal invariant set containing the current state is determined and a state feedback gain is calculated by linear interpolation between the pre-computed state feedback gains. Although the algorithm substantially reduces on-line computational burdens, the algorithm is rather conservative because the invariant ellipsoids used provides small domain of attraction.

An ellipsoidal off-line MPC algorithm for linear parameter varying (LPV) systems was introduced [4]. For LPV systems, the algorithm is less conservative as compared with [3] because the scheduling parameter is included in the controller synthesis. However, the algorithm is still based on an ellipsoidal invariant set. Moreover, the algorithm can handle only an uncertainty in a state matrix.

The invariant sets generally used in the controller design are either ellipsoidal or polyhedral sets. Though the polyhedral invariant set has some advantages over the ellipsoidal invariant set such as better handling of asymmetric constraints and enlargement of domain of attraction, the ellipsoidal invariant set is usually used in RMPC formulation due to its relatively lower on-line computational burdens. In recent years, an off-line RMPC algorithm based on a polyhedral invariant set has been developed [5]. The algorithm computes off-line a sequence of state feedback gains corresponding to a sequence of polyhedral invariant sets. At each control iteration, a smallest polyhedral invariant set containing the current state is determined and a corresponding state feedback gain is implemented to the process. Although the polyhedral invariant set which usually provides larger domain of attraction is used, the conservatism is still obtained because the control law implemented at each time step is an approximation of an optimal control law. Moreover, a jerking of control input caused by a switching of state feedback gains is observed. Therefore, the algorithm requires constructing a large number of polyhedral invariant sets, hence large data storage is required, in order to improve a control performance and to reduce the jerking effect. Later, an interpolation technique for polyhedral invariant sets was introduced to off-line RMPC for polytopic uncertain systems in order to improve the control performances [6], [7]. Another technique to deal with polytopic uncertain systems with input and output constraints can be based on a vertex control which is also an interpolation-based controller [8].

Practically, the systems to be handled are increasing complexity. It is difficult to handle these systems with a centralized MPC due to a limitation on computational burdens. Thus, distributed MPC (DMPC) schemes have received increasing attention because of their advantage for providing

similar performance to a centralized MPC while maintaing flexibity and requiring lower computational burdens. The basic concept of DMPC is to implement a number of local controllers controlling different sets of process input and outputs [9].

Generally, the DMPC strategies developed are based on linear time invariant (LTI) systems [10]. The robustness of DMPC strategies to model uncertainty has been identified as an important factor for the successful implementation of DMPC [11]. However, only a few works have been studied on DMPC for linear time-varying (LTV) systems. An algorithm for robust DMPC (RDMPC) has been introduced for polytopic uncertain systems [12]. The algorithm decomposes the entire system into a number of subsystems and iteratively solves associated convex optimization problems to minimize an upper bound on a worst-case performance cost. However, this algorithm requires high on-line computational time. Later, an RDMPC algorithm with lower requirement on computational time has been developed [13]. This algorithm uses dual-mode approach, and involves off-line and on-line computations. Consequently, most of computational burdens are moved off-line. In [14], an RDMPC for polytopic uncertain systems subject to actuator saturation has been introduced.

In this paper, we present a robust distributed framework for interpolation-based control of polytopic uncertain systems. The paper is organized as follows. In section 2, the problem description is presented. In section 3, an on-line centralized RDMPC is presented, and polyhedral invariant set construction is described. The proposed algorithms are introduced in section 4. In section 5, we illustrate an implementation of the algorithms proposed. Finally, in section 6, we conclude the paper.

Notation: Throughout this paper, a superscript T denotes a transpose operation. I denotes an identity matrix. A symbol \ast denotes a corresponding transpose of a lower block part of symmetric matrices.

II. PROBLEM DESCRIPTION

In this work, the discrete-time linear time-varying (LTV) system as shown in Eq. 1 is taken into account.

$$x_{k+1} = A_k x_k + B_k u_k,$$

$$y_k = C_k x_k,$$
(1)

where $x_k \in R^{n_x}$ is a vector of states at time k. We assume that a full-state measurement is available. $u_k \in R^{n_u}$ is a vector of control inputs at time k, and $y_k \in R^{n_y}$ is a vector of outputs at time k. It is assumed that a system matrix A_k , a control matrix B_k , and an output matrix C_k are within a polytope,

$$[A_k, B_k, C_k] \in Co\{[A_1, B_1, C_1], ..., [A_L, B_L, C_L]\},\$$

Co denotes a convex hull with $[A_l, B_l, C_l]$ vertices. Any $[A_k, B_k, C_k]$ within the polytope is a convex combination of the vertices such that $[A_k, B_k, C_k] = \sum_{l=1}^L \lambda_{l,k} [A_l, B_l, C_l]$, $\sum_{l=1}^L \lambda_{l,k} = 1$, where $0 \le \lambda_{l,k} \le 1$ is an uncertain parameter vector. In addition, the system is observable and controllable.

The model described in Eq. 1 can be decomposed into N subsystems as shown in Eq. 2.

$$x_{k+1} = A_k x_k + \sum_{i=1}^{N} B_{k,i} u_{k,i},$$

$$y_k = C_k x_k,$$
(2)

where $u_{k,i} \in R^{n_{u_i}}$ is a vector of control inputs in subsystem i. The vectors of control inputs $u_{k,j} \in R^{n_{u_j}}$ in other subsystems $j \neq i$ are also available to subsystem i via data communication. A state matrix A_k , a control matrix $B_{k,i}$, and an output matrix C_k can be represented as a convex combination of the vertices such that $[A_k, B_{k,1}, \ldots, B_{k,N}, C_k] = \sum_{l=1}^L \lambda_{l,k} [A_l, B_{l,1}, \ldots, B_{l,N}, C_l], \sum_{j=1}^L \lambda_{l,k} = 1$, where $0 \leq \lambda_{l,k} \leq 1$ is an uncertain parameter vector. N is the number of subsystems. Our aim is to find a state feedback control law of each local controller i,

$$u_{k,i} = K_i x_k \tag{3}$$

that robustly stabilizes the system described in Eq. 2 and achieves the minimum worst-case performance cost while satisfying input, state and output constraints.

III. RMPC AND POLYHEDRAL INVARIANT SET

An on-line centralized robust model predictive control for LTV systems was introduced in [2]. For a distributed system defined as Eq. 2, a similar formulation can be derived. A control objective for the entire system is to minimize the upper bound on infinite horizon worst-case performance cost while satisfying input and output constraints.

The optimization problem for centralized robust model predictive control is shown in Eqs. 4-8.

$$\min_{\gamma, Y_{1}, \dots, Y_{i}, \dots, Y_{N}, Q} \gamma \qquad (4)$$
s.t.
$$\begin{bmatrix}
1 & * \\
x_{k} & Q
\end{bmatrix} \ge 0, \qquad (5)$$

$$\begin{bmatrix}
Q & * & * & * & * & \dots & * \\
A_{l}Q + \sum_{i=1}^{N} B_{l,i}Y_{i} & Q & * & * & \dots & * \\
\Theta^{\frac{1}{2}}Q & 0 & \gamma I & * & \dots & * \\
R_{1}^{\frac{1}{2}}Y_{1} & 0 & 0 & \gamma I & \dots & * \\
\vdots & \vdots & \vdots & \vdots & \vdots & \ddots & \vdots \\
R_{N}^{\frac{1}{2}}Y_{N} & 0 & 0 & 0 & \dots & \gamma I
\end{bmatrix}$$

$$\forall I = 1, \dots, L, \qquad (6)$$

$$\begin{bmatrix}
X & * \\
Y_{i}^{T} & Q
\end{bmatrix} \ge 0,$$

$$X_{hh} \le u_{i,h,\max}^{2}, h = 1, \dots, n_{u_{i}}, \forall i = 1, \dots, N, \qquad (7)$$

$$\begin{bmatrix}
S & * \\
(A_{l}Q + \sum_{i=1}^{N} B_{l,i}Y_{i})^{T}C^{T} & Q
\end{bmatrix} \ge 0, \forall I = 1, \dots, L,$$

where $\Theta > 0$ is a diagonal weighting matrix of states, $R_i > 0$ is a diagonal weighting matrix of control inputs of subsystem *i*. The optimization problem is solved in a centralized fashion. For each subsystem *i*, the control input $u_{k,i} = Y_i Q^{-1} x_k$ is implemented to the process.

(8)

Typically two types of invariant sets including ellipsoidal and polyhedral sets are usually considered. In this work, the algorithms proposed are based on a polyhedral set.

By giving a feedback gain K_i , and control input $u_{k,i} = K_i x_k$ for each subsystem i in the system defined in Eq. 2, the polyhedral invariant set with largest domain of attraction can be estimated. The polyhedral invariant set $S = \{x | Mx \le d\}$ can be constructed by using the following procedure.

Procedure 1

- 1) Set o = 0, $M_o = [C_1; -C_1; ...; C_L; -C_L; I; -I; K_1; -K_1; ...; K_N; -K_N]$, $d_o = [y_{\text{max}}; -y_{\text{min}}; ...; y_{\text{max}}; -y_{\text{min}}; x_{\text{max}}; -x_{\text{min}}; u_{1,\text{max}}; -u_{1,\text{min}}; ...; u_{N,\text{max}}; -u_{N,\text{min}}]$, $S_o = \{x | M_o x \le d_o\}$.
- 2) Set o = o + 1, $M_o = [M_{o-1}; M_{o-1}[A_1 + \sum_{i=1}^N B_{1,i}K_i];$...; $M_{o-1}[A_L + \sum_{i=1}^N B_{L,i}K_i]]$ and $d_o = [d_{o-1}; d_{o-1};$...; $d_{o-1}]$, $S_o = \{x|M_ox \leq d_o\}$ and eliminate redundant inequalities from the polytope S_o .
- 3) If $S_o \neq S_{o-1}$ then repeat step 2, if otherwise stop the algorithm and $S = \{x | M_o x \leq d_o\}$.

Theorem 1: For a distributed system as shown in Eq. 2, given the control law $u_{k,i} = K_i x_k$ for each subsystem i with a state feedback gain $K_i = Y_i Q^{-1}$ provided by solving the optimization problem presented in Eqs.4-8. The polyhedral set, $S = \{x | Mx \le d\}$, constructed by using Procedure 1 provides a set of states that the system will evolve to the origin without input, state and output constraints violation.

Proof: The satisfaction of Eq. 6 for all state feedback gains $K_1,...,K_N$ ensures that $\gamma x_k^T Q^{-1} x_k - [[A_l + \sum_{i=1}^N B_{l,i} K_i] x_k]^T \gamma Q^{-1} [[A_l + \sum_{i=1}^N B_{l,i} K_i] x_k] \geq [x_k^T \Theta x_k + \sum_{i=1}^N u_{k,i}^T R_i u_{k,i}], \forall l=1,...,L$ Thus, $V_k = x_k^T \gamma Q^{-1} x_k$ is a strictly decreasing Lyapunov function and the closed-loop system is robustly stabilized by the state feedback gains $K_1,...,K_N$. By following Procedure 1, we iteratively add output, state and input constraints at the time k+o, $o=0,...,o_{\max}$ to define a polyhedral invariant set $S_o = \{x | M_o x \leq d_o\}$, and eliminate all redundant constraints. There exists a finite index $o=o_{\max}$ such that $M_o = M_{o+1}$ because of the contraction as the closed-loop stability is guarantee. Thus, we can construct a set of initial states $S = \{x | Mx \leq d\}$ such that all future states remain inside S and approach to the origin while satisfying the constraints.

IV. THE PROPOSED ALGORITHM

In this section, the proposed algorithms of RDMPC are described. The algorithms proposed consist of off-line and on-line calculations.

A. Algorithm 1 (decentralized control)

- 1) off-line computation:
 - Choose a sequence of states $x_m, m = 1, ..., m_{\text{max}}$ such that x_{m+1} is closer to the origin than x_m . For each x_m , solve the optimization problem in Eqs. 4-7 by replacing x_k with x_m in order to obtain the corresponding state feedback gain $K_{i,m} = Y_{i,m}Q_m^{-1}$ for each subsystem i. x_m is chosen such that $\varepsilon_{m+1}^{-1} \subset \varepsilon_m^{-1}$, where $\varepsilon_m = \{x | x^T Q_m^{-1} x \le 1\}$. The

state feedback gains are derived based on the minimization of upper bound of infinite horizon worst-case performance. However, the output constraints are not taken into account here in order to enlarge the domain of attraction. The output constraints are then properly handled during polyhedral invariant set construction.

• Given the state feedback gains $K_{i,m} = Y_{i,m}Q_m^{-1}$, i = 1,...,N previously calculated. A polyhedral invariant set $S_m = \{x | M_m x \le d_m\}$ associated with each state feedback gain is constructed by using Procedure 1 previously described.

2) On-line computation:

At each control iteration, a current state x_k is measured, a smallest polyhedral invariant set $S_m = \{x | M_m x \le d_m\}$ containing the current state measured is determined. A state feedback control law $u_{k,i} = K_{i,m} x_k$ for each subsystem i is implemented.

Theorem 2: For a distributed system as shown in Eq. 2, given an initial measured state $x_k \in S_m$, the control law provided by Algorithm 1 assures robust stability to the closed-loop system with input, output and state constraints satisfaction.

Proof: From Theorem 1, with the state feedback control law $u_{k,i}=K_{i,m}x_k$ for each subsystem i, the polyhedral set S_m provides a set of states that the system will evolve to the origin without input and output constraints violation. Thus, any initial states $x_k \in S_m$ are guaranteed that all future state trajectories evolve closer to the origin by passing S_{m+1} , S_{m+2} , ..., and $S_{m_{\max}}$. Thus, the control law provided by Algorithm 1 assures robust stability to the closed-loop system with input, output and state constraints satisfaction.

B. Algorithm 2 (centralized control)

1) off-line computation:

An off-line computation used in this algorithm is as same as that of Algorithm 1. However, x_m , $m = 1,...,m_{\text{max}}$ must be chosen such that for each $m \neq m_{\text{max}}$, there must exist a matrix P > 0 satisfying

$$P - (A_l + \sum_{i=1}^{N} B_{l,i} K_{i,m})^T P(A_l + \sum_{i=1}^{N} B_{l,i} K_{i,m}) > 0,$$
(9)

$$P - (A_l + \sum_{i=1}^{N} B_{l,i} K_{i,m+1})^T P(A_l + \sum_{i=1}^{N} B_{l,i} K_{i,m+1}) > 0,$$
(10)

for all l = 1,...,L, to assure robust stability satisfaction of a convex combination between $K_{i,m}$ and $K_{i,m+1}$.

2) On-line computation:

A state feedback gain for each subsystem is calculated by linear interpolation between the pre-computed state feedback gains to obtain the minimum violation of the constraints γ_k of the adjacent inner invariant sets. The state feedback gain calculated has to regulate the state from the current invariant set to the adjacent inner invariant set as fast as possible.

At each control iteration, if $x(k) \in S_m$ and $x(k) \notin S_{m+1}, \forall m \leq m_{\max} - 1$, for subsystem i a control law $u_{k,i} = K_{k,i}x_k$ with a state feedback gain $K_{k,i} = \lambda_{k,i}K_{i,m} + (1 - \lambda_{k,i})K_{i,m+1}$ can be obtained by solving the optimization problem in Eqs. 11-16.

$$\min_{\lambda_{k,1},\dots,\lambda_{k,N},\gamma_k} \gamma_k \tag{11}$$

s.t.

$$M_m[A_l + \sum_{i=1}^{N} B_{l,i} K_{k,i}] x_k - d_m \le 0, l = 1, ..., L$$
 (12)

$$M_{m+1}[A_l + \sum_{i=1}^{N} B_{l,i} K_{k,i}] x_k - d_{m+1} \le \gamma_k, l = 1, ..., L$$
 (13)

$$u_{i,\min} \le K_{k,i} x_k \le u_{i,\max}, i = 1, ..., N,$$
 (14)

$$K_{k,i} = \lambda_{k,i} K_{i,m} + (1 - \lambda_{k,i}) K_{i,m+1}, i = 1,...,N,$$
 (15)

$$0 \le \lambda_{k,i} \le 1, i = 1, ..., N. \tag{16}$$

If $x(k) \in S_{m_{\max}}$, a control law $u_i(k) = K_{i,m_{\max}} x(k)$ is implemented in each subsystem i.

Theorem 3: For a distributed system as shown in Eq. 2, given an initial measured state $x_k \in S_m$, the control law provided by Algorithm 2 assures robust stability to the closed-loop system with input, output and state constraints satisfaction.

Proof: As Eqs. 9 and 10 are satisfied, a Lyapunov function $V_k = x_k^T P x_k$ ensures robust stability of each feedback gain $K_{k,i} = \lambda_{k,i} K_{i,m} + (1 - \lambda_{k,i}) K_{i,m+1}$, $0 \le \lambda_{k,i} \le 1$, which is a convex combination of $K_{i,m}$ and $K_{i,m+1}$. In solving the problem in Eqs. 11-16, Eqs. 15 and 16 restrict $K_{k,i}$ to be a convex combination of $K_{i,m}$ and $K_{i,m+1}$. The input constraint is guarantee by Eq. 13. State and output constraints do not need to be explicitly incorporated into the problem formulation because the satisfaction of Eq. 12 also guarantees state and output constraints satisfaction. The constraints in Eq. 12 guarantee that one step prediction of x_{k+1} remains in x_k . Thus, any initial states $x_k \in x_k$ are guaranteed that all future state trajectories evolve closer to the origin by passing x_{k+1} , x_{k+2} , ..., and x_{k+1} are x_{k+1} are x_{k+1} are x_{k+1} and x_{k+1} remains in x_{k+1} and x_{k+1} remains in x_{k+1} and x_{k+1} remains in x_{k+1} r

C. Algorithm 3 (cooperative control)

1) off-line computation:

An off-line computation used in this algorithm is as same as that of Algorithm 2.

2) On-line computation:

The state feedback gain is also calculated by linear interpolation between the pre-computed state feedback gains to obtain the minimum violation of the constraints γ_k of the adjacent inner invariant sets. An ideal communication network is assumed so that the controllers can exchange their information without delays. The goal of performing communication and exchanging solutions among controllers is to achieve the optimal solution of the entire system in an iterative fashion.

At each control iteration, if $x_k \in S_m$ and $x_k \notin S_{m+1}, \forall m \le m_{\max} - 1$, all the controllers exchange their

local states measurements and initial estimates $\lambda_{k,i} = 1$ via communication. The optimization problem in Eqs. 17-22 is then solved for $\lambda_{k,i}$. The information of $\lambda_{k,i}$ calculated is then broadcasted to all subsystems. The optimization problem is then recursively solved and exchange information. The state feedback control law for subsystem i, $u_{k,i} = [\lambda_{k,i}K_{i,m} + (1 - \lambda_{k,i})K_{i,m+1}]x(k)$ is then obtained.

$$\min_{\lambda_{k,i},\gamma_k} \gamma_k \tag{17}$$

s.t.

$$M_m[A_l + \sum_{i=1}^{N} B_{l,i} K_{k,i}] x_k - d_m \le 0, l = 1, ..., L$$
 (18)

$$M_{m+1}[A_l + \sum_{i=1}^{N} B_{l,i} K_{k,i}] x_k - d_{m+1} \le \gamma_k, l = 1, ..., L$$
 (19)

$$u_{i,\min} \le K_{k,i} x_k \le u_{i,\max}, i = 1, ..., N,$$
 (20)

$$K_{k,i} = \lambda_{k,i} K_{i,m} + (1 - \lambda_{k,i}) K_{i,m+1}, i = 1,...,N,$$
 (21)

$$0 \le \lambda_{k,i} \le 1, i = 1, ..., N. \tag{22}$$

If $x(k) \in S_{m_{\max}}$, a control law $u_i(k) = K_{i,m_{\max}} x(k)$ is implemented in each subsystem i.

Theorem 4: For a distributed system as shown in Eq. 2, given an initial measured state $x_k \in S_m$, the control law provided by Algorithm 3 assures robust stability to the closed-loop system with input, output and state constraints satisfaction.

Proof: As Eqs. 9 and 10 are satisfied, a Lyapunov function $V_k = x_k^T P x_k$ ensures robust stability of each feedback gain $K_{k,i} = \lambda_{k,i} K_{i,m} + (1 - \lambda_{k,i}) K_{i,m+1}$, $0 \le \lambda_{k,i} \le 1$, which is a convex combination of $K_{i,m}$ and $K_{i,m+1}$. In solving the problem in Eqs. 17-22, Eqs. 21 and 22 restrict $K_{k,i}$ to be a convex combination of $K_{i,m}$ and $K_{i,m+1}$. The input constraint is guarantee by Eq. 19. State and output constraints do not need to be explicitly incorporated into the problem formulation because the satisfaction of Eq. 18 also guarantees state and output constraints satisfaction. The constraints in Eq. 18 guarantee that one step prediction of x_{k+1} remains in S_m . Thus, any initial states $x_k \in S_m$ are guaranteed that all future state trajectories evolve closer to the origin by passing S_{m+1} , S_{m+2} , ..., and $S_{m_{max}}$.

V. SIMULATION OF QUADRUPLE TANK SYSTEM

In this section, we present an example that illustrates the implementation of the proposed algorithms. The numerical simulations have been performed in 2.3 GHz Intel Core i-5 with 16 GB RAM, using SDPT3[15], Gurobi[16] and YALMIP [17] within Matlab R2011b environment. We illustrate our proposed algorithms in a quadruple tank system, which is similar to the system considered in [18]. The system is described by Eqs. 23-26.

$$\dot{h_1} = -5.91\sqrt{h_1} + 5.91\sqrt{h_3} + 0.74u_1,\tag{23}$$

$$\dot{h}_2 = -5.91\sqrt{h_2} + 5.91\sqrt{h_4} + 0.74u_2,$$
 (24)

$$\dot{h}_3 = -5.91\sqrt{h_3} + 1.73u_2,\tag{25}$$

$$\dot{h_4} = -5.91\sqrt{h_4} + 1.73u_1. \tag{26}$$

Where h_t is a water level in tank t,t=1,2,3,4. u_1 and u_2 are water flowrates. Let $\bar{h}_t=h_t-h_{t,eq},\,t=1,2,3,4$ and $\bar{u}_t=u_t-u_{t,eq},t=1,2$. Subscript eq denotes a corresponding variable at equilibrium condition, $h_{t,eq}=14.98$ cm, t=1,2 and $h_{t,eq}=7.34$ cm, t=3,4. Our aim is to regulate $\bar{h}_1,\,\bar{h}_2,\,\bar{h}_3$ and \bar{h}_4 to the origin by manipulating \bar{u}_1 and \bar{u}_2 . Input constraints are symmetric $\bar{u}_i \leq 9.25$ cm³/min. In addition, symmetric output constraints $-13.98 \leq \bar{h}_t \leq 13.98,\,t=1,2$ and $-6.34 \leq \bar{h}_t \leq 6.34,\,t=3,4$ are considered.

By rewriting Eqs. 23-26 in deviation form and rearranging along all uncertainty vertices. Our system is written in differential inclusion form as following

$$[\dot{\bar{h}}_1; \dot{\bar{h}}_2; \dot{\bar{h}}_3; \dot{\bar{h}}_4] \in \sum_{l=1}^{16} \lambda_l [A_l[\bar{h}_1; \bar{h}_2; \bar{h}_3; \bar{h}_4] + B_l[\bar{u}_1; \bar{u}_2]], \quad (27)$$

The discrete-time model is obtained by discretization of Eq. 27 using Euler first-order approximation with a sampling period of 0.2 min and it is omitted here for brevity. The tuning parameters are

The system is decomposed into two subsystems. A sequence of six polyhedral invariant sets with associated state feedback gains are generated by using the following states, [13.5; 13.5; 6.3; 6.3], [4.0; 4.0; 2.0; 2.0], [2.5; 2.5; 1.0; 1.0], [1.0; 1.0; 0.5; 0.5], [0.2; 0.2; 0.1; 0.1] and [0.05; 0.05; 0.01; 0.01]. Algorithm 1, Algorithm 2, Algorithm 3, and decentralized control based on ellipsoidal invariant set [2] are performed to stabilize the system from a deviated state of [12.0; 12.0; 6.0; 6.0] to the origin. The performance of each algorithm is then compared. Figures 1 and 2 depict the performance of each algorithm in terms of the regulated states \bar{h}_1 and \bar{h}_3 . The profiles of \bar{h}_2 is identical to \bar{h}_1 . In the same manner, the profiles of \bar{h}_3 is identical to \bar{h}_4 With only two iterations, the performance of Algorithm 3 (cooperative control) approaches that of Algorithm 2 (centralized control). Both algorithms is less conservative as compared to Algorithm 1 (decentralized control) and decentralized control based on ellipsoidal invariant set [2].

Figure 3 shows the profiles of control input \bar{u}_1 . The profiles of \bar{u}_2 is identical to \bar{u}_1 . A jerking in control input appeares in case of Algorithm 1 (decentralized control) and decentralized control based on ellipsoidal invariant set [2]. This jerking effect is caused by the switching of feedback gains. by a switching of state feedback gains. In comparison, we can overcome this problem by using centralized control

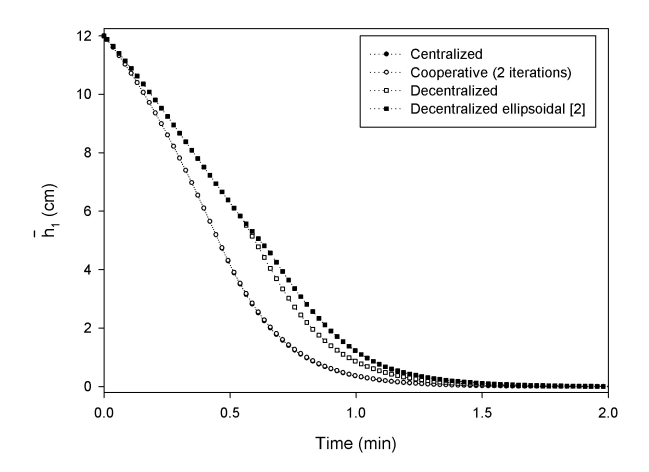


Fig. 1. Regulated state \bar{h}_1 of the quadruple tank system.

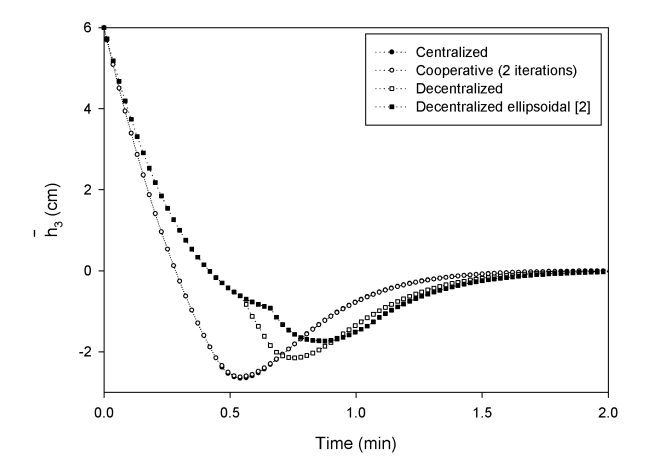


Fig. 2. Regulated state \bar{h}_3 of the quadruple tank system.

or cooperative control. The cooperative algorithm is capable of inheriting the properties of centralized control scheme, and provides similar control performance.

Figure 4 shows the cumulative performance cost. The lowest cumulative performance cost is obtained by using decentralized control based on ellipsoidal invariant set [2]. In addition, the cooperative control converges to centralized control within two iterations.

The on-line computational burdens are shown in Table I. For all algorithms, most of the computational burdens are moved off-line so the on-line computation is tractable. The optimization problem involved in cooperative control and centralized control is independent of the number of vertices of the uncertain polytope. Algorithms 2 and 3 require solving a linear programming. The number of decision variables involved in Algorithm 3 is lower than that of Algorithm 2. Thus, Algorithm 2 requires higher computational time compared with other Algorithms. In contrast, Algorithm 1 does not solve any optimization problems.

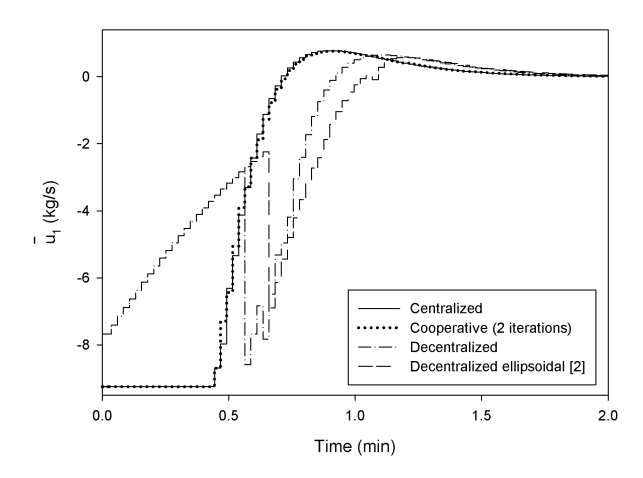


Fig. 3. Control input \bar{u}_1 of the quadruple tank system.

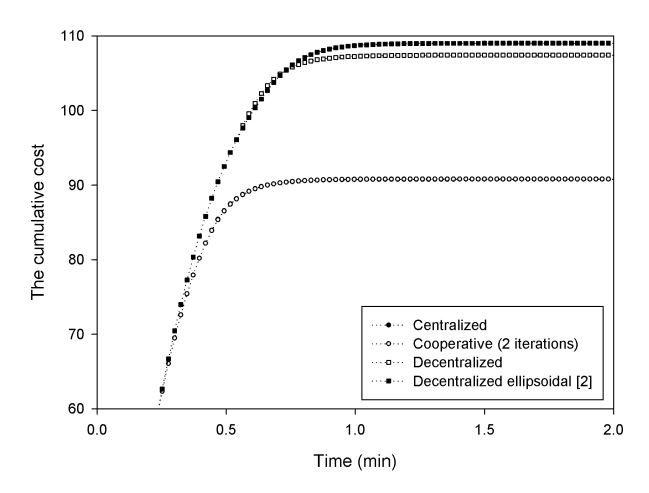


Fig. 4. The cumulative cost $\sum_{k=0}^{t} [x_k^T \Theta x_k + \sum_{i=1}^{N} u_{k,i}^T R u_{k,i}]$.

VI. CONCLUSIONS

We have proposed a framework for robust distributed interpolation-based control targeting at polytopic uncertain systems. The algorithm satisfies a cooperative scheme, and requires iteratively solving a number of linear programming problems in parallel. Simulation example of quadruple tank system are used to illustrate the application of the algorithm. The algorithm is favorable for large-scale systems with many inputs and states, because of reduction of on-line computational burdens. The cooperative algorithm is capable of inheriting the properties of centralized control scheme, and provides similar control performance.

ACKNOWLEDGMENT

This work was supported by Rajadapisek Sompoj Fund, Chulalongkorn University Centenary Academic Development Project, and the Thailand Research Fund (TRF).

TABLE I
THE ON-LINE COMPUTATIONAL BURDENS

| Algorithm | On-line CPU time(s)/step |
|---|--------------------------|
| Decentralized control | |
| with ellipsoidal set [2] | < 0.0001 |
| Algorithm 1 | |
| (decentralized control) | < 0.0001 |
| Algorithm 2 | |
| (centralized control) | 0.01 |
| Algorithm 3 | |
| (cooperative control with 2 iterations) | 0.002 |

REFERENCES

- S. Qin and T. Badgwell, "A survey of industrial model predictive control technology," *Control Engineering Practice*, vol. 11, pp. 733– 764, 2003.
- [2] M. Kothare, V. Balakrishnan, and M. Morari, "Robust constrained model predictive control using linear matrix inequalities," *Automatica*, vol. 32, pp. 1361–1379, 1996.
- [3] Z. Wan and M. Kothare, "An efficient off-line formulation of robust model predictive control using linear matrix inequalities," *Automatica*, vol. 39, pp. 837–846, 2003.
- [4] P. Bumroongsri and S. Kheawhom, "An ellipsoidal off-line model predictive control strategy for linear parameter varying systems with applications in chemical processes," Syst. Control Lett., vol. 61, pp. 435–442, 2012.
- [5] P. Bumroongsri and S. Kheawhom, "An off-line robust mpc algorithm for uncertain polytopic discrete-time systems using polyhedral invariant sets," J. Process Contr., vol. 22, pp. 975–983, 2012.
- [6] S. Kheawhom and P. Bumroongsri, "Constrained robust model predictive control based on polyhedral invariant sets by off-line optimization," *Chemical Engineering Transactions*, vol. 32, pp. 1417–1442, 2013.
- [7] P. Bumroongsri and S. Kheawhom, "An interpolation-based robust mpc algorithm using polyhedral invariant sets," in *Proceedings of the 2013 European Control Conference (ECC)*, 2013, pp. 3161–3166.
- [8] H.-N. Nguyen, P.-O. Gutman, S. Olaru, and M. Hovd, "Implicit improved vertex control for uncertain, time-varying linear discretetime systems with state and control constraints," *Automatica*, vol. 49, pp. 2754 – 2759, 2013.
- [9] R. Scattolini, "Architectures for distributed and hierarchical model predictive control a review," J. Process Contr., vol. 19, pp. 723 – 731, 2009.
- [10] P. D. Christofides, R. Scattolini, D. M. de la Pea, and J. Liu, "Distributed model predictive control: A tutorial review and future research directions," *Comput. Chem. Eng.*, vol. 51, pp. 21 – 41, 2013.
- [11] J. B. Rawlings and B. T. Stewart, "Coordinating multiple optimization-based controllers: New opportunities and challenges," *J. Process Contr.*, vol. 18, pp. 839 845, 2008.
- [12] W. Al-Gherwi, H. Budman, and A. Elkamel, "A robust distributed model predictive control algorithm," J. Process Contr., vol. 21, pp. 1127–1137, 2011.
- [13] W. Al-Gherwi, H. Budman, and A. Elkamel, "A robust distributed model predictive control based on a dual-mode approach," *Comput. Chem. Eng.*, vol. 50, pp. 130–138, 2013.
- [14] L. Zhang, J. Wang, and C. Li, "Distributed model predictive control for polytopic uncertain systems subject to actuator saturation," *J. Process Contr.*, vol. 23, pp. 1075 – 1089, 2013.
- [15] R. Tütüncü, K. Toh, and M. Todd, "Solving semidefinite-quadratic-linear programs using sdpt3," *Math. Prog. Series B*, vol. 95, pp. 189–217, 2003.
- [16] Gurobi Optimization Inc., "Gurobi optimizer reference manual," 2013. [Online]. Available: http://www.gurobi.com
- [17] J. Löfberg, "Yalmip: A toolbox for modeling and optimization in matlab," in *Proc. IEEE international symposium on computer aided* control systems design, 2004, pp. 284–289.
- [18] I. Alvarado, D. Limon, D. Muñoz de la Peña, J. Maestre, M. Ridao, H. Scheu, W. Marquardt, R. Negenborn, B. D. Schutter, F. Valencia, and J. Espinosa, "A comparative analysis of distributed mpc techniques applied to the hd-mpc four-tank benchmark," *Control Engineering Practice*, vol. 21, pp. 800–815, 2011.

Interpolation-based robust constrained model predictive output feedback control

Soorathep Kheawhom¹ and Pornchai Bumroongsri²

Abstract—In this paper, a problem of output feedback robust control of polytopic uncertain discrete-time systems is addressed. The output feedback control law proposed is a function of estimated state determined by mapping of the current output measured. An appropriate estimator is defined, and a sequence of feedback gains is computed by solving off-line a series of optimal control optimization problems. A sequence of nested polyhedral invariant sets associated with each feedback gain pre-computed is then constructed as a mapping on a system output. At each control iteration, a smallest polyhedral invariant set containing the current output is determined. A corresponding feedback gain is then implemented to the process. Further, an interpolation algorithm is proposed to improve control performance. In the interpolation scheme, a feedback gain is computed from convex combination between a feedback gain associated with the current invariant set and that of the adjacent smaller invariant set, where a parameter used in the combination is minimized subjected to a set of constraints associated with the current invariant set. The controller design is illustrated with a case study of nonlinear two-tank system formulated as a polytopic uncertain system. The simulation results showed that the proposed algorithms can drive the system to the origin without input and output constraints violation. The interpolation algorithm proposed can improve control performances while on-line computation is still tractable.

I. INTRODUCTION

Model predictive control (MPC) is an advanced control technique capable of dealing with multiple input multiple output processes with constraints on process variables. Generally, MPC is designed based on a linear time invariant (LTI) system. Robust model predictive control (RMPC) has been developed to guarantee satisfaction on robustness against model uncertainties.

RMPC proposed in [1] is a classic example of algorithm which can deal with polytopic parametric uncertainties. At each control iteration, the optimal state feedback gain that robustly stabilizes the closed-loop system is determined by minimizing the worst-case performance cost subject to input, output and stability criteria constraints. The optimization problem involved is a convex problem with linear matrix inequalities (LMI). This problem is required to be solved on-line. Thus, the algorithm usually requires high on-line computational burdens. Therefore, its application is rather

restricted to the relatively slow dynamic processes. Therefore, the synthesis approaches for off-line RMPC have been widely investigated.

An off-line formulation of RMPC using LMI was developed [2]. A sequence of state feedback gains corresponding to a sequence of ellipsoidal invariant sets is computed off-line. At each sampling instant, the smallest ellipsoidal invariant set containing the currently measured state is determined and the state feedback control law is calculated by linear interpolation between the pre-computed feedback gains. Although the algorithm substantially reduces on-line computational burdens compared with an on-line RMPC, the algorithm is rather conservative due to the fact that the algorithm is designed based on invariant ellipsoids providing small domain of attraction.

An ellipsoidal off-line MPC algorithm for linear parameter varying (LPV) systems was introduced [3]. For LPV systems, the algorithm is less conservative as compared with the algorithm proposed by [2], because the scheduling parameter is included in the controller synthesis. However, the algorithm is still based on an ellipsoidal invariant set. Moreover, the algorithm can handle only the uncertainty in the state matrix.

The invariant sets generally used in the controller design are either ellipsoidal or polyhedral sets. Though the polyhedral invariant set has some advantages over the ellipsoidal invariant set such as better handling of asymmetric constraints and enlargement of domain of attraction [4], the ellipsoidal invariant set is usually used in RMPC formulation due to its relatively low computational complexity. In recent years, an off-line RMPC algorithm based on polyhedral invariant set has been developed [5]. The algorithm computes offline a sequence of state feedback gains corresponding to a sequence of polyhedral invariant sets. At each control iteration, the smallest polyhedral invariant set containing the currently measured state is determined and the corresponding state feedback gain is implemented to the process. Although the polyhedral invariant set which usually provides larger domain of attraction is used, the algorithm is still conservative because the control law implemented at each control iteration is only an approximation of the optimal feedback gain. Moreover, the jerking in control input caused by the switching between state feedback gains is occurred. In order to improve the control performance and to eliminate jerking in control input, the algorithm requires constructing high number of polyhedral invariant sets, hence a large data storage is required. An interpolation technique for polyhedral invariant sets was introduced to off-line RMPC for polytopic uncertain systems in order to reduce conservatism and im-

¹Soorathep Kheawhom is with Computational Process Engineering, Department of Chemical Engineering, Faculty of Engineering, Chulalongkorn University, Bangkok 10330 Thailand soorathep.k@chula.ac.th, corresponding author

²Pornchai Bumroongsri is with Department of Chemical Engineering, Faculty of Engineering, Mahidol University, Nakhon Pathom 73170 Thailand pornchai.bum@mahidol.ac.th

prove the control performance [6], [7]. Another technique to deal with polytopic uncertain systems with input and output constraints can be based on a vertex control which is also an interpolation-based controller [8].

Information on a system state is also important to the performance of RMPC. In a state feedback RMPC, full state information is required in order to predict behaviours of a system. Unfortunately, the system state is not always accurately measurable, only information on a system output is available. In this case, an output feedback control is more practical than the state feedback control. [9] proposed an output feedback MPC, where a stable Luenberger state estimator was used, and an error on a state estimation was incorporated. [10] developed an output feedback RMPC (OFRMPC) for polytopic uncertain systems by also using a Luenberger state estimator. [11] developed OFRMPC based on dynamic output feedback control, where the control law is parameter-dependent.

In this paper, we present an off-line robust constrained output feedback model predictive control based on polyhedral invariant sets for polytopic uncertain systems. Moreover, an interpolation scheme to further improve control performances of the proposed algorithm is introduced. The paper is organized as follows. In section 2, the problem description is presented. The robust model predictive control and polyhedral invariant set construction are presented in section 3. In section 4, the proposed algorithms are described. In section 5, we illustrate the implementation of the algorithms proposed. Finally, in the last section, we conclude the paper.

Notation: For a matrix A, A^T denotes its transpose, A^{-1} denotes its inverse. I denotes the identity matrix. For a state vector x, x_k denotes the state measured at real time k, x_{k+i} denotes the state at prediction time k+i predicted at real time k. \hat{x}_k is the estimated state at real time k. y_k and y_k denote the output measured and the control input at real time k, respectively. The symbol * denotes the corresponding transpose of a lower block part of symmetric matrices.

II. PROBLEM DESCRIPTION

In this work, a discrete-time linear time-varying (LTV) system with polytopic parametric uncertainties as shown (1) is taken into account.

$$x_{k+1} = A_k x_k + B_k u_k,$$

$$y_k = C_k x_k,$$
(1)

where $x_k \in R^n$ is a vector of state variables. $u_k \in R^{n_u}$ is a vector of control inputs, and $y_k \in R^n$ is a vector of control outputs. The states cannot be accurately measured, but can be estimated by using the current outputs, which are accurately measureable. In addition, the system matrix A_k , the control matrix B_k , and the output matrix C_k are assumed to be within a polytope,

$$[A_k, B_k, C_k] \in Co\{[A_1, B_1, C_1], ..., [A_L, B_L, C_L]\},\$$

Co denotes convex hull with $[A_l, B_l, C_l]$ vertices. Any $[A_k, B_k, C_k]$ within the polytope is a convex combination of

the vertices such that $[A_k, B_k, C_k] = \sum_{l=1}^L \lambda_{l,k} [A_l, B_l, C_l]$, $\sum_{l=1}^L \lambda_{l,k} = 1$, where $0 \le \lambda_{l,k} \le 1$ is an uncertain parameter vector. C_k is assumed to be an invertible matrix. In addition, the system is observable and controllable.

As the state vector x_k cannot be accurately measured online, the estimated state vector \hat{x}_k are determined through a mapping of the output vector.

$$\hat{x}_k = E y_k, \tag{2}$$

where E is an $n \times n$ estimator matrix.

Our aim is to find a feedback control law

$$u_k = K\hat{x}_k = KEy_k, \tag{3}$$

that stabilizes the LTV system as shown in (1) and achieves the minimum worst case performance cost defined as in (4) subjected to input, output and state constraints as in (5)-(7).

$$\min_{u_{k+i}} \max_{[A,B,C] \in \Omega} \sum_{i=0}^{\infty} {x_{k+i} \brack u_{k+i}}^T \begin{bmatrix} \Theta & 0 \\ 0 & R \end{bmatrix} {x_{k+i} \brack u_{k+i}}, \tag{4}$$

$$s.t.u_{h,\min} \le u_{h,k+i} \le u_{h,\max}, h = 1,...,n_u,$$
 (5)

$$y_{r,\min} \le y_{r,k+i} \le y_{r,\max}, r = 1,...,n,$$
 (6)

$$x_{s,\min} \le x_{s,k+i} \le x_{s,\max}, s = 1, ..., n,$$
 (7)

where $\Theta > 0$ and R > 0 are diagonal weighting matrices of states and control inputs, respectively.

III. ROBUST MODEL PREDICTIVE CONTROL AND POLYHEDRAL INVARIANT SET

An on-line robust model predictive state feedback control for LTV systems was introduced in [1]. The optimization problem is shown in (8)-(12).

$$\min_{\gamma \neq 0} \gamma \tag{8}$$

$$\text{s.t.} \begin{bmatrix} 1 & * \\ x_k & Q \end{bmatrix} \ge 0, \tag{9}$$

$$\begin{bmatrix} Q & * & * & * \\ A_{l}Q + B_{l}Y & Q & * & * \\ \Theta^{\frac{1}{2}}Q & 0 & \gamma I & * \\ R^{\frac{1}{2}}Y & 0 & 0 & \gamma I \end{bmatrix} \ge 0, \forall l = 1, ..., L, \quad (10)$$

$$\begin{bmatrix} X & * \\ Y^T & Q \end{bmatrix} \ge 0, X_{hh} \le u_{h,\text{max}}^2, h = 1, ..., n_u,$$

$$\begin{bmatrix} S & * \\ (A_lQ + B_lY)^T C_l^T & Q \end{bmatrix} \ge 0, \forall l = 1, ..., L,$$

$$(11)$$

$$S_{rr} \le y_{r,\text{max}}^2, r = 1, ..., n,$$
 (12)

where Q is a symmetric matrix.

By solving the optimization problem presented in (8)-(12), we obtain a state feedback control law $u_k = Kx_k$ with a state feedback gain $K = YQ^{-1}$ that can stabilize the system while satisfying the input and output constraints.

However, the current state vector x_k cannot be accurately measured on-line. The estimated state vector \hat{x}_k is estimated via estimator matrix E as $\hat{x}_k = Ey_k$. The estimator matrix E can be chosen as an inverse of a nominal output matrix \bar{C}^{-1} . The nominal output matrix is obtained by taking the centroid

of all output matrices at each uncertainty vertex. We design a feedback control law of the form $u_k = KEy_k$.

$$x_{k} = C_{k}^{-1}y_{k}$$

$$y_{k} = y_{k}$$

$$u_{k} = KEy_{k}$$

$$x_{k+1} = [A_{k} + B_{k}KEC_{k}]C_{k}^{-1}y_{k}$$

$$y_{k+1} = C_{k+1}[A_{k} + B_{k}KEC_{k}]C_{k}^{-1}y_{k}$$

$$u_{k+1} = KEC_{k+1}[A_{k} + B_{k}KEC_{k}]C_{k}^{-1}y_{k}$$

$$\vdots = \vdots$$

$$x_{k+n} = [\prod_{i=1}^{n} [A_{k+n-i} + B_{k+n-i}KEC_{k+n-i}]]C_{k}^{-1}y_{k}$$

$$y_{k+n} = C_{k+n}[\prod_{i=1}^{n} [A_{k+n-i} + B_{k+n-i}KEC_{k+n-i}]]C_{k}^{-1}y_{k}$$

$$u_{k+n} = KEC_{k+n}[\prod_{i=1}^{n} [A_{k+n-i} + B_{k+n-i}KEC_{k+n-i}]]C_{k}^{-1}y_{k}$$

To guarantee that the estimator matrix E can be used incorporation with feedback gain K in an output feedback scheme, there must exist a matrix P > 0 satisfying

$$P - [A_l + B_l K E C_l]^T P[A_l + B_l K E C_l] \ge 0, l = 1, ..., L.$$
 (13)

Theorem 1: For an LTV system as shown in (1), given the initial measured output y_k with the estimator matrix E, the control law $u_k = KEy_k$ with a state feedback gain $K = YQ^{-1}$ provided by solving the optimization problem presented in (8)-(12) and satisfication of (13), provides robust stability to the closed-loop system.

Proof: The satisfaction of (13) for the feedback gain K and the estimator matrix E ensures that $x_k^T P x_k - [[A_l + B_l K E C_l] x_k]^T P [[A_l + B_l K E C_l] x_k] \ge 0$, l = 1, ..., L. That means $x_k^T P x_k - x_{k+1}^T P x_{k+1} \ge 0$. Thus, $V_k = x_k^T P x_k$ is a strictly decreasing Lyapunov function and the closed-loop system is robustly stabilized.

By giving a state feedback gain K with an estimator matrix E satisfying (13), and control inputs $u_k = KEy_k$, the polyhedral invariant set with largest domain of attraction can be constructed. The polyhedral invariant set mapped on the output vector, $S = \{y|My \le d\}$, can be constructed by using the following procedure.

Procedure 1

- 1) Set i = 0, $M_i = [C_1^{-1}; -C_1^{-1}; \dots; C_L^{-1}; -C_L^{-1}; I; -I; \dots; I; -I; KE; -KE; \dots; KE; -KE]$, $N_i = [I; -I; \dots; I; -I; C_1; -C_1; \dots; C_L; -C_L; KEC_1; -KEC_1; \dots; KEC_L; -KEC_L]$, $d_i = [x_{\max}; -x_{\min}; \dots; x_{\max}; -x_{\min}; y_{\max}; -y_{\min}; \dots; y_{\max}; -y_{\min}; y_{\max}; -y_{\min}; \dots; y_{\max}; -y_{\min}; y_{\min}; y_{\max}; -y_{\min}; y_{\min}; y_{\min$
- 2) Set i = i + 1, $M_i = [M_{i-1}; N_{i-1}[A_1 + B_1KEC_1]C_1^{-1};$...; $N_{i-1}[A_L + B_LKEC_L]C_L^{-1}]$, $N_i = [N_{i-1}; N_{i-1}[A_1 + B_1KEC_1];$...; $N_{i-1}[A_L + B_LKEC_L]]$, $d_i = [d_{i-1}; d_{i-1};$...; $d_{i-1}]$, $S_i = \{y|M_iy \le d_i\}$, and eliminate redundant inequalities from the polytope S_i , and also eliminate the corresponding row from N_i .

3) If $S_i \neq S_{i-1}$ then repeat step 2, if otherwise stop the algorithm and $S = \{y | M_i y \leq d_i\}$.

Theorem 2: For an LTV system as shown in (1), given the estimator matrix E, and the control law $u_k = KEy_k$ with a state feedback gain K satisfying Theorem 1. The polyhedral set, $S = \{y|My \le d\}$, constructed by using Procedure 1 provides a set of outputs that the system will evolve to the origin without input and output constraints violation.

Proof: By following Procedure 1, we iteratively add state, output and input constraints at the time k+i, $i=0,...,i_{\max}$ to define a polyhedral invariant set $S=\{y|My \leq d\}$, and eliminate all redundant constraints. Thus, we can construct a set of initial outputs, $y \in S$, such that all future outputs from time k to $k+i_{\max}$ remain inside S and satisfy the constraints. In addition, there exists a finite index $i=i_{\max}$ such that $M_i=M_{i+1}$ because of the contraction as the satisfaction of Theorem 1 ensures the closed-loop stability. Thus, we can construct a set of initial outputs $S=\{y|My \leq d\}$ such that all future outputs remain inside S and approach to the origin while satisfying the constraints.

IV. THE PROPOSED ALGORITHM

In this section, the proposed algorithms of robust constrained output feedback control are described. The algorithms proposed consist of off-line and on-line calculations. *Algorithm 1*

- 1) off-line computation:
 - Choose a sequence of states $x_m, m = 1, ..., m_{\max}$, where x_{m+1} is close to the origin than x_m . For each x_m , solve the optimization problem in (8)-(12) by replacing x_k with x_m in order to obtain a corresponding state feedback gain $K_m = Y_m Q_m^{-1}$. Moreover, x_m is chosen such that $\varepsilon_{m+1}^{-1} \subset \varepsilon_m^{-1}$, where $\varepsilon_m = \{x | x^T Q_m^{-1} x \le 1\}$. The estimator matrix E is chosen such that (13) is satisfied. The estimator matrix E can be chosen as an inverse of a nominal output matrix \bar{C}^{-1} .
 - By using the estimator matrix E, and a sequence of state feedback gains $K_m = Y_m Q_m^{-1}, m = 1, ..., m_{\text{max}}$ previously calculated. A polyhedral invariant set $S_m = \{y | M_m y \le d_m\}$ associated with each state feedback gain is constructed by using Procedure 1 previously described.
- 2) on-line computation: At each control iteration, y_k is measured, a smallest polyhedral invariant set $S_m = \{y | M_m y \le d_m\}$ containing the current output measured is determined. The feedback control law $u_k = K_m E y_k$ is implemented to the system.

Theorem 3: For an LTV system as shown in (1), given the initial measured output $y_k \in S_m$, the control law provided by Algorithm 1 assures robust stability to the closed-loop system, while satisfying input, output and state constraints.

Proof: From Theorem 2, with the estimator matrix E, and the control law $u_k = K_m E y_k$, the polyhedral set S_m provides a set of outputs that the system will evolve to the origin without input and output constraints violation.

Thus, any initial states with measured outputs $y_k \in S_m$ are guaranteed that all future output trajectories evolve closer to the origin by passing S_{m+1} , S_{m+2} , ..., and $S_{m_{max}}$. Thus, the control law provided by Algorithm 1 assures robust stability to the closed-loop system with input, output and state constraints satisfaction.

The output feedback control algorithm proposed in Algorithm 1 is further improved by implementing an interpolation technique. In this technique, a feedback gain is calculated from convex combination between a feedback gain associated with the current invariant set and that of the adjacent smaller invariant set, where a parameter used in the combination is minimized subjected to a set of constraints associated with the current invariant set.

Algorithm 2

1) off-line computation: An off-line computation used in this algorithm is as same as that of Algorithm 1. However, x_m , $m = 1,...,m_{\text{max}}$ must be chosen such that for each $m \neq m_{\text{max}}$, there must exist a matrix P > 0

$$P - [A_l + B_l K_m E C_l]^T P[A_l + B_l K_m E C_l] \ge 0, \quad (14)$$

$$P - [A_l + B_l K_{m+1} E C_l]^T P[A_l + B_l K_{m+1} E C_l] \ge 0, \quad (15)$$

for all l = 1,...,L, to assure robust stability satisfaction of a convex combination between K_m and K_{m+1} .

2) on-line computation: At each control iteration, when $y_k \in S_m$ and $y_k \notin S_{m+1}, \forall m \leq m_{\text{max}} - 1$, the feedback gain $K_k = \lambda_k K_m + (1 - \lambda_k) K_{m+1}$ can be obtained by solving the problem in (16)-(20).

$$\min_{\lambda_k} \lambda_k \tag{16}$$

s.t.
$$M_m[C_i(A_j + B_j K_k E C_j) C_j^{-1} y_k] - d_m \le 0,$$
 (17)

$$i = 1, ..., L, j = 1, ..., L,$$

$$u_{\min} \le K_k E y_k \le u_{\max},\tag{18}$$

$$K_k = \lambda_k K_m + (1 - \lambda_k) K_{m+1}, \tag{19}$$

$$0 \le \lambda_k \le 1. \tag{20}$$

If $y_k \in S_{m_{\text{max}}}$, the feedback control law $u_k = K_{m_{\text{max}}} E y_k$ is implemented to the system.

The optimization problem involved is formulated as a linear programming and the number of constraints involved grows with the number of vertices of the uncertain polytope.

Theorem 4: For an LTV system as shown in (1), given the initial measured output $y_k \in S_m$, the control law provided by Algorithm 2 assures robust stability to the closed-loop system, while satisfying input, output and state constraints.

Proof: As (14) and (15) are satisfied, a Lyapunov function $V_k = x_k^T P x_k$ ensures robust stability of the feedback gain $K_k = \lambda_k K_m + (1 - \lambda_k) K_{m+1}$, $0 \le \lambda_k \le 1$, which is a convex combination of K_m and K_{m+1} . In solving the problem in (16)-(20), (20) restricts K_k to be a convex combination of K_m and K_{m+1} . The input constraint is guaranteed by (18). The state constraint does not need to be explicitly incorporated into the problem formulation because the satisfaction of (17) also guarantees state and output constraints satisfaction.

The constraints in (17) guarantee that one step prediction output y_{k+1} remains in S_m . Thus, the feedback control law $u_k = K_k E y_k$ obtained from solving the optimization problem in (16)-(20) assures robust stability to the closed-loop system with input, output and state constraints satisfaction.

V. CASE STUDY

In this section, we present an example that illustrates the implementation of the proposed algorithms. The numerical simulations have been performed in 2.3 GHz Intel Core i-5 with 16 GB RAM, using SDPT3[12], Gurobi[13] and YALMIP [14] within Matlab R2011b environment. We consider the application of our approach to the nonlinear twotank system, which is described by (21)-(22).

$$\dot{h}_1 = -0.0161\sqrt{h_1} + 0.4u,\tag{21}$$

$$\dot{h}_2 = 0.0252\sqrt{h_1} - 0.0112\sqrt{h_2}. (22)$$

Where h_1 is the water level in tank 1, h_2 is the water level in tank 2 and u is the water flowrate.

Let $\bar{h}_1 = h_1 - h_{1,eq}$, $\bar{h}_2 = h_2 - h_{2,eq}$ and $\bar{u} = u - u_{eq}$. Subscript eq denotes the corresponding variable at equilibrium condition, $h_{1,eq} = 14$ cm and $h_{2,eq} = 70$ cm. The objective is to regulate \bar{h}_1 and \bar{h}_2 to the origin by manipulating \bar{u} . The input constraint is asymmetric -1.5kg/s $\leq \bar{u} \leq 1.0$ kg/s. Similarly, asymmetric state constraints $-13\text{cm} \le \bar{h}_1 \le 71\text{cm}$, and -69cm $\leq \bar{h}_2 \leq 29$ cm are considered.

By evaluating the Jacobian matrix of (21)-(22) along the vertices of the constraints set, the solutions of (21)-(22) are also the solution of the following differential inclusion

$$\begin{bmatrix} \bar{h}_1 \\ \bar{h}_2 \end{bmatrix} \in \sum_{l=1}^4 \lambda_l [A_l \begin{bmatrix} \bar{h}_1 \\ \bar{h}_2 \end{bmatrix} + B_l \bar{u}], \tag{23}$$

where $\sum_{l=1}^{L} \lambda_l = 1$, and $0 \le \lambda_l \le 1$. The measurable outputs, $\tilde{h_1}$ and $\tilde{h_2}$, are assumed to be inside the following polytopes,

$$\begin{bmatrix} \tilde{h}_1 \\ \tilde{h}_2 \end{bmatrix} \in \sum_{l=1}^2 \lambda_l C_l \begin{bmatrix} \bar{h}_1 \\ \bar{h}_2 \end{bmatrix}, \tag{24}$$

$$C_{1} = \begin{bmatrix} 0.9 & 0.0 \\ 0.0 & 0.8 \end{bmatrix},$$

$$C_{2} = \begin{bmatrix} 1.2 & 0.0 \\ 0.0 & 1.1 \end{bmatrix},$$
(25)

$$C_2 = \begin{bmatrix} 1.2 & 0.0 \\ 0.0 & 1.1 \end{bmatrix},\tag{26}$$

where $\sum_{l=1}^{L} \lambda_l = 1$, and $0 \le \lambda_l \le 1$.

The discrete-time model is obtained by discretization of (23) using Euler first-order approximation with a sampling period of 0.1 s and it is omitted here for brevity. The tuning parameters are $\Theta = \begin{bmatrix} 0 & 0 \\ 0 & 1 \end{bmatrix}$ and R = 0.01.

The estimator matrix of $E = \begin{bmatrix} 0.95 & 0.00 \\ 0.00 & 1.05 \end{bmatrix}$ is used to construct a sequence of six polyhedral invariant sets by using the following states, [-12;28], [1.4;1.8], [0.6;0.6], [0.2;0.3], [0.08; 0.12] and [0.01; 0.04]. Figure 1 shows the constructed polyhedral invariant sets mapping on $\tilde{h_1}$ and $\tilde{h_2}$. By using a different estimator matrix or a different sequence of states, the invariant set obtained may be different.

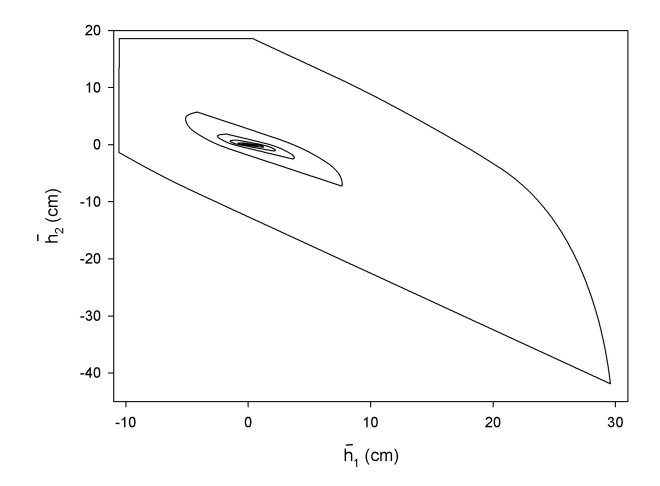


Fig. 1. The invariant sets with mapping on outputs for the case study

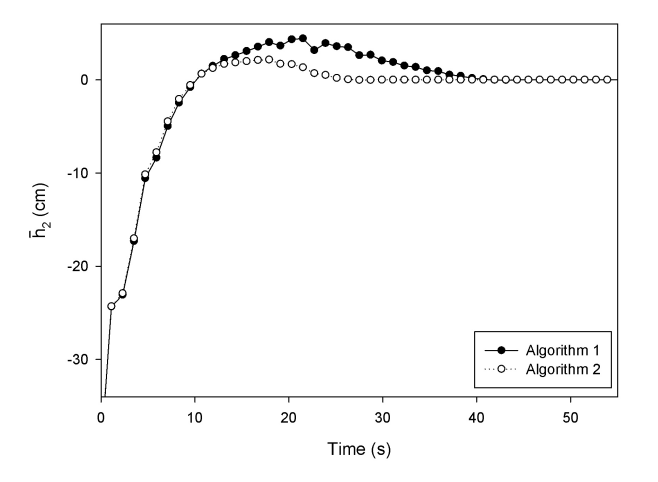


Fig. 2. The profiles of regulated state (\bar{h}_2) for the case study

We regulate the system from the initial state with measured output of $(h_1, h_2) = [29, -40]$ to the origin. Figure 2 shows the profiles of regulated state (\bar{h}_2) . Both algorithms can drive the states to the origin without input and state constraints violation. Algorithm 1 provides a slower response than Algorithm 2, because the real-time feedback gain used in Algorithm 1 is an approximation of the optimal feedback gain. For instance, by Algorithm 1, if we start from an initial state with output $y_k \in S_m$ but $y_k \notin S_{m+1}$, a feedback gain K_m is implemented. The system is driven to the next state x_{k+1} where the Lyapunov function $V_{k+1} < V_k$. If $y_{k+1} \in S_m$ but $y_{k+1} \notin S_{m+1}$, K_m is still used as a feedback gain. We see that $|u_{k+1}| < |u_k|$, as $V_{k+1} < V_k$. In other words, Algorithm 1 implements the feedback gain K_m for the whole region $y_k \in S_m$ but $y_k \notin S_{m+1}$. By using interpolation as in Algorithm 2, we can achieve a better control performance. For each $y_k \in S_m$ but $y_k \notin S_{m+1}$, a feedback gain K_k obtained by solving an optimization problem is implemented. We see that $K_k \neq K_m$. Thus, a preferable control performance can

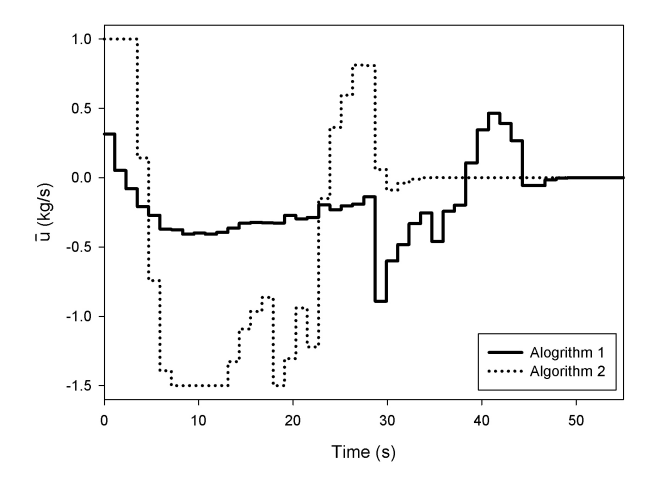


Fig. 3. The profiles of control input \bar{u} for the case study

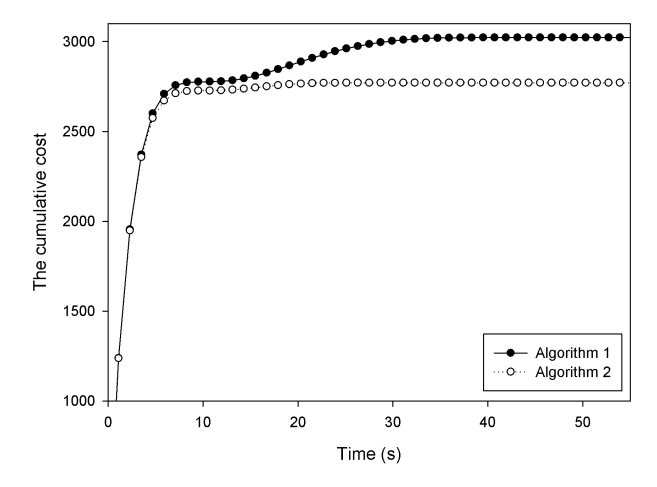


Fig. 4. The cumulative cost for the case study

be obtained. Therefore, Algorithm 1 is more conservative that Algorithm 2.

Figure 3 shows the profiles of control input \bar{u} . Algorithm 1 does not implement any interpolation techniques, thus, the feedback gain used updates only when the current output measured switches from one invariant set to another smaller invariant set. Consequently, a conservative control input profile is observed in Algorithm 1. In comparison, Algorithm 2 implements more aggressive control input profile, as the interpolation technique is implemented.

Figure 4 shows the cumulative performance cost. The cumulative performance cost of Algorithm 2 is lower than the cumulative cost of Algorithm 1.

Figures 5 and 6 show state, estimated state and output trajectories from initial output of $(\tilde{h}_1, \tilde{h}_2) = [29; -40]$ to the origin. The discrepancies between states and estimated states decrease as the system evolves. Algorithm 2 produces the trajectory with better control performances.

For both algorithms, most of the computational burdens

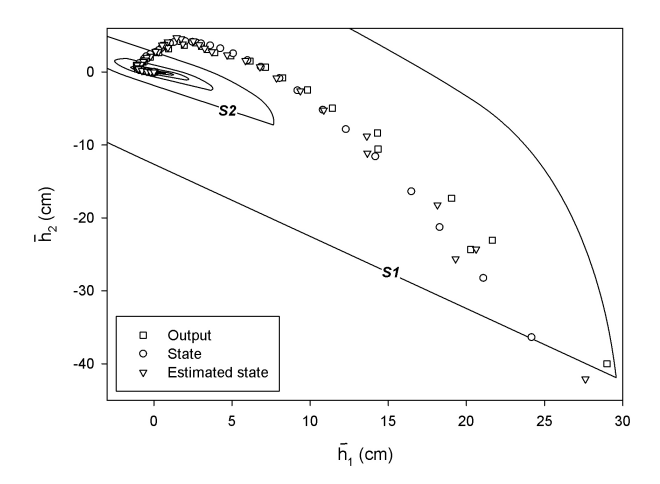


Fig. 5. State, estimated state and output trajectories of the algorithm 1 for the case study

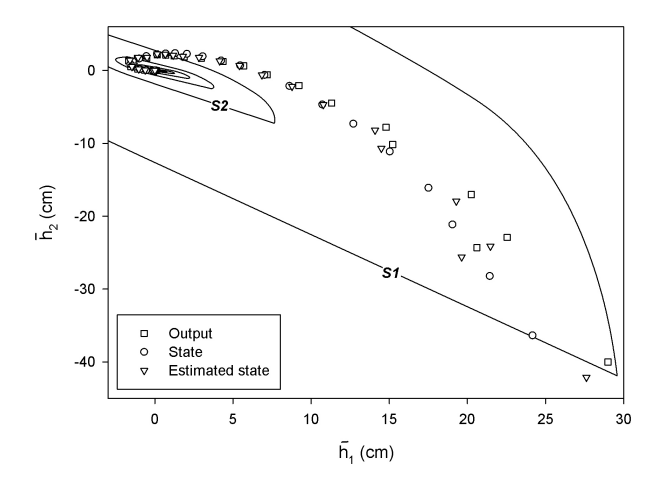


Fig. 6. State, estimated state and output trajectories of the algorithm 2 for the case study

are moved off-line so the on-line computation is tractable. The optimization problem involved in Algorithm 2 is a linear programming and the constraints involved is dependent of the number of vertices of the uncertain polytope. In each time step, computational times required for Algorithm 1 and 2 are 1 and 4 ms., respectively.

VI. CONCLUSIONS

In this paper, we have presented an output feedback robust model predictive control of polytopic uncertain discrete-time systems. The output feedback control law is parameterized as a function of estimated state determined by mapping of the current output measured. The proposed algorithms use an off-line solution of a series of optimal control optimization problems to determine a sequence of feedback gains. A sequence of nested polyhedral invariant sets associated with each feedback gain pre-computed is constructed. At each control iteration, the smallest invariant containing the measured output is identified, and the corresponding feedback

gain is implemented. In addition, the interpolation algorithm is proposed to improve control performance. A case study of nonlinear two-tank system formulated as a polytopic uncertain system is used to illustrate the algorithms proposed. The simulation results showed that the proposed algorithms can drive the system to the origin while satisfying input, output and state constraints. An interpolation-based algorithm can improve control performance. The interpolation technique used requires on-line solving a linear programming, where the complexity of the problem is dependent of the number of vertices of the uncertain polytope.

ACKNOWLEDGMENT

This work was supported by Rajadapisek Sompoj Fund, Chulalongkorn University Centenary Academic Development Project, and The Commission on Higher Education of Thailand, the Thailand Research Fund (TRF), and Chulalongkorn University under the research project RES56-25521050.

REFERENCES

- M. Kothare, V. Balakrishnan, and M. Morari, "Robust constrained model predictive control using linear matrix inequalities," *Automatica*, vol. 32, pp. 1361–1379, 1996.
- [2] Z. Wan and M. Kothare, "An efficient off-line formulation of robust model predictive control using linear matrix inequalities," *Automatica*, vol. 39, pp. 837–846, 2003.
- [3] P. Bumroongsri and S. Kheawhom, "An ellipsoidal off-line model predictive control strategy for linear parameter varying systems with applications in chemical processes," *Syst. Control Lett.*, vol. 61, pp. 435–442, 2012.
- [4] P. Pluymers, J. Rossiter, J. Suykens, and B. Moore, "The efficient computation of polyhedral invariant sets for linear systems with polytopic uncertainty," in *Proc. of the American Control Conference*, 2005, pp. 804–809.
- [5] P. Bumroongsri and S. Kheawhom, "An off-line robust mpc algorithm for uncertain polytopic discrete-time systems using polyhedral invariant sets." J. Process Contr., vol. 22, pp. 975–983, 2012.
- ant sets," J. Process Contr., vol. 22, pp. 975–983, 2012.
 [6] S. Kheawhom and P. Bumroongsri, "Constrained robust model predictive control based on polyhedral invariant sets by off-line optimization," Chemical Engineering Transactions, vol. 32, pp. 1417–1442, 2013.
- [7] P. Bumroongsri and S. Kheawhom, "An interpolation-based robust mpc algorithm using polyhedral invariant sets," in *Proceedings of the 2013 European Control Conference (ECC)*, 2013, pp. 3161–3166.
- [8] H.-N. Nguyen, P.-O. Gutman, S. Olaru, and M. Hovd, "Implicit improved vertex control for uncertain, time-varying linear discretetime systems with state and control constraints," *Automatica*, vol. 49, no. 9, pp. 2754 – 2759, 2013.
- [9] D. Mayne, S. Rakovic, R. Findeisen, and F. Allgower, "Robust output feedback model predictive control of constrained linear systems," *Automatica*, vol. 42, pp. 1217–1222, 2006.
- [10] B. Ding, Y. Xi, M. Cychowski, and T. O'Mahony, "A synthesis approach for output feedback robust constrained model predictive control," *Automatica*, vol. 44, pp. 258–264, 2008.
- [11] B. Ding, "Constrained robust model predictive control via parameterdependent dynamic output feedback," *Automatica*, vol. 46, pp. 1517– 1523, 2010.
- [12] R. Tütüncü, K. Toh, and M. Todd, "Solving semidefinite-quadratic-linear programs using sdpt3," *Math. Prog. Series B*, vol. 95, pp. 189–217, 2003.
- [13] Gurobi Optimization Inc., "Gurobi optimizer reference manual," 2013. [Online]. Available: http://www.gurobi.com
- [14] J. Löfberg, "Yalmip: A toolbox for modeling and optimization in matlab," in *Proc. IEEE international symposium on computer aided* control systems design, 2004, pp. 284–289.



Robust MPC Based on Polyhedral Invariant Sets for LPV Systems

Soorathep Kheawhom* and Pornchai Bumroongsri**

* Computational Process Engineering, Department of Chemical Engineering, Faculty of Engineering, Chulalongkorn University, Bangkok 10330 Thailand (e-mail: soorathep.k@chula.ac.th). ** Department of Chemical Engineering, Faculty of Engineering, Mahidol University, Nakhon Pathom 73170 Thailand (e-mail: pornchai.bum@mahidol.ac.th).

Abstract: A robust model predictive control (RMPC) using polyhedral invariant sets for linear parameter varying (LPV) systems is presented in this work. A sequence of state feedback gains associated with a sequence of nested polyhedral invariant sets is constructed off-line in order to reduce the computational burdens. At each control iteration, when the measured state lies between any two adjacent polyhedral invariant sets constructed, a state feedback gain is determined by interpolation of two pre-computed state feedback gains incorporated with scheduling parameters. Three interpolation algorithms are proposed. In the first algorithm, the real-time state feedback gain is determined by maximizing the state feedback gain with subjected to a set of constraints associated with current invariant set. In the second algorithm, the real-time state feedback gain is calculated by minimizing the violation of the constraints of the adjacent inner invariant set with subjected to a set of constraints associated with current invariant set. In the last algorithm, the real-time state feedback gain is obtaned by minimizing the upper bound of infinite horizon worst case performance cost, which is estimated by Lyapunov function at current state, with subjected to a set of constraints associated with current invariant set. The controller design is illustrated with a case study of nonlinear two-tank system. The simulation results showed that the proposed RMPC with interpolation provides a better control performance while on-line computation is still tractable as compared to previously reported algorithms.

Keywords: linear parameter varying system; polyhedral invariant set; model predictive control; robust stability; stabilizable region.

1. INTRODUCTION

Model predictive control (MPC) is known as an effective control algorithm to deal with multiple input-multiple output processes. At each control iteration, MPC uses an explicit model to solve an optimal control problem, and implements the first element of the optimal input sequence computed. However, conventional MPC based on a linear model is often unsuitable for controlling nonlinear systems. The performance of linear MPC will deteriorate as the discrepancy between the real process and the model used increases (Morari and Lee, 1999).

Though, the behaviour of a nonlinear system is preferably captured by a nonlinear process model, MPC based on nonlinear model is computationally prohibitive in practical situations. To overcome the excessive computational cost of MPC application for large-scale nonlinear systems, representing the process model in a form of Linear Parameter Varying (LPV) systems has been recieving increasing attention(Paijmans et al., 2008). Thus, the synthesis of MPC for LPV system has been motivated(Lu and Arkun, 2000).

An on-line RMPC for LPV systems using parameter-dependent Lyapunov function was introduced by Wada et al. (2006). At each control iteration, the ellipsoidal invariant set containing the measured state is constructed in order to guarantee robust stability. However, the associated optimization problem must be solved on-line, the algorithm requires a relatively high computational effort.

Bumroongsri and Kheawhom (2012a) introduced an offline RMPC for LPV systems. The sequences of state feedback gains corresponding to the sequences of ellipsoidal invariant sets are pre-computed off-line. At each control iteration, the smallest ellipsoid containing the state measured is determined. The corresponding real-time state feedback gain is obtained by linear interpolation between the pre-computed state feedback gains. The ellipsoidal invariant set computed at each control iteration is only an approximation. Thus, the algorithm trades off optimality in order to reduce on-line computational time.

Though the polyhedral invariant set has some advantages over the ellipsoidal invariant set such as better handling of asymmetric constraints and enlargement of stabilizable region (Pluymers et al., 2005), the ellipsoidal invariant set is usually used in robust model predictive control(RMPC)

formulation due to its relatively low on-line computational complexity. In recent years, an off-line RMPC algorithm based on polyhedral invariant set has been developed by Bumroongsri and Kheawhom (2012b). A sequence of polyhedral invariant sets corresponding to a sequence of pre-computed state feedback gains is constructed off-line. At each control iteration, the smallest polyhedral invariant set containing the measured state is determined. The corresponding state feedback gain is then implemented to the process without interpolation of the pre-computed state feedback gains. Unfortunately, the conservativeness is obtained because the control law implemented at each control iteration is an approximation of the optimal control law. Moreover, the input discontinuities caused by a switching between state feedback control laws are occurred. Therefore, the algorithm requires constructing a large number of polyhedral invariant sets, hence large data storage, in order to improve the control performance and reduce the input discontinuities. Later, an interpolation technique for polyhedral invariant sets was introduced to off-line RMPC for polytopic uncertain systems in order to reduce conservativeness and improve the control performances (Kheawhom and Bumroongsri, 2013; Bumroongsri and Kheawhom, 2013).

In this paper, we present a robust model predictive control (RMPC) based on polyhedral invariant sets for LPV systems. The algorithm constructs off-line a sequence of nested polyhedral invariant sets corresponding to a sequence of state feedback gains. At each control iteration, when the state measured lies between any two adjacent polyhedral invariant sets constructed, a real-time state feedback gain is determined by interpolation of two precomputed state feedback gains incorporated with scheduling parameters. Three interpolation algorithms are proposed. The algorithm proposed requires very small computation complexity. The paper is organized as follows. In section 2, the problem description is presented. In section 3, the RMPC with interpolation algorithms proposed are presented. In section 4, we illustrate the implementation of the algorithms proposed. Finally, in section 5, we conclude the paper.

Notation: For a matrix A, A^T denotes its transpose, A^{-1} denotes its inverse. I denotes the identity matrix. For a vector x, x(k/k) denotes the state measured at real time k, x(k+i/k) denotes the state at prediction time k+i predicted at real time k. The symbol * denotes the corresponding transpose of the lower block part of symmetric matrices.

2. PROBLEM DESCRIPTION

In this work, the discrete-time LPV system as shown in Eq. 1 is taken into accounted.

$$x(k+1) = A(p(k))x(k) + B(p(k))u(k), y(k) = Cx(k),$$
(1)

where $x(k) \in \mathbb{R}^{n_x}$ is the state of the plant and $u(k) \in \mathbb{R}^{n_u}$ is the control input. The scheduling parameter p(k) is assumed to be on-line measurable at each control iteration k. In addition, the system matrix A(p(k)) and the control matrix B(p(k)) are assumed to be within a polytope Ω ,

$$\Omega = Co\{[A_1, B_1], [A_2, B_2], ..., [A_L, B_L]\}. \tag{2}$$

Co denotes convex hull. $[A_j, B_j]$ is the vertex of the convex hull. Any [A(p(k)), B(p(k))] being inside the polytope Ω is a convex combination of all vertices such that

$$[A(p(k)), B(p(k))] = \sum_{j=1}^{L} p_j(k)[A_j, B_j],$$
(3)

$$\sum_{j=1}^{L} p_j(k) = 1, 0 \le p_j(k) \le 1.$$
(4)

The objective is to find a state feedback control law

$$u(k+i/k) = Kx(k+i/k), (5)$$

that stabilises the LPV system and achieves the minimum worst case performance cost.

$$\min_{u(k+i/k)} \max_{[A,B] \in \Omega} \sum_{i=0}^{\infty} {x(k+i/k) \choose u(k+i/k)}^T {\Theta \choose 0}_R {x(k+i/k) \choose u(k+i/k)}, (6)$$

s.t.
$$|u_h(k+i/k)| \le u_{h,\text{max}}, h = 1, 2, ..., n_u,$$
 (7)

$$|y_r(k+i/k)| \le y_{r,\max}, r = 1, 2, ..., n_y.$$
 (8)

3. THE PROPOSED ALGORITHM

In this section, the RMPC based on polyhedral invariant set with interpolation algorithms proposed are described. The on-line computational time is reduced by solving off-line the optimization problem shown in Eqs. 9-12 in order to find a sequence of state feedback gains K_i , i=1,2,...,N associated with a sequence of polyhedral invariant sets. An approach to construct the polyhedral invariant set proposed by (Pluymers et al., 2005) is adopted here. At each control iteration, when the measured state lies between two adjacent polyhedral invariant sets, the real-time state feedback gain is calculated by solving optimization problem based on linear interpolation between two precomputed state feedback gains.

Off-line:

(1) Choose a sequence of states $x_i, i = 1, 2, ..., N$. For each x_i , solve the optimization problem in Eqs. 9-12 by replacing x(k/k) with x_i in order to obtain the corresponding state feedback gain $K_i = Y_i G_i^{-1}$,

$$\min_{\gamma_{i}, Y_{i}, Q_{i}} \gamma_{i}$$
 (9) s.t.
$$\begin{bmatrix} 1 & * \\ x_{i} & Q_{i} \end{bmatrix} \geq 0,$$
 (10)
$$\begin{bmatrix} Q_{i} & * & * & * \\ A_{j}Q_{i} + B_{j}Y_{i} & Q_{i} & * & * \\ \Theta^{\frac{1}{2}}Q_{i} & 0\gamma_{i}I & * \\ R^{\frac{1}{2}}Y_{i} & 0 & 0 & \gamma_{i}I \end{bmatrix} \geq 0,$$
 (11)
$$\begin{bmatrix} X & * \\ Y_{i}^{T} & Q_{i} \end{bmatrix} \geq 0, X_{hh} \leq u_{h,\max}^{2}, h = 1, 2, ..., n_{u}.$$
 (12)

 x_i is chosen such that $Q_{i+1}^{-1}\subset Q_i^{-1}$. Moreover, for each $i\neq N$, the following inequality must be satisfied

 $Q_i^{-1}-(A_j+B_jK_{i+1})^TQ_i^{-1}(A_j+B_jK_{i+1})\geq 0, \forall j=1,2,...,L$ to assure robust stability satisfaction of a convex combination between K_i and K_{i+1} . The state feedback gains are derived based on the minimization of upper bound of infinite horizon worst-case performance proposed by (Kothare et al., 1996). However, the output constraints are not taken into account here in order to enlarge the stabilizable region. The ouput constraints are then properly handled in the

- (2) Given the state feedback gains $K_i = Y_i Q_i^{-1}, i = 1, 2, ..., N$ previously calculated from step 1. For each K_i , the corresponding polyhedral invariant set $S_i =$ (a) Set $M_i = [C^T, -C^T, K_i^T, -K_i^T]^T$, $d_i = [y_{\max}^T, y_{\min}^T, u_{\max}^T, u_{\min}^T]^T$ and m = 1. (b) Select row m from (M_i, d_i) and check $\forall j$ whether
 - $M_{i,m}(A_j + B_j K_i)x \leq d_{i,m}$ by solving the following problem 13:

$$\max_{T} W_{i,m,j} \tag{13}$$

$$\max_{x} W_{i,m,j}$$
(1)
s.t. $W_{i,m,j} = M_{i,m} (A_j + B_j K_i) x - d_{i,m},$ (1)

$$M_i x \le d_i. \tag{15}$$

If $W_{i,m,j} \geq 0$, the constraint $M_{i,m}(A_j + B_j K_i)x \leq$ $d_{i,m}$ is non-redundant with respect to (M_i, d_i) , then, add non-redundant constraints to (M_i, d_i) by assigning $M_i = [M_i^T, (M_{i,m}(A_j + B_jK_i))^T]^T$ and $d_i = [d_i^T, d_{i,m}^T]^T$. (c) Let m = m + 1 and return to step (b). If m

is strictly larger than the number of rows in (M_i, d_i) , the algorithm is stopped.

On-line: The real-time state feedback gain is calculated by linear interpolation between the pre-computed state feedback gains. Three interpolation algorithms are proposed.

Algorithm 1: In the first algorithm, the pre-computed state feedback gains $K_i = 1, 2, ..., N$ are interpolated in order to get the largest possible state feedback gain while robust stability is still guaranteed. At each control iteration, when $x(k) \in S_i$ and $x(k) \notin S_{i+1}, \forall i \leq N-1$, the real-time state feedback gain $K(k) = \lambda(k)\overline{K_i} + (1 - k)\overline{K_i}$ $\lambda(k)K_{i+1}$ can be obtained by solving the problem in Eqs. 16-20.

$$\min_{\lambda(k)} \lambda(k) \tag{16}$$

s.t.
$$M_i \sum_{j=1}^{L} p_j(k) (A_j + B_j K(k)) x(k) - d_i \le 0,$$
 (17)

$$|K(k)x(k)_h| \le u_{h,\max}, h = 1, 2, ..., n_u,$$
 (18)

$$K(k) = \lambda(k)K_i + (1 - \lambda(k))K_{i+1}, \tag{19}$$

$$0 \le \lambda \le 1. \tag{20}$$

If $x(k) \in S_N$, the real-time state feedback gain is K_N .

 K_{i+1} is always larger than K_i because input and output constraints impose less limit on the state feedback gain as i increases. Thus, the largest possible state feedback gain can be obtained by minimizing $\lambda(k)$, while robust stability is still guaranteed by Eq. 17. The input constraint is guaranteed by Eq. 18. The output constraint does not need to be incorporated into the problem formulation because the satisfaction of Eq. 17 also guarantees output constraint satisfaction. The optimization problem involved is formulated as a linear programming and the number of constraints is independent of the number of vertices of the polytope Ω .

Algorithm 2: The real-time state feedback gain is obtained by minimizing the violation of the contraints $(\gamma(k))$ of the adjacent inner invariant sets, so the real-time state feedback gain calculated has to regulate the state from the current invariant set to the adjacent inner invariant set as fast as possible. At each control iteration, when $x(k) \in S_i$ and $x(k) \notin S_{i+1}, \forall i \leq N-1$, the real-time state feedback gain $K(k) = \lambda(k)K_i + (1 - \lambda(k))K_{i+1}$ can be obtained by solving the optimization problem in Eqs. 21-26.

$$\min_{\lambda(k),\gamma(k)} \gamma(k) \tag{21}$$

s.t.
$$M_i \sum_{j=1}^{L} p_j(k) (A_j + B_j K(k)) x(k) - d_i \le 0,$$
 (22)

$$M_{i+1} \sum_{j=1}^{L} p_j(k) (A_j + B_j K(k)) x(k) - d_{i+1} \le \gamma(k),$$

$$|K(k)x(k)_h| \le u_{h,\text{max}}, h = 1, 2, ..., n_u,$$
 (24)

(23)

$$K(k) = \lambda(k)K_i + (1 - \lambda(k))K_{i+1},$$
 (25)

$$0 \le \lambda \le 1. \tag{26}$$

If $x(k) \in S_N$, the real-time state feedback gain is K_N .

By minimizing $\gamma(k)$, the real-time state feedback gain calculated has to regulate the state from the current invariant set to the adjacent inner invariant set as fast as possible. Robust stability as well as output constraint satisfaction are guaranteed by Eq. 22. The input constraint is guaranteed by Eq. 24. The optimization problem involved is formulated as a linear programming and the number of constraints is independent of the number of vertices of the polytope Ω . However, the number of constraints involved is larger than that of algorithm 1.

Algorithm 3: In the last algorithm, the real-time state feedback gain is obtained by minimizing the upper bound of infinite horizon worst case performance cost, which is estimated by Lyapunov function at current state, with subjected to a set of constraints associated with current invariant set. At each control iteration, when $x(k) \in S_i$ and $x(k) \notin S_{i+1}, \forall i \leq N-1$, the real-time state feedback gain $K(k) = \lambda(k)K_i + (1 - \lambda(k))K_{i+1}$ can be obtained by solving the optimization problem in Eqs. 27-32.

$$\min_{\lambda(k),\gamma(k)} \gamma(k) \tag{27}$$

s.t.
$$M_i \sum_{j=1}^{L} p_j(k) (A_j + B_j K(k)) x(k) - d_i \le 0,$$
 (28)

$$\begin{bmatrix} \gamma(k) & x(k)^T \\ x(k) & Q_i \end{bmatrix} \ge 0, \tag{29}$$

$$|K(k)x(k)_h| \le u_{h,\text{max}}, h = 1, 2, ..., n_u,$$
 (30)

$$K(k) = \lambda(k)K_i + (1 - \lambda(k))K_{i+1}, \tag{31}$$

$$0 \le \lambda \le 1. \tag{32}$$

If $x(k) \in S_N$, the real-time state feedback gain is K_N .

By minimizing $\gamma(k)$, the real-time state feedback gain calculated has to regulate the system by using the minimum infinite horizon worst case performance cost. Robust stability and output constraint satisfaction are guaranteed by Eq. 28. The input constraint is guaranteed by Eq. 30. The optimization problem involved is formulated as a convex optimization involving linear matrix inequalities (LMIs) and the number of constraints is independent of the number of vertices of the polytope Ω .

4. CASE STUDY

In this section, we present an example that illustrates the implementation of the proposed robust MPC algorithms. The numerical simulations have been performed in 2.3 GHz Intel Core i-5 with 16 GB RAM, using SDPT3(Tütüncü et al., 2003), Gurobi(Gurobi Optimization, 2012) and YALMIP (Löfberg, 2004) within Matlab R2011b environment. We will consider the application of our approach to the nonlinear two-tank system (Angeli et al., 2000), which is described by Eqs. 33-34.

$$\rho s_1 \dot{h_1} = -\rho a_1 \sqrt{2gh_1} + u, \tag{33}$$

$$\rho s_2 h_2 = \rho a_1 \sqrt{2gh_1} - \rho a_2 \sqrt{2gh_2}. \tag{34}$$

Where h_1 is the water level in tank 1, h_2 is the water level in tank 2 and u is the water flowrate. The operating parameters are shown in table 1.

Table 1. The parameters of two-tank system

| Parameters | Value |
|------------|-------------------------|
| s_1 | 2500 cm^2 |
| s_2 | $1600 \; {\rm cm}^2$ |
| a_1 | 9 cm^2 |
| a_2 | $4 \mathrm{~cm^2}$ |
| g | 980 cm/s^2 |
| ho | 0.001 kg/cm^3 |
| $h_{1,eq}$ | $14~\mathrm{cm}$ |
| $h_{2,eq}$ | 70 cm |

Let $\bar{h_1} = h_1 - h_{1,eq}$, $\bar{h_2} = h_2 - h_{2,eq}$ and $\bar{u} = u - u_{eq}$. Subscript eq denotes the corresponding variable at equilibrium condition. The objective is to regulate $\bar{h_2}$ to the origin by manipulating \bar{u} . The input constraint are symmetic $\bar{u} \leq 1.5 \text{kg/s}$. In contrast, asymmetric output constraints $-13 \leq h_1 \leq 71$, and $-69 \leq \bar{h_2} \leq 29$ are considered.

By evaluating the Jacobian matrix of Eqs. 33 and 34 along the vertices of the constraints set, the solutions of Eqs. 33 and 34 are also the solution of the following differential inclusion

$$\begin{bmatrix}
\rho s_1 \dot{\bar{h_1}} \\
\rho s_2 \dot{\bar{h_2}}
\end{bmatrix} \in \sum_{i=1}^4 p_j A_j \begin{bmatrix} \bar{h_1} \\ \bar{h_2} \end{bmatrix} + \begin{bmatrix} 1 \\ 0 \end{bmatrix} \bar{u}, \tag{35}$$

where A_j , j = 1, ..., 4 are given by

$$A_{1} = \begin{bmatrix} -\rho a_{1} \sqrt{\frac{2g}{h_{1,\min}}} & 0 \\ \rho a_{1} \sqrt{\frac{2g}{h_{1,\min}}} & -\rho a_{2} \sqrt{\frac{2g}{h_{2,\min}}} \end{bmatrix}, \\ A_{2} = \begin{bmatrix} -\rho a_{1} \sqrt{\frac{2g}{h_{1,\max}}} & 0 \\ \rho a_{1} \sqrt{\frac{2g}{h_{1,\max}}} & -\rho a_{2} \sqrt{\frac{2g}{h_{2,\min}}} \end{bmatrix}, \\ A_{3} = \begin{bmatrix} -\rho a_{1} \sqrt{\frac{2g}{h_{1,\min}}} & 0 \\ \rho a_{1} \sqrt{\frac{2g}{h_{1,\min}}} & -\rho a_{2} \sqrt{\frac{2g}{h_{2,\max}}} \end{bmatrix}, \\ A_{4} = \begin{bmatrix} -\rho a_{1} \sqrt{\frac{2g}{h_{1,\max}}} & 0 \\ \rho a_{1} \sqrt{\frac{2g}{h_{1,\max}}} & 0 \\ \rho a_{1} \sqrt{\frac{2g}{h_{1,\max}}} & -\rho a_{2} \sqrt{\frac{2g}{h_{2,\max}}} \end{bmatrix}, \end{cases}$$
(36)

and p_i , j = 1, ..., 4 are given by

$$p_{1} = \left[\frac{\frac{1}{\sqrt{h_{1,\max}}} - \frac{1}{\sqrt{h_{1}}}}{\frac{1}{\sqrt{h_{1,\max}}} - \frac{1}{\sqrt{h_{1}}}}\right] \left[\frac{\frac{1}{\sqrt{h_{2,\max}}} - \frac{1}{\sqrt{h_{2}}}}{\frac{1}{\sqrt{h_{2,\max}}} - \frac{1}{\sqrt{h_{2,\min}}}}\right],$$

$$p_{2} = \left[\frac{\frac{1}{\sqrt{h_{1}}} - \frac{1}{\sqrt{h_{1,\min}}}}{\frac{1}{\sqrt{h_{1,\min}}} - \frac{1}{\sqrt{h_{1,\min}}}}\right] \left[\frac{\frac{1}{\sqrt{h_{2,\max}}} - \frac{1}{\sqrt{h_{2}}}}{\frac{1}{\sqrt{h_{2,\min}}} - \frac{1}{\sqrt{h_{2,\min}}}}\right],$$

$$p_{3} = \left[\frac{\frac{1}{\sqrt{h_{1,\max}}} - \frac{1}{\sqrt{h_{1,\min}}}}{\frac{1}{\sqrt{h_{1,\min}}} - \frac{1}{\sqrt{h_{1,\min}}}}\right] \left[\frac{\frac{1}{\sqrt{h_{2,\max}}} - \frac{1}{\sqrt{h_{2,\min}}}}{\frac{1}{\sqrt{h_{2,\min}}} - \frac{1}{\sqrt{h_{2,\min}}}}\right],$$

$$p_{4} = \left[\frac{\frac{1}{\sqrt{h_{1,\max}}} - \frac{1}{\sqrt{h_{1,\min}}}}{\frac{1}{\sqrt{h_{1,\min}}} - \frac{1}{\sqrt{h_{1,\min}}}}\right] \left[\frac{\frac{1}{\sqrt{h_{2,\max}}} - \frac{1}{\sqrt{h_{2,\min}}}}{\frac{1}{\sqrt{h_{2,\min}}} - \frac{1}{\sqrt{h_{2,\min}}}}\right].$$

$$(37)$$

The discrete-time model is obtained by discretization of Eq.35 using Euler first-order approximation with a sampling period of 0.1 s and it is omitted here for brevity. The proposed algorithm will be compared with an off-line RMPC algorithm based on polyhedral invariant set without interpolation(Bumroongsri and Kheawhom, 2012b). The tuning parameters are $\Theta = \begin{bmatrix} 0 & 1 \\ 0 & 1 \end{bmatrix}$ and R = 0.01.

A sequence of four polyhedral invariant sets is constructed. Figure 1 shows the polyhedral invariant sets constructed. As the output constraints considered in this case are not symmetric. It affects the constructed polyhedral invariant sets of S_1 and S_2 . Thus, these two invariant sets are also asymmetric.

Figure 2 shows the regulated output $(\bar{h_2})$. The RMPC without interpolation gives the slowest response, because the real-time state feedback gain used is an approximation of optimal state feedback gain. For instance, if we start from an initial state $x(k) \in S_i$ but $x(k) \notin S_{i+1}$, a state feedback gain K_i is implemented. The system is driven to x(k+1), where |x(k+1)| < |x(k)|. If $x(k+1) \in S_i$ but $x(k+1) \notin S_{i+1}$, K_i is still used as a state feedback gain. We see that |u(k+1)| < |u(k)|, as |x(k+1)| < |x(k)|. In

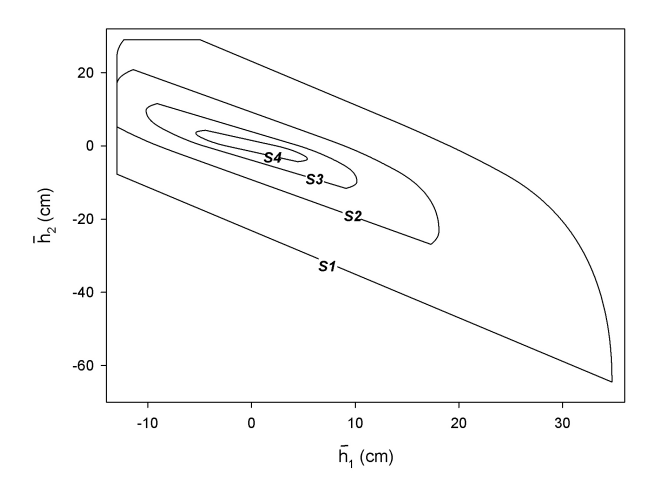


Fig. 1. The constructed polyhedral invariant sets.

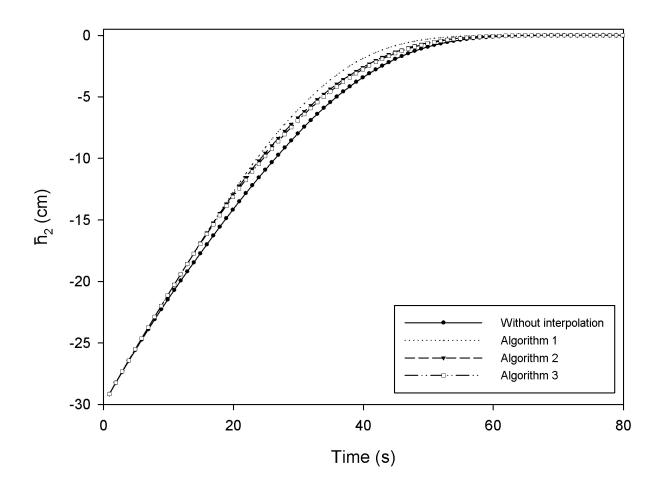


Fig. 2. Regulated output of the nonlinear two-tank system.

other words, this algorithm implements the state feedback gain K_i for the whole region $x(k) \in S_i$ but $x(k) \notin S_{i+1}$.

By using interpolation, we can achieve better control performance. For each $x(k) \in S_i$ but $x(k) \notin S_{i+1}$, a state feedback gain K(k) obtained by solving a simple optimization problem is implemented. We see that $K(k) \neq K_i$. Thus, a preferable control performance can be obtained.

Algorithm 1 yields the best control performance. In comparison, algorithms 2 and 3 give similar responses being slower than that of algorithm 1. In algorithm 1, the precomputed state feedback gains are interpolated to get the largest possible real-time state feedback gain, so algorithm 1 tends to produce fastest responses. In algorithm 2, the violation of the contraints of the adjacent inner invariant sets is minimized. Thus, a state feedback gain obtained from algorithm 2 leads to the shortest path to the inner adjacent invariant set. However, the shortest path to the inner adjacent invariant set does not guarantee the smallest worst case performance cost. Algorithm 3 minimizes the upper bound of infinite horizon worst case performance cost, which is estimated by Lyapunov function at current state. Unfortunately, Lyapunov function at each state is not determined on-line. Thus, Lyapunov function

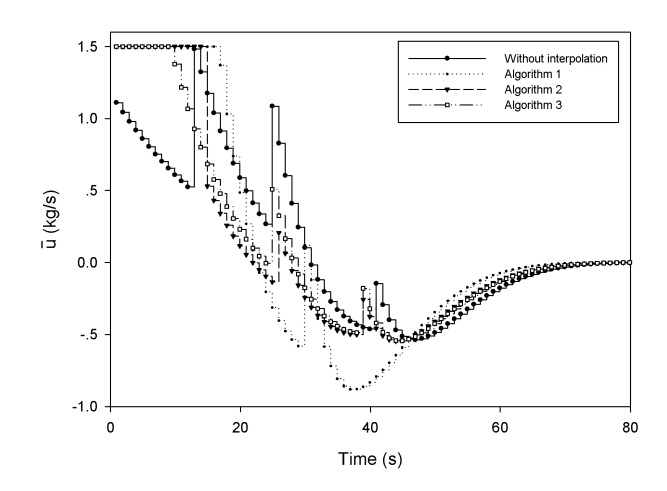


Fig. 3. Control input of the nonlinear two-tank system.

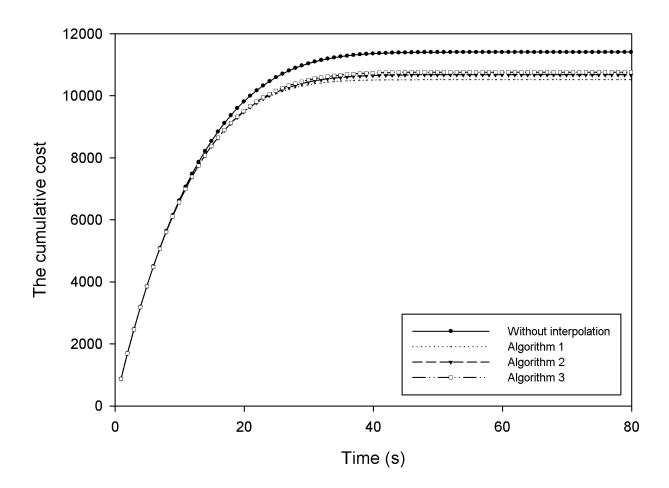


Fig. 4. The cumulative cost $\sum_{i=0}^{t} x(i)^T \Theta x(i) + u(i)^T R u(i)$.

obtained off-line is used. That is for each $x(k) \in S_i$ but $x(k) \notin S_{i+1}$, Lyapunov function Q_i^{-1} is used for the whole region. Therefore, algorithm 3 becomes more conservative than algorithm 1.

Figure 3 shows the profiles of control input \bar{u} . The input discontinuities appeared in the response of the RMPC without interpolation are caused by the switching of feedback gains based on the distance between the state and the origin. In comparison, we can overcome this issue by using the interpolation algorithms proposed.

Figure 4 shows the cumulative performance cost. The cumulative performance costs of RMPC with interpolation are lower than the cumulative cost of the RMPC without interpolation. The lowest cumulative performance cost is obtained by using algorithm 1.

Table 2. The on-line computational burdens

| Algorithm | On-line CPU time(s)/step |
|-----------------------|--------------------------|
| Without interpolation | < 0.0001 |
| Algorithm 1 | 0.0001 |
| Algorithm 2 | 0.0001 |
| Algorithm 3 | 0.1800 |

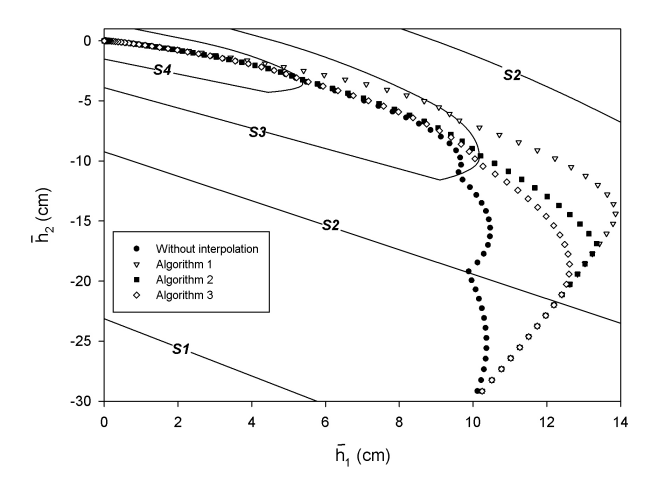


Fig. 5. State trajectories from initial condition of $(\bar{h_1}, \bar{h_2}) = (10, -30)$ to the origin.

Figure 5 shows state trajectories from initial condition of $(\bar{h}_1, \bar{h}_2) = (10, -30)$ to the origin. Algorithm 1 produces the trajectory with lowest control performance cost.

The on-line computational burdens are shown in table 2. For all algorithms, most of the computational burdens are moved off-line so the on-line computation is tractable. The optimization problem involved in each interpolation algorithm is independent of the number of vertices of the polytope Ω . Algorithms 1 and 2 use a linear programming. The number of constraints involved in algorithm 1 is lower than that of algorithm 2. In contrat, algorithm 3 uses a convex optimization involving LMIs. Thus, algorithm 3 requires higher computational time compared with other algorithms.

5. CONCLUSIONS

In this paper, we have presented an interpolation-based RMPC algorithms using polyhedral invariant sets for LPV systems. The proposed algorithms computes off-line a sequence of polyhedral invariant sets. The real-time control law is then calculated by interpolation between the two state feedback gains corresponding to two adjacent polyhedral invariant sets. Three interpolation algorithms are proposed. The controller design is illustrated with a case study of nonlinear two-tank system. The simulation results showed that the proposed RMPC with interpolation provides a better control performance while on-line computation is still tractable.

ACKNOWLEDGEMENTS

This work was supported by Rajadapisek Sompoj Fund, Chulalongkorn University Centenary Academic Development Project, and the Thailand Research Fund (TRF).

REFERENCES

Angeli, D., Casavola, A., and Mosca, E. (2000). Constrained predictive control of nonlinear plants via polytopic linear system embedding. *Int. J. Robust Nonlin.*, 10, 1091–1103.

Bumroongsri, P. and Kheawhom, S. (2012a). An ellipsoidal off-line model predictive control strategy for linear parameter varying systems with applications in chemical processes. *Syst. Control Lett.*, 61, 435–442.

Bumroongsri, P. and Kheawhom, S. (2012b). An off-line robust mpc algorithm for uncertain polytopic discrete-time systems using polyhedral invariant sets. *J. Process Contr.*, 22, 975–983.

Bumroongsri, P. and Kheawhom, S. (2013). An interpolation-based robust mpc algorithm using polyhedral invariant sets. In *Proceedings of the 2013 European Control Conference (ECC)*, 3161–3166.

Gurobi Optimization, I. (2012). Gurobi optimizer reference manual. URL http://www.gurobi.com.

Kheawhom, S. and Bumroongsri, P. (2013). Constrained robust model predictive control based on polyhedral invariant sets by off-line optimization. *Chemical Engineering Transactions*, 32, 1417–1442. doi: 10.3303/CET1332237.

Kothare, M., Balakrishnan, V., and Morari, M. (1996). Robust constrained model predictive control using linear matrix inequalities. *Automatica*, 32, 1361–1379.

Löfberg, J. (2004). Yalmip: A toolbox for modeling and optimization in matlab. In *Proc. IEEE international symposium on computer aided control systems design*, 284–289.

Lu, Y. and Arkun, Y. (2000). Quasi-min-max mpc algorithms for lpv systems. *Automatica*, 36, 527–540.

Morari, M. and Lee, J. (1999). Model predictive control: past, present and future. *Comput. Chem. Eng.*, 23, 667–682.

Paijmans, B., Symens, W., Brussel, H., and Swevers, J. (2008). Experimental identification of affine lpv models for mechatronic systems with one varying parameter. *Eur. J. Contr.*, 14, 16–29.

Pluymers, P., Rossiter, J., Suykens, J., and Moore, B. (2005). The efficient computation of polyhedral invariant sets for linear systems with polytopic uncertainty. In *Proc. of the American Control Conference*, 804–809.

Tütüncü, R., Toh, K., and Todd, M. (2003). Solving semidefinite-quadratic-linear programs using sdpt3. *Math. Prog. Series B*, 95, 189–217.

Wada, N., Saito, K., and Saeki, M. (2006). Model predictive control for linear parameter varying systems using parameter dependent lyapunov function. *IEEE T. Circuits Syst.*, 53, 1446–1450.



Interpolation-based Off-line MPC for LPV systems

P. Bumroongsri^{a,b}, S. Kheawhom^{a,*}

^aComputational Process Engineering, Department of Chemical Engineering, Faculty of Engineering, Chulalongkorn University, Bangkok, 10330, Thailand (e-mail: soorathep.k@chula.ac.th).
 ^bDepartment of Chemical Engineering, Faculty of Engineering, Mahidol University, Nakhon Pathom, 73170 Thailand (e-mail: pornchai.bum@mahidol.ac.th).

Abstract: Interpolation-based off-line MPC for LPV systems is presented in this work. The on-line computational time is reduced by pre-computing off-line the sequences of state feedback gains corresponding to the sequences of ellipsoidal invariant sets. At each sampling time, the real-time state feedback gain is calculated by linear interpolation between the pre-computed state feedback gains. Four interpolation techniques are presented. In the first technique, the smallest ellipsoid containing the current state measured is approximated and the corresponding real-time state feedback gain is calculated. In the second technique, the pre-computed state feedback gains are interpolated in order to get the largest possible real-time state feedback gain while robust stability is still guaranteed. In the third technique, the real-time state feedback gain is calculated by minimizing the violation of the constraints of the adjacent inner ellipsoids so the real-time state feedback gain calculated has to regulate the state from the current ellipsoids to the adjacent inner ellipsoids as fast as possible. In the last technique, the real-time state feedback gain is calculated by minimizing the one-step cost function so the real-time state feedback gain calculated has to regulate the next predicted state to the origin as fast as possible. A case study of nonlinear CSTR is presented to illustrate the implementation of the proposed techniques. The results show that the proposed interpolation techniques 2, 3 and 4 tend to produce less sluggish responses than the technique 1.

Keywords: Off-line MPC, LPV systems, Interpolation techniques.

1. INTRODUCTION

Model predictive control (MPC) has originated in the industries as an effective control algorithm to solve multivariable control problem. Although MPC based on a linear model has been successfully implemented in many industrial applications, it is well-known that the stability of MPC based on a linear model cannot be guaranteed in the presence of process nonlinearity (Morari and Lee, 1999). This has motivated the synthesis of MPC using linear parameter varying (LPV) model whose dynamics depend on the scheduling parameter that can be measured on-line (Lu and Arkun, 2000).

Wada et al. (2006) proposed on-line MPC for LPV systems using parameter-dependent Lyapunov function. At each sampling instant, the ellipsoidal invariant set containing the measured state is constructed so robust stability is guaranteed. Since the optimization problem has to be solved on-line at each sampling instant, the algorithm requires a relatively high computational effort.

Some researchers have proposed a dual-mode MPC for LPV systems (Casavola et al., 2002; Bumroongsri and Kheawhom, 2012a). The control law has the form u = Kx + c for the first N steps and u = Kx for the rest of the infinite horizon. Although the degrees of freedom are increased, larger on-line

computational time is required because the size of on-line optimization problem grows significantly with respect to N.

In order to reduce on-line computational time, off-line formulation of MPC have been proposed (Wan and Kothare, 2003; Bumroongsri and Kheawhom, 2012c). A sequence of state feedback gains corresponding to a sequence of invariant sets is pre-computed off-line. At each sampling instant, the real-time state feedback gain is calculated by linear interpolation between the pre-computed state feedback gains. Although the on-line computational time is significantly reduced, the conservativeness can be obtained in control of LPV systems because the scheduling parameter is not included in the controller design.

Off-line MPC for LPV systems was proposed by Bumroongsri and Kheawhom (2012b). The sequences of state feedback gains corresponding to the sequences of ellipsoids are pre-computed off-line. At each sampling instant, the scheduling parameter is measured and the smallest ellipsoid containing the measured state is approximated. The corresponding real-time state feedback gain is then calculated by linear interpolation between the pre-computed state feedback gains. The ellipsoid computed at each sampling instant is only an approximation so the algorithm sacrifices optimality in order to reduce on-line computational time. To improve the control performances of off-line MPC algorithm, an interpolation technique has been introduced (Kheawhom

and Bumroongsri, 2013; Bumroongsri and Kheawhom, 2013.)

In this paper, interpolation-based off-line MPC for LPV systems is presented. Four interpolation techniques based on different ideas are proposed. The aim is to develop new interpolation techniques that can achieve good control performance while robust stability is still guaranteed.

The paper is organized as follows. In section 2, the problem description is presented. In section 3, interpolation-based off-line MPC for LPV systems is presented. In section 4, we present an example to illustrate the implementation of the proposed techniques. Finally, in section 5, we conclude the paper.

Notation: For a matrix A, A^T denotes its transpose, A^{-1} denotes its inverse. I denotes the identity matrix. For a vector x, x(k/k) denotes the state measured at real time k, x(k+i/k) denotes the state at prediction time k+i predicted at real time k. The symbol * denotes the corresponding transpose of the lower block part of symmetric matrices.

2. PLOBLEM DESCRIPTION

The model considered here is the following discrete-time LPV system:

$$x(k+1) = A(p(k))x(k) + Bu(k)$$

$$y(k) = Cx(k)$$
 (1)

where x(k) is the state of the plant and u(k) is the control input. We assume that the scheduling parameter p(k) is measurable on-line at each sampling time. Moreover, we assume that

$$A(p(k)) \in \Omega, \ \Omega = Co\{A_1, A_2, \dots, A_L\}$$
 (2)

where Ω is the polytope, Co denotes the convex hull, A_j are the vertices of the convex hull. Any A(p(k)) within the polytope Ω is a linear combination of the vertices such that

$$A(p(k)) = \sum_{j=1}^{L} p_j(k) A_j, \sum_{j=1}^{L} p_j(k) = 1, 0 \le p_j(k) \le 1$$
 (3)

The aim of this research is to find the state feedback control law

$$u(k) = K(p(k))x(k) \tag{4}$$

that stabilizes (1) and satisfies the input and output constraints

$$|u_h(k+i/k)| \le u_{h \max}, h = 1, 2, 3, ..., n_u$$
 (5)

$$|y_r(k+i/k)| \le y_{r,\text{max}}, r = 1,2,3,...,n_y$$
 (6)

Wada et al. (2006) proposed on-line MPC for LPV systems using parameter-dependent Lyapunov function. At each sampling instant, the state feedback control law which minimizes the upper bound γ on the following worst-case performance cost

$$\min_{u(k+i/k)} \max_{A(p(k+i)) \in \Omega, i \ge 0} J_{\infty}(k)$$

$$J_{\infty}(k) = \sum_{i=0}^{\infty} \begin{bmatrix} x(k+i/k) \\ u(k+i/k) \end{bmatrix}^{T} \begin{bmatrix} \Theta & 0 \\ 0 & R \end{bmatrix} \begin{bmatrix} x(k+i/k) \\ u(k+i/k) \end{bmatrix}$$
 (7)

where Θ and R are weighting matrices, and asymptotically stabilizes the discrete-time LPV system (1) is given by

$$u(k) = K(p(k))x(k), K(p(k)) = \sum_{j=1}^{L} p_j(k)K_j, K_j = Y_jG_j^{-1}$$
 where

 Y_i and G_i are obtained by solving the following problem

$$\min_{\gamma, Y_i, G_i, Q_i} \gamma \tag{8}$$

s.t.
$$\begin{bmatrix} 1 & x(k/k)^T \\ x(k/k) & Q_j \end{bmatrix} \ge 0, \forall j = 1,2,3,...,L$$
 (9)

$$\begin{bmatrix} G_{j} + G_{j}^{T} - Q_{j} & * & * & * \\ A_{j}G_{j} + BY_{j} & Q_{l} & * & * \\ \frac{1}{\Theta^{2}}G_{j} & 0 & \gamma I & * \\ \frac{1}{R^{2}}Y_{j} & 0 & 0 & \gamma I \end{bmatrix} \geq 0,$$

$$\forall j = 1, 2, 3, \dots, L, \ \forall l = 1, 2, 3, \dots, L$$

$$(10)$$

$$\begin{bmatrix} X & Y_j \\ Y_j^T & G_j + G_j^T - Q_j \end{bmatrix} \ge 0,$$

$$\forall j = 1, 2, 3, ..., L, \ X_{hh} \le u_{h, \text{max}}^2, \ h = 1, 2, 3, ..., n_u$$
(11)

$$\begin{bmatrix} S & * \\ (A_j G_j + BY_j)^T C^T & G_j + G_j^T - Q_j \end{bmatrix} \ge 0,$$

$$\forall j = 1, 2, 3, ..., L, S_{rr} \le y_{r, \max}^2, r = 1, 2, 3, ..., n_y$$
(12)

Since the optimization problem has to be solved on-line at each sampling instant, the algorithm requires a relatively high computational effort.

3. INTERPOLATION-BASED OFF-LINE MPC

In this section, interpolation-based off-line MPC for LPV systems is presented. The sequences of state feedback gains

 $K_{i,j}$ corresponding to the sequences of ellipsoids $\varepsilon_{i,j} = \left\{ x/x^T Q_{i,j}^{-1} x \leq 1 \right\}$ are pre-computed off-line where i=1,2,3,...,N denote the number of ellipsoids in each sequence and j=1,2,3,...,L denote the vertices of the polytope Ω . At each sampling time, the real-time state feedback gain is calculated by linear interpolation between the pre-computed state feedback gains.

3.1 Interpolation-based off-line MPC

Off-line: Choose a sequence of states x_i , i = 1,2,3,...,N. For each x_i , substitute x(k/k) in (9) by x_i and solve the optimization problem (8) to obtain the corresponding state feedback gain $K_{i,j} = Y_{i,j}G_{i,j}^{-1}$ and ellipsoids $\varepsilon_{i,j} = \left\{x/x^TQ_{i,j}^{-1}x \le 1\right\}$. Note that x_i should be chosen such that $\varepsilon_{i+1,j} \subset \varepsilon_{i,j}$. Moreover, for each $i \ne N$, the inequality $Q_{i,j}^{-1} - (A_j + BK_{i+1,j})^TQ_{i,l}^{-1}(A_j + BK_{i+1,j}) > 0$, $\forall j = 1,2,3,...,L$, $\forall l = 1,2,3,...,L$ must be satisfied.

On-line: The real-time state feedback gain is calculated by linear interpolation between the pre-computed state feedback gains. Four interpolation techniques are proposed as follows

Technique 1: (Bumroongsri and Kheawhon, 2012b) The first technique is based on an approximation of the smallest ellipsoid containing the measured state. At each sampling time, when x(k) satisfies $x(k) \in \varepsilon_{i,j}$, $x(k) \notin \varepsilon_{i+1,j}$, $\forall j = 1,2,3,...,L$, $i \neq N$, the real-time state feedback gain

$$K(\lambda(k)) = \lambda(k) \left[\sum_{j=1}^{L} p_{j}(k) K_{i,j} \right] + (1 - \lambda(k)) \left[\sum_{j=1}^{L} p_{j}(k) K_{i+1,j} \right]$$

can be calculated from $\lambda(k) \in (0,1]$ obtained by solving

$$x(k)^{T} (\lambda(k) [\sum_{j=1}^{L} p_{j}(k) Q_{i,j}^{-1}] + (1 - \lambda(k)) [\sum_{j=1}^{L} p_{j}(k) Q_{i+1,j}^{-1}]) x(k) = 1$$
(13)

It is seen that $\lambda(k) = 0$ and $\lambda(k) = 1$ correspond to the ellipsoids $\mathcal{E}_{i+1,j}$ and $\mathcal{E}_{i,j}$, respectively. In this technique, no optimization problem is needed to be solved on-line. Figure 1 shows the graphical representation of the state feedback gain in each prediction horizon. It is seen that the state feedback gain $K(\lambda(k))$ is implemented throughout the prediction horizon. Thus, the state must be restricted to lie in the smallest ellipsoid approximated by (13) and robust stability is guaranteed.

Technique 2: In the second technique, the pre-computed state feedback gains $K_{i,j}$ are interpolated in order to get the largest possible real-time state feedback gain while robust stability is still guaranteed. At each sampling time, when x(k) satisfies $x(k) \in \varepsilon_{i,j}$, $x(k) \notin \varepsilon_{i+1,j}$, $\forall j = 1,2,3,...,L$,

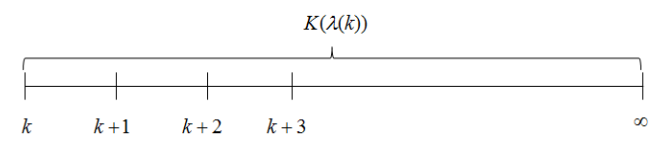


Fig.1. The graphical representation of the state feedback gain in each prediction horizon of technique 1.

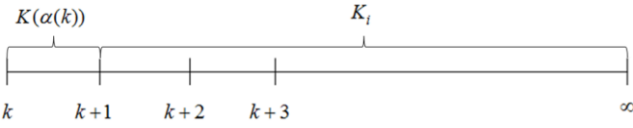


Fig.2. The graphical representation of the state feedback gain in each prediction horizon of technique 2.

$$i \neq N$$
, the real-time state feedback gain
$$K(\alpha(k)) = \alpha(k) [\sum_{j=1}^{L} p_j(k) K_{i,j}] + (1 - \alpha(k)) [\sum_{j=1}^{L} p_j(k) K_{i+1,j}]$$

can be calculated from $\alpha(k)$ obtained by solving the following problem

$$\min \alpha(k)$$
 (14)

s.t.
$$\begin{bmatrix}
1 & ((A(p(k)) + BK(\alpha(k)))x(k))^{T} \\
(A(p(k)) + BK(\alpha(k)))x(k) & Q_{i,j}
\end{bmatrix} \ge 0,$$

$$j = 1,2,3,...,L$$
(15)

$$\begin{bmatrix} u_{h,\max}^2 & * \\ (K(\alpha(k))x(k))_h & 1 \end{bmatrix} \ge 0$$
 (16)

$$0 \le \alpha(k) \le 1 \tag{17}$$

 $K_{i+1,j}$ is always larger than $K_{i,j}$ because input and output constraints impose less limit on the state feedback gain as i increases. Thus, the largest possible real-time state feedback gain $K(\alpha(k))$ can be calculated by minimizing $\alpha(k)$ in (14) while robust stability is still guaranteed by (15). The input constraint is guaranteed by (16).

Figure 2 shows the graphical representation of the state feedback gain in each prediction horizon. It is seen that the largest possible real-time state feedback gain $K(\alpha(k))$ is only implemented at each sampling time k. At time k+1

and so on, the state feedback gain
$$K_i = \sum_{j=1}^{L} p_j(k) K_{i,j}$$
 is

implemented. Thus, the state must be restricted to lie in the ellipsoids $\varepsilon_{i,j}$ and robust stability is guaranteed.

Technique 3: In the third technique, the real-time state feedback gain is calculated by minimizing the violation of the constraints of the adjacent inner ellipsoids so the real-time state feedback gain calculated has to regulate the state from the current ellipsoids $\varepsilon_{i,j}$ to the adjacent inner ellipsoids

$$\begin{split} \varepsilon_{i+1,j} & \text{ as fast as possible. At each sampling time, when } x(k) \\ & \text{ satisfies } \quad x(k) \in \varepsilon_{i,j}, \ x(k) \notin \varepsilon_{i+1,j}, \ \forall j=1,2,3,...,L, \ i \neq N, \quad \text{the real-time} & \text{ state } & \text{feedback } & \text{gain} \\ & K(\delta(k)) = \delta(k) [\sum_{j=1}^L p_j(k) K_{i,j}] + (1-\delta(k)) [\sum_{j=1}^L p_j(k) K_{i+1,j}] \end{split}$$

can be calculated from $\delta(k)$ obtained by solving the following problem.

$$\min \sigma(k)$$
 (18)

s.t. $\begin{bmatrix}
1 + \sigma(k) & ((A(p(k)) + BK(\delta(k)))x(k))^T \\
(A(p(k)) + BK(\delta(k)))x(k) & Q_{i+1,j}
\end{bmatrix} \ge 0,$ j = 1,2,3,...,L(19)

$$\begin{bmatrix} 1 & ((A(p(k)) + BK(\delta(k)))x(k))^{T} \\ (A(p(k)) + BK(\delta(k)))x(k) & Q_{i,j} \end{bmatrix} \ge 0,$$

$$j = 1, 2, 3, ..., L$$
(20)

$$\begin{bmatrix} u_{h,\max}^2 & * \\ (K(\delta(k))x(k))_h & 1 \end{bmatrix} \ge 0$$
 (21)

$$0 \le \delta(k) \le 1 \tag{22}$$

By applying Schur complement to (19), we obtain $x(k+1)^T Q_{i+1,j}^{-1} x(k+1) \le 1 + \sigma(k)$. By minimizing $\sigma(k)$ in (18), the real-time state feedback gain $K(\delta(k))$ calculated has to regulate the state from the current ellipsoids $\varepsilon_{i,j}$ to the adjacent inner ellipsoids $\varepsilon_{i+1,j}$ as fast as possible. Robust stability is guaranteed by (20). The input constraint is guaranteed by (21).

Figure 3 shows the graphical representation of the state feedback gain in each prediction horizon. It is seen that the real-time state feedback gain $K(\delta(k))$ calculated is only implemented at each sampling time k. At time k+1 and so on, the state feedback gain $K_i = \sum_{j=1}^L p_j(k) K_{i,j}$ is

implemented. Thus, the state must be restricted to lie in the ellipsoids $\varepsilon_{i,j}$ and robust stability is guaranteed.

Technique 4: In the last technique, the real-time state feedback gain is calculated by minimizing the one-step cost function so the real-time state feedback gain calculated has to regulate the next predicted state to the origin as fast as possible. At each sampling time, when the measured state x(k) satisfies $x(k) \in \mathcal{E}_{i,j}$, $x(k) \notin \mathcal{E}_{i+1,j}$, $\forall j = 1,2,...,L$, $i \neq N$, the real-time state feedback gain

$$K(\beta(k)) = \beta(k) \left[\sum_{i=1}^{L} p_{j}(k) K_{i,j} \right] + (1 - \beta(k)) \left[\sum_{i=1}^{L} p_{j}(k) K_{i+1,j} \right]$$

can be calculated from $\beta(k)$ obtained by solving the following problem.

$$\min J_{\nu}$$
 (23)

s.t.

$$\begin{bmatrix} J_k & ((A(p(k)) + BK(\beta(k)))x(k))^T \\ (A(p(k)) + BK(\beta(k)))x(k) & \Theta^{-1} \end{bmatrix} \ge 0,$$
(24)

$$\begin{bmatrix} 1 & ((A(p(k)) + BK(\beta(k)))x(k))^{T} \\ (A(p(k)) + BK(\beta(k)))x(k) & Q_{i,j} \end{bmatrix} \ge 0,$$

$$j = 1, 2, ..., L$$
(25)

$$\begin{bmatrix} u_{h,\max}^2 & * \\ (K(\beta(k))x(k))_h & 1 \end{bmatrix} \ge 0$$
 (26)

$$0 \le \beta(k) \le 1 \tag{27}$$

By applying Schur complement to (24), we obtain $J_k \ge x(k+1)^T \Theta x(k+1)$ where Θ is the weighting matrix. Thus, J_k in (23) is the one-step cost function. Robust stability is guaranteed by (25). The input constraint is guaranteed by (26).

Figure 4 shows the graphical representation of the state feedback gain in each prediction horizon. It is seen that the real-time state feedback gain $K(\beta(k))$ calculated is only implemented at each sampling time k. At time k+1 and so on, the state feedback gain $K_i = \sum_{j=1}^{L} p_j(k) K_{i,j}$ is implemented. Thus, the state must be restricted to lie in the ellipsoids $\varepsilon_{i,j}$ and robust stability is guaranteed.

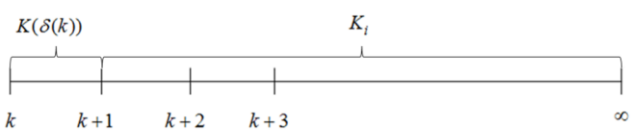


Fig.3. The graphical representation of the state feedback gain in each prediction horizon of technique 3.

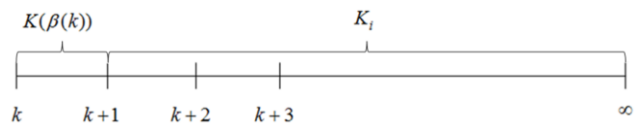


Fig.4. The graphical representation of the state feedback gain in each prediction horizon of technique 4.

4. EXAMPLE

In this section, we present an example that illustrates the implementation of the proposed off-line MPC algorithm. The numerical simulations have been performed in Intel Core i-5 (2.4GHz), 2 GB RAM, using SeDuMi (Sturm, 1998) and YALMIP (Löfberg, 2004) within Matlab R2008a environment. We will consider the application of our approach to the following nonlinear model for CSTR where the consecutive reaction $A \longrightarrow B \longrightarrow C$ takes place

$$\begin{bmatrix} \dot{x}_1 \\ \dot{x}_2 \\ \dot{x}_2 \end{bmatrix} = \begin{bmatrix} -1 - Da_1 & 0 \\ Da_1 & -1 - Da_2 x_2 \end{bmatrix} \begin{bmatrix} x_1 \\ x_2 \end{bmatrix} + \begin{bmatrix} 1 \\ 0 \end{bmatrix} u \quad (28)$$

where x_1 denotes the dimensionless concentration of A and x_2 denotes the dimensionless concentration of B. The control variable u corresponds to the inlet concentration of A. The operating parameters are $Da_1 = 1$ and $Da_2 = 2$.

Let $\bar{x}_1 = x_1 - x_{1,eq}$, $\bar{x}_2 = x_2 - x_{2,eq}$ and $\bar{u} = u - u_{eq}$ where subscript eq is used to denote the corresponding variable at the equilibrium condition, the input and output constraints are given as

$$|x_1| \le 0.5, |x_2| \le 0.5, |u| \le 0.5$$
 (29)

By evaluating the Jacobian matrix of (28) along the vertices of the constraints set (29), we have that all the solutions of (28) are also the solutions of the following differential inclusion

$$\begin{bmatrix} \frac{\cdot}{x_1} \\ \frac{\cdot}{x_2} \\ \frac{\cdot}{x_2} \end{bmatrix} \in \left(\sum_{j=1}^2 p_j A_j \right) \begin{bmatrix} \frac{\cdot}{x_1} \\ \frac{\cdot}{x_2} \end{bmatrix} + \begin{bmatrix} 1 \\ 0 \end{bmatrix} u$$
 (30)

where A_j , j = 1,2 are given by

$$A_{1} = \begin{bmatrix} -1 - Da_{1} & 0 \\ Da_{1} & -1 - Da_{2}x_{2,\text{min}} \end{bmatrix}, A_{2} = \begin{bmatrix} -1 - Da_{1} & 0 \\ Da_{1} & -1 - Da_{2}x_{2,\text{max}} \end{bmatrix}$$
(31)

and p_i , j = 1,2 are given by

$$p_1 = \frac{x_{2,\text{max}} - x_2}{x_{2,\text{max}} - x_{2,\text{min}}}, p_2 = \frac{x_2 - x_{2,\text{min}}}{x_{2,\text{max}} - x_{2,\text{min}}}$$
(32)

The discrete-time model is obtained by discretization of (30) using Euler first-order approximation with a sampling period of 0.1 min and it is omitted here for brevity. The weighting matrices are $\Theta = \begin{bmatrix} 1 & 0 \\ 0 & 1 \end{bmatrix}$ and R = 0.01.

Figure 5 shows two sequences of ellipsoids constructed offline. Each sequence has three ellipsoids $(\varepsilon_{i,j}, i=3, j=2)$. In this example, two sequences of ellipsoids are constructed because the polytope Ω has two vertices.

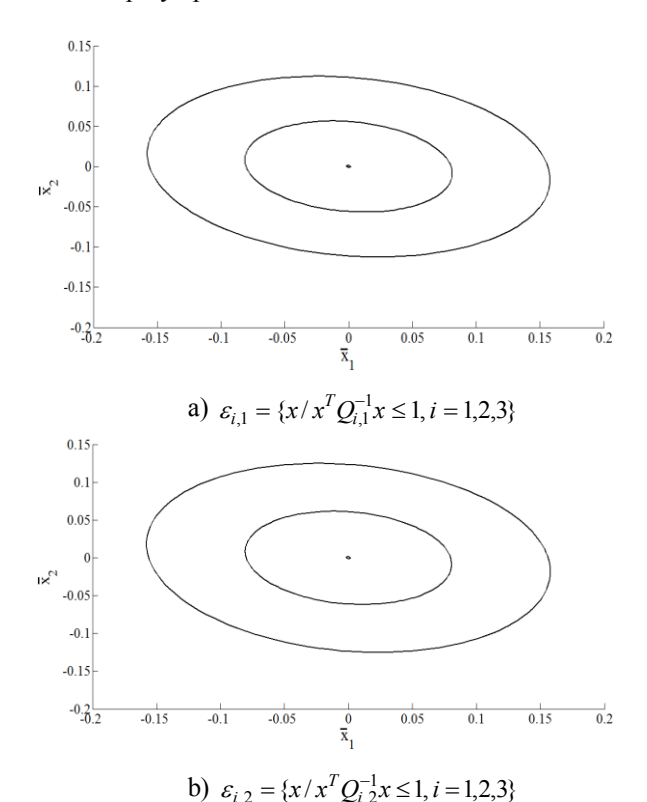
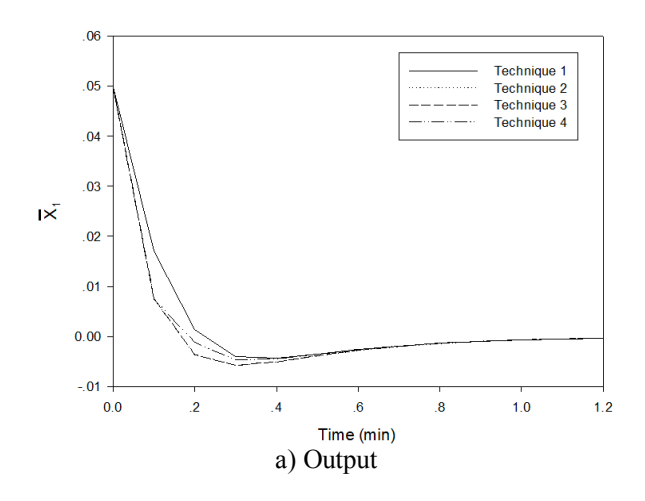


Fig. 5. Two sequences of ellipsoids constructed off-line.

Figure 6 shows the closed-loop responses of the system. In technique 1, the smallest ellipsoid containing the measured state is approximated at each sampling instant and the corresponding real-time state feedback gain is calculated. Since the same real-time state feedback gain $K(\lambda(k))$ is implemented throughout the prediction horizon as shown in Fig. 1, technique 1 tends to produce relatively slow responses compared to other techniques. In technique 2, the precomputed state feedback gains are interpolated in order to get the largest possible real-time state feedback gain $K(\alpha(k))$. At each sampling time, the largest possible real-time state feedback gain is implemented as shown in Fig. 2 so technique 2 tends to produce less sluggish responses than technique 1. In this example, technique 2 gives 0.5% better performance cost (7) compared to technique 1. In technique 3, the real-time state feedback gain is calculated by minimizing the violation of the constraints of the adjacent inner ellipsoids. At each sampling time, the real-time state feedback gain $K(\delta(k))$ is implemented as shown in Fig. 3 so the state has to be regulated from the current ellipsoids $\varepsilon_{i,j}$ to the adjacent inner ellipsoids $\mathcal{E}_{i+1,j}$ as fast as possible. In this example, technique 2 and technique 3 behave almost identically in regulating the output. In technique 4, the realtime state feedback gain is calculated by minimizing the onestep cost function so the real-time state feedback gain calculated has to regulate the next predicted state to the origin as fast as possible. As shown in Fig. 6, technique 4 tends to produce the fastest responses among all techniques. In this example, technique 4 gives 0.6% better performance cost (7) compared to technique 1.



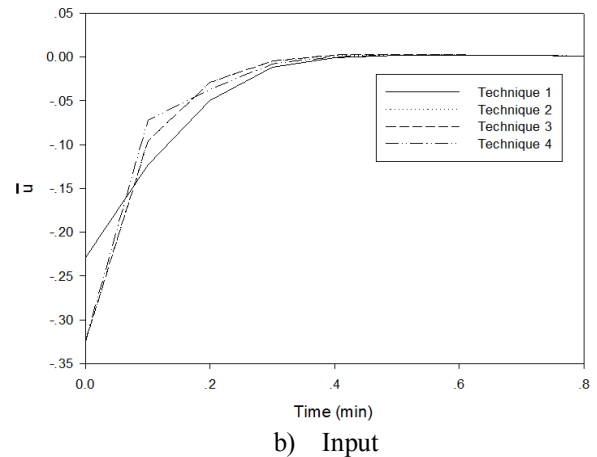


Fig. 6. The closed-loop responses.

Table 1. The on-line computational time.

| Algorithm | CPU time (s) |
|-------------|--------------|
| Technique 1 | 0.001 |
| Technique 2 | 0.047 |
| Technique 3 | 0.101 |
| Technique 4 | 0.075 |

Table 1 shows the on-line computational time. It is seen that technique 1 has the smallest on-line computational time because no optimization problem is needed to be solved on-line. In comparison, technique 3 has the largest on-line computational time because many LMIs constraints are involved in the on-line optimization problem.

5. CONCLUSIONS

In this paper, we have presented interpolation-based off-line MPC for LPV systems. The sequences of state feedback gains are pre-computed off-line. The real-time state feedback gain is calculated by linear interpolation between the pre-

computed state feedback gains. Four interpolation techniques are presented. It is shown that the proposed techniques give better control performance than the old technique.

ACKNOWLEDGEMENTS

This work was supported by Rajadapisek Sompoj Fund, Chulalongkorn University Centenary Academic Development Project, and the Thailand Research Fund (TRF).

REFERENCES

Bumroongsri, P. and Kheawhom, S. (2012a). MPC for LPV systems based on parameter-dependent Lyapunov function with perturbation on control input strategy. *Engineering Journal*, 16, 61-72. doi: 10.4186/ej.2012.16.2.61.

Bumroongsri, P. and Kheawhom, S. (2012b). An ellipsoidal off-line model predictive control strategy for linear parameter varying systems with applications in chemical processes. *Syst. Control Lett.*, 61, 435-442.

Bumroongsri, P. and Kheawhom, S. (2012c). An off-line robust mpc algorithm for uncertain polytopic discrete-time systems using polyhedral invariant sets. *J. Process Contr.*, 22, 975-983.

Bumroongsri, P. and Kheawhom, S. (2013). An interpolation-based robust mpc algorithm using polyhedral invariant sets. *In Proc. of the 2013 European Control Conference (ECC)*, 3161-3166.

Casavola, A. Famularo, D., and Franze, G. (2002). A feedback min-max MPC algorithm for LPV systems subject to bounded rates of change of parameters. *IEEE T. Automat. Contr.*, 47, 1147-1152.

Kheawhom, S. and Bumroongsri, P. (2013). Constrained robust model predictive control based on polyhedral invariant sets by off-line optimization. *Chemical Engineering Transactions*, 32, 1417-1442. doi:10.3303/CET1332237.

Lu, Y., and Arkun, Y. (2000). Quasi-min-max MPC algorithms for LPV systems. *Automatica*, 36, 527-540.

Löfberg, J. (2004). YALMIP: A toolbox for modeling and optimization in MATLAB. *in Proc. IEEE international symposium on computer aided control systems design*, 284-289.

Morari, M., and Lee, J.H. (1999). Model predictive control: past, present and future. *Comput. Chem. Eng.*, 23, 667-682

Sturm, J.F. (1998). Using Sedumi 1.02, a MATLAB toolbox for optimization over symmetric cones. *Optim. Method Softw.*, 11, 625-653.

Wada, N., Saito, K., and Saeki, M. (2006). Model predictive control for linear parameter varying systems using parameter dependent lyapunov function. *IEEE T. Circuits Syst.*, 53, 1446-1450.

Wan, Z., and Kothare, M.V., (2003). An efficient off-line formulation of robust model predictive control using linear matrix inequalities. *Automatica*, 39, 837-846.